

Molecular evaluation of IgE reactivity
in Hymenoptera venom allergy

Dissertation

zur Erlangung des Doktorgrades der Naturwissenschaften

der Fakultät für Mathematik, Informatik und Naturwissenschaften
der Universität Hamburg

vorgelegt von

Frank I. Bantleon

aus Hamburg

Hamburg 2014

The experimental part of this work was performed from September 2010 until January 2014 in the group of Prof. Dr. Reinhard Bredehorst at the Department of Chemistry, Institute for Biochemistry and Molecular Biology, University of Hamburg.

Gutachter der Dissertation: Prof. Dr. Reinhard Bredehorst
Prof. Dr. Bernd Meyer

Gutachter der Disputation: Prof. Dr. Reinhard Bredehorst
Prof. Dr. Markus Fischer
Dr. Thomas Hackl

Datum der Disputation: 28.03.2014

Abstract:

The background of this PhD-thesis is based on the Hymenoptera venom allergy and the associated complex of problems of severe anaphylactic reactions. In general around 0.3 to 8.9% of the population suffer from systemic reactions after a Hymenoptera sting. Allergic reactions are frequently provoked by stings of honeybee (*Apis mellifera*) and yellow jacket (*Vespula vulgaris*). In this context 10 to 20 fatal casualties are reported in Germany per annum; in other countries the rate is between 0.1 to 0.5 per million inhabitants and it can be assumed that the estimated number of unreported cases is much higher. As permanent therapy of allergies the so called "specific immunotherapy" (SIT) has been established. In the case of Hymenoptera venom allergy a proper diagnosis and identification of the allergy provoking insect is a prerequisite for such therapy. *In vitro* diagnostic is based i.a on determination of IgE reactivities against the venom; however this is hampered by the complexity of the venoms.

A molecular, component resolved analysis of IgE reactivities offers an opportunity to distinguish relevant IgE reactivities from clinical irrelevant cross-reactivities.

Therefore in the context of this work several different honeybee venom allergens were expressed in insect cells. The choice of the expression system offers the opportunity to avoid the establishment of cross-reactive carbohydrate determinants (CCDs). Beside biochemical and allergogenic characterisation of the allergens, coupling on a diagnostic surface allowed analyses of IgE reactivities to the allergens by the use of a great cohort of patient sera. Thereby for the first time insights into the recognition patterns of allergic patients and the relevance of particular allergens could be obtained. Additional allergens relevant for therapy could be identified and the diagnostic sensitivity could be enhanced and improved from 72 to 94% by this component resolved diagnostic.

Another aspect of this work is represented by the phenomena of IgE reactivities to CCDs. In this case IgE antibodies are binding specific to the α -1,3-core fucose epitope, which is present on glycosylated Hymenoptera venom allergens. The circumvention of the epitope formation offers diagnostic benefits, however the relevance of this reactivity is still unclear. For the detection of such reactivities marker proteins which bear different CCD epitopes are widely used rendering a differentiation and fine analysis difficult. Therefore a set of glyco-engineered insect cell lines was established by the stable transfection of different Lepidoptera species with CCD relevant glycosyltransferases. These cell lines were used for the expression of a human serum protein with defined glycosylation pattern. The resulting glycoproteins were used to obtain reactivity profiles of Hymenoptera venom and pollen allergic patients and to analyse the prevalence of IgE reactivity for particular carbohydrate structures. As inert scaffold protein alpha-2HS-glycoprotein was chosen, because as high

abundance serum protein it should not show any protein-based cross-reactivity. Additionally it bears two glycosylation-sites, which can be easily modified upon expression in the different glyco-engineered insect cell lines. It could be shown, that IgE reactivities to the fucose epitope dominate compared to the xylose epitope in the case of Hymenoptera venom allergic patients.

Moreover analyses for the establishment and recognition of CCDs by specific antibodies and glycosyltransferases were performed. By the use of recombinant expressed glycosyltransferases and using STD NMR based analyses, first insights into the recognition of the carbohydrate core by human fucosyltransferase 8 and the honeybee α -1,3-core fucosyltransferase could be obtained. Interestingly an appropriate affinity of the enzyme to its acceptor is secured by the previous binding of the donor. To obtain findings of the recognition of CCDs by high affinity antibodies, α -1,3-core fucose specific antibody fragments were selected from a rabbit immune library for the first time. Subsequently this antibody fragments were converted into different human antibodies classes and used for structural as well as for functional analysis. By the recombinant approach the pronounced potential to activate effector cells of these antibodies was demonstrated, which confirms the biological relevance and therefore also the potential clinical significance. In structural analyses the relevance of core fucose as well as the importance of the carbohydrate core for the binding of CCD specific antibodies could be confirmed. The obtained insights contribute significantly to the comprehension of the interaction of the adaptive immune system with the environment and the allergy in particular.

Zusammenfassung:

Den Hintergrund dieser Arbeit bildet die Hymenopterengiftallergie und die mit ihr verbundene Problematik schwerer anaphylaktischer Reaktionen. Generell zeigen ca. 0.3-8.9% der Bevölkerung systemische Reaktionen auf Insektenstiche, wobei häufig allergische Reaktionen nach Stichen der Honigbiene (*Apis mellifera*) und der Wespe (*Vespula vulgaris*) auftreten. Hierbei kommt es zu ca. 10-20 Todesfällen pro Jahr in Deutschland; in anderen Ländern liegt die Rate bei 0.1-0.5 pro 1 Million Einwohnern, wobei generell anzunehmen ist, dass die Dunkelziffer weit höher liegt. Zur dauerhaften Therapie von Allergien hat sich die sogenannte „spezifische Immuntherapie“ (SIT) etabliert, wobei im Falle der Hymenopterengiftallergie zunächst eine sorgfältige Diagnose und Identifikation des allergieauslösenden Insekts erfolgen muss. Eine *in vitro* Diagnostik basiert u.a. auf der Bestimmung von IgE-Reaktivitäten gegen das Gift, was jedoch durch die Komplexität des Giftes erschwert wird. Eine molekulare, Komponenten-aufgelöste Analyse der IgE-Reaktivität ist hier die einzige Option, relevante IgE-Reaktivitäten und klinisch irrelevante Kreuzreaktivitäten zu unterscheiden.

Im Rahmen dieser Dissertation wurden daher unterschiedliche Allergene des Giftes der Honigbiene durch Expression in Insektenzellen dargestellt. Die Wahl des Expressionssystems bot hier die Möglichkeit, die Etablierung kreuzreaktiver Carbohydrat-Determinanten (CCD) zu umgehen. Neben einer biochemischen und allergologischen Beschreibung der Allergene konnten selbige nach Kopplung an Träger unter Verwendung eines großen Kollektivs von Patientenseren hinsichtlich ihrer IgE-Reaktivität analysiert werden. Hierbei konnten erstmalig Einblicke in die individuellen Erkennungsmuster allergischer Patienten und die Bedeutung der jeweiligen Allergene gewonnen sowie die für eine Therapie besonders kritischen Allergene identifiziert werden. Darüber hinaus kann durch Komponenten-Auflösung die Sensitivität der Diagnostik von ca. 72% auf 94% verbessert werden.

Einen weiteren interessanten Aspekt der Arbeit stellt das Phänomen der IgE-Reaktivität mit CCDs dar. Hierbei binden IgE-Antikörper spezifisch das α -1,3-core Fukose-Epitop, welches auf glykosylierten Insektengift-Allergenen vorhanden ist. Die Umgehung der Etablierung dieser Epitope bietet diagnostische Vorteile, allerdings ist die Bedeutung dieser Reaktivität nach wie vor unklar. Für die Detektion einer solchen Reaktivität werden bislang Marker-Proteine eingesetzt, die unterschiedliche CCD-Epitope tragen, was eine Differenzierung und Feinanalyse verhindert. Aus diesem Grunde wurde ein Satz von glykomodifizierten Insektenzelllinien etabliert, indem Zelllinien unterschiedlicher Lepidoptera-Arten mit CCD-relevanten Glycosyltransferasen transfiziert wurden. Diese Zelllinien wurden dann zur Expression eines humanen Serumproteins verwendet, das entsprechend definierte

Glykosylierungsmuster aufwies. Die so erhaltenen Glykoproteine wurden dann eingesetzt um Reaktivitätsprofile von Hymenopterengift- und Pollen-Allergikern zu erstellen und die Prävalenz einer IgE-Reaktivität für einzelne Carbohydrat-Strukturen zu analysieren. Als inertes Trägerprotein wurde α -2-Heremans-Schmid-Glykoprotein verwendet, da dieses als humanes Serumprotein keine Reaktivität mit humanen IgE-Antikörpern zeigen sollte und es zwei Glykosylierungsstellen aufweist, die durch die Expression in den unterschiedlichen Zelllinien modifiziert werden können. Hierbei konnte klar gezeigt werden, dass IgE-Reaktivitäten mit dem Fukose-basiertem Epitop gegenüber dem Xylose-Epitope bei Insektengift-Allergikern dominieren.

Im Weiteren wurden Analysen zur Etablierung bzw. Erkennung von CCDs durch spezifische Antikörpern bzw. Glykosyltransferasen durchgeführt. Unter Verwendung rekombinant produzierter Glykosyltransferasen und mittels STD NMR basierter Untersuchungen konnten erste mechanistische Einblicke in die Erkennung des Zucker-Cores durch die humane Fukosyltransferase 8 und α -1,3-core Fukosyltransferase der Honigbiene gewonnen werden. Interessanterweise wird z.B. eine adäquate Affinität des Enzyms zu seinem Akzeptor erst durch die Bindung des Donors sichergestellt.

Um Erkenntnisse zur Erkennung von CCDs durch hochaffine IgE zu erhalten, wurden erstmalig α -1,3-core Fukose-spezifische Antikörper-Fragmente aus einer leporiden Immunrepertoire-Bibliothek selektiert. Anschließend wurden diese Antikörper-Fragmente in unterschiedliche humane Antikörpertypen konvertiert und diese sowohl für strukturelle als auch funktionelle Analysen eingesetzt. Durch den rekombinanten Ansatz konnte erstmalig ein ausgeprägtes Potential dieser Antikörper zur Aktivierung von Effektor-Zellen nachgewiesen werden, was die biologische Relevanz und damit die mögliche klinische Relevanz bestätigt. In strukturellen Analysen konnte die Relevanz der core-Fukose sowie die Bedeutung der core-Struktur als solche für die Bindung von CCD-spezifischen Antikörpern bestätigt werden.

Die in dieser Arbeit erhaltenen Einblicke tragen wesentlich zum Verständnis der Interaktion des adaptiven Immunsystems und der Umwelt generell und in der Allergie im Besonderen bei

Table of Content

1. Introduction.....	1
1.1 Allergy.....	1
1.1.1 Hypersensitivity reaction Type I.....	2
1.1.2 Hymenoptera venom allergy diagnosis and therapy	8
1.2 Glycosylation and biological function.....	11
1.2.1 The role of glycosylation in allergy.....	12
1.2.2 Glycosyltransferases involved in establishment and biological function of CCDs..	14
1.2.3 Carbohydrate specific antibodies	16
1.3 Objective.....	16
2. Material and Methods	18
2.1 Formation of the immunogenic α -1,3 fucose epitope: elucidation of substrate specificity and enzyme mechanism of core fucosyltransferase A	18
2.1.1 In vitro fucosylation.....	18
2.1.2 Preparation of asialo complex type N-glcans.....	18
2.1.3 Preparation of asialo agalacto complex type N-glycans.....	19
2.1.4 Preparation of 1- β -N-acetyl asialo agalacto complex type N-glycans.....	19
2.1.5 Immobilisation of FucTA	19
2.1.6 SPR affinity assays for ligands of FucTA.....	20
2.1.7 Enzyme kinetic studies by progress curve analysis	21
2.1.8 Other methods.....	21
2.2 Donor substrate binding and enzymatic mechanism of human core α -1,6 fucosyltransferase (FUT8).....	22
2.2.1 Cloning, recombinant expression, and purification of human fucosyltransferase	22
2.2.2 Preparation of 1- β -N-acetyl asialo agalacto complex type heptasaccharide	23
2.2.3 NMR experiments	23
2.2.4 Preparation of NMR samples.....	23

2.2.5 STD NMR experiments	23
2.2.6 Enzyme kinetic studies by progress curve analysis	24
2.2.7 SPR affinity studies	24
2.2.8 Molecular modelling	25
2.2.9 Other methods.....	26
2.3 Donor assists acceptor binding and catalysis of human α -1,6 fucosyltransferase	26
2.3.1 Established methods.....	26
2.3.2 STD NMR experiments	26
2.3.3 SPR affinity studies	26
2.3.4 Molecular modelling	27
2.4 Component resolution reveals additional major allergens in patients with bee venom allergy	27
2.4.1 Patients.....	27
2.4.2 Allergens and IgE antibody measurements.....	28
2.4.3 Immunoreactivity of patient sera	28
2.4.4 CAP-FEIA inhibition.....	28
2.5 <i>Polistes</i> species venom is devoid of carbohydrate-based cross-reactivity and allows interference-free diagnostics.....	29
2.5.1 Analysis of glycosylation pattern of Hymenoptera venoms.....	29
2.5.2 Other methods.....	29
2.6 Fine specificity of IgE carbohydrate reactivity dissected by establishing xenobiotic epitopes with glycoengineered cell lines.....	29
2.6.1 Patient sera.....	29
2.6.2 Cloning of cDNA	29
2.6.3 Recombinant baculovirus production	30
2.6.4 Expression in baculovirus-infected insect cells.....	31
2.6.5 Stable transfection of insect cells.....	31
2.6.6 Protein purification.....	31

2.6.7 Immunoreactivity of patient sera with recombinant proteins	31
2.6.8 Other methods.....	32
2.7 Structural and functional insights into the high affinity recognition of xenobiotic N-glycan core structures by mammalian antibodies.....	32
2.7.1 Generation and selection by phage display of rabbit immune repertoires.....	32
2.7.2 Conversion and production of human IgE and IgG formats.....	33
2.7.3 Surface plasmon resonance analysis.....	33
2.7.4 Cellular mediator release assays	34
2.7.5 Epitope mapping by STD NMR	34
2.7.6 Other methods.....	35
3. Results	36
3.1 Formation of the immunogenic α -1,3 fucose epitope: elucidation of substrate specificity and enzyme mechanism of core fucosyltransferase A	36
3.1.1 Recombinant expression and immunochemical characterisation of soluble FucTA	37
3.1.2 Preparation of core fucosyltransferase acceptor substrates for structural analyses	38
3.1.3 Donor substrate specificity of core fucosyltransferase A.....	40
3.1.4 Acceptor substrate specificity of core fucosyltransferase A.....	42
3.1.5 Characterisation of the enzyme kinetics of core fucosyltransferase A.....	44
3.2 Donor substrate binding and enzymatic mechanism of human core α -1,6 fucosyltransferase (FUT8).....	47
3.2.1 Expression, purification and characterisation of fucosyltransferase 8.....	50
3.2.2 Donor substrate binding of core α -1,6 fucosyltransferase.....	51
3.2.3 In silico model of core α -1,6 fucosyltransferase in complex with GDP-Fuc.....	52
3.2.4 Molecular dynamics simulation.....	54
3.3 Donor assists acceptor binding and catalysis of human α -1,6 fucosyltransferase	56
3.3.1 Acceptor shows moderate affinity and dissociation Rate	57
3.3.2 FUT8 recognises a large epitope of the acceptor substrate	58

3.3.3 Donor contributes significantly to acceptor binding	60
3.3.4 Recognition of the branches	61
3.3.5 Role of the essential Lys369 in donor binding and GDP release.....	63
3.3.6 FUT8 acts via an ordered Bi Bi mechanism	63
3.3.7 FUT8 employs a substrate-assisted mechanism.....	65
3.4 Component resolution reveals additional major allergens in patients with bee venom allergy	67
3.4.1 IgE reactivity to HBV allergens in patients with HBV allergy, patients with YJV allergy, and HBV-nonallergic control subjects.....	68
3.4.2 Sensitisation profiles in patients with HBV allergy.....	69
3.4.3 IgE reactivity to HBV allergens in relation to whole HBV	70
3.4.4 HBV allergen-specific IgG ₄ during HBV immunotherapy	72
3.5 <i>Polistes</i> species venom is devoid of carbohydrate-based cross-reactivity and allows interference-free diagnostics.....	73
3.5.1 CCD-reactivity analysis of <i>Polistes</i> venom	73
3.5.2 Screening of CCD reactive Hymenoptera venom allergic patients sera	74
3.6 Fine specificity of IgE carbohydrate reactivity dissected by establishing xenobiotic epitopes with glyco-engineered cell lines.....	76
3.6.1 Cloning of β -1,2 xylosyltransferase and alpha-2HS-glycoprotein	77
3.6.2 Establishment of insect cell lines with variant glycosylation	79
3.6.3 Expression of AHSG in glyco-engineered insect cells lines.....	80
3.6.4 Analyses of CCD-phenotype of AHSG variants.....	81
3.6.5 Screening of allergic patients sera with diversely glycosylated AHSG variants	82
3.7 Structural and functional insights into the high affinity recognition of xenobiotic complex-type N-glycan core structures by mammalian antibodies.....	84
3.7.1 Establishment of leporid immune repertoire libraries and selection of CCD specific antibodies.....	85
3.7.2 Generation and characterisation of carbohydrate specific IgE and IgG ₁ immunoglobulins	87
3.7.3 Cellular activation by recombinant CCD specific antibodies.....	89

3.7.4 Epitope recognition by CCD specific antibodies	91
4. Discussion	93
4.1 Identification and characterisation of Hymenoptera venom allergens	93
4.2 Fine specificity of IgE carbohydrate reactivity	95
4.3 Carbohydrate core recognition by glycosyltransferases and affinity purified antibodies	96
4.4 Generation of α -1,3-core fucose specific antibodies for evaluation of affinity and biological activity	97
4.5 Relevance of glycosylation in immune modulation, vaccination approaches and tumor targeting	101
5. Summary	105
6. Outlook.....	107
7. References	109
Appendix	127

1. Introduction

1.1 Allergy

The term allergy was established by the Austrian paediatrician Clemens Freiherr von Pirquet in 1906 and conduces the discrimination between a beneficial and a harmful immune response [1]. Today the term comprises an abnormal and exaggerated adaptive immune response against harmless, exogenous, non-infectious, environmental substances [2]. Atopic disorders like anaphylaxis, hay fever, eczema and asthma afflict approximately 25% of individuals in the developed countries [2, 3]. These disorders are characterised by the involvement of allergen specific IgE and T helper 2 cells (T_H2 cells) that recognise allergen derived antigens. In allergic subjects persistent or repetitive exposure to allergens, which typically are intrinsically innocuous substances common in the environment, results in chronic allergic inflammation [2].

In 1963 Coombs and Gell have developed a concept for the understanding of allergic reactions, including the cutaneous immediate and delayed hypersensitive reactions, by classification of the different immunopathologic mechanisms underlying the disease [4]. Of the four major hypersensitivity reactions, Type I underlies the clearest distinct immunopathologic principles [5]. In the Gell-Coombs classification disorders like hay fever, allergic asthma and Hymenoptera venom allergy are classical examples for Type I reactions, which is also known as immediate hypersensitivity [5, 6]. These disorders are characterised by the fact that the reaction is predominately driven by IgE antibodies bound to mast cells. The degranulation of mast cells is triggered on the binding of IgE to the high-affinity receptor ($Fc\epsilon RI$) located on the surface of tissue mast cells [7]. Antigen-clustering of $Fc\epsilon RI$ by bound antigen specific IgE results in the initiation of multiple events, which induces mast cell activation and subsequent degranulation of the mast cell [8]. The mediators released by the mast cells are include histamine, cytokines and granulocyte macrophage colony stimulating factors, which mediate the characteristic symptoms of Type I allergy [9].

Type II allergic reactions are characterised by antibody-antigen interactions resulting in cell lysis of the target cell [5, 10]. In this case cytotoxic antibodies, mainly IgG and IgM, are directed against antigens of the individuals own cells [10]. Subsequent cell damage can be induced by two different mechanisms. The first mechanism is the direct action of macrophages, neutrophils and eosinophils that are linked to immunoglobulin coated target cells on the Fc receptor of the antibody. The second mechanism is the antibody mediated activation of the complement system that results in cell lysis [10].

The formation of immune complexes is typical for Type III allergic reactions [5, 10]. This response occurs when the antigen reacts in the tissue space with potentially precipitating antibodies, mainly IgM, forming microprecipitates in and around small vessels, causing secondary damage to cells [10]. If the antigen is present in excess, soluble immune complexes are formed and further deposited in the endothelial lining of blood vessels walls, fixing complement and causing local inflammation [10]. Immune complexes are primarily deposited in the lung, joints, kidneys and the skin [10]. Tissue injury is initiated by the local inflammation response involving activation of the complement [10]. Various cells, such as macrophages, neutrophils and platelets, are subsequently attracted to the deposition site, and further contribute to the tissue damage [10].

Type IV allergic reactions are characterised by the activation of T cells, instead of involvement of IgE [10].

Typical for this allergic reactions are skin eruptions (contact dermatitis) due to skin contact of drugs, cosmetics and environmental chemicals [10, 11]. Type IV is also known as delayed hypersensitivity, because the symptoms develop usually within of 2-14 days after exposure to the allergen [10]. Type IV reactions are triggered when the allergen encounters T lymphocytes, and is presented to T lymphocytes by antigen presenting cells, which results in lymphocyte stimulation and cytokine release [10].

1.1.1 Hypersensitivity reaction Type I

In most cases the term allergy is used for hypersensitivity reactions of Type I, which are characterised as IgE-induced diseases [12]. The term atopy from the Greek atopos, meaning out of place, is often used when describing IgE mediated diseases [12]. Atopy characterises the personal or familial tendency to produce IgE antibodies in response to minute doses of allergens and to develop typical allergic symptoms like asthma [13].

The primary response to an allergen is known as sensitisation, which reflects the allergen's ability to promote the differentiation of CD4⁺ T cells into T_H2 cells during priming [2, 3]. There are different CD4⁺ helper T cell effector lineages, which control the host defences against distinct classes of pathogens. T helper type 1 cells (T_H1 cells), controlled by the transcription factors T-bet (T box expressed in T cells), provide protective immunity to intracellular microorganisms, like bacterial, viral and protozoan pathogens [14, 15]. IL-17 expressing T helper cells (T_H17 cells), characterised by the transcription factor ROR γ t (RAR-related orphan receptor γ t), control host defences against extracellular bacterial and fungal pathogens. T_H2 cells orchestrate immunity to multicellular parasites, including helminthes [15, 16]. Inappropriate activation of these three arms of adaptive immunity can lead to

different types of immunopathologies, including autoimmunity in the case of T_H1 and T_H17 responses and allergies in the case of T_H2 responses (Fig. 1.1) [15].

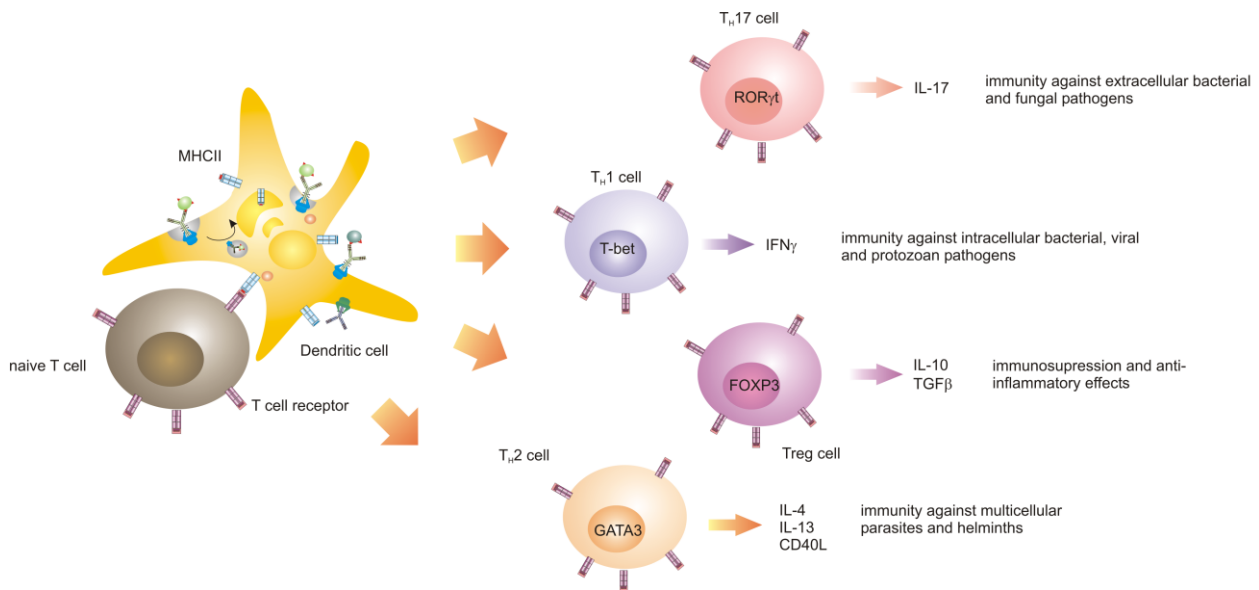


Fig. 1.1 T_H cell differentiation

Schematic representation of different ways of T_H cell differentiation and overview of immunological functions of T_H cell subsets

Sensitisation begins with the uptake of allergens by antigen presenting cells (APCs) like Dendritic cells (DCs) [3]. This event can happen e.g. in the airway lumen or the allergen enters the tissue through epithelium disruptions where it is sampled by DCs [2]. Another possibility of allergen uptake by DCs may occur if the allergen is a proteolytic enzyme, which can access submucosal DCs by cleaving epithelium tight junctions [2]. DCs efficiently sample the periphery for foreign antigens by using a set of different receptors, like pattern recognition receptors (PRRs), Toll like receptors (TLRs) and C-type lectin receptors (CTLRs), which increase internalisation efficiency and deliver information regarding danger signals [17]. Newer findings suggest a link between glycosylation of allergens and recognition as well as uptake of them by DCs. For example allergens like Der p 1, Fel d 1, Ara h 1 and Can f 1 are recognised by a mannose receptor (MR) of DCs [18]. The internalised allergens are processed and the resulting peptides are presented by the MHC (Major histocompatibility complex) II of APCs to naïve T cells in the lymph nodes (Fig. 1.2) [2].

To induce the differentiation of naïve T cells to T_H2 cells a T_H2 promoting milieu is essential [19]. This milieu is generated by the secretion of epithelial cell derived cytokines, like IL (Interleukin)-25, IL-33 and TSLP (Thymic stromal lymphopoietin), which are released during tissue damage, pathogen recognition or allergen exposure [19-21]. Several different cell types, like monocytes, DCs, B cells and T cells are stimulated by TSLP [21]. TSLP and IL-33 act on dendritic cells to induce a T_H2 differentiation tendency [19]. T_H2 cells respond

stronger to TSLP than T_H1 cells or T_H17 cells, due to higher expression rates of TSLPR (TSLP receptor) and a TSLP improved cell proliferation. Furthermore TSLP promotes the differentiation and cytokine secretion of T_H2 cells [20, 22].

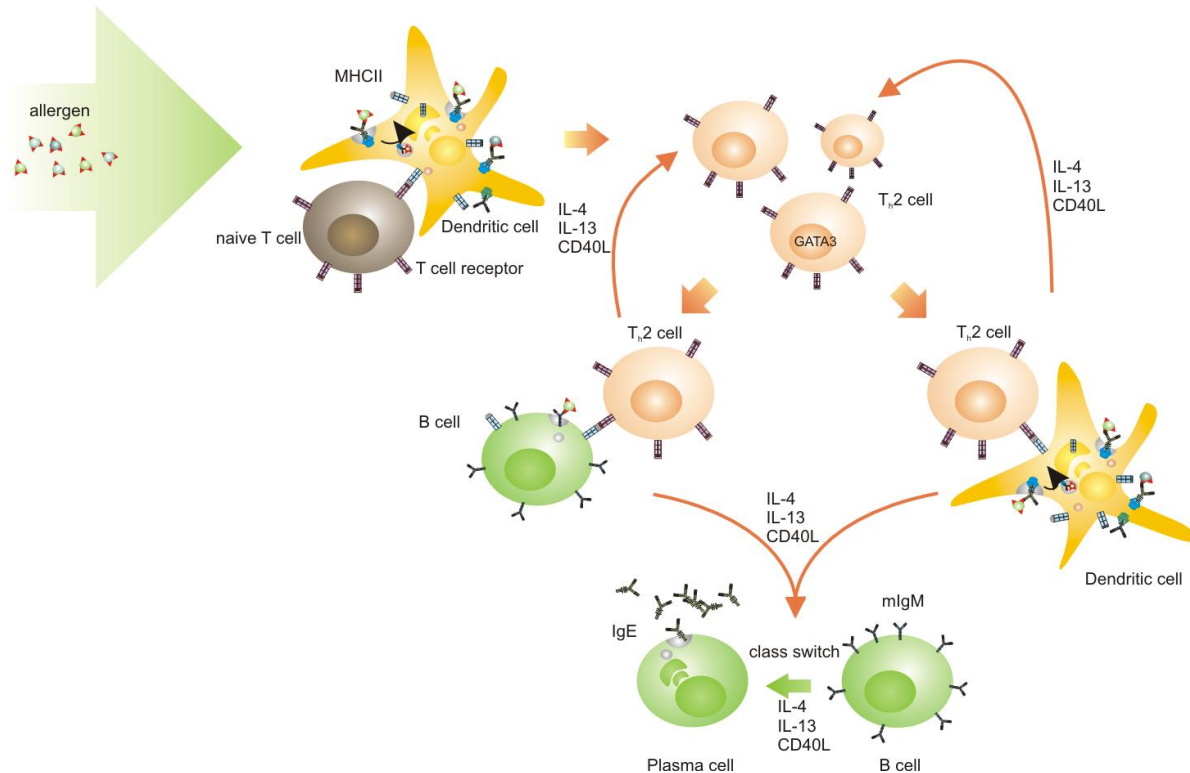


Fig. 1.2 Sensitisation and B cell class switch induction

Schematic representation of allergen uptake by DCs, APC-T cell interaction and induction of B cell class switch and IgE production

Allergen exposure or helminth and fungal infections upregulate the expression of IL-25 in epithelial cells [20, 23, 24]. IL-25 binds to IL-17Rb (IL-17 receptor b) on naïve T cells and promotes the differentiation of these cells into T_H2 cells in an IL-4-dependent manner [24].

IL-33 is expressed and found all over the vascular tree, in epithelial cells and tissue exposed to the environment, in fibroblastic cells, in lymphoid organs and in the brain where it is stored in the nucleus of cells [25, 26]. After cell damage or allergen exposure this cytokine is immediately released into the extracellular space where it is processed by several enzymes that are secreted by recruited neutrophils, resulting in an enhanced activity of IL-33 [25, 26]. IL-33 induces the production of IL-5 and IL-13 by innate type immune cells, such as mast cells or basophils, which contribute to a T_H2 -promoting milieu [25, 26].

In combination IL-25 and IL-33 also activate lineage negative lymphoid like populations, like type 2 innate lymphoid cells (ILC2), nuocytes or natural helper cells [27, 28]. These cells secrete significant levels of IL-5, IL-9 and IL-13. These cytokines promote the differentiation, survival and expansion of T_H2 cells [19].

Beside the cytokine milieu also the strength of T cell receptor (TCR) signalling contributes to the fate of naïve T cells. In general weak signalling favours T_H2 differentiation, whereas strong TCR signals lead to T_H1 differentiation [29]. When naïve $CD4^+$ T cells receive weak TCR signals, these weakly stimulated T cells rapidly induce expression of the T_H2 master regulatory transcription factor GATA (GATA transcription factor)-3 in an IL-4/STAT (Signal Transducer and Activator of Transcription) 6 independent manner and produce IL-2 that in turn activates STAT5 [29]. GATA-3 cooperates with STAT5 to induce TCR dependent, IL-4/STAT6 independent early IL-4 production that occurs 14-24 h after activation [29]. The endogenously produced IL-4 acts on the weakly stimulated T cells through IL-4R to further upregulate GATA-3 expression [29]. The expressed GATA-3, in cooperation with continued STAT5 activation, amplifies the production of IL-4. This positive feedback loop leads to the completion of differentiation into T_H2 cells [29].

The activated T_H2 cells express and secrete the cytokines IL-4, IL-13, IL-5 and IL-9 [30]. Especially IL-4 and IL-13 are potent inducers of $C\epsilon$ germline transcription in B cells [31, 32]. IL-4 binds to the IL-4 receptor α -chain (IL-4R α) that is part of both the IL-13R and IL-4R of B cells [32]. The IL-4R in addition contains the common cytokine receptor γ -chain. Activation of the IL-4R triggers the activation of the Janus family tyrosine Kinases JAK (Janus kinase) 1, JAK3, IRS1 (Insulin receptor substrate) and TYK1 (Tyrosine kinase 1). The IL-13R, which additionally consists of a unique IL-13-binding chain, activates JAK1 and TYK2. The activated JAKs phosphorylate tyrosine residues in the intracellular domains of IL4R α , which act as signal transducer and activator of transcription 6-binding site (STAT6)-binding sites. STAT6 is phosphorylated, dimerises and is translocated to the nucleus, where it can activate transcription of the ϵ promoter [32].

Beside signals from the cytokines IL-4 and IL-13 also cell surface receptors collaborate to regulate class switch recombination in B cells [32]. Activated T_H2 cells also upregulate the cell surface receptors CD (cluster of differentiation) 40L. CD40L interacts with CD40 of B cells, which results in the upregulation of co-stimulatory molecules CD80 and CD86, which allows a more efficient T cell expression of CD40L and thereby an enhanced stimulation of B cells. CD40-mediated stimulation of B cells also synergises with IL-4R signals to enhance the transcription of $C\epsilon$ germline transcripts. The subsequent activation induces cytidine deaminase, the rearrangement of the IgE genomic locus and finally the production of IgE antibodies by the stimulated B cells [32]. The concentration of IgE in the serum is normally low due to the fact that most IgE is bound to receptors of mast cells or basophils, but after allergen contact the IgE levels and the sensitivity of the patient to allergens is enhanced [3, 33, 34]. There are two main IgE receptors on immune cells, which differ in structure, function and location [35]. One of these is the Fc ϵ RI, the high-affinity IgE receptor and the other one

is the FcεRII, the so called low-affinity IgE receptor [34]. Human FcεRI consists of up to four protein chains of three kinds, the α-, the β- and the γ-subunit [36]. Solely the α-subunit binds the Fc part of IgE, as also demonstrated by the crystallisation of the subunit alone and in complex with the Fc of IgE [37, 38]. The other subunits are involved in stable formation of the FcεRI or are also part of other Fc receptors [34, 36]. On mast cells and basophils FcεRI shows a tetrameric structure comprising one α-, one β- and two γ-subunits (αβγ₂) [2, 34, 36, 39-41]. The α-subunit itself consists of two extracellular immunoglobulin-like domains, a hydrophobic transmembrane region and a short cytoplasmic tail [34].

Expression of the β-subunit in mast cells and basophils results in an increased FcεRI expression and amplifies signalling through the receptor [42]. Additionally the FcεRI density on the surface of mast cells is also upregulated by increased IgE levels and in the presence of IL-4 [42].

In allergic patients, whose tissue mast cells and basophils provide antigen specific IgE bound to the FcεRI, re-exposure to antigen results in the crosslinking of FcεRI-bound IgE and the aggregation of surface FcεRI [40, 41, 43]. The consequence of the FcεRI aggregation is the activation of mast cells and basophils and the secretion of diverse biologically active mediators (Fig. 1.3) [41].

Mediators produced by mast cells are divided into preformed mediators, newly synthesised lipid mediators, cytokines/chemokines and growth factors [42, 44]. These categories are not absolutely exclusive because at least one cytokine, TNF-α (Tumor necrosis factor-α), is known as both preformed and newly synthesised molecule [42]. Preformed mediators, including histamine, serine proteases (tryptase and chymase), carboxypeptidase A and proteoglycans are stored in cytoplasmic granules [9, 42, 45]. As a consequence of mast cell activation the granules fuse with the plasma membrane and the contents are released into the extracellular environment [42]. The released mediators have different effects, e.g. histamine has effects on smooth muscle (contraction), endothelial cells, nerve endings and mucous secretion [42]. The allergic inflammation can be classified into different temporal phases. Early- or immediate-phase reaction occurs within seconds to minutes after allergen contact, whereas late-phase reaction occurs within several hours [2]. In contrast, chronic allergic inflammation is a persistent inflammation that occurs at the site of repeated allergen exposure [2]. The early-phase reaction is characterised by the described activation of mast cells at the affected site and the action of the preformed mediators, lipid mediators and platelet activating factor, which are also released by some mast cells [2]. These signs and symptoms vary according to the site of the reaction, but can include vasodilation (reflecting the action of mediators on local nerves, and causing erythema of the skin), contraction of bronchial smooth muscle (producing airflow obstruction and wheezing) and increased

secretion of mucus (causing a runny nose) [2]. The mediators can also stimulate nociceptors of sensory nerves in the nose, skin and airway, resulting in sneezing, itching or coughing [2, 46-48].

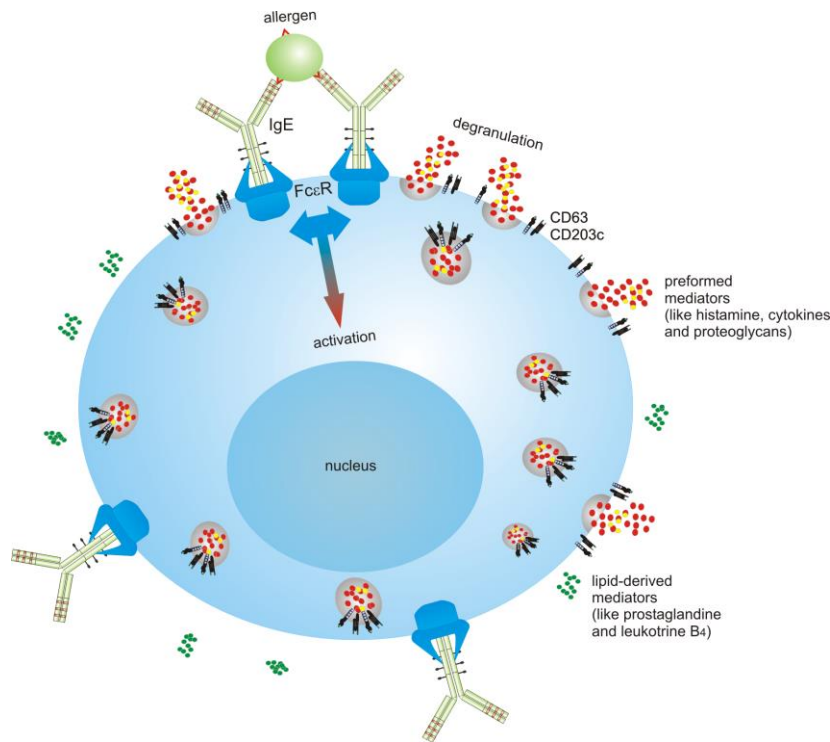


Fig. 1.3 Mast cell activation

Schematic representation of mast cell activation and secretion of biological active mediators, causing acute symptoms of allergic reactions

The rapid and systemic release of such mediators from mast cells and basophils accounts for much of the pathology associated with anaphylaxis [2, 49].

The late phase reaction, which occurs 12 to 48 hours after allergen exposure, is characterised by an excessive inflammation of the local tissue induced by various mediators secreted from inflammatory cells, like mast cells, basophils, DCs, neutrophils, eosinophils, T cells and macrophages [50].

For example mast cells also release a broad range of newly synthesised cytokines, chemokines and growth factors [2, 44]. Some of these mediators have the potential to attract other immune cells either directly or indirectly, like TNF- α and IL-8 [2, 51]. Other secreted products can activate innate immune cells or affect T cells, DCs and B cells [2]. Beside immune cells also structural cells, like vascular endothelial cells, epithelial cells, fibroblasts and smooth muscle cells are affected by some mast cell products [2, 52].

Cytokines like IL-17 and IL-25 are secreted from T cells that recognise allergen-derived peptides [2, 53-55]. These T cells may be either resident at the site of allergen contact or they are attracted to these sites. Late phase reactions are thought to be coordinated in part

by certain long term consequences of the mediators released by mast cells during early phase reaction, and in part by antigen stimulated T cells. The clinical features of late-phase reactions reflect the activities of both resident cells and circulating leukocytes that are attracted to the inflammatory site. In the skin, for example, to the recruited leukocytes belong T cells, granulocytes and monocytes. These cells secrete pro-inflammatory mediators, which cause tissue damage [2, 56].

1.1.2 Hymenoptera venom allergy diagnosis and therapy

In general the relative frequency of an anaphylactic reaction after a hymenoptera sting is between 0.3% to 8.9% in the population and 19% for severe local reactions [57-60].

A local reaction is classified as confinement of the symptoms like erythema, itching, redness or swelling to tissue contiguous with the sting site. Local reactions may swell to greater than 10 cm, increase for 24-48 hours, last 5 to 10 days and generally resolve without treatment [57, 61, 62].

Systemic reactions on the other hand are characterised by symptoms that are beyond a local reaction at the site of the sting [57]. These reactions include a spectrum of manifestations, ranging from mild to life threatening [61]. Symptoms of a mild systemic reaction are often limited to the skin and include flushing, urticaria and angioedema [61]. More severe systemic reactions can be fatal and life threatening. Upper airway obstruction, including tongue and throat swelling as well as laryngeal edema, are probably the most common cause of fatal anaphylaxis [61]. Additional signs of anaphylaxis may be gastrointestinal such as nausea, diarrhea and abdominal pain. Neurological manifestation of anaphylaxis can include seizures [61]. In the most fatal degree the anaphylactic reaction can lead to a cardiac arrest and death of the patient [57].

In Europe fatal reactions are mainly induced by stings from honeybee (*Apis mellifera*) or yellow jacket (*Vespula vulgaris*), but, e.g. in the USA, also stings of the fire ant (*Solenopsis invicta*) can provoke such reactions [58, 63, 64]. Moreover members of the genus *Polistes* are prominent anaphylaxis provoking Hymenopteras. Notably, the species *Polistes dominula* is increasingly spreading all over Europe and the USA [65]. Other Hymenoptera species, like bumblebee (*Bombus spp.*), hornets (*Vespa crabro*) and *Dolichovespula* represent clinically relevant species, too, but with less sting events compared to e.g. the frequency of *A. mellifera* stings [57].

The venom of Hymenoptera species comprises a variety of different components including low-molecular weight substances, peptides and proteins [57]. The best characterised Hymenoptera venom is the honeybee's (Table 1). It contains several allergens with enzymatic properties, e.g. Api m 1 (phospholipase A2), Api m 2 (hyaluronidase), Api m 3

(acid phosphatase) and Api m 5 (dipeptidylpeptidase IV) [66-70]. Furthermore the majority of allergens is glycosylated, like Api m 2, Api m 5 and Api m 10 [70-72]. The most prominent low-molecular weight substance in the venom is Api m 4, a peptide of 70 amino acids [73].

Venoms of other Hymenoptera species have many similar and sometimes cross-reactive allergens [70]. Although there are some components in the vespid venom, which are cross-reactive with components from the honeybee venom, as Ves v 3 and Api m 5, the cross-reactivity of the venoms between members of the *Vespidae* is much higher compared to the protein-based cross-reactivity of honeybee and yellow jacket venom [64, 70, 71]. Structure analysis suggests a higher cross-reactivity for Ves v 2 and the homologue in the venom of *Dolichulavespula maculata* Dol m 2, compared to the structural cross-reactivity of Api m 2 and Ves v 2 [74].

In the venoms of yellow jacket and honeybee are also venom and species specific allergens, which have no homologues in the corresponding venom, like Ves v 5 or Api m 10 [75].

Table 1 Overview of known honeybee and yellow jacket venom allergens in 2014

Allergen	common name/function	MW	glycosylation sites	rec. expression
<i>Apis mellifera</i>				
Api m 1	phospholipase A2	17 kDa	1	+
Api m 2	hyaluronidase	45 kDa	2	+
Api m 3	acid phosphatase	49 kDa	2-3	+
Api m 4	melittin	3 kDa	-	
Api m 5	DPPIV	100 kDa	5-6	+
Api m 6	protease inhibitor	8 kDa	-	+
Api m 7	cub protease	39 kDa	2-4	+
Api m 8	carboxyesterase	70 kDa	4	+
Api m 9	carboxypeptidase	60 kDa	4-5	+
Api m 10	icarapin	55 kDa	3	+
Api m 11	MRJP9	45 kDa	2	+
Api m 12	vitellogenin	200 kDa	2	+
<i>Vespula vulgaris</i>				
Ves v 1	phospholipase A1	35 kDa	-	+
Ves v 2	hyaluronidase	45 kDa	2-3	+
Ves v 3	DPPIV	100 kDa	3-6	+
Ves v 4	cub protease	35 kDa	?	+
Ves v 5	antigen 5	25 kDa	-	+
Ves v 6	vitellogenin	200 kDa	1	+

Honeybee and yellow jacket differ also in the kind of stinging. Honeybees normally sting only once and inject 50-140 µg venom protein per sting and the stinger remains in the skin [76, 77]. In contrast yellow jacket and *Polistes* are able to sting several times, but the injected venom amount is significantly lower (yellow jacket inject 1,7-3,1 µg/sting, *Polistes* 4,2-17 µg/sting) and the stinger does not remain in the skin [64, 76].

To therapy a Hymenoptera venom allergy patient proper diagnosis of the culprit Hymenoptera venom is a prerequisite [62]. The diagnosis of Hymenoptera allergy requires both the history of a sting event that resulted in a systemic reaction and the evidence of venom specific IgE, either by skin testing or *in vitro* testing [61, 62]. Due to the fact that insect stings are painful, most patients are aware of the occurrence of the sting [61]. If the patient can identify the stinging insect, this can be helpful for the following diagnosis and treatment [61]. But many patients cannot identify the culprit insect reliably, so the physician may need to use additional evidence. The presence of the stinger is most common with honeybees and the presence of pustules is often associated with stings from fire ants [61, 62].

Another important step in the diagnosis of Hymenoptera allergy is to determine whether the patient's reaction was local or systemic, based on a careful history of the sting event [61].

Once the physician determines that the sting resulted in a systemic anaphylactic reaction, testing for venom specific IgE is essential for the diagnosis [61]. Venom specific IgE may be assigned either by skin testing or *in vitro* testing [61, 78]. In Hymenoptera venom allergy skin testing is normally performed with both honeybee and yellow jacket venom, but also other insect venoms are used if necessary [57]. To reduce the risk of systemic side effects, testing is done with increasing venom concentrations [57]. The skin prick test starts with venom concentrations of 1 µg/mL, which is increased until a positive reaction is elicited [57]. Every 15 minutes, readings are conducted and the concentration is increased to 10 and 100 µg/mL [57]. If there is no reaction, an intradermal test is performed with a venom concentration of 1 µg/mL [57].

To date *in vitro* sIgE measuring is routinely performed by a fluorescence enzyme immunoassay, which has replaced the radioallergosorbent test (RAST) for *in vitro* sIgE measuring, since the new test systems are more accuracy [59, 64, 78]

However a common problem in diagnosis of Hymenoptera venom allergy is that 50% of patients with a history of a systemic reaction after a Hymenoptera sting have venom specific IgE to venoms of honeybee and yellow jacket [79, 80]. This double positivity can be provoked by three factors:

A patient can be sensitised against both venoms, therefore possesses venom specific IgE for allergens of honeybee and yellow jacket venom [80]. Or a patient, which is sensitised only against one Hymenoptera venom, reacts with a cross-reactive allergen in another

Hymenoptera venom. Some allergens in Hymenoptera venoms share homologous structure due to a high amino acid identity, as shown for the dipeptidylpeptidases, the vitellogenins or the hyaluronidases [70, 81].

The majority of double positive test results is induced by cross-reactive carbohydrate determinants (CCDs). Up to 75% of Hymenoptera venom double positive allergic patients react with these carbohydrates [82].

In the *in vitro* IgE testing, usage of CCD-free recombinant allergens can avoid and circumvent the mentioned problems [71, 78].

Recently, it could be shown that the diagnostic sensitivity in *in vitro* IgE testing could be increased by using a set of recombinant allergens. Compared to the application of only one allergen (Api m 1), the use of the set (Api m 1, Api m 2, Api m 3, Api m 4, Api m 5 and Api m 10) of honeybee venom allergens increased the diagnostic sensitivity dramatically from 72 to 94% [83].

Some Hymenoptera venom allergic patients with negative venom specific IgE could be diagnosed by the use of the basophil activation test (BAT) [84]. The BAT is a flow-cytometry-based functional assay that assesses the degree of cell activation by CD63 cell surface presentation after exposure to an allergen [85, 86].

After final identification of the culprit insect the patient can be treated with a specific immunotherapy.

Venom immunotherapy (VIT) is the most effective treatment, reducing the risk of systemic reactions in individuals with Hymenoptera venom allergy [87]. VIT can restore normal immunity against venom allergens and can induce venom specific immune tolerance [87, 88]. During VIT, peripheral tolerance is induced by the generation of allergen specific regulatory T (T_{reg}) cells, which suppress proliferative and cytokine responses against the venom allergens [87]. T_{reg} cells are characterised by IL-10 secretion that influences effector cells of allergic inflammation, like mast cells and basophils [87]. T_{reg} cells also have influence on B cells by suppressing IgE production and increasing the levels of the blocking antibody IgG₄ [87, 88]. IgG₄ inhibits allergen-induced and IgE-mediated release of inflammatory mediators from basophils and mast cells, IgE-facilitated allergen presentation to T cells, and allergen-induced boost of memory IgE production during allergen exposure [88].

1.2 Glycosylation and biological function

Glycosylation is probably the most abundant posttranslational modification of proteins [89]. Protein glycosylation is a very heterogeneous group of posttranslational modifications that can be found in all living organisms, ranging from eubacteria to eukaryotes [90]. It is divided

into O- and N-glycosylation. O-glycans are built up by the sequential enzymatic transfer of monosaccharides starting with the glycosylation of hydroxyl groups of amino acids like serine [90-92]. In contrast N-glycosylation starts by *en-bloc* transfer of a 14 monosaccharide building block onto asparagine residues of polypeptides that have entered the endoplasmic reticulum (ER) [92, 93]. There is also a bacterial N-glycosylation pathway, which differs from the eukaryotic way [94].

In eukaryota, after the sugar bloc is transferred to asparagine residues, the original 14 monosaccharide building block is stepwise modified by several enzymes while the glycoprotein is transported along the secretory pathway [95]. The modifications include removal of glucose and mannose residues to generate high mannose type glycans and eventually the addition of new sugar residues in the Golgi apparatus (GA) to build up complex type glycans [95]. Hybrid-type glycans are established by the addition of N-acetylglucosamine to the $\alpha 3$ arm of an acceptor containing five mannose residues. These glycans can be further modified as well [96].

Glycosylation is a very heterogeneous process in terms of glycan composition, tissue expression of glycosyltransferases, species specific residues and the fact that not all possible glycosylation sites are glycosylated [89, 96-100].

Glycosylation plays an important role in many aspects, like protein folding, protein quality control, protein trafficking, cell cell contact, cell adhesion, developmental processes and for many diseases [101-105]

1.2.1 The role of glycosylation in allergy

Glycosylation affects many aspects in allergy, like recognition and uptake of allergens by immune cells, diagnostic approaches and clinical effects [18, 106, 107].

Allergens are recognised at the site of entry by epithelial cells and DCs, which activate innate inflammatory systems that can collectively induce T_H2 immune response [18]. This initial recognition and uptake of allergens by immune cells can also be triggered by the glycosylation of the allergen [18]. It could be shown that the allergens Der p 1, Bla g 2, Fel d 1, Ara h 1 and Can f 1 are glycosylated and the main sugar subunits of these allergens is mannose [18, 108]. These allergens are recognised by the MR, expressed on the surface of DCs and epithelial cells [18, 109, 110]. Epithelial cells, stimulated with glycosylated Der p 1, secrete higher levels of TSLP compared to stimulation with deglycosylated Der p 1. This finding supports the importance of glycosylation of allergens for development of allergic inflammation [18].

Beside cell surface receptors, also soluble receptors like galectins might play a role in developing allergic inflammation [17, 111]. Galectins are a family of proteins that bind

β -galactosides and are expressed by diverse cell types, including monocytes and DCs. In murine models it was shown that ovalbumin-sensitised Gal-3 knockout mice had lower eosinophil levels and a lower T_H2 response compared to control mice [112]. The contribution of Gal-3 in T_H2 responses was further confirmed in murine models of atopic dermatitis and chronic allergic inflammation [17].

Beside its role in immune cell recognition and uptake of allergens, glycosylation has also to be considered in diagnostic approaches. The CCDs present on the surface of hymenoptera venom and plant derived allergens may hamper a correct diagnosis of Hymenoptera venom or pollen allergic patients. Due to the fact that the CCDs are present on plant derived material, these glyco-structures are considered as the most abundant environmental immune determinants [107].

Since the CCDs are lacking on human proteins, these structures are highly immunogenic and provoke a pronounced immune response in men.

On insect N-glycans the relevant epitope is defined by an α -1,3 fucose linked to the innermost *N*-acetylglucosamine (GlcNAc) of the core-glycan [113]. Beside insect N-glycans the α -1,3-core fucose epitope is also present on the glycans of parasitic nematode *Ascaris suum* [114]. Plant N-glycans bear an additional β -1,2 xylose residue linked to the innermost mannose residue of the core glycan (Fig. 1.4) [115]. Both residues are also detectable on *Shistosoma mansoni* derived N-glycans, in contrast to N-Glycans of *Helix pomatia* haemocyanin, where only xylose is present [116-118]. In mice using *S. mansoni* infection the fucosylated and xylosylated N-glycans induce a glycan specific T_H2 cellular response and elicit T cell-dependend anti- α -1,3-core fucose and anti- β -1,2 xylose specific antibodies [116].

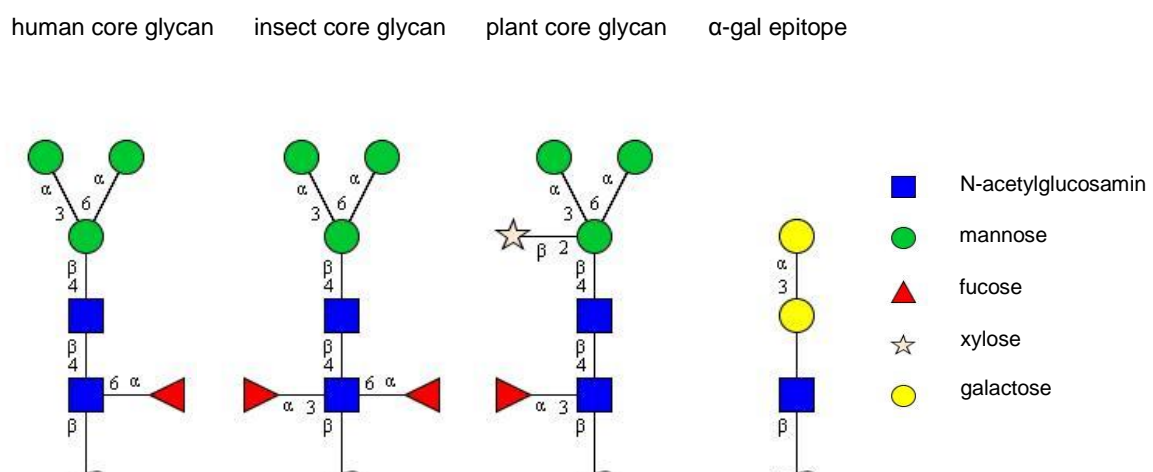


Fig. 1.4 Cross-reactive carbohydrate determinants in overview
Schematic representation of human and immunogenic core-glycan structures

In diagnostic approaches the CCDs are often responsible for false positive test results [82, 119]. In a group of 1831 patients with an allergic respiratory disease 23% of the sera showed reactivity with CCDs [120]. The diagnostic problem caused by the CCDs can be abolished by the use of recombinant CCD-free allergens, non-glycosylated natural allergens or recombinantly modified allergens lacking the glycosylation site [71]. While the diagnostic importance of the CCDs is evident, the clinical relevance of the α -1,3-core fucose and β -1,2 xylose epitope is generally considered low, because these CCDs seem to be unable to induce severe clinical symptoms [107]. For example, in a nasal provocation test of CCD positive Hymenoptera venom allergic patients with grass pollen, these patients did not show any clinical effects [121]. Despite of the low or not detectable clinical effects in skin prick test and provocation tests, CCD bearing molecules are able to induce histamine release or basophil activation *in vitro*, however these results are considered clinically irrelevant [122, 123].

Whereas the clinical effects provoked by α -1,3-core fucose- and β -1,2 xylose specific IgE antibodies remain unclear and controversially discussed, IgE antibodies specific for the α -gal epitope are clearly able to induce clinical effects and even severe anaphylactic reactions. The α -gal epitope is composed of a terminal α -1,3 linked galactose attached to a galactose residue at the end of a glycan (Fig. 1.4) [124]. The epitope is abundantly found on glycans of non-primate mammals including marsupials and on the glycans of prosimians and new world monkeys [125]. Apart from mammals the α -gal epitope is also expressed on glycans of *Leishmania* and *Trypanosoma* and is present on the therapeutic antibody cetuximab [126, 127]. Antigens bearing the α -gal epitope are able to induce anaphylactic reactions, which differ in the period of occurrence of clinical symptoms [106, 128-131]. On the one hand IgE antibodies specific for the α -gal epitope are able to induce a classical immediate reaction, when the α -gal bearing antigen is applied by intravenous injection as seen for cetuximab [127]. On the other hand in meat allergy delayed anaphylactic reactions are reported, which also seem to be induced by α -gal specific IgE antibodies [106, 130]. The delayed appearance in the latter case can be possibly explained by the time needed for red meat to be digested and α -gal carrying antigens presented to the circulation [132]. IgE antibodies specific for the α -gal epitope clearly demonstrate the potential of carbohydrate specific IgE to induce anaphylactic reactions.

1.2.2 Glycosyltransferases involved in establishment and biological function of CCDs

The glycosyltransferases involved in the establishment of the α -1,3-core fucose and β -1,2 xylose epitopes both are localised in the GA and share a common topology with most GA localised glycosyltransferases, which is composed of a short cytoplasmatic tail, a

transmembrane region, a stem region and the catalytic domain in the lumen of the GA [133-135]. The α -1,3-core fucose epitope, present on Hymenoptera venom components, is established by an α -1,3-core fucosyltransferase [136]. This enzyme transfers fucose from the donor GDP (guanosine diphosphate) -fucose to the innermost GlcNAc, preferentially after the transfer of fucose to the same GlcNAc in α -1,6 linkage [137, 138]. The genes of the α -1,3-core fucosyltransferases of honeybee and yellow jacket have been identified and the epitope assembled by these glycosyltransferases has been immunologically characterised. Homologous enzymes also establishing the α -1,3-core fucose epitope could be found e.g. in *Arabidopsis thaliana*, *Drosophila melanogaster*, *Trichoplusia ni* and *Schistosoma mansoni* [71, 116, 139-141]. *A. thaliana* mutants, lacking the α -1,3-core fucosyltransferase, a higher salt sensitivity was detected by root growth assays. In this case the fucose residue has influence in the stress response of the plant [142]. For *D. melanogaster* a role of the fucose epitope in developmental processes of the nervous system was suggested, especially in the organisation of the central nervous system [143].

In plants and *Trematoda* the β -1,2 xylose epitope is established additional to the α -1,3-core fucose epitope on N-glycans [107]. The enzyme responsible for composition of the β -1,2 xylose epitope formation is a GA-located β -1,2 xylosyltransferase [133]. In plants the formation of the β -1,2 xylose epitope occurs prior to transfer of fucose to the innermost GlcNAc residue of the N-glycan [144]. The function of β -1,2 xylosylation is suggested to be a quality control to prevent the production of immature N-glycosylated proteins in plants [144].

The α -1,3 galactosyltransferase transfers galactose from UDP (uridine diphosphate) -galactose, forming an α -1,3-glycosidic linkage to a glycolipid or glycoprotein acceptor terminating in N-acetyllactosamin, [106, 145]. Besides the role of the α -gal epitope in allergy, it has also tremendous influence on xenotransplantation, for this epitope is an inducer of complement-dependent cytotoxicity of transplanted organs [145, 146]. In the human genome located on chromosome 12 a pseudogene of the α -1,3 galactosyltransferase is found and it was shown that this pseudogene contains the same exon/intron organisation as the active gene in mice [147, 148]. Unlike the active murine gene the human pseudogene contains two point mutations which result in a frame shift and a premature stop codon [148, 149]. The gene was inactivated probably 28 million years ago due to the threat of an infectious agent, for instance a virus, to produce antibodies against the α -gal epitope or a similar structure present on the infectious agent [148]. The putative biological role of the α -gal epitope is in cell-cell or cell-matrix interactions [148].

1.2.3 Carbohydrate specific antibodies

Antibodies against carbohydrate antigens are crucial to study bacteria, tumors, blood groups and cell cell adhesion interactions. Moreover they can be used to analyse viral, hormone and toxin receptors as well as to analyse the glycosylation of recombinant proteins.

The first evidence that carbohydrates were antigenic arose from the discovery that the human blood group AB0 antigens were glycans and that antibodies against these structures inhibited the transfer of blood from an improper donor.

However, antibodies specific for carbohydrate antigens are more difficult to develop because of the T cell-independent response to carbohydrates. This can result in the production of low affinity IgM antibodies [150]. The low affinity of antibodies specific for glycans is consistent with the general observation, that carbohydrate-protein interactions are relatively weak (micromolar range), compared to protein-protein interactions [151]. Prominent examples for carbohydrate specific antibodies with low affinities are naturally occurring antibodies directed against carbohydrate tumor antigens [152, 153].

Carbohydrate-antibody interactions with low affinity are difficult to analyse and this analysis can be additionally hampered by the flexibility of the glycans [154].

However, carbohydrates attached to a protein surface and/or the continuous stimulation by carbohydrate antigens can induce the production of high affinity antibodies [150, 155].

Also repetitive glycan elements of bacterial lipopolysaccharides can induce the production of such antibodies [156]. Antibodies with high affinities allow insights into the recognition of glycans by antibodies and some crystal structures are available of antibodies in complex with their carbohydrate antigens. For instance interactions of HIV glycans with broadly neutralizing antibodies, like 2G12, PGT127 and PGT128 or the interaction of Lewis X with a Lewis X specific Fab (fragment of antigen binding) [151, 157-159]. The HIV neutralizing antibody 2G12 reflects a special case due to its characteristic domain swapped structure, which provides an extended surface for multivalent interaction with a conserved cluster of oligomannose type glycans on the surface of gp (envelope glycoprotein)120 [151].

Over the last years it could be shown that antibodies specific for CCDs have an extraordinary high affinity. Analysis of polyclonal human IgE antibodies specific for CCDs revealed the outstanding high affinity if both, α -1,3-core fucose and additional β -1,2 xylose were present on the same glycan [160].

1.3 Objective

The diagnosis of Hymenoptera venom allergy can still be hampered by double-positive test results provoked by CCDs or protein-based cross reactivity. To circumvent these problems a

set of Hymenoptera venom allergens should be produced recombinantly, devoid of CCDs. This set should be used to evaluate the benefit for diagnosis in Hymenoptera venom allergy. Molecular tools offering the opportunity to dissect xylose and/or fucose specific IgE antibodies in an epitope resolved diagnosis are not yet available. Therefore a set of glyco-engineered insect cell lines with various abilities in the formation of CCDs should be established by the stable transfection of insect cells with different glycosyltransferases. These cell lines allow the production of scaffold proteins with variant CCD composition. By the use of these proteins IgE reactivity profiles of pollen and Hymenoptera venom allergic patients with regard to the different glycotopes should be revealed and analysed.

To obtain first insights into the recognition of carbohydrates by proteins, the honeybee α -1,3-core fucosyltransferase and human fucosyltransferase 8 should be expressed in insect cells. Subsequently these enzymes will allow STD NMR based analyses to elucidate functional mechanisms and structural information.

To gain further information into recognition of carbohydrates by proteins the before mentioned analysis should be completed by the use of CCD specific antibodies. These antibodies are difficult to generate, therefore combinatorial approaches will be used to address this problem. Hence, immune libraries should be established from HRP immunised rabbits, allowing the selection of CCD specific phages. The genetic information of the obtained CCD specific phages can be converted into different antibody formats, allowing structural as well as functional analysis.

2. Material and Methods

2.1 Formation of the immunogenic α -1,3 fucose epitope: elucidation of substrate specificity and enzyme mechanism of core fucosyltransferase A

2.1.1 In vitro fucosylation

For *in vitro* fucosylation 96 well microtiter plates (Greiner, Frickenhausen, Germany) were coated with recombinant honeybee venom allergen Api m 2 (20 mg/mL) devoid of detectable α -1,3-core fucosylation at 4 °C overnight and blocked with 40 mg/mL milk powder in PBS. Thereafter, 2 mg of sFucTA in PBS with a final concentration of 1 mM GDP-fucose were incubated in a final volume of 50 μ L for 2 h at room temperature. After washing 4 times with PBS α -1,3-core fucosylated Api m 2 was detected using anti-HRP antiserum as primary antibody and alkaline phosphataseconjugated anti-rabbit IgG as secondary antibody. After washing 4 times with PBS 50 μ L of substrate solution (5 mg/mL 4-nitrophenylphosphate, AppliChem, Darmstadt, Germany) per well were added. The plates were read at 405 nm.

2.1.2 Preparation of asialo complex type N-glcans

Asialo N-glycans were isolated from bovine and porcine fibrinogen (Sigma) as described previously [161] with minor modifications. Briefly, 5 g of fibrinogen was denatured in 40 mL 8 M guanidinium hydrochloride in 200 mM Tris-HCl, pH 8.3, and 1.1 g of dithiothreitol (Fluka) was added. After 1 h incubation at RT, 5.1 g of iodoacetamide (Sigma) was added followed by 0.5 h incubation at RT. The alkylated glycoprotein was dialyzed in an MWCO 10,000 Da tubing (Sigma) against 3x10 L ultrapure water (SGWater, 18 mS), centrifuged to remove precipitated protein and freeze dried. The retentate was dissolved in 12 mL 8 M guanidinium hydrochloride and diluted by adding 80 mL 200 mM TriseHCl, pH 8.3. The pH of the fibrinogen solution was adjusted to 7.6 by adding 1 M HCl and the protein was digested by adding 50 mg of trypsin (Sigma) and incubating at 37 °C for 24 h. Afterwards, the digest was dialyzed in an MWCO 1000 Da tubing (SpectrumLabs) against 3x10 L ultrapure water, centrifuged at 6000 xg to remove precipitated protein and freeze dried. The glycopeptide mixture was digested with PNGase F (Roche) by dissolving into 25 mL of 50 mM ammonium acetate buffer, pH 7.5, containing 0.05% sodium azide, and the pH was adjusted by adding 1 M ammoniumhydroxide. 10 U (10 mL) PNGase F was added and the reaction was allowed to proceed for 24 h at 37 °C. A second portion of 10 U PNGase F was added and the incubation was continued for further 48 h. Desialylation was performed by adjusting the pH to 5.0 by adding 1 M acetic acid followed by addition of 2 U sialidase from *Clostridium perfringens* (Roche) and incubation for 48 h at 37 °C. The digest was freeze dried and the

retentate was dissolved into 6 mL of ultrapure water. Precipitated protein was removed by centrifugation at 6000 xg and the supernatant was chromatographed in two equal parts of a mixed bed ion exchange column (3x30 cm each; top: AG50W-X2 (Biorad), H⁺ form; bottom AG1-X2 (Biorad), acetate form). Asialo Nglycan- containing fractions were identified by ESI-TOF MS analysis, pooled and freeze dried.

2.1.3 Preparation of asialo agalacto complex type N-glycans

For degalactosylation of the asialo N-glycan, 10 mg asialo N-glycan were dissolved in 1 mL of 50 mM Bis Trise HCl buffer, pH 7.2, containing 100 mM sodium chloride, 5 mM magnesium chloride, 0.05% sodium azide. 1000 U (1 mg) β -galactosidase from *E. coli* overproducer (Sigma), dissolved in 100 μ L of the same buffer were added. The reaction was allowed to proceed for 48 h at 37 °C. At completion of the reaction as verified by ¹H NMR, galactosidase was separated from the solution by ultrafiltration (MWCO 50,000) and the filtrate was dialyzed against ultrapure water. The freeze dried oligosaccharide was purified by porous graphitised carbon (PGC) HPLC (Thermo Fisher, Hypercarb 150x4.6 mm; particle size 3 mm), flow rate 0.8 mL/min, eluent A: ultrapure water; eluent B: acetonitrile; gradient (share of eluent B): 0 min: 0%; 10 min: 2%; 22 min: 9%; 75 min: 17%; 95 min: 40%; 105-115 min: 100%.

2.1.4 Preparation of 1- β -N-acetyl asialo agalacto complex type N-glycans

1- β -N-acetyl oligosaccharides were synthesised as described previously [162]. Briefly, 1-5 mg of reducing oligosaccharide were dissolved into 500 μ L of saturated ammoniumbicarbonate and incubated at 50 °C for 72 h. Solid ammonium bicarbonate was added several times during incubation to maintain saturation of the solution. After the reaction had finished, ammonium bicarbonate was removed by repeated freeze-drying cycles. The glycosyl amine was dissolved into 200 μ L of saturated sodium bicarbonate solution on ice and 10 μ L of acetic anhydride were added. The reaction was allowed to proceed for 10 min on ice. Then, another 10 μ L of acetic anhydride were added and the solution was incubated at room temperature for 1 h. After dialysis against ultrapure water and freeze drying, the reaction product was subjected to PGC HPLC as described above. The reaction yielded 60-80% 1- β -N-acetyl oligosaccharide as determined by PGC HPLC (UV detection, 215 nm).

2.1.5 Immobilisation of FucTA

All SPR experiments were performed at a Biacore T100 (GE Helthcare). FucTA was immobilised using the standard amide coupling method: The SPR chip surface (coated with

carboxymethylated dextrane, CM5 (GE Helthcare)) was activated by injecting a solution containing 50 mM of N-hydroxysuccinimide and 50 mM of 1-ethyl-3-(3-dimethylaminopropyl)carbodiimide at a flow rate of 10 μ L/min for 15 min on both flow cells. Subsequently, FucTA (30 μ g/mL in 25 mM BisTris/10 mM sodium acetate buffer, pH 6.0) was injected into one flowcell at a flow rate of 10 μ L/min for 30 min yielding 4000-6000 RU (70-100 fmol) immobilised protein. Finally, unreacted carboxy functions in both flow cells were capped by injecting 1 M ethanolamine for 7 min at a flow rate of 10 μ L/min. We found immobilised FucTA to be stable for a couple of weeks.

2.1.6 SPR affinity assays for ligands of FucTA

Sterile filtered 50 mM BisTris, pH 6.7, containing 100 mM sodium chloride and 5 mM magnesium chloride was used as buffer system throughout the experiments. All ligand samples were injected for 1 min (contact time) followed by 3 min injection of buffer (dissociation time) at a flow rate of 30 μ L/min into both flow cells. In order to determine thermodynamic binding constants, each ligand concentration was assayed twice. Donor substrate and related ligands (GDP-Fuc (Jennewein Biotechnology), GDP (Sigma), guanosine (Fluka)) were dissolved in buffer and diluted to the indicated concentrations (typically 0.25-500 mM). For acceptor substrates 1a and 2a, concentrations between 0.5 mM and 10 mM were employed. β -N-Asparaginyll chitobiose (prepared as described [163], was analysed in concentrations of 2 mM and 10 mM and α -methylfucoside in concentrations of 10 mM and 100 mM. The sensorgrams with the highest ligand concentrations possible were recorded and no SPR response could be detected. Therefore, no further experiments were conducted.

2.1.7 STD NMR experiments

STD NMR spectra were obtained at 300 K using a Bruker Avance 700 MHz NMR spectrometer equipped with a TXI triple resonance cryoprobe head incorporating gradients in the z-axis. Samples (150 μ L in 3 mm sample tubes) contained 10 mM protein and 0.1-1.5 mM ligand. Deuterium oxide buffered with 50 mM BisTris- d_{19} (Euroisotope Laboratories), pH 6.7 and containing 100 mM sodium chloride and 5 mM magnesium chloride was used as solvent. Data was acquired using a Bruker standard sequence (stdiffesgp.3) incorporating an excitation sculpting sequence with a 180° soft pulse of 8 ms duration for selective suppression of the HDO resonance. On resonance irradiation was applied at -0.9 ppm or at 0 ppm and off resonance irradiation at 40 ppm. Saturation was achieved by a cascade of 40 Gaussian pulses with duration of 50 ms (field strength 120 Hz or 100 Hz) to give a total saturation time of 2 s. STD spectra and reference spectra were

acquired with 32,768 data points and a total of 4048 transients. FIDs were multiplied with an exponential function (line broadening 3) before Fourier transformation. All ligands were assigned using ^1H - ^1H total correlation and ^1H - ^{13}C heteronuclear single quantum correlation spectra. To determine the size of STD effects, resonances in the STD spectrum were integrated with respect to the reference spectrum. Therefore, an STD effect of 100% results if the resonances in both spectra show the same intensity. For the competition experiment, GDP was added in concentrations of 130 mM, 450 mM, 740 mM, 1.0 mM, 1.4 mM, 1.7 mM and 2.1 mM to a sample containing 10 mM FucTA and 100 mM GDP-Fuc. STD effects of GDP-Fuc and GDP resonances were multiplied with the excess of the respective ligand over FucTA to obtain the STD amplification factor.

2.1.7 Enzyme kinetic studies by progress curve analysis

For analysis of enzyme kinetics of FucTA, samples were prepared as described above. They contained 1.5 mM FucTA, 10 U alkaline phosphatase, sequencing grade, from calf intestine (Roche) and 1.0 mM heptasaccharide 1a or 1.6 mM octasaccharide 2a, respectively. Spectra were recorded at 300 K. Prior to adding donor substrate, a 1D proton spectrum employing an excitation sculpting sequence as was acquired with 32 transients (2 min experiment duration). Resonances from this spectrum yielded the intensities for $t = 0$. Thereafter, GDP-Fuc was added to the sample to give a concentration of 2 mM and the sample solution was mixed quickly. The sample was then reinserted into the magnet and after applying a short shimming routine, ^1H NMR spectra using identical parameters as mentioned above were recorded at different time points for 18 h. FIDs were multiplied with an exponential function (line broadening 0.5) prior to Fourier transformation. All well dispersed resonances were integrated with respect to the sum integral of the H-10 resonances of GDP and GDP-Fuc, which corresponds to a concentration of 2 mM. From the integrals, substrate and product concentrations were calculated at each time point.

2.1.8 Other methods

SDS-PAGE, Western blotting and molecular biology standard procedures such as PCR, DNA-restriction, ligation, transformation, and plasmid-isolation were performed according to established protocols [164].

2.2 Donor substrate binding and enzymatic mechanism of human core α -1,6 fucosyltransferase (FUT8)

2.2.1 Cloning, recombinant expression, and purification of human fucosyltransferase 8

Total RNA was isolated from HEK293 (human embryonic kidney) cells using peqGold TriFast (PepLab Biotechnologie, Erlangen, Germany). SuperScript III RT (Invitrogen, Karlsruhe, Germany) and the genespecific primer 5'-GATCGCGGCCGCTTATTTCTCAGCCTCAG GATATGTGGG-3' was used to synthesise cDNA of FUT8 from the isolated total RNA. The FUT8 coding region (Arg68 to Lys575) was amplified from cDNA with Pfu DNA polymerase (Fermentas, St. Leon-Rot, Germany) using the primers 5'-GATCTCTAGAGGGAT CGAGGGAAGGCGGATACCAGAAGGCCCTATTG-3' adding an XbaI restriction site and 5'-GATCGCGGCCGCTTATTTCTCAGCCTCAGGATATGTGGG-3' adding a NotI restriction site. The PCR product was subcloned via XbaI and NotI into the digested baculovirus transfer vector pACGP67B (BD Pharmingen, Heidelberg, Germany) which was modified by addition of an N-terminal 10 fold His-tag, a V5 epitope, a factor Xa cleavage site as well as an XbaI restriction site. The sequence of selected subclones was verified by sequencing. *Spodoptera frugiperda* insect cells (Sf9) (Invitrogen) were grown at 27 °C in serum-free medium (Express Five SFM; Lonza, Verviers, Belgium containing 10 µg/mL gentamycin; Invitrogen). Cell density was determined by hemocytometer counts, cell viability was evaluated by staining with Trypan Blue. Recombinant baculovirus was generated by cotransfection of Sf9 cells with BaculoGold bright DNA (BD Pharmingen, Heidelberg, Germany) and the baculovirus transfer vector pACGP67B containing FUT8. High titer stocks were produced by three rounds of virus amplification and optimal MOI for protein expression was determined empirically by infection of Sf9 cells in 100 mL suspension flasks (1.5×10^6 cells/mL in 20 mL suspension culture) with serial dilutions of high titer virus stock. The high titer stock of recombinant baculovirus was used to infect 400 mL suspension cultures of Sf9 cells (1.5×10^6 cells/mL) in 2000 mL flasks. For protein production the cells were incubated at 27 °C and 110 rpm for 72 h. The supernatant of baculovirus-infected cells was collected, the buffer exchanged to PBS, pH 8 applying the QuixStand Benchtop System (GE Healthcare, Munich, Germany), and applied to a nickelchelating affinity matrix (NTA-agarose, Qiagen, Hilden, Germany). The column was washed with binding buffer (50 mM sodium phosphate, pH 8, 500 mM NaCl) and pre-eluted with NTA binding buffer containing 20 mM imidazole. The recombinant protein was eluted from the matrix using NTA-binding buffer containing 300 mM imidazole. Purification was confirmed by SDS-PAGE. For immunoblot procedures purified recombinant FUT8 was separated by SDS-PAGE and immobilised onto nitrocellulose membranes. Anti-V5 epitope mAb (Invitrogen) was applied

according to the recommendations of the manufacturer and bound antibodies visualised via anti-mouse IgG conjugated to alkaline phosphatase (Sigma, Taufkirchen, Germany) and nitrotertrazolium blue chloride/5-bromo-4-chloro-3-indoyl phosphate according to the recommendations of the manufacturer.

2.2.2 Preparation of 1- β -N-acetyl asialo agalacto complex type heptasaccharide

Asialo N-glycans were isolated from bovine fibrinogen (Sigma) as described previously with minor modifications [138, 161]. Consequently, the asialo N-glycans were degalactosylated and 1- β -N-acetylated as described [138, 162].

2.2.3 NMR experiments

STD NMR spectra of the donor substrate and enzyme kinetic analysis were obtained using a Bruker Avance 700 MHz NMR spectrometer equipped with a TXI triple resonance probe with z-gradients.

2.2.4 Preparation of NMR samples

After purification of the enzyme, the samples in 50 mM PBS buffer pH 7.0 were exchanged to deuterium oxide buffered with 50 mM Mes- d_{13} (Cambridge Isotope Laboratories), pH 7.0 and concentrated via centrifugal filtering using Amicon Ultra filter devices (Millipore, MWCO 10,000 Da). Protein concentration was determined by absorption at 280 nm using a nanodrop UV-spectrometer. All NMR samples were prepared in 160 μ L of buffer solution and measured using 3 mm NMR tubes.

2.2.5 STD NMR experiments

Spectra were obtained at 285 K. Samples contained 10 μ M protein and 1.0 mM ligand. Data was acquired using a Bruker standard sequence (stdiffesgp) incorporating an excitation sculpting sequence with a 180° soft pulse of 2–8 ms duration for selective suppression of the HDO resonance. On resonance irradiation was applied at -0.9 ppm and off resonance irradiation at 40 ppm. Saturation was achieved by a cascade of 40 Gaussian pulses with duration of 50 ms (field strength 120 Hz) to give a total saturation time of 2 s. STD spectra and reference spectra were acquired with 32,768 data points and a total of 4048 transients. FIDs were multiplied with an exponential function (line broadening 3) before Fourier transformation. To determine the size of STD effects, resonances in the STD spectrum were integrated with respect to the reference spectrum. Therefore, a STD effect of 100% results if the resonances in both spectra show the same intensity. The resulting relative STD percentages were subsequently corrected by their T_1 relaxation constants as determined by

means of inversion recovery experiments [165].

2.2.6 Enzyme kinetic studies by progress curve analysis

For analysis of enzyme kinetics of FUT8, samples contained 2.0 μ M FUT8, 10 U alkaline phosphatase, sequencing grade, from calf intestine (Roche) and 0.9 mM GlcNAc β 1-2Man α 1-3(GlcNAc β 1-2Man α 1-6)Man β 1-4GlcNAc β 1-4GlcNAc β 1-N-Ac(heptasaccharide), respectively. BSA (Fluka, >98%) was added to give a concentration of 1.0 mg/mL in the sample to prevent adhesion and subsequent degeneration of FUT8 to the glass surface of the NMR tube at such low concentrations. Spectra were recorded at 310 K. Prior to adding donor substrate, a 1D proton spectrum employing an excitation sculpting sequence as described above (zgesgp) was acquired with 64 transients (4 min experiment duration). Resonances from this spectrum yielded the intensities for $t=0$. Thereafter, GDP-Fuc was added to the sample to give a concentration of 3.0 mM and the sample solution was mixed quickly. The sample was then reinserted into the magnet and after applying a short shimming routine, ^1H NMR spectra using identical parameters as mentioned above were recorded at different time points for 30 min. FIDs were multiplied with an exponential function (line broadening 0.5) prior to Fourier transformation. All well dispersed resonances were integrated with respect to the sum integral of the H-1' resonances of GDP and GDP-Fuc, which corresponds to a concentration of 3.0 mM. From the integrals, substrate and product concentrations were calculated at each time point.

2.2.7 SPR affinity studies

All SPR experiments were performed at a Biacore T100 (GE Healthcare). FUT8 was immobilised using the standard amide coupling method: The SPR chip surface (coated with carboxymethylated dextrane, CM5 (GE Healthcare)) was activated by injecting a solution containing 50 mM of N-hydroxysuccinimide and 50 mM of 1-ethyl-3-(3-dimethylaminopropyl) carbodiimide at a flow rate of 10 μ L/min for 15 min on both flow cells. Subsequently, FUT8 (30 μ g/mL in 25 mM PBS/25 mM sodium acetate buffer, pH 5.5) was injected into one flow cell at a flow rate of 10 μ L/min for 60 s yielding 7300 RU (120 fmol) immobilised protein. Finally, unreacted carboxy functions in both flow cells were capped by injecting 1 M ethanolamine for 5 min at a flow rate of 10 μ L/min. We found immobilised FUT8 to be stable for one day at 25 $^{\circ}\text{C}$. Sterile filtered 50 mM Mes-NaOH, pH 7.0, was used as buffer system throughout the experiments. All ligand samples were injected for 40 s (contact time) followed by 1 min injection of buffer (dissociation time) at a flow rate of 30 μ L/min into both flow cells. In order to determine thermodynamic binding constants, each ligand concentration was assayed twice. Donor substrate and related ligands (GDP-Fuc (Jennewein Biotechnology),

GDP (Sigma), GMP (Sigma) and guanosine (Fluka)) were dissolved in buffer and diluted to the indicated concentrations (typically 0.25–500 μ M).

2.2.8 Molecular modelling

All simulations were performed using the Desmond Molecular Dynamics System, version 2.2, D 2009 (E. Shaw Research, New York, NY) as implemented in Maestro-Desmond Interoperability Tools, version 2.2 2009 (Schrödinger, New York, NY) [166]. MD simulations are based on the crystal structure of human FUT8 [PDB ID: 2DE0] [167]. The donor binding site was determined by using the structure of cePOFUT in complex with GDP-Fuc [PDB ID: 3ZY6]. All hydrogen atoms were added and ionizable side chains as well as the C- and N-terminus were converted into their default ionisation state and the system was minimised using a steepest descend algorithm. We identified peptide segments in both proteins that possess high structural similarity. In the first step, the proteins were aligned along backbones of the beta sheets from Lys302 to Ser308 (cePOFUT) and from Lys402 to Thr408 (FUT8) in order to find further regions with high structural similarity. Four regions were identified to have high structural similarity. In a second step, the segments Arg40-Leu58, Pro233-Arg240, Leu348-Asn352 and Val354-Gly369 of cePOFUT were aligned with Gly219-Thr237, Pro358-Arg365, Phe462-Thr466 and Ser468-His483 of FUT8, respectively. Further, GDP-Fuc from the cePOFUT structure was positioned at the putative binding site in the FUT8 crystal structure. After alignment of the side chain conformation of Arg365 of FUT8 to that of Arg240 in cePOFUT, the complex of FUT8 and GDP-Fuc was minimised. The system was immersed into an orthorhombic water box containing 0.2 M sodium chloride and 16,847 solvent molecules in total. The box dimensions were calculated with the buffer method in such a way that the minimal distance between the periodic images of the box was 10 Å in each dimension and the box volume was 631,032 Å³. The total number of atoms during our MD simulations was 59,073. For the MD simulation, the system was simulated at 310 K and at a pressure of 1.01325 bar over 1.5 ns with recording intervals of 0.1 ps for energy and 0.5 ps for the trajectory. We used the OPLS 2005 Force Field [168] in combination with the SPC model for water [169]. The method employed for electrostatic interactions was the Particle mesh Ewald (PME) with a real space cut-off of 9.0 Å [170]. The system was coupled to a Nose–Hoover–Chain thermostat with a relaxation time of 1.0 ps and to an isotropic Martyna–Tobias–Klein barostat with a relaxation time of 2.0 ps [171, 172]. The integration time step was set to 2.0 fs. Data analysis was conducted using Desmond Simulation Event Analysis, and all molecular images were made with PyMol (The PyMOL Molecular Graphics System, Schrödinger, LLC, 2011).

2.2.9 Other methods

Molecular biology standard procedures such as PCR, DNA restriction, ligation, transformation, and plasmid-isolation were performed according to established protocols.

2.3 Donor assists acceptor binding and catalysis of human α -1,6 fucosyltransferase

2.3.1 Established methods

Human FUT8 was cloned from HEK293 cells and expressed as soluble enzyme lacking the transmembrane region as previously described in 2.2.1 [173]. Asialo N-glycans were isolated from bovine fibrinogen (Sigma) as described in 2.1.2 [138]. Consequently, the asialo N-glycans were degalactosylated and 1- β -N-acetylated as described in 2.1.3 [138].

2.3.2 STD NMR experiments

STD NMR spectra of the acceptor substrate with FUT8 were obtained using a Bruker Avance 700 MHz NMR spectrometer equipped with a TXI triple resonance probe with z-gradients. Samples contained 10 μ M protein and 1.0 mM ligand. Data was acquired using a Bruker standard sequence (stdiffesgp) incorporating an excitation sculpting sequence with a 180° soft pulse of 8 ms duration for selective suppression of the HDO resonance. On resonance irradiation was applied at 0.2 ppm and off resonance irradiation at 40 ppm. Saturation was achieved by a cascade of 40 Gaussian pulses with duration of 50 ms (field strength 120 Hz) to give a total saturation time of 2 s. STD spectra and reference spectra were acquired with 32,768 data points and a total of 4048 transients. FIDs were multiplied with an exponential function (line broadening 3) before Fourier transformation. STD spectra from a sample without enzyme were acquired to determine artifact STD effects. This artifact spectrum was subtracted from the actual STD spectrum to give artifact adjusted STD effects. The heptasaccharide was assigned using ^1H - ^1H total correlation (TOCSY) and ^1H - ^{13}C heteronuclear single quantum correlation spectra (HSQC) [138].

To determine the size of STD effects, resonances in the artifact adjusted STD spectrum were integrated with respect to the reference spectrum. Therefore, an absolute STD effect of 100% results if the resonances in both spectra show the same intensity. Artifacts are between 0.2 and 0.6%.

2.3.3 SPR affinity studies

All SPR experiments were performed on a Biacore T100 (GE Healthcare). FUT8 was immobilised as described in 2.2.7 yielding 7300 RU (120 fmol) immobilised protein. S-20

Sterile filtered 50 mM Mes-NaOH, pH 7.0, was used as buffer system throughout the experiments. Ligand samples were injected for 40 seconds (contact time) followed by 1 minute injection of buffer (dissociation time) at a flow rate of 30 $\mu\text{L min}^{-1}$ into both flow cells. The heptasaccharide was dissolved in buffer and diluted to the final concentrations (0.25–1000 μM).

2.3.4 Molecular modelling

All simulations were performed using the Desmond Molecular Dynamics System, version 2.2, D 2009 (E. Shaw Research, New York, NY) as implemented in Maestro-Desmond Interoperability Tools, version 2.2 2009 (Schrödinger, New York, NY) [166]. MD simulations are based on the model the complex of FUT8 and GDP-Fuc [173]. The system was immersed into an orthorhombic water box containing 0.2 M sodium chloride and 16,847 solvent molecules in total. The box dimensions were calculated with the buffer method in such a way that the minimal distance between the periodic images of the box was 10 Å in each dimension and the box volume was 713,764 Å³ [173]. The total number of atoms during our MD simulations was 66,429. For the MD simulation, the system was simulated at 310 K and at a pressure of 1.01325 bar over 1.5 ns with recording intervals of 0.1 ps for energy and 0.5 ps for the trajectory. We used the OPLS 2005 Force Field4 in combination with the SPC model for water [169]. The method employed for electrostatic interactions was the Particle mesh Ewald (PME) with a real space cut-off of 9.0 Å [170]. The system was coupled to a Nose-Hoover-Chain thermostat with a relaxation time of 1.0 ps and to an isotropic Martyna-Tobias-Klein barostat with a relaxation time of 2.0 ps [171, 172]. The integration time step was set to 2.0 fs. Data analysis was conducted using Desmond Simulation Event Analysis, and all molecular images were made with PyMol (The PyMOL Molecular Graphics S-21 System, Schrödinger, LLC, 2011).

2.4 Component resolution reveals additional major allergens in patients with bee venom allergy

2.4.1 Patients

Sera from 184 patients with anaphylactic reactions to either honeybee (n = 144) or yellow jacket (n = 40) stings (as identified by the patient) and 40 HBV-nonallergic control subjects were analysed. Diagnosis of HBV allergy was based on a combination of the patient's history of an anaphylactic sting reaction, a positive skin test result, and positive IgE levels to HBV (ImmunoCAP i1), as recently described [174]. As defined by the inclusion criteria, all patients with HBV allergy displayed IgE to HBV (>0.35 kUA/L), and 90 (62.5%) also had positive test

results to YJV (ImmunoCAP i3). Diagnosis of YJV allergy was based on a combination of the patient's history of yellow jacket sting anaphylaxis, a positive skin test result, and positive IgE results for YJV (ImmunoCAP i3) and negative results for HBV (ImmunoCAP i1). The HBV-nonallergic control subjects had all experienced a bee sting, although without an anaphylactic or large local reaction. All patients and control subjects had provided informed written consent, and the study was approved by the local ethics committee.

2.4.2 Allergens and IgE antibody measurements

rApi m 2, rApi m 3, rApi m 5, and rApi m 10 were expressed as secreted full-length proteins by *Spodoptera frugiperda* (Sf9) insect cells, as recently described [69, 71]. In brief, Sf9 cells were grown in suspension at 27 °C in serum-free medium (Lonza, Verviers, Belgium) containing 10 µg/mL gentamicin (Invitrogen, Carlsbad, Calif) to a density of 1.5×10^6 cells/mL and then infected with a high-titer stock of recombinant baculovirus containing the allergen gene to be expressed. For protein production, the cells were incubated at 27 °C and 110 rpm for 72 h. The recombinant proteins were then purified from culture medium by using a nickel-chelating affinity matrix (NTA-agarose; Qiagen, Hilden, Germany). The purity of each recombinant protein was assessed by using SDS-PAGE. Api m 4 was purified from HBV by means of sequential steps of ion exchange and size exclusion chromatography.

2.4.3 Immunoreactivity of patient sera

Serum IgE reactivity was analysed on a CAP-FEIA platform (Phadia 250) using commercially available ImmunoCAP tests for HBV (ImmunoCAP i1), YJV (ImmunoCAP i3), rApi m 1 (ImmunoCAP i208), rVes v 5 (ImmunoCAP i209), rVes v 1 (ImmunoCAP i211), and the CCD marker MUXF3 (ImmunoCAP i213) and experimental ImmunoCAP tests for rApi m 2, rApi m 3, nApi m 4, rApi m 5, and rApi m 10. Selected sera were also analysed for IgE reactivity to major royal jelly protein 8 and 9 (Api m 11.0101 and Api m 11.0201) and 3 additional HBV proteins (not been assigned as allergens) by using ELISA. Allergen specific IgG₄ reactivity to rApi m 1, nApi m 4, rApi m 3, and rApi m 10 in selected sera was analysed by using a Phadia 250 instrument and 1:100 or 1:20 serum dilutions.

2.4.4 CAP-FEIA inhibition

Inhibition of allergen specific IgE (sIgE) binding to HBV (ImmunoCAP i1) by nApi m 1 (Latoxan, Valence, France), rApi m 3, or rApi m 10 was performed by means of preincubation of patient sera and inhibitors at the indicated concentrations for 2 h at room temperature before the CAP-FEIA analysis. Alternatively, sera were preincubated with a

crude HBV preparation (Latoxan) or solubilised freeze-dried therapeutic HBV preparations (ie, not absorbed to alum) at 300 mg/mL.

2.5 *Polistes* species venom is devoid of carbohydrate-based cross-reactivity and allows interference-free diagnostics

2.5.1 Analysis of glycosylation pattern of Hymenoptera venoms

For this analysis AlaBlots (Siemens Healthcare Diagnostics, Los Angeles, Calif) with the venoms of *Apis mellifera*, *Vespula vulgaris* and *Polistes* species were applied and analysed using *Galanthus nivalis* agglutinin (GNA) and rabbit anti-horseradish peroxidase (HRP) serum. GNA-reactivity suggest the presence of N-glycosylated proteins, whereas HRP-reactivity is a hint for the presence of CCDs. AlaBlot-analysis was performed according Western blot in 2.1.8.

2.5.2 Other methods

SDS-PAGE, Western blotting and ELISA were performed according to established protocols [164].

2.6 Fine specificity of IgE carbohydrate reactivity dissected by establishing xenobiotic epitopes with glycoengineered cell lines

2.6.1 Patient sera

Three groups of sera were selected at random from the institutional serum bank: (i) Sera with a positive sIgE to honeybee and/or vespid venom ($i1$ and/or $i3 < 0.35$ kU/L) ($n = 30$); (ii) Sera with a positive sIgE to pollen (pollen IgE < 0.35 kU/L) ($n = 30$); (iii) Sera of non-atopic patients (sIgE < 100 kU/L) ($n = 30$). All patients had given their informed written consent to draw an additional serum sample and all experiments applying human sera were approved by the local ethics committee.

2.6.2 Cloning of cDNA

Total RNA was isolated from leaves of *Glycin max* using peqGold Trifast™ (Peqlab Biotechnologie, Erlangen, Germany). *Accuscript*™ High Fidelity Reverse Transcriptase (Agilent Technologies Inc., Santa Clara, USA) was used to synthesise cDNA from the isolated total RNA. Ribolock ribonuclease inhibitor (Fermentas, St.-Leon-Rot, Germany) was added to the 20 µl standard reaction mix containing 5 µg leave-RNA. Reverse transcription was performed at 42 °C for 60 min. First strand cDNA was used as template for PCR

amplification of DNA sequences. Due to high GC-content the aminoterminal part of the β -1,2 xylosyltransferase to amino acid 240 was chemical synthesized (Geneart, Life Technologies, Regensburg) including an 17 amino acid long overlapping region, on the other hand the carboxyterminal part from amino acid 240 to 503 was amplified from cDNA by using the primers 5'-GTTTCTTCTAGAGTGACTGG-3' and 5'-GACATAATGAAAAGCCTTGGATGTCGCTCGAGGATC-3. Using PCR approaches both parts were combined using Primer 5'-GATCAAGCTTATGAACCGTCGTACCACC-3' and 5'-GACATAATGAAAAGCCTTGGATGTCGCTCGAGGATC-3'. Full-length xylosyltransferase was cloned into the insect cell expression vector pIB/V5-His (Invitrogen, Karlsruhe, Germany) via HindIII and XhoI restriction enzyme sites and was fused with a C-terminal V5 epitope and a 6 fold His-tag. The ligated DNA was transformed into *E. coli* XL1Blue by electroporation and selected on ampicillin agar plates.

Utilizing the oligonucleotides 5'-GCCCCACATGGCCCAGGGCTG-3' and 5'-CCTTGAA GTGTCTGATCCT-3', full-length human α -2HS-glycoprotein was amplified from cDNA of human PBMCs. The DNA was isolated from 1% agarose gel using the peqGOLD Gel Extraktion kit (Peqlab). Subcloning for sequencing was done using the Zero Blunt Topo PCR Cloning Kit (Invitrogen) with the pCR-Blunt II-Topo vector. The ligated DNA was transformed into the *E. coli* XL1Blue strain by electroporation (2 mm cuvettes, Easy-Ject+, Eurogentec, Seraing, Belgium) and selected on ampicillin agar plates.

After sequencing of selected cDNA subclones and verification of the sequence, the clones were used for secondary amplification of the coding region using Pfu DNA polymerase in two consecutive PCR reactions adding a 10 fold His-tag and V5 epitope. The PCR product was subcloned via BamHI and NotI restriction enzyme sites into baculovirus transfer vector pACGP67B (BD Pharmingen, Heidelberg, Germany).

Full-length fucosyltransferase X was amplified from *A. mellifera* venom-gland as described in [71].

2.6.3 Recombinant baculovirus production

Spodoptera frugiperda cells (Sf9) (Invitrogen, Karlsruhe, Germany) were grown at 27 °C in serum-free medium (Express Five SFM; Lonza, Verviers, Belgium containing 10 μ g/mL gentamycin; Invitrogen, Karlsruhe, Germany). Cell density was determined by haemocytometer counts, cell viability was evaluated by staining with Trypan Blue. Recombinant baculovirus was generated by cotransfection of Sf9 cells with BaculoGold bright DNA (BD Pharmingen, Heidelberg, Germany) and the baculovirus transfer vector pACGP67B containing AHSG. High titer stocks were produced by three rounds of virus amplification and optimal MOI for protein expression was determined empirically by infection

of Sf9 cells in 100 mL suspension flasks (1.5×10^6 cells/mL in 20 mL suspension culture) with serial dilutions of high titer virus stock.

2.6.4 Expression in baculovirus-infected insect cells

High titer stocks of recombinant baculovirus was used to infect 400 mL suspension cultures of Sf9, Sf9-FucTX, Sf9-XylIT, HighFive or HighFive-XylIT cells (Invitrogen, Karlsruhe, Germany) (1.5×10^6 cells per mL) in 2000 mL flasks. For protein production the cells were incubated at 27 °C and 110 rpm for 72 h.

2.6.5 Stable transfection of insect cells

For transfection of purified DNA into cells, the reagent Cellfectin II (Invitrogen, Karlsruhe, Germany) was used. Sf9 cells were grown in serum-free medium and selected for stable integration of the recombinant product by addition of 80 µg/mL Blasticidin S (Invivogen) antibiotic to the medium.

2.6.6 Protein purification

The supernatant of baculovirus-infected cells was collected, adjusted to pH 8, centrifuged at 4000 xg for 5 min., and applied to a nickel-chelating affinity matrix (NTA-agarose, Qiagen, Hilden, Germany). The column was washed with binding buffer (50 mM sodium phosphate, pH 7.6, 500 mM NaCl) and pre-eluted with NTA binding buffer containing 20 mM imidazole. The recombinant protein was eluted from the matrix using NTA-binding buffer containing 300 mM imidazole. Purification was confirmed by SDS-PAGE.

2.6.7 Immunoreactivity of patient sera with recombinant proteins

For assessment of specific IgE immunoreactivity of human sera in ELISA, 384 well microtiter plates (Greiner, Frickenhausen, Germany) were coated with purified recombinant proteins (20 µg/mL) at 4 °C overnight and blocked with 40 mg/mL milkpowder in PBS. Thereafter, human sera were diluted 1:2 with PBS and incubated in a final volume of 20 µl for 4 h at room temperature. After washing 4 times with PBS bound IgE were detected with a monoclonal alkaline phosphatase-conjugated anti-human IgE antibody (BD Pharmingen, Heidelberg, Germany) diluted 1:1000. After washing 4 times with PBS 50 µl of substrate solution (5 mg/mL 4-nitrophenylphosphate, AppliChem, Darmstadt, Germany) per well were added. The plates were read at 405 nm. The lower end functional cut-off indicated as lines was calculated as the mean of the negative controls plus 2 SDs. Reactivities only slightly higher than the cut-off were excluded. For ELISA procedures with anti-V5 epitope mAb and anti-HRP antiserum the antibodies were applied according to the recommendations of the

manufacturer and bound antibodies visualised via corresponding secondary antibodies conjugated to alkaline phosphatase as described above.

2.6.8 Other methods

SDS-PAGE, Western blotting, ELISA and molecular biology standard procedures such as PCR, DNA-restriction, ligation, transformation, and plasmid-isolation were performed according to established protocols [164].

2.7 Structural and functional insights into the high affinity recognition of xenobiotic N-glycan core structures by mammalian antibodies

2.7.1 Generation and selection by phage display of rabbit immune repertoires

Rabbit spleen and bone marrow derived mRNA were prepared from the Trizol-solubilised samples after extraction with chloroform and precipitation with ice-cold isopropanol. The cDNA was prepared by using Superscript III reverse transcriptase (Life Technologies) and 5'-CTGCGGTGTTKTAAGTCTCG-3' primer for light chain cDNA and 5'-GCTCCGGGAGGTAGCCTTTG-3' for heavy chain cDNA. The cDNAs of the light chains served as template for the amplification of primary products using the primers 5'-GATTAGCGTCTCCAATGGAGCTCGTGMTGACCCAGACTCCA-3', 5'-GATTAGCGTCTCC AATGGAGCTCGTGMTGACCCAGACTCCA-3', 5'-GATTAGCGTCTCCAATGGAGCTCGT GMTGACCCAGACTCCA-3', 5'-GATTAGCGTCTCCAATGGAGCTCGTGMTGACCCAGAC TCCA-3' and the primer 5'-AGTAGGTGCAACTGGATCACC-3' (back). In a nested PCR approach these products were used as templates to amplify using the same forward primers as above and the primers 5'-GATTAGCGTCTCCTCCCTAGGATCTCCAGCTCG GTCCC-3', 5'-GATTAGCGTCTCCTCCCTTTGATTTCCACATTGGTGCC-3', 5'-GATTAG CGTCTCCTCCCTTTGACSACCACCTCGGTCCC-3' and 5'-GATTAGCGTCTCCTCCCG CCTGTGACGGTCAGCTGGGTCCC-3' in all possible combinations to obtain the final sequence pool containing genetic information of diverse variable light chains. The heavy chain cDNA was the template for a PCR using the forward primers 5'- GATTAGCGTCTCCAATGCAGTCGGTGGAGGAGTCCRGG-3', 5'-GATTAGCGT CTCCAATGCAGTCGGTGAAGGAGTCCGAG-3', 5'-GATTAGCGTCTCCAATGCAGTCGY TGGAGGAGTCCGGG-3' and 5'-GATTAGCGTCTCCAATGCAGSAGCAGCTGRTGGAGT CCGG-3' combined with the back primer 5'-GACTGAYGGAGCCTTAGGTTGC-3'. In a nested PCR approach these products were used as templates to amplify using the same forward primers as above and the primer 5'-GGCACCTGGTCACCYTCTCBTCAGGGAGG AGACGCTAATC-3' to obtain the final pool of variable heavy chain sequences. The PCR

products were introduced into the StarGate[®]-System and the genetic information of variable heavy chains were cloned into the vector pNFuse-IBA-link11, whereas the genetic informations of variable light chains were introduced into the vector pCFuse-IBA1. After sequence analysis both vector systems were used to fuse variable heavy and light chains in another StarGate[®]-reaction using the vector pENTRY-IBA51. The fused sequences were amplified from the vector using the forward primers 5'-GATCGGCCAGCCGGCCATGGCGCAGTCGGTGGAGGAGTCCRGG-3', 5'-GATCGGCCAGCCGGCCATGGCGCAGTCGGTGAAGGAGTCCGAG-3', 5'-GATCGGCCAGCCGGCCATGGCGCAGTCGYTGGAGGAGTCCGGG-3' and 5'-GATCGGCCAGCCGGCCATGGCGCAGSAGCAGCTGRTGGAGTCCGG-3' combined with the back primers 5'-GATCGCGGCCGCTAGGATCTCCAGCTCGGTCCC-3', 5'-GATCGCGGCCGCTTTGATTTCCACATTGGTGCC-3', 5'-GATCGCGGCCGCTTTGACSACCACCTCGGTCCC-3' and 5'-GATCGCGGCCGCGCCTGTGACGGTCAGCTGGGTCCC-3'. These primers allow introducing the sequences into the vector pHen2 by restriction with the enzymes NcoI and NotI. The correctness of the sequences was verified by sequencing and the pHen2-vectors were electroporated into *E. coli* TG1 cells. Sequencing of randomly picked clones confirmed that the library carried members with a different genetic background.

The selection of repertoires was essentially performed according to established protocols [175]. Briefly, immunotubes coated with the CCD-carrying protein and blocked with 20 g/L MPBS were incubated with a total volume of 4 mL of 20 g/L MPBS containing 10^{12} to 10^{13} phages. After incubation, washing, elution of bound phages, reinfection of *E. coli* TG1 and rescue by M13KO7 helper phage, recombinant phages were subjected to the next round of selection. Immunoreactivity of polyclonal or monoclonal phages was assessed in ELISA with anti-M13-horseradish peroxidase conjugate (GE Healthcare) and 2,2-azino-bis(3-ethyl-benzothiazoline-6-sulfonic acid) di-ammonium salt for detection. Expression of soluble single chain formats in *E. coli* was essentially performed as described in the literature.

2.7.2 Conversion and production of human IgE and IgG formats

Recombinant production of IgE and IgG was essentially performed as described recently [175, 176] Oligonucleotides for amplification of the rabbit V_H and V_L provided restriction sites for ligation into the expression vector.

2.7.3 Surface plasmon resonance analysis

The interaction affinity of CCD carrying proteins and IgE has been determined by surface plasmon resonance (SPR) measurements were performed on a Biacore T100 (GE Healthcare). CCD-bearing molecules were immobilised as described in 2.2.7 on a CM5 chip.

HSA coupled on the surface served as reference. Measurements were performed at 20 °C in 0.22 µm filtered PBS buffer. For the kinetic analyses, increasing concentrations of the CCD specific (0-150 µg/mL) antibodies were injected at a flow rate of 25 µl/min. The association phase was monitored for 720 s, the dissociation phase for 600 s. Sensor surfaces were regenerated after each binding cycle by subsequent injections of Tris-HCl pH 11 for 30 s and sodium acetate pH 1 also 30 s. After subtracting reference cell signals, resulting binding data were fitted to a two-state binding model and the dissociation constant at equilibrium K_D was calculated.

2.7.4 Cellular mediator release assays

In vitro degranulation was analysed as described previously [176]. After sensitisation of RBL-SX38 cells with IgE and washing with incomplete Tyrode's buffer, different CCD carrying proteins were added to the wells and incubated for 60 min at 37 °C. As reference, cross-linking was achieved by addition of polyclonal anti-human IgE serum (1 µg/mL from goat, Bethyl). Beta-hexosaminidase release of viable versus lysed cells was assessed with *p*-nitrophenyl N-acetyl-glucosaminide (Sigma Aldrich) as a substrate.

2.7.5 Epitope mapping by STD NMR

Asialo N-glycans were isolated from bovine fibrinogen (Sigma) as described in 2.1.2 [177] with minor modifications. Consequently, the asialo N-glycans were degalactosylated and 1-β-N-acetylated. Enzymatic fucosylation was performed using recombinant human FUT8 and apid core α-1,3 fucosyltransferase as described [138].

Buffer exchange against deuterated PBS and concentrating affinity-purified antibodies to 450 µg/mL of was performed by using AMICON Ultra-4 10K centrifugal filter devices.

Saturation transfer difference (STD) NMR experiments were performed at 298 K on a Bruker 500 MHz spectrometer equipped with a 5 mm inverse triple resonance probe head and a Bruker 700 MHz spectrometer equipped with a 5 mm inverse triple resonance probe head with cryo technology. The PBS NMR buffer contained 137 mM NaCl, 2.7 mM KCl, 10 mM Na₂HPO₄ and 176 mM KH₂PO₄ in D₂O and was adjusted to pH 7.4. The on resonance pulse for antibody saturation was set to 0 Hz (500 MHz) or -500 Hz (700 MHz), respectively, and the off resonance pulse to 28500 Hz (500 MHz) or 28000 Hz (700 MHz). Saturation was achieved by a train of 90° Gaussian-shaped pulses of 50 ms yielding a total saturation time of 2 s with an attenuation of 45 dB (500 MHz) or 40 dB (700 MHz). The spectra were acquired with a spectral width of 8000 Hz, 64k time domain data points and 2 transients using a pseudo-2D Bruker standard pulse sequence (stdiff.3, 500 MHz). A relaxation delay of 4 s was applied. For suppression of protein background a T1ρ-filter was used applying a

field strength of 11.5 kHz and a duration of 15 ms. Each experiment was performed with a total of 1024 scans. STD experiments on serum were performed using a pseudo-2D Bruker standard pulse sequence (stddiffesgp2d) that contained the excitation sculpting sequence for the suppression of residual HDO (700 MHz). The spectra were recorded with a spectral width of 7000 Hz, 32k time domain data points and 2 transients. The FIDs of the on and off resonance spectrum were stored and processed separately. Subtraction of the on and off resonance spectrum resulted in the STD NMR spectrum.

2.7.6 Other methods

SDS-PAGE, Western blotting, ELISA and molecular biology standard procedures such as PCR, DNA-restriction, ligation, transformation, and plasmid-isolation were performed according to established protocols [164].

3. Results

The results presented in this thesis were obtained in collaboration with different members of different research groups as evident from the published and submitted manuscripts listed in the appendix section.

3.1 Formation of the immunogenic α -1,3 fucose epitope: elucidation of substrate specificity and enzyme mechanism of core fucosyltransferase A

A highly acute and severe pathological condition is represented by generalised systemic reactions to Hymenoptera venom that has been recognised as potentially fatal and is mediated by IgE antibodies in venom-allergic patients. Pronounced IgE reactivities directed against cross-reactive carbohydrate determinants (CCDs), present on venom glycoproteins and other more common xenobiotics, like birch pollen, severely hamper diagnosis of the causative agent and therefore its therapy [82, 178-180]. These problems are associated with the presence of a core α -1,3 linked fucosyl residue [113]. Such CCDs however are characteristic not only for Hymenoptera but also for plant derived glycosylated allergens that in addition often carry a β -1,2 xylose residue as a second immunogenic moiety. Interestingly and in addition to a plethora of other glycotopes, helminthes also exhibit both α -1,3 linked fucose and β -1,2 xylose residues resulting in pronounced immune reactions [107]. Although immunomodulation and adjuvant effects have been reported, the impact of these glycotopes for biology, pathogenesis and clinical outcome of disease and therapy is not fully understood. The xenobiotic nature of the epitope renders it highly immunogenic, resulting in the induction of IgE as well as IgG antibodies, key compounds in different immune mechanisms. Hence, avoidance of xenobiotic glycosylation and optimisation by glyco-engineering are a central issue in biotechnology, in which a variety of cell types are increasingly used as host for the production of diagnostically and therapeutically relevant glycoproteins [107]. Invertebrate N-glycans often exhibit both an α -1,3- and an α -1,6 linked fucose residue at the proximal GlcNAc, as for example found in *Drosophila*. In contrast to diptera, like *Drosophila*, Hymenoptera show predominantly only α -1,3-fucosylation, suggesting different acceptor substrate specificities [181, 182]. Honeybee (*Apis mellifera*) core α -1,3-fucosyltransferase (FucTA) has recently been identified [139]. Similar enzymes are present in other invertebrates and have been cloned from *Caenorhabditis elegans*, *Vigna radiata* and *Drosophila melanogaster* [140, 183, 184]. The α -1,6 linked fucosyl residue is attached by core α -1,6-fucosyltransferase (FUT8). FucTA can act upon a fucosylated or non-fucosylated core oligosaccharide. FUT8 can only attach the 6 linked fucosyl residue onto a core oligosaccharide that does not carry the α -1,3 linked fucosyl residue. In general, fucosyltransferases form a diverse class of glycosyltransferases. They catalyze the transfer

of fucosyl residues mostly onto carbohydrate structures (for review see, [185]). Various human, insect and bacterial fucosyltransferases have been characterised and they differ only with respect to the acceptor substrate [135, 186]. They all utilise β -L-fucopyranosylguanosine 50-diphosphate (GDP-fucose) as the donor substrate. Structural information and detailed mechanistic studies on fucosyltransferases are very scarce. Available X-ray crystal structures are limited to that of human FUT8, the fucosyltransferase from a *Rhizobium* that produces NodZ and a fucosyltransferase from *Helicobacter pylori* [167, 187, 188]. The sequence homology of these fucosyltransferases is very low and none of them is related to FucTA from invertebrates. The substrate binding model derived from *H. pylori* involves a deep nucleotide binding pocket whereas the acceptor binding region is shallow and only few residues are involved in acceptor binding [189]. The molecular basis underlying the acceptor specificity however remains elusive. Most glycosyltransferases are believed to operate in a Bi Bi sequential mechanism in which the donor sugar nucleotide binds to the enzyme together with the acceptor oligosaccharide and after transfer, the glycosylated product and the nucleotide are released from the ternary complex [190]. Molecular details of the catalytic mechanism of glycosyltransferases are only known in few cases. In this study, we present a structure based characterisation of the substrate specificity of honeybee FucTA. Therefore, we established a high-level expression system of soluble FucTA (sFucTA) that allowed STD NMR and SPR studies on molecular recognition of both donor and acceptor substrates. Finally, we show an enzyme kinetic characterisation of this transferase reaction by progress curve analysis using an explicit solution of the integrated MichaeliseMenten equation.

3.1.1 Recombinant expression and immunochemical characterisation of soluble FucTA

Recently, functionality of a Golgi-resident full length form of FucTA from *A. mellifera* expressed in baculo virus infected *Spodoptera frugiperda* insect cells (Sf9) could be demonstrated [71]. As basis for further studies of the enzyme mechanism, we established a high-level expression and purification protocol for recombinant soluble honeybee FucTA. For glycosylated transferases, defects in their own glycosylation are reported to have significant impact on catalytic activity. Therefore, we established a nearly autologous expression system in baculovirus infected Sf9 cells to guarantee a natural posttranslational processing, including glycosylation, of FucTA lacking only the transmembrane domain composed of amino acids 1 to 29. From the supernatant, we obtained 10 mg/mL FucTA after purification using a nickel nitrilotriacetic acid (Ni NTA) column. The purified FucTA had an apparent molecular mass of 60 kDa (Fig. 3.1A). The enzyme gave one band on SDS page as well as in the Western blot and showed enzymatic activity, e.g., on glycoprotein substrates native to *A. mellifera*. α -1,3 core fucosylation of proteins produced in Sf9 cells can be established by stable

transfection with the honeybee FucTA gene [66, 71]. Hence, cellular lysates of Sf9 cells infected with sFucTA baculo virus were analysed using anti-horseradish peroxidase (HRP) antiserum recognizing the α -1,3-core fucose epitope [178, 191, 192]. In contrast to non-infected Sf9 cells, sFucTA expressing cells showed reactivity of a variety of glycoproteins suggesting pronounced core α -1,3-fucosyltransferase activity and functionality (Fig. 3.1B). Analysis of purified sFucTA demonstrated that the enzyme itself undergoes core α -1,3 fucosylation (Fig. 3.1A) and is therefore a substrate for its own enzymatic activity.

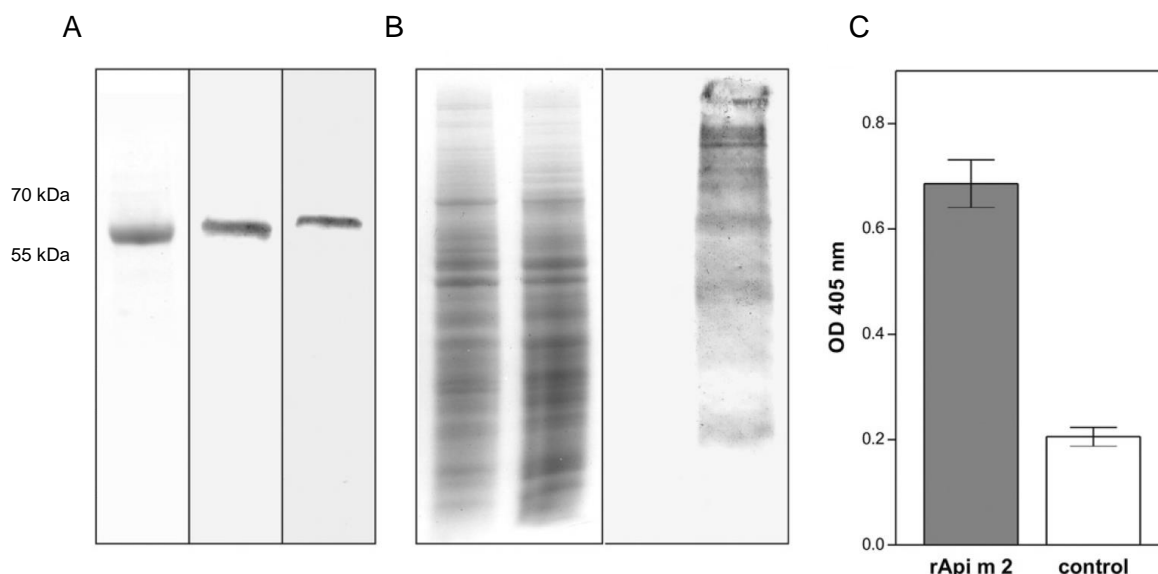


Fig. 3.1: Expression and immunochemical characterisation of honeybee sFucTA

A. SDS-PAGE and immunoblot analysis of purified sFucTA produced in Sf9 insect cells visualised by either Coomassie blue staining (left), anti-V5 epitope antibody (middle), and anti-HRP antiserum (right). B. Fucosyltransferase activity in cellular lysates. After SDS-PAGE using equal amounts of lysates from Sf9 (left lane) and Sf9 cells infected with sFucTA baculovirus (right lane) detection was performed using either Coomassie blue staining (left panel) or anti-HRP antiserum (right panel). C. ELISA analysis of *in vitro* fucosylation of recombinant non-fucosylated honeybee venom allergen Api m 2 by purified sFucTA in the presence of 1 mM GDP-fucose using HRP antiserum.

Moreover, the ability of purified sFucTA to fucosylate a proteinogenic acceptor was investigated applying an *in vitro* fucosylation assay. Here, recombinant honeybee venom allergen Api m 2, devoid of immunologically detectable core α -1,3 fucosylation but carrying glycan structures that are potential acceptors for the core α -1,3 fucosylation reaction, was used as an acceptor substrate [139, 193]. Api m 2 was incubated with sFucTA and GDP-fucose and functionality of FucTA was demonstrated by the HRP-antiserum (Fig. 3.2C).

3.1.2 Preparation of core fucosyltransferase acceptor substrates for structural analyses

The detailed structural analysis of the substrate binding mode of sFucTA by NMR and SPR required about 1 mmol of acceptor substrate. Therefore, we prepared reducing asialo

The oligosaccharides 1a and 2a were prepared by enzymatic digestion of bovine and porcine fibrinogen, respectively [161]. The core α -1,3-fucosylated structures 3a and 4a are products of FucTA using acceptors 1a and 2a, respectively. β 1-Aminoacetylated oligosaccharides (marked by an asterisk) were synthesised from the reducing oligosaccharides. All compounds were purified by PGC HPLC, retention times (Rt) are listed in the table.

Number	Structure	Mass	R _t [min]	Characterization
1a		1316.487	β 39.4 α 45.6	NMR, LC-ESI-MS
1b*		1357.547	β 40.1	NMR, LC-ESI-MS
2a		1462.544	β 49.4 α 55.7	NMR, LC-ESI-MS
2b*		1503.604	β 51.3	NMR, LC-ESI-MS
3a		1462.544	β 26.4 α 27.2	NMR, LC-ESI-MS
3b*		1503.604	β 27.8	NMR, LC-ESI-MS
4a		1608.602	β 30.6 α 36.2	NMR, LC-ESI-MS
4b*		1649.662	β 33.4	LC-ESI-MS

Digesting the pure asialo nonasaccharide with β -galactosidase resulted in heptasaccharide 1a. Acceptor substrate 2a was prepared from porcine fibrinogen that dominantly carries core α -1,6 fucosylated N-glycans. 5 g fibrinogen yielded 2-5 mg pure asialo agalacto N-glycans. Identity and purity of PGC HPLC purified oligosaccharides were unambiguously confirmed by MS, ^1H and ^{13}C NMR. The reducing oligosaccharides 1a and 2a served as substrates for honeybee FucTA. Generally, reducing oligosaccharides give rise to complex NMR spectra due to two sets of signals originating from the α and the β anomers, respectively. Since 1D ^1H STD NMR epitope mapping experiments require unambiguous assignment of ligand resonances we prepared 1-aminoactetylated derivatives [162]. The N-acetate in the 1-position of the oligosaccharides is a very close related mimic of the natural linkage to the side chain of asparagine. The 1- β -N-acetyl oligosaccharides 1b and 2b were characterised by MS, NMR, and 2D NMR techniques.

3.1.3 Donor substrate specificity of core fucosyltransferase A

Like all fucosyltransferases, honeybee FucTA uses GDP- β -L-fucose as donor substrate (Fig. 3.2).

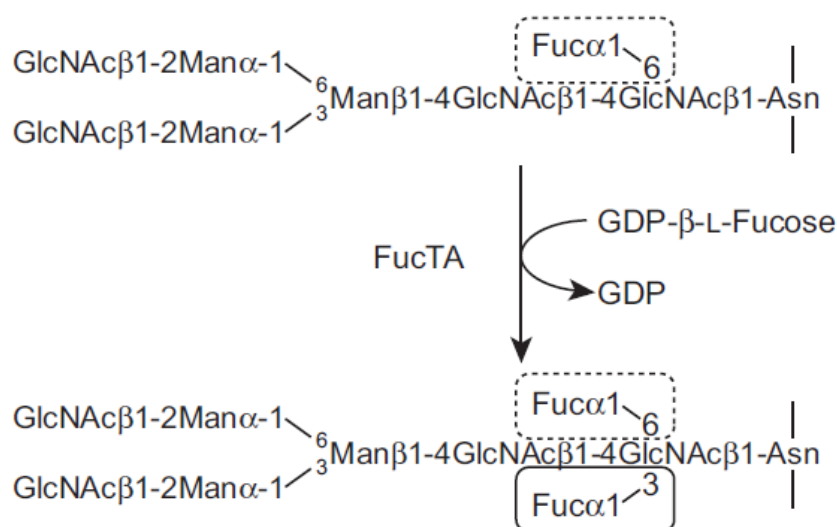


Fig. 3.2 Reaction catalysed by FucTA

Insect core α -1,3-fucosyltransferase transfers a fucose residue from the donor substrate GDP-Fucose (GDP-Fuc) to the proximal N-acetylglucosamine of an N-glycan (acceptor substrate). Whereas the non-reducing GlcNAc at the 3-Man arm is required for activity, the linkage to the Asn side chain is not necessary and reducing oligosaccharides are accepted as substrates. N-glycans already carrying an α -1,6 linked core fucose (dashed boxes) are preferred by drosophila FucTA over unfucosylated substrates [140].

Commonly, donor substrates bind to glycosyltransferases with dissociation constants in the 10 mM range. Here we characterised the interaction of the GDP-fucose donor with FucTA

using surface plasmon resonance (SPR) by analyzing binding of the building blocks GDP-Fuc, GDP and guanosine to sFucTA (Fig. 3.3B).

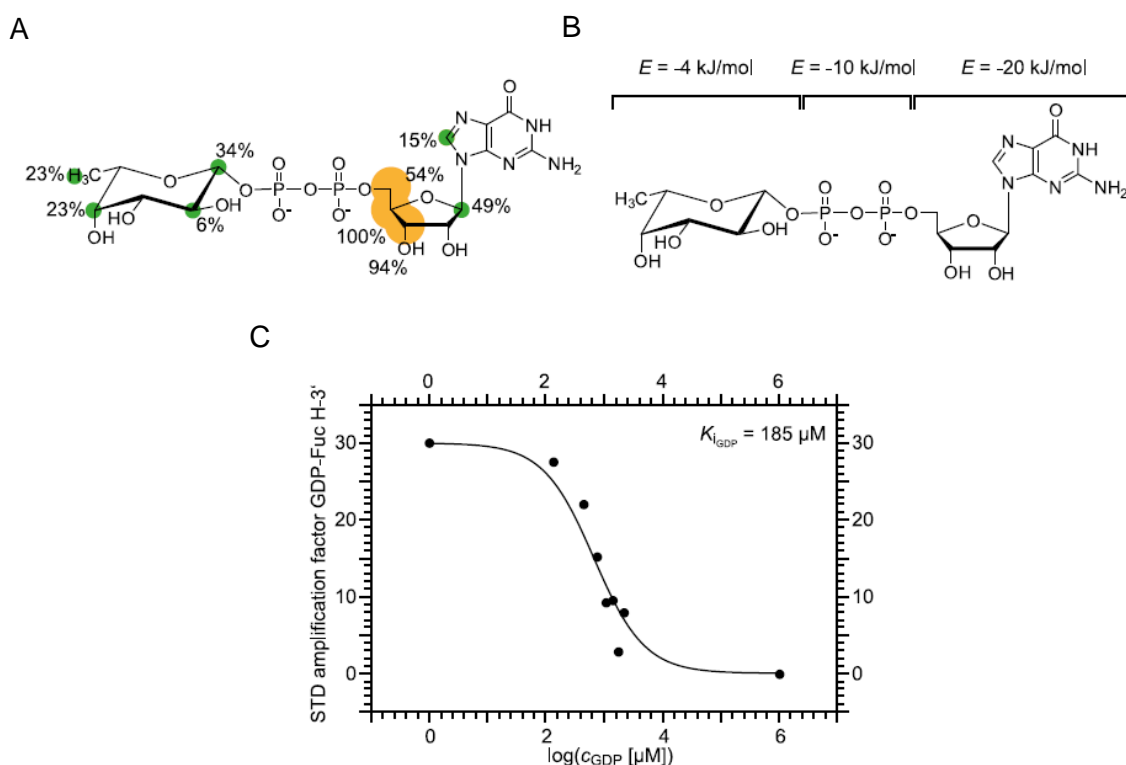


Fig. 3.3 Interaction of sFucTA with its donor substrate

A Binding epitope of GDP-Fucose as determined by STD NMR. Circles indicate the relative STD effects which are proportional to the distance of the respective protons to the enzyme's surface. The ribose is clearly closest to the enzyme surface. B Fragment based screening of the donor substrate binding pocket of FucTA. The brackets indicate the fragments used to elucidate donor substrate specificity by SPR. C Product inhibition of FucTA by GDP. The STD amplification factor for each inhibitor concentration is plotted against the inhibitor concentration. A fit using the one-site competition model yields the IC_{50} value from which the K_i of 185 mM was calculated.

All binding assays of donor substrates were performed in absence of acceptor substrate. For sFucTA the nucleoside part contributes dominantly to binding affinity with a $K_{D,guanosine} = 410$ mM (corresponding to a binding energy $E = -19.5$ kJ/mol). GDP gave $K_{D,GDP} = 7.0$ mM, equivalent to a binding energy $E = -29.8$ kJ/mol, indicating that the pyrophosphate bridge accounts for ~ 10 kJ/mol binding energy. GDP-fucose binds to sFucTA with a slightly weaker dissociation constant compared to GDP ($K_{D,GDP-Fuc} = 37.5$ mM, equivalent to $E = -25.7$ kJ/mol). The detailed epitope of the substrate was determined using STD NMR [196-198]. The results supported the data obtained by SPR (Fig. 3.3A). Protons of the ribose show the largest relative saturation transfer suggesting that the nucleoside moiety binds closest to the enzyme surface in the binding pocket. STD effects of the guanine cannot be

evaluated, as the protons attached to nitrogen atoms exchange too quickly with deuterium oxide. However, the proton at C-8 showed only low STD effects. Also, the contribution of the pyrophosphate cannot be assessed by STD NMR due to the lack of covalently linked protons. However, the fucosyl residue clearly gains saturation transfer indicating that it is in close contact to FucTA in the bound state. To further elucidate the role of the fucose moiety for the binding substrate, we performed a competitive binding assay monitored by STD NMR (Fig. 3.3C). For this analysis we added GDP-Fuc to a solution of the enzyme and then titrated GDP. For quantitative analysis of the inhibition constant K_i , eight titration points were determined. STD amplification factors were recorded as a function of the total concentration of the inhibitor GDP (cGDP) [199].

Here, we used the STD signal of H-3' of GDP-fucose to track the occupancy of the donor binding site with GDP-fucose in presence of different GDP concentrations. A fit of the one-site competition model to the semi-logarithmic affinity plot yielded a value of $K_i = 185$ mM for GDP using a $K_D = 37.5$ mM for GDP-fucose as determined by SPR experiments. This fact indicates that the fucose enhances the affinity by 4 kJ/mol which is in contrast to the SPR data, where the fucosyl residue weakened binding by about 2 kJ/mol. There are several possible explanations for this small discrepancy: first, the enzyme is in different states in the NMR and SPR based assays e dissolved vs. immobilised. Here especially the immobilisation may alter the enzyme dynamics and in consequence the binding affinity. Second, in the NMR experiment, we used a deuterated buffer which might affect the binding strength of hydrogen bonds. Third, SPR experiments are performed under flow conditions which may affect the binding contribution. However, overall we find only a small (almost negligible) contribution of the fucosyl residue to binding. These findings are in agreement with data from other glycosyltransferases and, thus, like in other glycosyltransferases, the nucleobase directs the binding process of the donor substrate to FucTA [190, 200, 201]. However, a quantitative analysis of the K_i value of GDP revealed that GDP is the weaker binder compared with the natural donor GDP-fucose and the fucosyl residue increases the relative binding energy by a small contribution.

3.1.4 Acceptor substrate specificity of core fucosyltransferase A

Generally, glycosyltransferases show very low affinity towards their acceptor substrates [190, 202]. Determination of binding constants of the acceptor substrates 1a and 2a by SPR yielded a dissociation constant of 10 mM for heptasaccharide 1a. Up to the concentrations used for 1a we could not detect binding for 2a. Thus, octasaccharide 2a has an even higher dissociation constant. These extremely high ligand concentrations (e.g., 10 mM and higher)

were accompanied by detrimental effects on the chip surface resulting in negative sensorgrams. Therefore, we could not determine the binding affinity of 2a to FucTA.

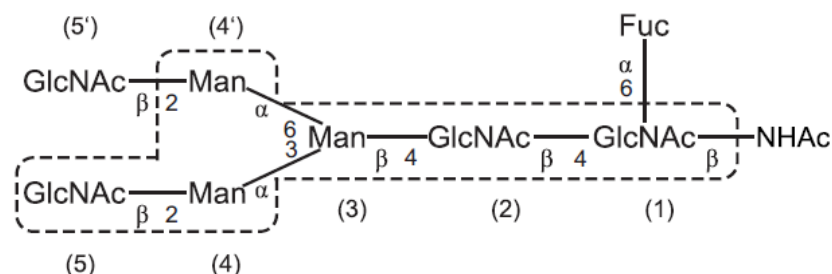


Fig. 3.4 Interaction of sFucTA with its acceptor substrate

Epitope of the acceptor substrate 2b as determined by 1D ^1H STD NMR of the structural reporter groups. The structural reporter groups of the chitobiose core, the β linked mannose and the α -1,3 linked mannose residue (dashed boxes) receive relative STD percentages of >50%.

Obviously, oligosaccharides with core α -1,6 linked fucose residues do not favourably bind to the acceptor region of FucTA. Asn linked chitobiose and α -methylfucoside gave no SPR response even at concentrations as high as 20 mM. This is in agreement with the fact that the core pentasaccharide of complex type N-glycans is not sufficient to bind to FucTA and to undergo fucosylation [139]. These data suggest that in contrast to other FucTs and other glycosyltransferases core-modifying fucosyltransferases such as FucTA require a much larger oligosaccharide as acceptor [202, 203]. STD NMR experiments with octasaccharide 2b showed only very small absolute STD percentages of 0.3-1.0%, most likely due to its transient binding and short residence time in the pocket. Virtually all structural reporter groups in the 1D ^1H STD NMR spectrum of acceptor substrate 1b were found to exhibit STD effects indicating that large portions of the molecule are in contact with the enzyme [204]. However, core N-acetylglucosamines and the 3-mannose branch seem to be closer to the enzyme surface compared to the fucose and the 6-mannose branch, which show relative STD percentages below 50%. Since the resonances of the two terminal GlcNAc residues cannot be distinguished in the spectra, it is unclear which GlcNAc residue gives rise to the corresponding STD signal. It is likely that the GlcNAc of the 3-branch has a shorter distance to the protein surface. Analysis of the STD effects of the N-acetate groups reveals that both GlcNAc residues of the branches have similar distances to the protein surface. The N-acetate groups of the “reducing” GlcNAc1 have the highest STD effect overall. Further information on the enzyme’s acceptor substrate specificity was obtained by fucosylation of a mixture of heptasaccharide 1a and two hexasaccharides lacking the respective GlcNAc residues at the non-reducing end that originate from cleavage of either terminal GlcNAc

residue. NMR analysis revealed that the hexasaccharide lacking the GlcNAc in the 3-branch is not fucosylated (data not shown).

3.1.5 Characterisation of the enzyme kinetics of core fucosyltransferase A

Several methods to study enzyme kinetics of core fucosyltransferases have been published [205-208]. In many cases, complex type asialo agalacto N-glycans have been derivatised with fluorescence dyes in order to apply reversed phase HPLC separation employing UV detection [140, 201]. However, fluorescence labelling of oligosaccharides is a laborious procedure and the hydrophobic scaffold might give rise to unwanted protein ligand interactions. Radiolabeled substrates are the basis for the second established method which offers sensitive detection without changing chemical properties of the substrate. However, all steady state initial rate assays based on detecting substrate conversion after a given time interval are relatively material and time consuming, as several samples with starting concentrations have to be prepared. In addition, conditions for the steady state have to be found in separate experiments. NMR spectroscopy presents an attractive analytical method because substrate conversion can be directly detected from specific resonances of substrates and products without special probing, quenching or work-up procedures during the enzyme reaction [209]. Direct analysis of the time course (progress curve) of the enzymatic reaction yields K_M and k_{cat} [210]. It can be realised by solving the integrated Michaelise-Menten equation (Eq. (1)) [211-213]. Recently, the Lambert-W function, defined as the function that satisfies Eq. (3), has been described as solution for the integrated Michaelise-Menten equation (Eq. (1)) [214]. A non-linear fitting procedure employing the Lambert-W function (Eq. (2)) allows for determining K_M and V_{max} directly from the progress curve [215]. ^1H NMR provides an ideal tool to transiently record the concentrations of all substrates and products, respectively, as a function of time through integration of their resonances. Product inhibition might influence the velocity of the reaction and thus has to be considered when analyzing progress curves. In line with data obtained from the binding assays (cf. above), samples containing 10 mM FucTA, 1 mM acceptor 1a and 2 mM GDP-fucose reached equilibrium after 1.5 h. However, only 60% of the substrate was converted documenting strong product inhibition by GDP. The kinetic model of such a reaction cannot be described by a MichaeliseMenten equation. To determine kinetic constants of the FucTA reaction, product inhibition was circumvented by adding alkaline phosphatase to a sample of 1.5 mM FucTA, 2 mM GDP-fucose and 1.1mMacceptor substrate 1a or 1.6 mM acceptor substrate 2a, respectively. The excess of donor substrate ensured the reaction to proceed under pseudo first order conditions required to apply MichaeliseMenten kinetics. No GDP

resonances appeared at any time of reaction indicating the high efficiency of the phosphatase.

$$V_{\max}t = K_M \ln \frac{[S]_0}{[S]} + [S]_0 - [S] \quad (1)$$

$$[S] = K_M W \left\{ \frac{[S]_0}{K_M} \exp \left(\frac{[S]_0 - V_{\max}t}{K_M} \right) \right\} \quad (2)$$

$$W(z)e^{W(z)} = z \quad (3)$$

Like other glycosyltransferases, honeybee FucTA hydrolyses its donor substrate in absence of acceptor substrate [216]. This hydrolysis reaction corresponds to a transfer of a fucosyl residue to a water molecule. For FucTA, we found a $k_{cat} = 2 \text{ min}^{-1}$ for GDP-fucose hydrolysis, which is somewhat slower than the transfer of the fucosyl residue to its natural acceptor (6 min^{-1}). In presence of the acceptor, however, no hydrolysis of the substrate is observed. In this study we established the NMR-based characterisation of glycosyltransferase reactions based on progress curves, to gain insights into molecular and kinetic characteristics of fucosyltransferases and their interaction with the corresponding substrate. The data illustrate that direct observation of enzymatic processes by NMR spectroscopy allows a label-free observation of all substrates and products and it has the potential for obtaining information on molecular interplay of substrates and products with the enzyme. When run as part of an STD NMR experiment one has additional molecular information on binding processes. FucTA binds its acceptor with a high dissociation constant. The thermodynamic binding constant determined for the heptasaccharide 1a by SPR is 10 mM, which is a typical binding constant of acceptor substrates to glycosyltransferases. For the core α -1,6 fucosylated acceptor substrate 2a, the dissociation constant was even higher suggesting that the enzyme, unlike its homologue from *D. melanogaster*, prefers the unfucosylated N-glycan over the fucosylated structure [140]. This finding is supported by results of enzyme kinetics: The K_M value for the heptasaccharide 1a was determined to 400 mM, whereas the octasaccharide 2a showed $K_M = 1 \text{ mM}$.

The discrepancy between the K_D and K_M values for each acceptor substrate is remarkable. This has been shown for other glycosyltransferases already [217]. The acceptor substrate binding seems to be dependent on the presence of donor substrate. Thus, thermodynamic binding constant K_D is often found to be much weaker than the kinetic constant K_M [218].

We also considered SPR in presence of GDP-Fuc, but discarded the idea because under these conditions, substrate conversion will occur and thus SPR results will be meaningless and could not be interpreted on the basis of a one site-binding model. Importantly, SPR assays with the acceptors in presence of GDP yielded the same results as the assay with acceptor substrate only (data not shown). The weak K_D values are also not uncommon for protein carbohydrate interaction as it is known from lectin interactions with oligosaccharides. Still lectin chromatography is widely used in purification protocols of carbohydrates. The substrate specificity is one possible explanation for the rather high proportion of mono α -1,3 fucosylated N-glycans in comparison to other species found in the glycoproteins of honeybees [181]. However, for detailed elucidation of the order of fucosylation in honeybees, knowledge on substrate specificity of the involved glycosidases is required. Furthermore, we observed no binding affinity of the enzyme to α -methylfucoside and GlcNAc β 1,4-GlcNAc β 1,4-Asn by SPR. As the proximal GlcNAc is the focus of action of the enzyme, it is unexpected that no detectable affinity is found for this structure. To dissect which molecular features of the acceptor are actually recognised by the enzyme, we determined the binding epitope of ligand 2b by STD NMR. Due to the high dissociation constant and the resulting short residence time of 2b in the enzyme pocket, the absolute STD percentages detected were low. Core GlcNAc-1 and-2, β -Man and α -1,3 linked Man residues receive significantly more saturation than other monosaccharide units. Also, the GlcNAc residue of the 3-branch shows considerable saturation, which, however, cannot be quantified because of overlap with the corresponding residue of the 6-branch. Taken together with the data from SPR experiments with acceptor substrates and its fragments, recognition of the pentasaccharide from GlcNAc-1 to the GlcNAc of the 3-branch is proposed. All STD contacts of the ring protons are very weak which is to be expected because of the low affinity of the heptasaccharide. We therefore conclude that the oligosaccharide included in the dashed line in Fig. 3.4 is specifically recognised by the enzyme. It is known from previous studies of the specificity of the acceptor substrate of honeybee FucTA that at least one of the GlcNAc residues in the antennae is essential for activity [139]. For *Drosophila* FucTA and vertebrate core α -1,6 FucT, the GlcNAc at the 3-Man arm is required and according to the above mentioned STD NMR data, the same is true for honeybee FucTA [140]. In this context, it should be mentioned that we observed an unusual enzymatic activity of our FucTA sample. In presence of its acceptor substrate 2b and absence of the donor substrate, the terminal GlcNAc of the 1,6-Man branch was selectively hydrolysed as indicated by a time-dependent decay of the corresponding α -1,3-Man H-1 and H-2 resonances. We also found products that showed the fucosylation and that were lacking the GlcNAc residue in the 6-branch even though no such starting material had been present. This indicates presence of a GlcNAcase

activity specific for the 6-branch. This observation is also in agreement with the binding epitope shown in Fig. 3.4.

3.2 Donor substrate binding and enzymatic mechanism of human core α -1,6 fucosyltransferase (FUT8)

Human α -1,6 fucosyltransferase (FUT8) catalyzes the transfer of a fucosyl residue from guanine nucleotide diphosphate (GDP)- β -L-fucose to the 6-hydroxy function of the innermost N-acetyl glucosamine (GlcNAc) residue of asparagine linked oligosaccharides (N-glycans) with inversion of the anomeric configuration (Fig.3.5) [219].

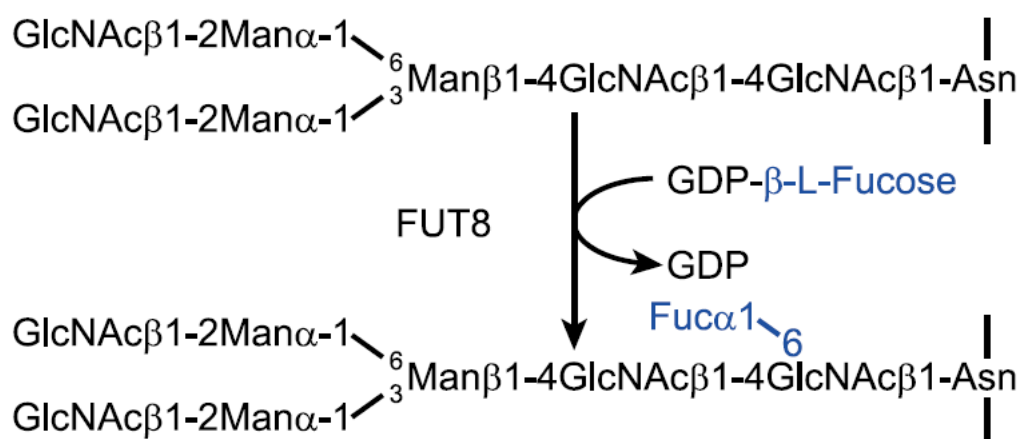


Fig. 3.5 Enzymatic reaction catalysed by FUT8

A fucosyl moiety is transferred from the activated sugar nucleotide GDP-Fuc to the 6-hydroxy group of the proximal GlcNAc of the acceptor with inversion of the anomeric configuration. The acceptor, a branched N-type oligosaccharide, has to exhibit an unsubstituted GlcNAc residue at the 3-mannose to be recognised by the enzyme. In contrast, the linkage of the proximal GlcNAc to the asparagine side chain is not essential.

The products of FUT8, glycoproteins carrying core α -1,6 fucosylated N-glycans, are widely distributed in human and animal tissues and various biological functions are regulated by this common modification of glycoproteins [220, 221]. The physiological significance of FUT8 has been demonstrated in FUT8-null mice, of which 80% died within three days after birth [222, 223]. FUT8 knock-out mice exhibit severe growth retardation and emphysema-like changes in the lung. This phenotype is thought to be caused by inactivation of growth factor receptors due to the lack of core-fucosylation of their glycans. The receptors include the transforming growth factor beta (TGF β) receptor, the epidermal growth factor (EGF) receptor and the vascular endothelial growth factor (VEGF) receptor 2 [222-224]. Further studies suggest that core-fucosylation is involved in turnover and expression levels of E-cadherin and regulates the activity of α 3 β 1 integrin [225, 226]. FUT8 therefore influences cell adhesion and cell migration processes. Also, core-fucosylated N-glycans were found to be of diagnostic

value for tumor diseases. For instance, the level of core fucosylation of α -fetoprotein is a well-known tumor marker in hepatocellular carcinoma, very likely due to high expression of the GDP-fucose transporter and enhances cell–cell adhesion in human colon carcinoma cells [225, 227-229]. Therapeutic antibodies show a 50–100 fold increase of Fc γ -mediated cytotoxicity if the core-fucosylation is deleted [230, 231]. Some of the putative mechanisms by which core-fucosylation regulates the functions of glycoproteins have been elucidated. It has been demonstrated that core-fucosylation as well as bisecting GlcNAc shift the conformational equilibria of N-glycans [232, 233]. Also, the modification has been shown to affect the serum clearance of glycoproteins [233]. Prolonging the half-life of the glycoprotein has also been suggested as a mechanism for the high expression of the membrane protein E-cadherin upon enhanced core-fucosylation [225]. Small molecules that could modulate the activity of FUT8 *in vivo* with a high selectivity would facilitate further elucidation of the biological function of this biologically important carbohydrate epitope. However, the design of specific, potent and permeable inhibitors for fucosyltransferases and glycosyltransferases in general remains a challenging task [234, 235]. FUT8 is a typical type-II transmembrane glycosyltransferase that resides in the medial Golgi and was first described by Wilson et al. [219, 236]. The enzyme has been purified and cloned from various human and animal tissues [236-238]. Detailed analyses of the FUT8 gene have revealed that the overall homology of FUT8 to any other known glycosyltransferases is very low [239-241]. However, distinct regions are highly conserved among α -1,2 fucosyltransferases, bacterial α -1,6 FucT (NodZ) and protein O-fucosyltransferases [241-244]. The existence of these conserved motifs has led to site-directed mutagenesis studies of FUT8 in order to determine residues that are essential for the catalytic activity [201, 244]. The data presented on a set of 15 mutants of highly conserved residues revealed eight amino acids that are essential for enzymatic activity of FUT8. As all fucosyltransferases use the same donor substrate GDP-Fuc but differ in their acceptor substrates, the conserved regions are supposedly involved in donor substrate binding. In fact, two conserved arginine residues (Arg365 and Arg366) have been shown to be involved in the binding of the nucleotide, although the latter is not essential for activity of FUT8 [244]. The high resolution crystal structure of FUT8 gives further implications on the donor substrate binding mode [167]. The 3D structure revealed that the fold of FUT8 can be classified as glycosyltransferase-B (GT-B). The enzyme exhibits a Rossman fold, a structural motif that is widely distributed among nucleotide-binding proteins. A comparison to the crystal structure of NodZ revealed that the conserved motifs are also structurally similar to the bacterial α -1,6 fucosyltransferase [187, 245, 246]. FUT8 acts via a Bi Bi mechanism and both donor and acceptor substrates bind to the enzyme in order to form a ternary complex [201]. After transfer of the fucosyl residue, both GDP and the fucosylated acceptor

are released [201, 247]. Potent inhibitors combine high efficiency, e.g. a low dissociation constant, with high specificity. Inhibitors that are either donor or acceptor substrate analogs exhibit only one of these properties. In the case of FUT8, donor substrate mimics will affect several fucosyltransferases in the organism. Blocking the acceptor substrate binding site is challenging because of the low binding affinity found in that region. Hence, bisubstrate analog inhibitors are most promising to feature both affinity and specificity [234, 235]. Yet, for the design of bisubstrate inhibitors, detailed knowledge of the recognition process of both substrates is indispensable. The general model for substrate binding in glycosyltransferases involves a deep cavity which binds the sugar nucleotide with relatively high affinity. In contrast, the acceptor substrate binding site is shallow and the dissociation constant is generally in the mM range [190, 202]. Fucosyltransferases that modify the proximal N-acetylglucosamine of complex type N-glycans are highly unusual concerning their acceptor substrate specificity [138, 140, 238, 247-250]. Contrary to most other glycosyltransferases, FUT8 requires a motif of at least six monosaccharides for fucosylation of the proximal N-acetylglucosamine (Fig. 3.5). As all fucosyltransferases use the same donor substrate, the recognition process of the acceptor substrate is responsible for the specificity of the fucosyl transfer. Detailed information on substrate binding mode and catalytic mechanism as required for structure-based inhibitor design cannot be derived from the FUT8 structure, as it does not include any substrates or substrate analogs and all attempts to co-crystallise or soak FUT8 with its substrates have failed so far [167]. On the other hand, protein NMR based methods are likewise demanding due to the size of FUT8 (62 kDa) and the fact that isotope labeling and particularly perdeuteration are difficult in eukaryotic expression systems required for functional expression of FUT8. 3D structural data for fucosyltransferases in complex with GDP-Fuc is available for only three other fucosyltransferases: Pioneering, for the α -1,3 fucosyltransferase of *Helicobacter pylori*, for the Protein O-fucosyltransferase 1 of *Caenorhabditis elegans* (cePOFUT1) and, very recently, also for NodZ from *Bradyrhizobium* sp. [188, 245, 251]. In the case of the enzyme of *H. pylori*, the substrate binding site is fundamentally different to that of FUT8. cePOFUT1, however, exhibits conserved motifs that are also present in FUT8 and NodZ. These segments of all three proteins are also structurally related to some extent [251]. In this work, we present a model of donor substrate binding for FUT8. As a basis, we used the crystal structure of FUT8 and the crystal structure of cePOFUT in complex with GDP-Fuc together with results from STD NMR and SPR studies of the ligands' binding. We combined the experimental information with in silico studies to create the first model of FUT8 in complex with GDP-Fuc. Our results provide detailed information about enzyme–substrate contacts and about the catalytic mechanism of FUT8.

3.2.1 Expression, purification and characterisation of fucosyltransferase 8

FUT8 was cloned and expressed as soluble enzyme lacking the transmembrane region with minor modifications as described [224]. In contrast to the recombinant FUT8 published by Ihara et al., our construct carries the 10 fold histidine affinity tag as well as the V5-epitope at the N-terminus as it is known that the catalytic domain is located near the C-terminus in most glycosyltransferases. Furthermore, the expression applying the baculovirus-mediated infection of Sf9 insect cells was conducted in serum-free medium. The modified protocol yielded soluble and secreted recombinant protein and allowed for direct His-tag affinity purification of FUT8 from the supernatant after exchange of the buffer (Fig. 3.6).

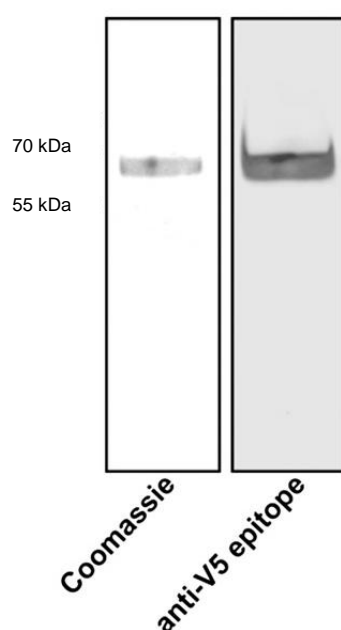


Fig. 3.6 SDS-PAGE analysis of purified recombinant FUT8

The expression and purification protocol yielded one band in the Coomassie stained gel (left) at the expected mass (62 kDa). The identity of the expression product was verified by Western-blot analysis using a monoclonal antibody against the V5 epitope (right).

Thus, no precipitation step was necessary and enhanced yields of purified FUT8 at 5 µg/mL culture supernatant were obtained. The identity of recombinant FUT8 was verified by Mascot MS analysis, SDS-PAGE and Western blot analysis. Analysis by MALDI TOF MS gave no evidence for the presence of dimers or oligomers of FUT8. This is in agreement with earlier data, including gel filtration analysis, on FUT8 isolated from human blood platelets [249]. Therefore, we assume that FUT8 is present as a monomer in solution. Many other glycosyltransferases are known to be present as dimer or tetramer. The MS analysis here was only intended to confirm that our construct has the same behavior as the native protein. The enzymatic characterisation with progress curve analysis using ^1H NMR allows the

determination of K_M and k_{cat} without special probing, quenching or work-up procedures [138, 210]. The change of substrate concentration with time is described by the integrated form of the Michaelis–Menten kinetics that has the Lambert-W function as solution [211–213, 252]. The Lambert-W function can be fitted to the data using a non-linear fitting routine. The kinetic constants were obtained as $K_{M,acceptor} = 12 \mu\text{M}$ and $k_{cat} = 0.45 \text{ s}^{-1}$.

These values are in perfect agreement with those reported by Ihara et al. using fluorescently labeled substrates [201]. We therefore conclude that the His-tag at the N-terminus present in our construct has no impact on the activity of FUT8. The data presented here were obtained in less than an hour using 0.3 nmol (=19 μg) of enzyme.

3.2.2 Donor substrate binding of core α -1,6 fucosyltransferase

In order to gain insight into substrate recognition of FUT8, we performed ligand-based NMR experiments. Saturation transfer difference (STD) NMR allows the determination of ligand epitopes without requirement of large protein amounts or labeling of the protein. Fig. 3.8 shows the epitope of GDP-Fuc in complex with FUT8 [196–198].

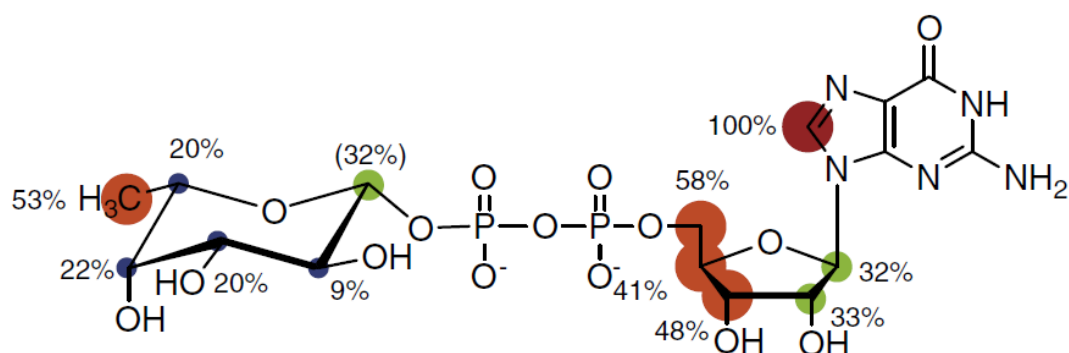


Fig. 3.8 Epitope of GDP-Fuc in complex with FUT8 as determined by STD NMR

The size of the relative STD effect of a resonance is proportional to the distance of the corresponding proton to the enzyme surface. Protons of the guanosine moiety receive highest saturation. In contrast, the protons of the fucose moiety show only minor STD effects, indicating that the fucose is located farther away from the FUT8 surface and thus is surrounded by solvent.

The different longitudinal relaxation constants of the different protons of GDP-Fuc may bias the absolute STD percentages measured and thus affect the epitope. Therefore, the STD percentages that were directly obtained from the experiment were corrected by the respective T_1 constants as described [165]. Clearly the nucleoside protons acquire relatively high saturation, indicating close proximity to the protein surface in the complex. The fucose moiety, in contrast, shows only minor saturation. Due to the lack of covalently linked protons, the contribution of the pyrophosphate group to the epitope remains elusive. These findings complement the results of inhibition studies by Ihara et al. They found that GDP is a strong inhibitor for FUT8 ($K_i = 3.6 \mu\text{M}$), whereas the absence of the β -phosphate group weakens the

inhibitor potential almost by a factor of 1000 ($K_{I,GM P} = 2.8$ mM). Taken together, our results suggest a binding mode where the nucleobase and the ribose direct the binding process to the enzyme. The fucosyl part, per contra, is positioned farther from the enzyme surface and is supposedly located towards the shallow acceptor binding site. We determined the dissociation constants for the complexes of FUT8 with its substrates and parts of the donor substrate (GDP, GMP and guanosine) with SPR. The obtained K_D values are listed in Table 3. Our data show that the affinity of GDP is 10 fold higher compared to that of GDP-Fuc. These findings are in good agreement with the inhibition constants determined by Ihara et al. [201]. A fit of the one-site-binding model to the SPR data of guanosine and GMP yields K_D values of approximately 2 mM for both ligands, indicating very weak binding (data not shown). From these data it becomes clear that the β -phosphate moiety has a major contribution to the binding affinity of the donor substrate. This is in stark contrast to other glycosyl transferases where the base is the dominant part of the donor substrate [226, 228].

Table 3 K_D values for FUT8 and ligands

K_D values for FUT8 and ligands occupying the binding site of the donor substrate as determined by SPR.

Ligand	K_D [mM]
GDP-Fuc	0.0093 (± 0.001)
GDP	0.00089 (± 0.0005)

We performed transferred NOE experiments to obtain information about the active conformation of GDP-Fuc bound to FUT8 at various protein to ligand ratios, mixing times, temperatures and pH values. However, the conditions that allow observation of transferred NOEs were not met. The problems that prevent observation of trNOEs are the very fast hydrolysis of the donor substrate by FUT8 even at moderate temperatures combined with a slow off-rate of 0.2 s^{-1} of GDP-Fuc.

3.2.3 In silico model of core α -1,6 fucosyltransferase in complex with GDP-Fuc

The crystal structure of the apo enzyme FUT8 was used as a starting point for an in silico model of FUT8 in complex with its two substrates [167]. In addition to the usual preparation steps of the structure for in silico calculations, we modeled five amino acids (Asn368-Thr372) at the tip of a loop that were not resolved in the crystal structure. In order to obtain a reliable position for the donor molecule GDP-Fuc, we started from the X-ray crystal structure of cePOFUT in complex with its donor GDP-Fuc. The binding sites of the donor molecule in

cePOFUT and FUT8 are structurally homologous [251]. We defined the amino acids of the donor binding site in cePOFUT by the distance of the amino acids to the donor molecule of less than 4 Å. Four peptide segments with a total of 48 residues were obtained and their structural motifs were structurally aligned with the backbone of the crystal structure of FUT8 (Fig. 3.9). The peptides Arg40-Leu58, Pro233-Arg240, Leu348-Asn352 and Val354-Gly369 of cePOFUT were simultaneously aligned with peptides Gly219-Thr237, Pro358-Arg365, Phe462-Thr466 and Ser468-His483 of FUT8). The two long sequences are forming α -helices and the two short β -strands. The backbones of the two enzymes matched within these five peptide segments with an RMSD of 1.49 Å (Fig. 3.9). Now the donor molecule was placed into the FUT8 by using the exact same positioning relative to the five peptide segments as was found in cePOFUT. As a result, GDP-Fuc was prepositioned in the putative binding pocket of the donor substrate of FUT8. The side chain of Arg365 is folded onto the enzyme surface in the FUT8 structure, probably because there is no substrate present. The conformation of the side chain of Arg365 in the apo structure of FUT8 results in clashes of the atoms of Arg365 with the donor molecule.

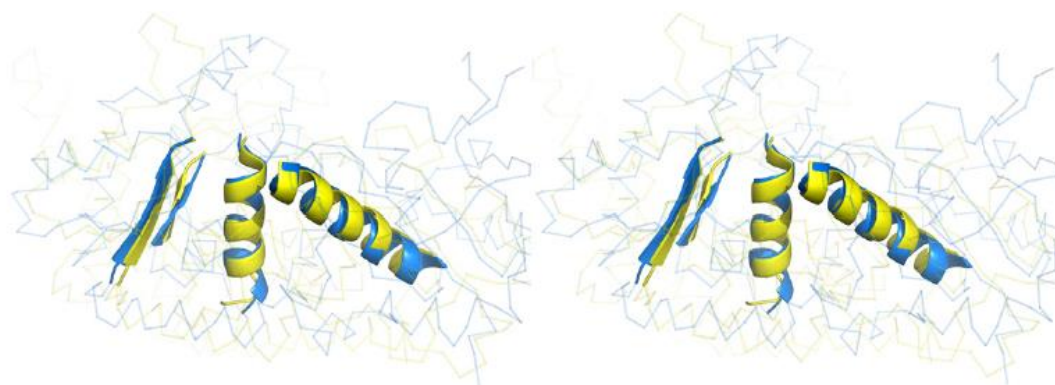


Fig. 3.9 Ribbon representation of structural alignment of the 3D structures of hFUT8 (yellow ribbon) and cePOFUT (blue ribbon)

The sections that were selected for the alignment are emphasised by opaque cartoon ribbons.

This explains why all our previous attempts to place GDP-Fuc into the FUT8 structure via docking algorithms were unsuccessful. However, if the donor substrate is present and the side chain of Arg365 of FUT8 is rotated into the conformation of the Arg240 of cePOFUT, a perfect fit is obtained. Subsequent energy minimisation of the FUT8/GDP-Fuc complex yielded a ‘homology’ model of GDP-Fuc bound to FUT8 derived from the structure of the cePOFUT complex as shown in Fig. 3.10. The guanine is bound via hydrogen bonds to two key residues, Asp453 and His363, which form a conserved binding motif as these key interactions are also found in the crystal structures of cePOFUT and NodZ [245, 251].

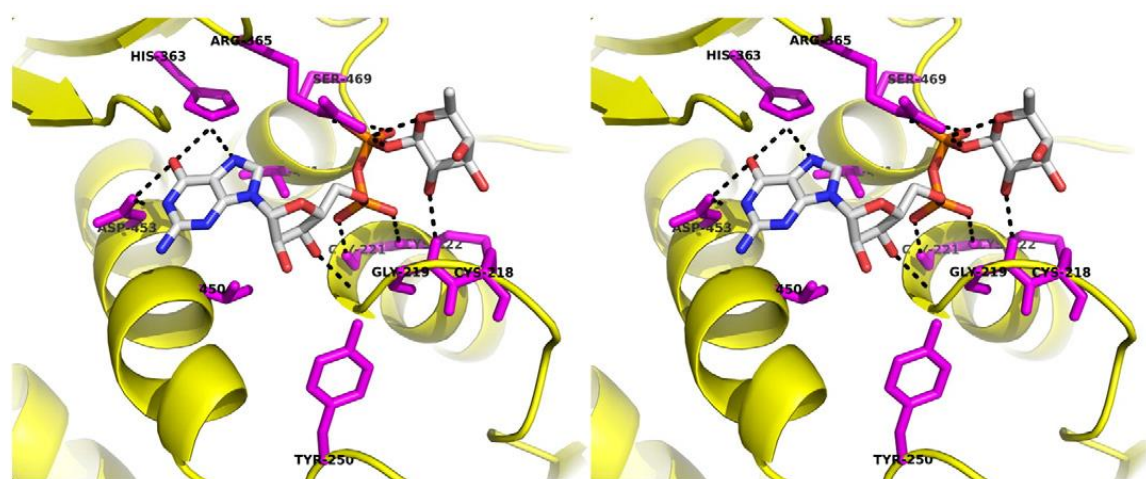


Fig. 3.10 Crossed-eye stereo plot of the initial placement of GDP-Fuc (sticks by atom color) into FUT8 (yellow cartoon ribbon)

Residues that directly interact with GDP-Fuc according to the model are shown in magenta. The structure was used as a starting point for the MD simulation.

In the cases of cePOFUT and NodZ, the ribose is mainly bound via hydrophobic interaction with a phenylalanine residue. In FUT8, this residue is substituted by valine residues forming the hydrophobic pocket for the ribose part. FUT8 also exhibits a tyrosine residue Tyr250 corresponding to the Tyr45 in NodZ. Tyr45 in NodZ forms H-bonds with the 2' and 3' OH groups of GDP-Fuc [245]. In FUT8 we found a similar interaction between the OH of Tyr250 and ribose OH-2' and OH-3' during the MD simulation. The pyrophosphate moiety in the FUT8 model is bound via multiple hydrogen bonds to the backbone NH atoms of the peptide chains forming two α -helices of the Rossman fold and the side chain hydroxy group of the essential Ser469. This binding mode of the pyrophosphate is very similar to that observed in the X-ray crystal structure of cePOFUT. Arg365 forms hydrogen bonds to the β -phosphate oxygen atoms and the 5' and 1' oxygen atoms of the fucose of GDP-Fuc and is also very close to the O-4'. (Fig. 3.10) The fucose moiety lies outside the donor substrate binding cavity and points towards a shallow area formed by the peptide segment from Asp494 to Gly501. The methyl group of Thr367 is close enough to interact with the methyl group of the fucose and probably gives rise to the high STD effects observed for these protons.

3.2.4 Molecular dynamics simulation

The positioning of the donor substrate was validated by a molecular dynamics simulation. The complex of donor substrate and protein was embedded into water box containing also 200 mM sodium chloride. After minimisation of the water box a 1.5 ns MD simulation time was run. During that time the position of the donor did not change significantly, indicating that the positioning was reasonable (Fig.3.11).

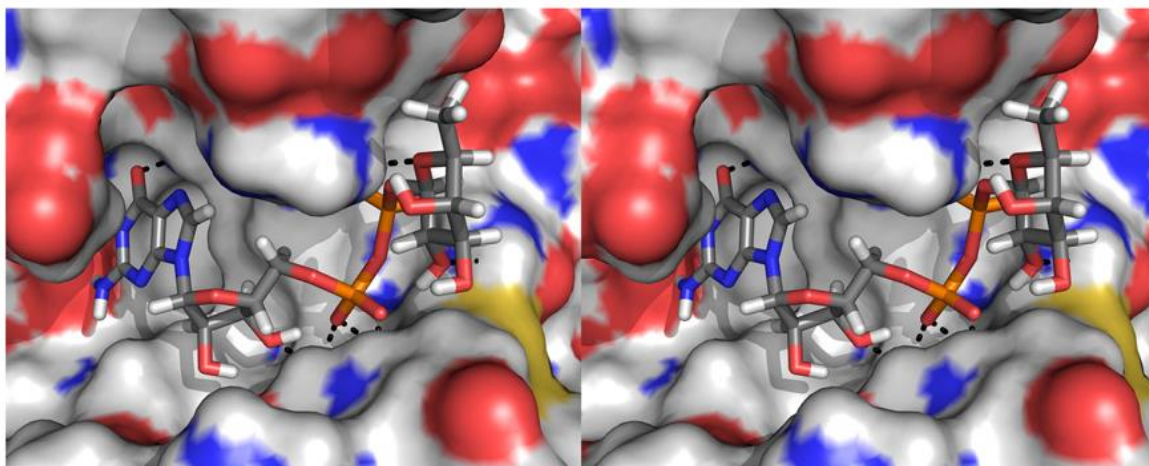


Fig. 3.11 Last frame of the MD simulation of GDP-Fuc in complex with FUT8

Polar contacts are indicated as black dotted lines. It is clearly visible that the pattern of hydrogen bonds as well as the positioning of the ligand has not changed throughout the MD.

For the donor substrate, the distances between the key amino acids (Fig. 3.12) and their hydrogen bonding partners in the nucleotide part of GDP-Fuc remained perfectly constant.

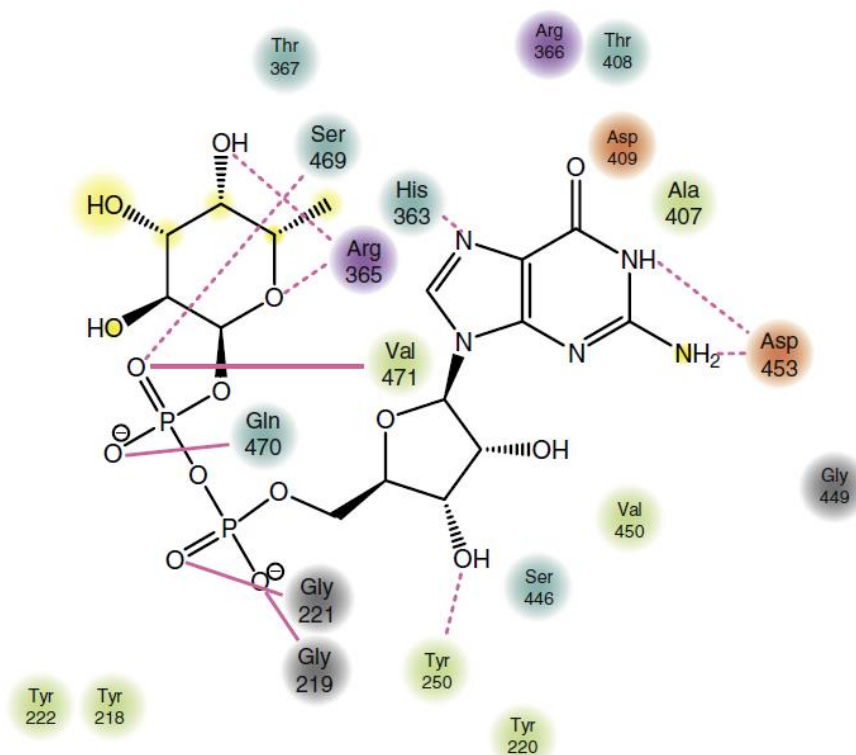


Fig. 3.12 2-dimensional plot taken from a representative frame of the MD simulation

2-dimensional plot taken from a representative frame of the MD simulation (frame 2278) illustrating the interactions of the donor substrate GDP-Fuc with residues in the active site of FUT8. Dotted lines show hydrogen bonds with functions from side chains and solid lines such with functions of the backbone. Other residues shown are close to the substrate and participate in hydrophobic interactions.

Especially the four hydrogen bonds binding the β -phosphate constantly kept their distance to the corresponding donor atoms between 2.5 and 3.0 Å, underlining the significance for binding of the donor substrate that was also found experimentally. Remarkably, new unpredicted interaction established after 200 ps simulation time. Namely, hydrogen bonds between the nitrogen atoms of the guanidinium group of Arg365 and the O-1" and O-5" of the fucosyl moiety of GDP-Fuc built up and remained for the rest of the simulation time, locking the fucosyl residue into a position perfectly suited for the nucleophilic attack.

3.3 Donor assists acceptor binding and catalysis of human α -1,6 fucosyltransferase

In mammals, fucosylation is accomplished by 14 fucosyltransferases (FUTs) that all transfer a fucosyl residue from the activated sugar nucleotide diphosphate, GDP-fucose (GDP-Fuc), to various acceptors [185, 189]. The specific fucosylation pattern found in tissue, developmental states, or under pathological conditions is determined by the expression level, the specific activity, and the unique acceptor substrate specificity of each of these individual fucosyltransferases. Human α -1,6 fucosyltransferase (FUT8) catalyzes the transfer of a fucosyl residue to the 6-hydroxy function of the innermost N-acetyl glucosamine (GlcNAc) residue of asparagine linked oligosaccharides (N-glycans) with inversion of the anomeric configuration (Fig. 3.5) [219]. The resulting so-called core α -1,6 fucosylation is a common modification of N-glycans [185, 186]. Gene knockout for FUT8 in mice has elucidated much of its biological function [222, 223]. FUT8-null mice suffer from early postnatal death, severe growth retardation, and emphysema-like changes in the lung. The results of these studies revealed that core fucosylation is crucial for the activation of growth factor receptors such as the transforming growth factor beta (TGF β) receptor, the epidermal growth factor (EGF) receptor, and the vascular endothelial growth factor (VEGF) receptor 2 [222-224].

Furthermore, core fucosylated N-glycans influence turnover and expression levels of E-cadherin and modulate the activity of α 3 β 1 integrin [225, 226]. FUT8 is therefore involved in cell adhesion and cell migration processes. In addition, the level of core fucosylation at N-glycans is associated with the prognosis and progression of tumor diseases. FUT8 was recently found to functionally regulate non-small cell lung cancer and to enhance cell-cell adhesion in human colon carcinoma cells [225, 253]. Another example is the core fucosylation of α -fetoprotein, which is a well-known tumor marker in hepatocellular carcinoma [227, 228]. Finally, therapeutic antibodies are 50–100 fold more active in terms of Fc γ -mediated cytotoxicity if the N-glycans of the immunoglobulin are not core fucosylated [230, 231]. Flexible tools for probing biological effects of core fucosylation in life animals are therefore of high interest. However, specific, potent, and membrane-permeable inhibitors for glycosyltransferases are lacking. Recent progress in the development of inhibitors for the

structurally well studied human blood group galactosyltransferase B demonstrates the significance of structural information. Most glycosyltransferases exhibit high affinity to their family wide shared donor substrate but have generally a low affinity to their specific acceptor substrate. Bisubstrate-analogues are thought to be most promising as inhibitors [234, 235, 254]. FUT8 is a type-II transmembrane protein located in the medial Golgi that has been purified and cloned from various human and animal tissues [219, 236, 238]. The gene of FUT8 has a very low homology to any other glycosyltransferases [241]. The specificity of FUT8 toward its acceptor substrate, a branched N-glycan (Fig. 3.5), is highly unusual in that it requires a hexasaccharide as minimal acceptor structure and strictly requires an unsubstituted GlcNAc residue in the 3-branch [247-250]. Interestingly, the linkage of the reducing end to the asparagine is not essential [201, 249]. Other core modifications like core α -1,3 fucosylation and bisecting GlcNAc were found to completely prevent fucosylation by FUT8 [238, 247, 248]. For some non-mammalian fucosyltransferases, X-ray structures with bound donor substrate were successfully solved [188, 245, 251]. Despite much effort, bound acceptor substrates have never been observed in X-ray structures of fucosyltransferases, probably due to their generically low binding affinity [138, 190, 202, 217]. FUT8 is the first mammalian fucosyltransferase for which a high resolution crystal structure was solved [167]. Its structure has been classified as glycosyltransferase B (GT-B) fold with, however, only one Rossmann fold. FUT8 also features an N-terminal coiled-coil structure and C-terminal β -sheets as part of an SH2-domain. Based on the X-ray structure of the apoenzyme, a structural model of GDP-Fuc binding was recently developed by our group [173]. The unusual acceptor binding specificity is addressed in this study.

3.3.1 Acceptor shows moderate affinity and dissociation Rate

We synthesised GlcNAc β 1-2Man α 1-3(GlcNAc β 1-2Man α 1-6)Man β 1-4GlcNAc β 1-4GlcNAc β 1-N-Ac (heptasaccharide 1) and used it as acceptor substrate throughout the experiments [138, 173]. This structure is a close mimic to the natural acceptor substrate also having an amide function in β -configuration at the reducing end. We determined the thermodynamic dissociation constant of heptasaccharide 1 with FUT8 by means of an SPR affinity assay and found an affinity of $K_D = 390 \mu\text{M}$. The recorded SPR sensorgrams also allow for analysis of the kinetic parameters of the binding process, e.g., the association rate constant k_{on} and the dissociation rate constant k_{off} . We observed a moderate association rate of $k_{on} = 4000 \text{ L s}^{-1} \text{ mol}^{-1}$ and a moderate dissociation rate of $k_{off} = 2 \text{ s}^{-1}$. The dissociation constant from the kinetic on and off rates is $K_D = k_{off}/k_{on} = 500 \mu\text{M}$, which is in excellent agreement with the thermodynamic determination of the K_D value described above.

3.3.2 FUT8 recognises a large epitope of the acceptor substrate

STD NMR allows for mapping the binding epitope of ligands binding to large molecules. This technique requires neither labeling nor high amounts of protein [196, 197]. The absolute and relative STD percentages of heptasaccharide 1 when binding to FUT8 were determined where higher STD effects indicate shorter distances to the enzyme's surface, and the resulting epitope is shown (Fig. 3.13). H-1 and H-2 of GlcNAc-1 and H-2 of Man-4 receive highest saturation transfer.

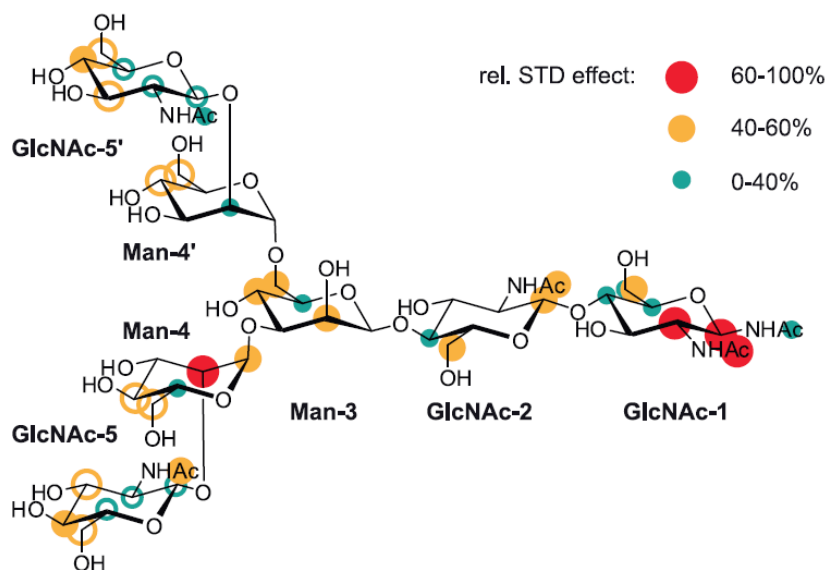


Fig. 3.13 FUT8 affinity analysis and epitope mapping

Acceptor substrate epitope of FUT8. Filled circles indicate the size of the relative STD effect (red = high, orange = medium, green = low). Open circles indicate the sum of STD effects of resonances that are overlapping pairwise.

Furthermore, the other two core residues GlcNAc-2 and Man-3 experience moderate saturation transfer at numerous positions. Thus, the three core saccharide units and the α -1,3 linked mannose unit make the most important protein contacts. However, the antennae also show clear STD effects. The model of GDP-Fuc in complex with FUT8 from our previous work represented the starting point for in silico modeling of the ternary complex [173]. Since there is no indication from protein crystallographic data for the position of the acceptor substrate, we used the molecular docking algorithm GLIDE as implemented in Maestro for initial positioning. The results were subsequently filtered using information of the STD NMR epitope in combination with four additional boundary conditions:

(1) The 6-hydroxy group of GlcNAc-1 of the acceptor substrate has to be in close proximity to the anomeric position of the fucosyl residue of the bound donor in order to allow a transfer of the fucosyl residue to the 6-position of the first GlcNAc residue.

(2) GlcNAc-5 at the 3-mannose branch of the acceptor is essential for the catalytic process and thus, we assumed, has to have contact to the protein.

(3) The shape and size of the acceptor has to match a complementary surface on the protein.

(4) The peptide part of the nascent glycopeptide chain has to be accommodated by the protein/acceptor complex. Taking all these facts together, only one position of the heptasaccharide was possible (Fig. 3.14A).

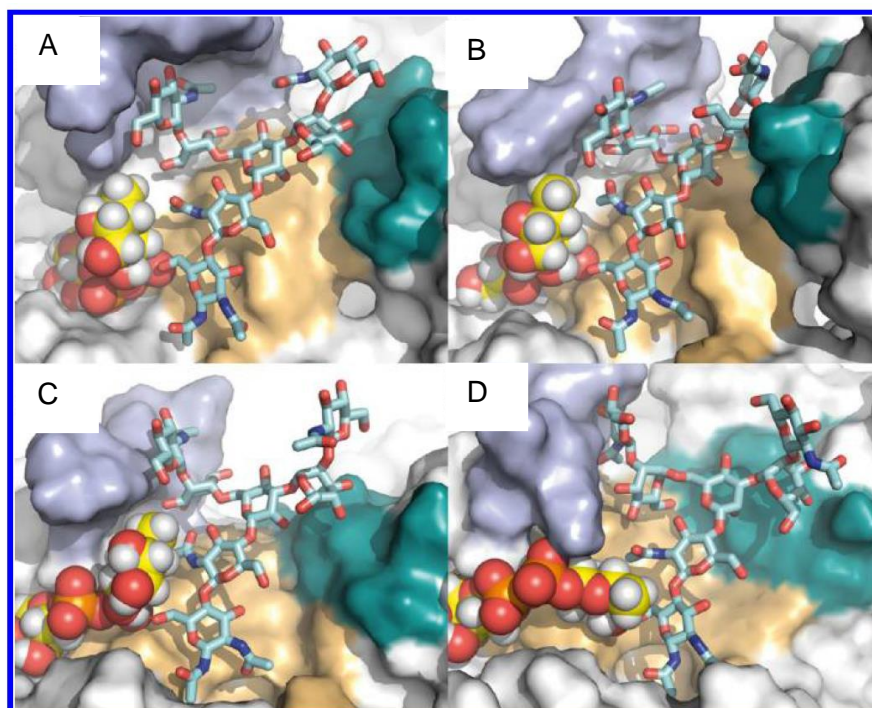


Fig. 3.14 Acceptor binding site of FUT8 at four time steps of the MD simulation

The acceptor oligosaccharide is shown in sticks with cyan carbon atoms, FUT8 with a gray surface, and GDP-Fuc as space filling model with yellow carbon atoms and gray hydrogen atoms. The peptides of FUT8 that form the acceptor binding site are indicated by different colors of the surface: flexible loop (Thr367–His377, blue, top), moderately hydrophobic cavity under the chitobiose (Ser468–Arg473 and Asp494–Gly501, orange) and the C-terminal β -sheets β 10 and β 11 (Ala532–Lys541, teal, right). The four frames clearly show the flexibility of the branches of the acceptor substrate and of the interacting parts of the acceptor substrate binding site.

The structural model of the heptasaccharide from acceptable GLIDE poses were corrected for torsional angles of the glycosidic linkages (neither GLIDE nor any other docking program take the exoanomeric effect into account) prior to the MD simulation. As a result, a pose was obtained, in which the 6-hydroxy function of GlcNAc-1 is close to the anomeric center of the donor, the hydroxymethyl group has a favorable *gt* conformation, the 3-mannose branch is located between the beta sheets β 9 and β 11, and the 6-mannose branch is positioned near the flexible loop (Fig. 3.14A). The positioning of both donor and acceptor substrates was validated by a molecular dynamics simulation (Fig. 3.14A–D) in a water box containing

sodium chloride for 20 ns. Over a large portion of the simulation time neither the position of the donor nor that of the acceptor changed significantly. However, a general change of the overall binding mode was observed after 16 ns in that the acceptor molecule dissociated from the protein. Running the simulation for another 20 ns (40 ns simulation time in total) did not re-establish the initial binding mode of the acceptor. Discussion of the overall binding mode of the heptasaccharide in the ternary complex is therefore based on the first 16 ns. The characteristics of the binding of the acceptor become obvious from the trajectories of the distances of selected atom pairs that participate in hydrogen bonds or hydrophobic contacts between enzyme and acceptor. Interactions of GlcNAc-1 and GlcNAc-2 do not change over the simulation time. All other distances of acceptor atoms from Man-3 and the two branches to enzyme atoms show a much higher variability, and most of them exist only for a fraction of the simulation time. The detailed analysis of the acceptor substrate binding during the MD simulation yields the following results: First, the acceptor is mainly bound via a shallow, large hydrophobic epitope established by the strands Ser468–Arg473 and Asp494–Gly501 that bind the core trisaccharide and Ala532–Lys541 that bind Man-4, both interactions resulting in relatively high STD values. Thus, for acceptor binding we identified a large, shallow cavity of approximately $18 \times 23 \text{ \AA}$ that is adjacent to the donor substrate binding site. Binding strengths are different for the core and the two branches of the acceptor. The general binding of the acceptor is therefore fundamentally different from that of the donor substrate, which is tightly bound in a network of hydrogen bonds and lipophilic interactions in a narrow fold of FUT8 [173]. This observation is also supported by the weak thermodynamic dissociation constant as determined by SPR. In addition, the experimental results from SPR and STD NMR show that the apo form of FUT8 is capable to bind the acceptor substrate with $K_D = 390 \text{ }\mu\text{M}$, although the affinity is weak compared to that of the donor substrate, whose K_D is $9.3 \text{ }\mu\text{M}$ [173].

3.3.3 Donor contributes significantly to acceptor binding

We observed strong interactions between the donor and the acceptor substrate during the MD simulation. First, a hydrogen bond between one of the oxygen atoms of the β -phosphate and the 6-OH of the GlcNAc-1 was observed. This intersubstrate interaction is the only hydrogen bond with a very short average distance of 2.6 \AA that remained in effect for first 16 ns. Second, the methyl group of the acetyl function of GlcNAc-2 is pointed toward the hydrophobic face of the fucose residue and exhibits a stable distance to the C-5 of fucose of 4.4 \AA . Our MD simulation shows the most stable interactions of the acceptor with GDP-Fuc indicating that the hydrogen bonds and hydrophobic interactions of these components contribute a significant proportion to the binding of the acceptor (Fig. 3.15).

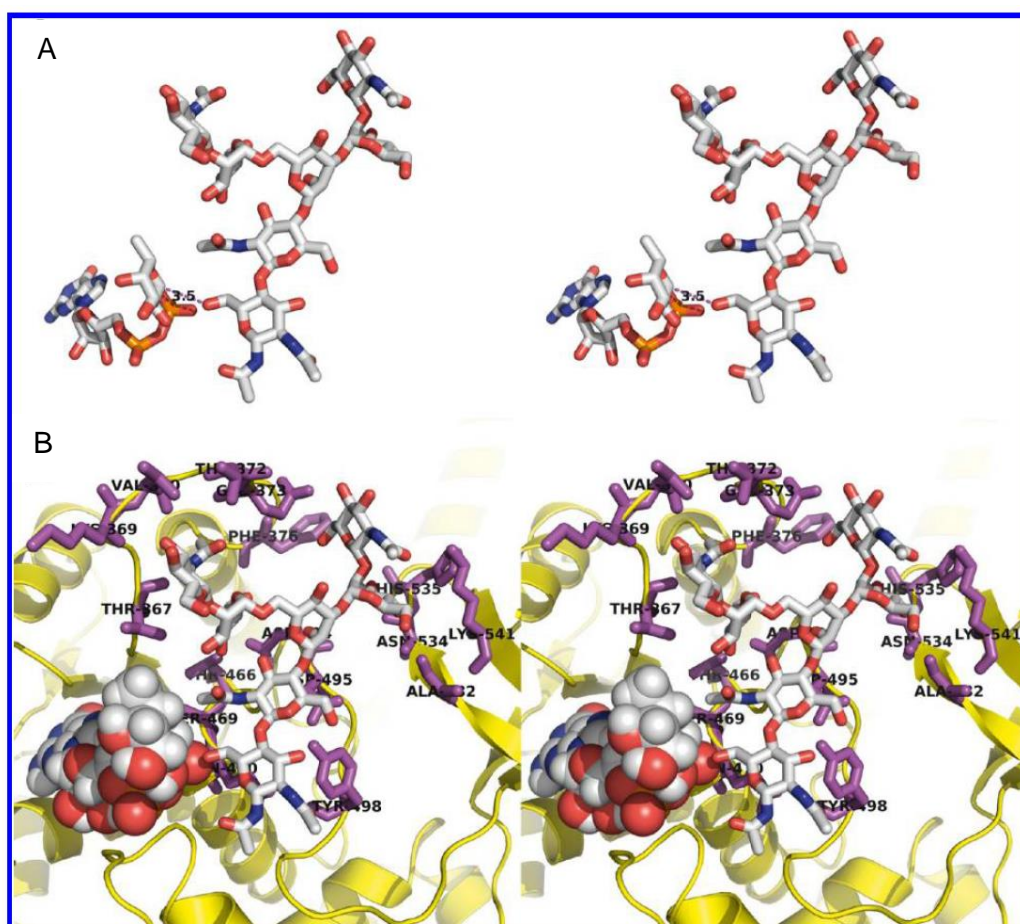


Fig. 3.15 MD simulation of FUT8 acceptor binding

A Cross-eyed stereo plot of donor and acceptor substrate when bound to FUT8 in the ternary complex (1.0 ns). Atoms involved in the nucleophilic attack are the 6-oxygen of the proximal GlcNAc and the anomeric carbon of the fucose (3.5 Å distance, magenta dotted line). B The same frame showing the complex including FUT8 (backbone = yellow ribbon, interacting side chains = magenta sticks). GDP-Fuc is shown as spacefill model, the acceptor heptasaccharide as stick model, and both are colored by atom type

The K_D of the acceptor with the apo enzyme is much larger than the K_M . The interactions listed above explain the increased affinity of the acceptor toward the GDP-Fuc/FUT8 complex compared to the apo enzyme very well. On the basis of the strength of hydrogen bonds in aqueous environment, we estimate an increase of the binding affinity of the acceptor to the FUT8/GDP-Fuc complex by a factor of 10–100 compared to the apo enzyme [255].

3.3.4 Recognition of the branches

The branch at the 3-position of mannose-3 is bound via multiple hydrogen bonds between the flexible loop and the C-terminal β -sheets (Fig. 3.16).

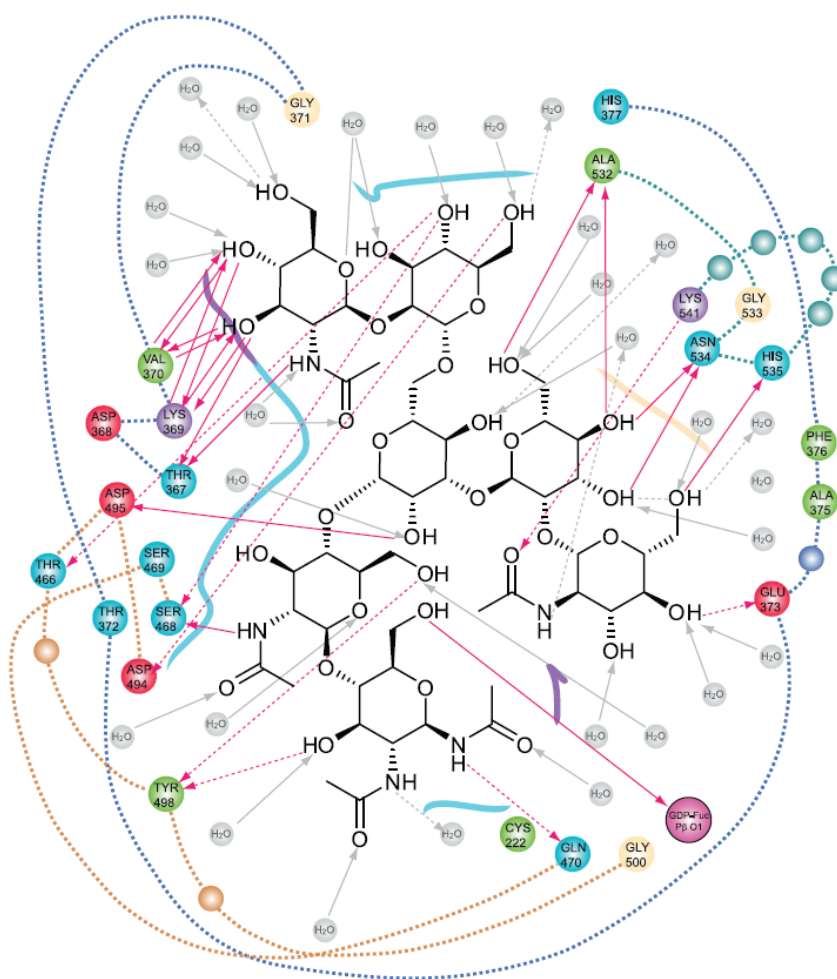


Fig. 3.16 Two-dimensional plot taken from a representative frame of the MD simulation

Two-dimensional plot taken from a representative frame of the MD simulation (1.0 ns) illustrating the interactions of the acceptor substrate with residues in the active site of FUT8. Dotted arrows show hydrogen bonds with functional groups from side chains and solid arrows such with functional groups of the backbone. Other residues shown are close to the substrate and likely to participate in hydrophobic interactions.

All three unsubstituted hydroxy functions of Man-4 are hydrogen bound to Ala532 and Asn534. Lys541 switches a hydrogen bond between the carbonyl of GlcNAc-5 and the OH-4 of Man-4. The epitope from STD NMR studies also indicates in agreement with the MD simulation strong binding of Man-4 to the enzyme. The binding behavior of GlcNAc-5 at the 3-mannose branch is of major interest, as this carbohydrate unit is essential for substrate activity although positioned far from the location of fucosyl transfer. Surprisingly, the essential GlcNAc-5 shows comparatively few interactions both experimentally and theoretically. GlcNAc-5 exhibits considerable flexibility in the MD simulation and shows short-lived interactions with the Lys541 side chain and with the flexible loop (Fig. 3.16). The carboxy function of Glu373 is essential for catalytic activity and was found here to be in contact with the OH-3 and OH-4 of GlcNAc-5 [167]. The more flexible 6-mannose branch is

bound between the strands Thr466–Arg473, Asp494–Gly501, and the flexible loop (Thr367–Glu373) and occupies a favorable *gg* conformation of the C5–C6 bond of Man-3 [256]. All hydroxyl functions of GlcNAc-5' are exclusively bound via hydrogen bonds to the backbone amide functions of residues of the flexible loop. FUT8 has been shown to be tolerant toward substitutions at the 6-mannose branch and the lack of GlcNAc-5' [238, 247, 248]. Three peptide bonds were observed to interact in a time-alternating manner with their carbonyl oxygen as hydrogen bond acceptor or with their nitrogen as hydrogen bond donors. This finding illustrates a highly adaptive nature of the flexible loop.

3.3.5 Role of the essential Lys369 in donor binding and GDP release

The dissociation of the acceptor substrate after 16 ns MD simulation requires a detailed consideration. Remarkably, the origin of this process lies in a change of the donor substrate binding mode. Normally, the guanidinium group of Arg365 interacts with the pyrophosphate of GDP-Fuc. However, the side chain of Arg365 offers considerable flexibility and pulls the pyrophosphate out of the Rossman fold at 16 ns. The hydrogen bond between donor and acceptor subsequently breaks because the β -phosphate is leaving its position. In the next step, the ammonium group of Lys369 binds to the pyrophosphate. This lysine residue is part of the flexible loop and was shown to be essential for catalytic activity of FUT8 [167]. The first 20 ns of the simulation showed the high flexibility of the loop that allows the ammonium group of Lys369 to interact with the β -oxygen of the pyrophosphate of GDP-Fuc if the pyrophosphate is partly released from the Rossman fold. After the pyrophosphate group has moved out of the original binding site mediated by the arginine 365, at 17 ns of simulation time Lys369 establishes a hydrogen bond to the β -phosphate of GDP-Fuc. Arg365 relocates at the same time to the α -phosphate. At the same time the conformation of the fucosyl-pyrophosphate segment changes to a stretched orientation, and the fucose leaves its position [173]. Adopting this orientation, the β -face of the fucose faces the protein surface as shown (Fig. 3.14D).

Hence, GlcNAc-1 and the core trisaccharide of the acceptor are displaced from their original binding site, rendering the complex unstable. As a result, the acceptor heptasaccharide dissociates partly from the binding site. This observation underlines that the proposed orientation of the fucose and the interaction between the substrates are crucial to the mechanism of FUT8.

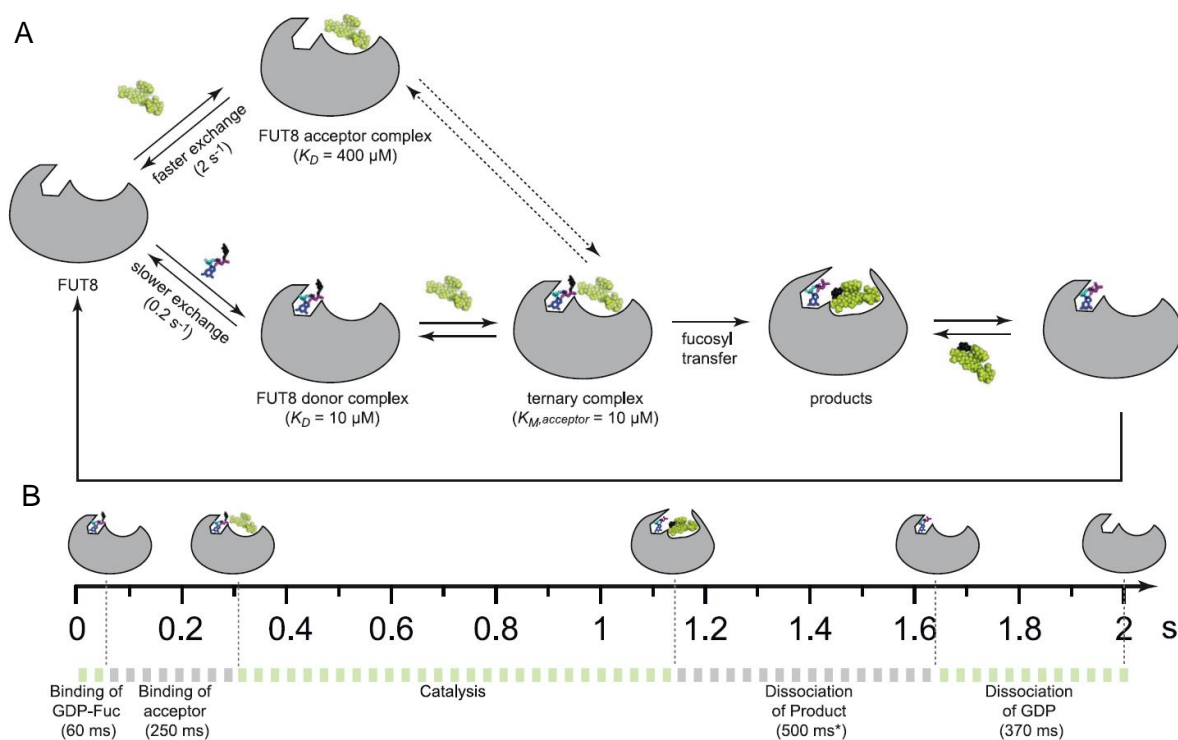
3.3.6 FUT8 acts via an ordered Bi Bi mechanism

FUT8 was proposed to act via a random Bi Bi mechanism, where donor and acceptor substrate bind to the enzyme in random order to form the ternary complex [201]. This

conclusion was drawn from the K_M values of donor and acceptor, which are very similar. The exchange rates of donor (0.2 Hz) and acceptor (2 Hz), however, indicate that the donor substrate binds first to FUT8. The FUT8/GDP-Fuc complex has a lifetime (5.0 s) 10 fold higher than that of the FUT8/acceptor complex (0.5 s). Therefore, it is much more likely that GDP-Fuc is already present in the binding pocket of FUT8 when the acceptor substrate binds. This fact is also supported by the thermodynamics: As the affinity of the apo form of FUT8 is 50 fold higher toward GDP-Fuc than the affinity toward the acceptor, the occupancy of the GDP-Fuc binding site is much higher, especially at lower substrate concentrations. Another indication for the ordered Bi Bi mechanism is the discrepancy between the K_M and K_D values of the acceptor substrate: Whereas the K_M and K_D value are the same for the donor substrate, the K_M is 50 fold lower for the acceptor substrate than the K_D . This difference shows that the affinity of FUT8 toward the acceptor substrate is much higher under the conditions of substrate conversion, i.e., when the donor is present. This mechanism also prevents the hydrolysis of the donor even at low concentrations of the acceptor substrate. Interestingly, GDP-Fuc is hydrolysed by FUT8 with a k_{cat} that is approximately 1/100 of the k_{cat} observed for the transfer to the natural acceptor (data not shown). However, with a 5 fold excess of acceptor substrate in the NMR assay no hydrolysis of the donor substrate is observed. The acceptor substrate is readily converted once it has bound to the FUT8/GDP-Fuc complex, which is indicated by the fact that the conversion rate k_{cat} is similar to the k_{off} of the acceptor. However, the actual mechanism of FUT8 *in vivo* depends on the concentrations of both substrates in the Golgi apparatus, which are difficult to estimate. The concentration of substrates is particularly critical to the association rates. On-rates determined for GDP-Fuc ($5500 \text{ L mol}^{-1} \text{ s}^{-1}$) and for the acceptor heptasaccharide ($4000 \text{ L mol}^{-1} \text{ s}^{-1}$) are a measure for the association events per second at a concentration of 1 M for enzyme and substrate. Multiplying k_{on} with the concentration of the ligand yields the binding events per second at the given concentration of the ligand. As the concentration of FUT8 is low compared to that of the substrates, it can be neglected in the calculation of the association events per second. The association rates given (Scheme 1) are calculated for the initial substrate concentrations employed in the assay (3 mM GDPFuc and 0.9 mM acceptor substrate), which convert to on-rates expressed as binding events per second to 16.5 s^{-1} for GDPFuc and 4 s^{-1} for the acceptor heptasaccharide. The reciprocal of the on-rates is equivalent to the time for the binding event to take place. These times are used to generate an approximate time line for the reaction (Scheme 1). The times for the products to leave the protein are calculated as the inverse of the off-rates. The off-rate of the fucosylated product was estimated to be the same as that of the acceptor heptasaccharide in the apo enzyme. Decreasing substrate concentrations during the enzymatic reaction lower the

number of association events per second and therefore reduce the turnover rate. Ordered Bi Bi mechanisms where the donor substrate binds first have been proposed for other glycosyltransferases [189, 190, 202]. However, it has only been proven in few select cases. Such a kinetic mechanism is often explained by a model in which the acceptor is stacked on top of the nucleotide sugar in the active site or, in some cases, by substrate-dependent ordering of flexible loops. The mechanism of FUT8 is different in that in the ternary complex the donor is necessary to induce a stable binding of the acceptor

Scheme 1 proposed kinetic mechanism for FUT8^a



^aA According to the exchange rates, the donor binds first to FUT8 (cf. text). After binding of the acceptor, which is assisted by the bound donor, the acceptor substrate is rapidly converted and both products are released in unknown order. Hypothetically, FUT8 undergoes one or more conformational changes upon substrate binding. It is unclear if the ternary complex can also form from the FUT8/acceptor complex (dotted lines).

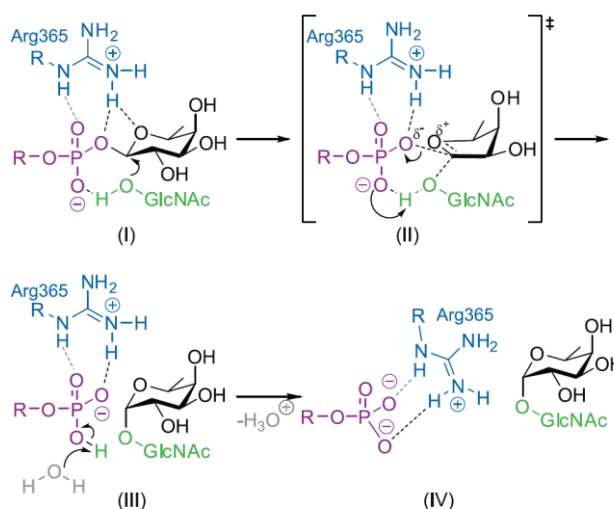
B Estimated time line indicating the statistical duration of the individual steps of the catalytic cycle of FUT8 (cf. text).

3.3.7 FUT8 employs a substrate-assisted mechanism

The mechanistic strategy applied by inverting glycosyltransferases is that of a direct displacement $\text{S}_{\text{N}}2$ -like reaction [257, 258]. In many inverting glycosyltransferases an active-site side chain, often glutamate or aspartate, serves as a base catalyst [257]. The base catalyst increases the nucleophilicity of the hydroxyl group of the acceptor by deprotonation and facilitates the direct displacement of the phosphate leaving group. The identity of the base catalyst is therefore a key question in the mechanism of inverting glycosyltransferases

[257]. In the structure of FUT8 there is no basic residue present that could act as an assisting base. Instead, our results strongly suggest that the β -phosphate of the bound GDP-Fuc acts as a base in the catalytic process of FUT8. The length of the hydrogen bond established between the oxygen of the β -phosphate of GDP-Fuc and the O-6 of GlcNAc-1 is 2.6 Å, indicating a very tight interaction due to a strong hydrogen bond. For a similar reason, such a mechanism has also been proposed for cePOFUT27 and, very recently, for hOGT, which is not related to FUT8 [259]. Furthermore, the importance of the β -phosphate group for catalysis is an explanation for very strong binding of the β -phosphate group by FUT8, an observation that is rather unusual for other glycosyltransferases [173, 201]. The tight binding of the β -phosphate guarantees a precise orientation of the incoming nucleophile with respect to the anomeric carbon of the fucose and to the residues that are active in catalysis, such as Arg365. The complete catalytic mechanism is deduced from the data for FUT8 (Scheme 2).

Scheme 2 proposed catalytic mechanism for the reaction catalysed by FUT8^a



^aAn oxygen of the β -phosphate group of GDP-Fuc assists in deprotonation of the 6-hydroxyl group of GlcNAc-1 of the acceptor substrate in order to promote a nucleophilic attack to the anomeric carbon of the fucose (I). The direct nucleophilic displacement mechanism involves a single transition state with oxocarbenium ionlike character (II). Protonation of the phosphate improves the leaving group qualities of GDP (III). The resulting negative charge is neutralised by the side chain of Arg365 (IV).

The key catalytic residue Arg365 binds the donor molecule and orients the fucose moiety by forming a bifurcated hydrogen bond with its N η to O-1'' and O-5'' [173]. The hydrogen bond between the oxygen of the β -phosphate of GDP-Fuc and O-6 of GlcNAc-1 ensures the nucleophile to be in close proximity to the anomeric carbon (3.6 Å). After the nucleophilic attack of O-6 at the anomeric carbon of fucose, a single transition state with delocalisation of a partial positive charge to the ring oxygen is traversed. The phosphate acts as leaving group, and the developing negative charge at the former O-1'' is further stabilised by Arg365.

Simultaneous protonation of the β -phosphate further enhances its qualities as a leaving group. After the transfer of the fucosyl residue is completed, Arg365 binds exclusively to the β -phosphate of GDP, which is quickly released as fast off-rates indicate [173]. The mechanism proposed here does not involve an oxocarbenium ion intermediate but rather a highly activated pyrophosphate as leaving group in a SN_2 -type mechanism. Some other FucTs have been proposed to act via an SN_1 -like mechanism involving a more or less separated oxocarbenium/ phosphate ion pair [251, 260]. However, for FUT8, there is evidence for an SN_2 -like mechanism. First, catalytic efficiency is easier to achieve for the enzyme selecting a mechanism with an intermediate species of lower energy. Second, the enzyme lacks a basic residue to stabilise an oxocarbenium ion. In accordance with the Hammond postulate this corresponds to a (stabilised) transition state of the lowest possible free energy.

3.4 Component resolution reveals additional major allergens in patients with bee venom allergy

Diagnosis of Hymenoptera venom allergy is commonly based on a history of anaphylactic sting reactions, positive skin test results, and/or detection of specific IgE to venom of honey bee or *Vespula* species [64]. Positive results on skin and serologic tests with conventional venom preparations are frequently caused by antibodies cross-reactive to conserved structures found in venom allergens. These include homologous primary structures of protein allergens (eg, hyaluronidases, dipeptidyl peptidases IV, and vitellogenins) and cross-reactive carbohydrate determinants (CCD), which are present on the majority of Hymenoptera venom allergens [113, 179, 180]. Double positivity to bee (HBV) and yellow jacket venom (YJV) in patients who have not been able to identify the culprit insect necessitates additional laboratory tests (eg, IgE inhibition assays or basophil activation tests) that are expensive, time-consuming, difficult to interpret, and therefore rarely used in the clinical routine [82, 261]. Recently, the diagnostic value of IgE detection to CCD-free, species specific recombinant Hymenoptera venom allergens, such as HBV phospholipase A2 (rApi m 1), YJV phospholipase A1 (rVes v 1), and antigen 5 (rVes v 5), was demonstrated [71, 74, 174, 262-265]. In contrast to the situation of YJV allergy, the frequency of sensitisation to rApi m 1, the only recombinant HBV allergen commercially available to date, in patients with HBV allergy ranges from 58% to 80%, which is insufficient to support a definitive diagnosis of HBV allergy [74, 174, 262, 263, 265-267]. This suggests that additional HBV allergens are of relevance for sensitisation and hence the diagnosis of HBV allergy. The best characterised HBV allergens are phospholipase A2 (Api m 1), hyaluronidase (Api m 2), and the basic peptide

melittin (Api m 4), which all constitute medium- to high-abundance proteins [268, 269]. More recently, additional HBV allergens of lower abundance have been cloned and characterised, such as acid phosphatase (Api m 3), dipeptidylpeptidase IV (Api m 5), Api m 6, major royal jelly proteins 8 and 9 (Api m 11.0101 and Api m 11.0201), icarapin (Api m 10), and vitellogenin (Api m 12) [69, 70, 72, 81, 270-272]. Insect cell-based expression strategies allowed for detection of IgE reactivity of these allergens independent of the presence of CCDs [71]. The recombinant availability enabled analysis of different venom preparations, demonstrating that lower-abundance components, such as Api m 3 and Api m 10, although present in the crude HBV, are absent or underrepresented in preparations used for HBV immunotherapy [271]. Here we analysed the sensitisation profile of patients with HBV allergy to a panel of CCD-free HBV allergens, including rApi m 1, rApi m 2, rApi m 3, nApi m 4, rApi m 5, and rApi m 10, by using the ImmunoCAP assay system (Thermo Fischer Scientific, Uppsala, Sweden). Inclusion of additional allergens improved the sensitivity of component-based diagnostics and demonstrated distinct sensitisation profiles, some of which displayed prominent sensitisations to Api m 3 and Api m 10. In the same line, we observed a lack of Api m 3- and Api m 10 specific IgG₄ induction during HBV immunotherapy, suggesting that sensitisation profiles to allergens that are not sufficiently present in therapeutic HBV preparations might be of relevance for the outcome of HBV immunotherapy.

3.4.1 IgE reactivity to HBV allergens in patients with HBV allergy, patients with YJV allergy, and HBV-nonallergic control subjects

IgE reactivity (>0.35 kUA/L) to the commercially available rApi m 1 (i208) was detected in 72.2%, to rApi m 2 in 47.9%, to rApi m 3 in 50.0%, to nApi m 4 in 22.9%, to rApi m 5 in 58.3%, and to rApi m 10 in 61.8% of patients with HBV allergy (Fig. 3.17). In patients with YJV allergy, no relevant IgE reactivity was detected, except to rApi m 5 (3/40, Fig. 3.17), the crossreactive dipeptidylpeptidase also present in YJV as Ves v 3. Of the 40 HBV-non allergic control subjects, 6 (15%) displayed IgE reactivity of 0.35 kUA/L or greater to HBV (ImmunoCAP i1), which is in line with previous reports [273]. In this subgroup of 6 control subjects, IgE reactivity to rApi m 1 was detected in 3, to rApi m 5 in 2, and to rApi m 10 in 1 subjects. No IgE reactivity to any of the tested HBV allergens was detected in the ImmunoCAP i1 negative control sera (Fig. 3.17).

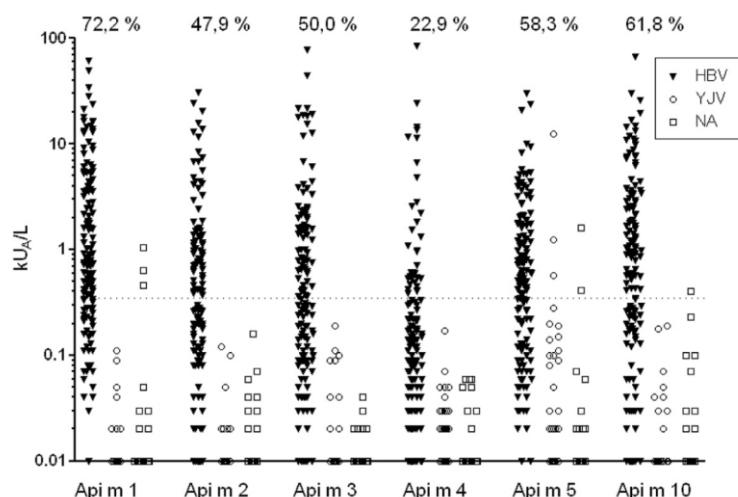


Fig. 3.17 IgE immunoreactivity of individual patient sera with recombinant allergens

IgE reactivity to HBV allergens of sera from patients with HBV allergy ($n = 144$), patients with YJV allergy ($n = 40$), and HBV-exposed but nonallergic control subjects (NA; $n = 40$). The lower-end cutoff of the CAP-FEIA (<0.35 kU_A/L) is represented as a dotted line.

Among the patients with HBV allergy, positive results to at least 1 HBV allergen were detected in 94.4%, and positive results to at least 1 of the HBV specific allergens Api m 1, 3, 4, or 10 were detected in 89.6% (Fig. 3.18).

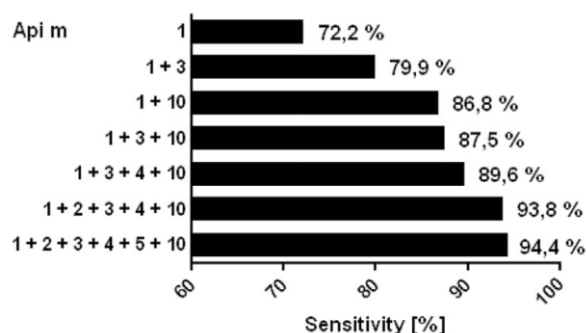


Fig. 3.18 Diagnostic sensitivity of sIgE to different combinations of HBV allergens

Detection of IgE reactivity to a panel of HBV allergens increases diagnostic sensitivity in patients with HBV allergy ($n = 144$).

The majority of patients with HBV allergy were sensitised to more than 1 allergen (74.3%), and a minority (9.7%) were sensitised to all allergens tested. Interestingly, HBV-monosensitised patients ($n = 54$) had lower total IgE levels, lower levels of sIgE to HBV (ImmunoCAP i1), and lower levels of sIgE to all HBV allergens tested when compared with patients with HBV allergy who were also sensitised to YJV (ImmunoCAP i3, $n=590$).

3.4.2 Sensitisation profiles in patients with HBV allergy

Among the patients with HBV allergy, 39 of 64 possible different sensitisation profiles were present, and the 10 most frequent profiles covered 64% of the study population. As

suggested from analysis of IgE profile complexity, the number of allergens detected showed a clear association with the concentration of sIgE to HBV. Interestingly, the mono sensitised patients mostly display lower sIgE levels to lower numbers of allergens, and double-sensitised patients recognise multiple bee venom allergens [274]. IgE reactivity to Api m 3, Api m 10, or both was detected in 68% of the patients, and 7 (4.8%) patients displayed IgE reactivity exclusively to Api m 3, Api m 10, or both. This is of particular interest because Api m 3 and Api m 10 have been demonstrated to be absent or underrepresented in HBV preparations used for immunotherapy [69, 70].

3.4.3 IgE reactivity to HBV allergens in relation to whole HBV

IgE reactivity to HBV (ImmunoCAP i1) displayed a significant correlation ($r = 0.94$, $P < .0001$) with the sum of IgE reactivity to Api m 1, Api m 2, Api m 3, Api m 4, Api m 5, Api m 10, and CCDs (Fig. 3.19A).

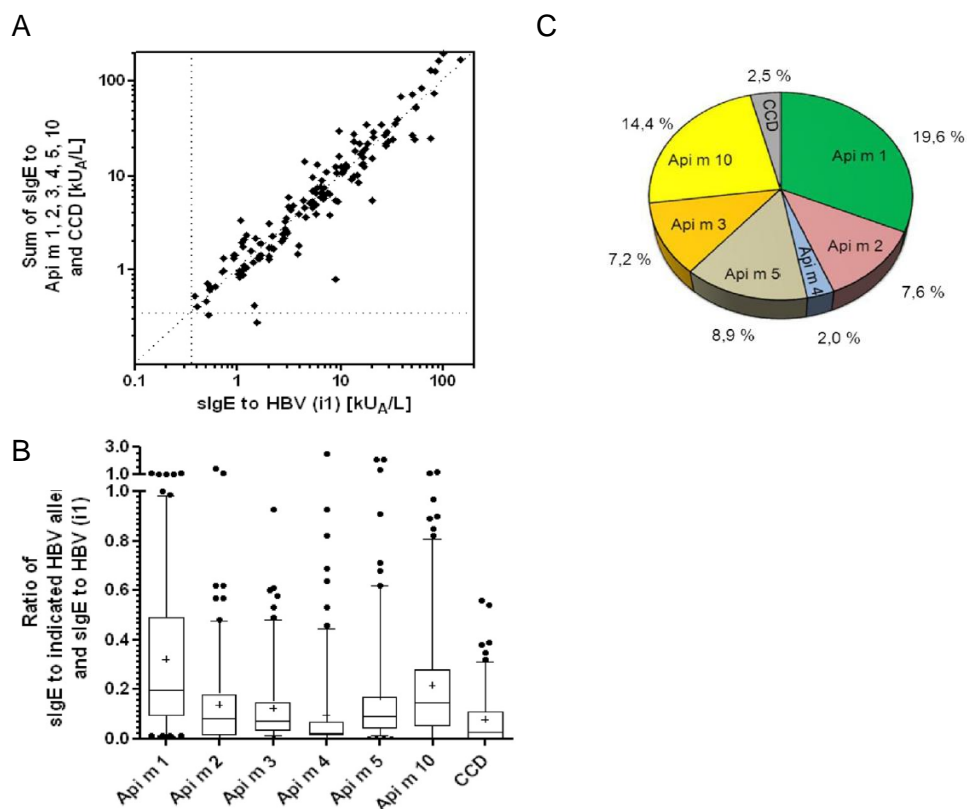


Fig. 3.19 IgE reactivity to single HBV allergens in relation to sIgE to HBV

A IgE reactivity to HBV (ImmunoCAP i1) in patients with HBV allergy (n 5 144) in relation to the sum of IgE reactivity to Api m 1, Api m 2, Api m 3, Api m 4, Api m 5, Api m 10, and CCDs. B The relative sIgE reactivity to single HBV allergens was calculated as a ratio of sIgE reactivity to HBV and displayed as a whisker plot with medians; 5th, 25th, 75th, and 95th percentiles; and outliers. C The median was used to present the relative contribution to IgE reactivity of single allergens as a pie chart.

The relative contribution of sIgE to the different allergens was calculated in relation to and expressed as a percentage of sIgE to HBV (ImmunoCAP i1; Fig 3.19, B and C). The relative IgE reactivity to Api m 3 (median, 7%; 25% to 75% interquartile range [IQR25/75], 3%/14%) and Api m 10 (median, 14%; IQR25/75, 5%/28%), even though lower than the relative IgE reactivity to Api m 1 (median, 20%; IQR25/75, 9%/49%), suggests a relevant role in HBV allergy. CAP-FEIA inhibition experiments with titrated doses of recombinant allergens in equimolar concentrations (Fig. 3.20A) in patients either sensitised to Api m 1 and not to Api m 10 or vice versa confirmed the relative contribution of IgE directed against Api m 1 and Api m 10.

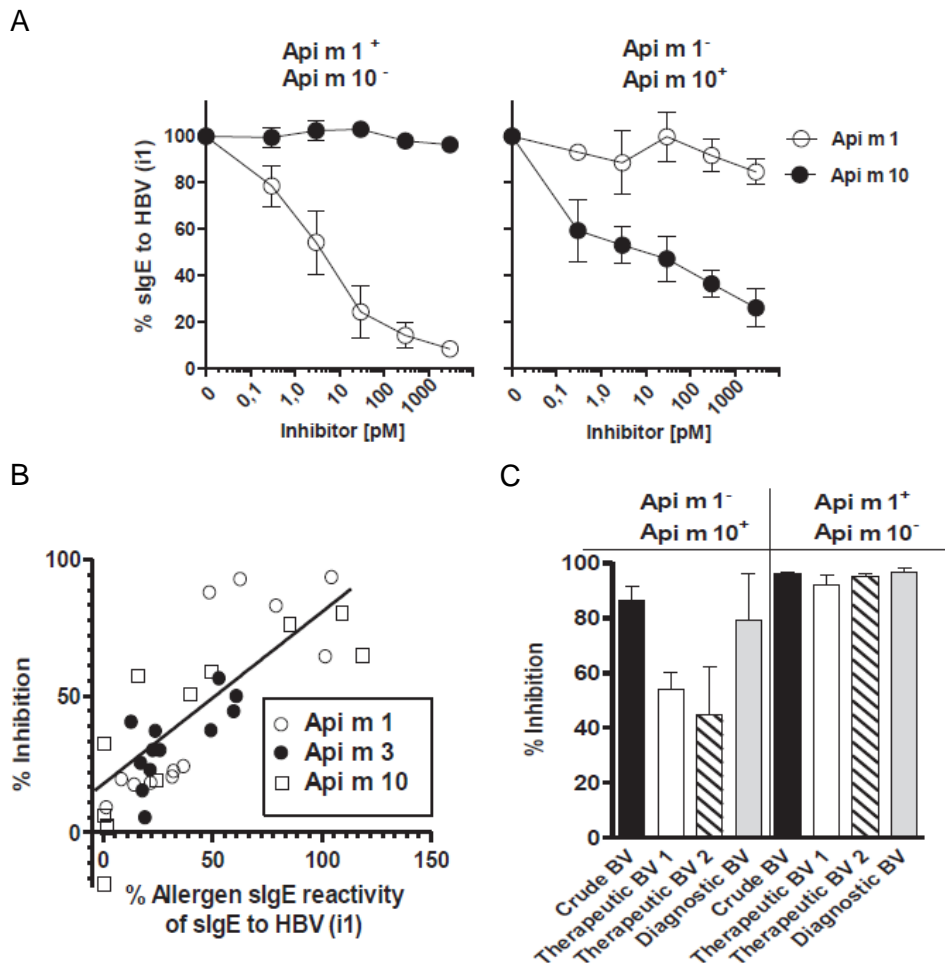


Fig. 3.20 Inhibition of IgE reactivity to HBV (ImmunoCAP i1) by single HBV allergens or crude or therapeutic HBV preparations

A CAP-FEIA inhibition of sIgE reactivity to HBV (ImmunoCAP i1) was performed with Api m 1 or Api m 10 as inhibitors at increasing concentrations in patients with predominant Api m 1 sensitisation or in patients with a predominant Api m 10 sensitisation. B CAP-FEIA inhibition of sIgE reactivity to HBV (ImmunoCAP i1) was performed with Api m 1, Api m 3, or Api m 10 at 300 nmol/L in patients with HBV allergy. The degree of CAP-FEIA inhibition was correlated with the relative IgE reactivity to Api m 1, Api m 3, or Api m 10, as calculated in Fig.3.19 ($P < .0001$, $r = 0.8082$). C CAP-FEIA inhibition of sIgE reactivity to HBV (ImmunoCAP i1) was performed with a crude HBV, a diagnostic HBV, or 2 different therapeutic HBV preparations at 300 mg/mL in patients with predominant Api m 1 sensitisation or in patients with predominant Api m 10 sensitisation BV, Bee venom.

Similarly, the degree of maximal inhibition with Api m 1, Api m 3, and Api m 10 correlated with the calculated relative IgE reactivity (Fig. 3.20B). Inhibition of HBV sIgE reactivity by different HBV preparations, such as crude HBV or therapeutic preparations, provided a means to demonstrate the presence of individual allergens in the preparation. For the predominantly Api m 1 positive sera, both a crude and a therapeutic HBV preparation blocked the IgE binding to a similar degree. In contrast, in predominantly Api m 10 positive sera (relative IgE reactivity, 54%; range, 35% to 72%), therapeutic HBV preparations were clearly less effective compared with a crude HBV preparation (Fig. 3.20C). This result is consistent with the previously reported absence of Api m 10 from therapeutic HBV preparations [271].

3.4.4 HBV allergen-specific IgG₄ during HBV immunotherapy

Finally, we analysed IgG₄ responses to the HBV specific allergens Api m 1, Api m 3, Api m 4, and Api m 10 in 20 patients who had undergone HBV immunotherapy for 12 to 48 months. A prominent induction of sIgG₄ was observed for the 2 highly abundant allergens Api m 1 and Api m 4, which was comparable with that observed with whole HBV. In contrast, no or very little sIgG₄ induction was observed for the low-abundance allergens Api m 3 and Api m 10 (Fig. 3.21), again supporting the notion that Api m 3 and Api m 10 might be underrepresented in therapeutic HBV preparations.

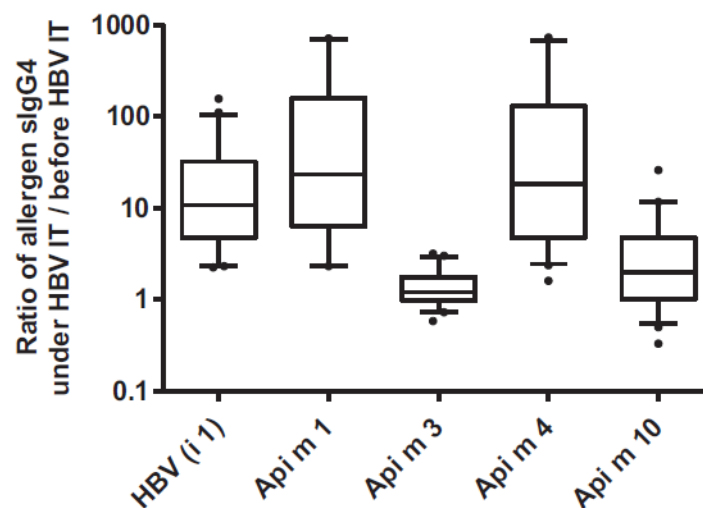


Fig. 3.21 Induction of allergen specific IgG₄ during HBV immunotherapy

sIgG₄ responses to Api m 1, Api m 3, Api m 4, and Api m 10 were analysed in patients before and 12 to 36 months after initiation of HBV immunotherapy (n = 20). The induction of sIgG₄ was expressed as the ratio of sIgG₄ during immunotherapy/sIgG₄ before immunotherapy and is displayed as whisker plots with medians; 5th, 25th, 75th, and 95th percentiles; and outliers.

3.5 *Polistes* species venom is devoid of carbohydrate-based cross-reactivity and allows interference-free diagnostics

Allergy to venom of paper wasps (*Polistinae*) is common in North America as well as in Europe, especially in Mediterranean areas. The most important *Polistes* species in Europe are *P. dominula* and *P. gallicus*, whereas in Northern America other species such as *P. annularis*, *P. apachus*, *P. exclamans*, *P. fuscatus*, and *P. metricus* are dominant. In the last few decades, *P. dominula* has increasingly spread across the North American continent and the central and northern parts of Europe. This phenomenon has been suggested to be associated with environmental changes, explaining the increasing importance of *Polistes* venom allergy as a cause for anaphylactic Hymenoptera sting reactions. A lack of molecular tools and the neglect of specific diagnosis in northern regions classically dominated by other Hymenoptera such as yellow jackets and honeybees are likely to additionally contribute to underestimating *Polistes* venom (PV) allergy [275, 276]. Diagnosis of Hymenoptera venom allergy is based on a history of anaphylactic sting reactions, positive skin test responses, and/ or detection of specific IgE to Hymenoptera venom. Positive results in skin and serological tests with conventional venom extracts, however, do not always reflect genuine sensitisations but are frequently caused by clinically irrelevant cross-reactive antibodies. Treatment modalities therefore often include different venoms, resulting in higher costs, increased risk of severe side effects, and possible de novo sensitisations [277]. A high percentage of cross-reactivity has been attributed to IgE directed against cross-reactive carbohydrate determinants (CCDs), namely, to α -1,3 linked core fucose residues of glycoproteins. Therefore, molecular diagnosis applying nonglycosylated species-specific allergens and strategies to circumvent α -1,3-core fucosylation led to a significant advance in the dissection of true double sensitisation versus irrelevant cross-reactivity [71, 174]. The molecular cross-reactivity between European and American *Polistes* species is described as rather low because they belong to different subgenera. In contrast, cross-reactivity between *Polistinae* and *Vespinae* (*Vespula*, *Dolichovespula*, and *Vespa*) venoms and purified venom proteins is frequently observed especially for *Vespula* and American as well as European PV [275, 276]. Moreover, it is widely accepted that IgE cross-reactivity in a significant fraction of patients can be attributed to CCDs [275].

3.5.1 CCD-reactivity analysis of *Polistes* venom

In this study, we addressed for the first time the CCD reactivity of European and American PV. We utilised *Galanthus nivalis* agglutinin, which indicates the general presence of N-linked glycans, and rabbit anti-horseradish peroxidase (HRP) serum that specifically detects α -1,3-core fucosylation of insect venoms [140]. Applying *Galanthus nivalis* agglutinin

in AlaBlots (Siemens Healthcare Diagnostics, Los Angeles, Calif) with *Polistes* species (i4), *A. mellifera* (i1), and *V. vulgaris* (i3) venom demonstrated the presence of several glycoproteins in all 3 venoms (Fig. 3.22A).

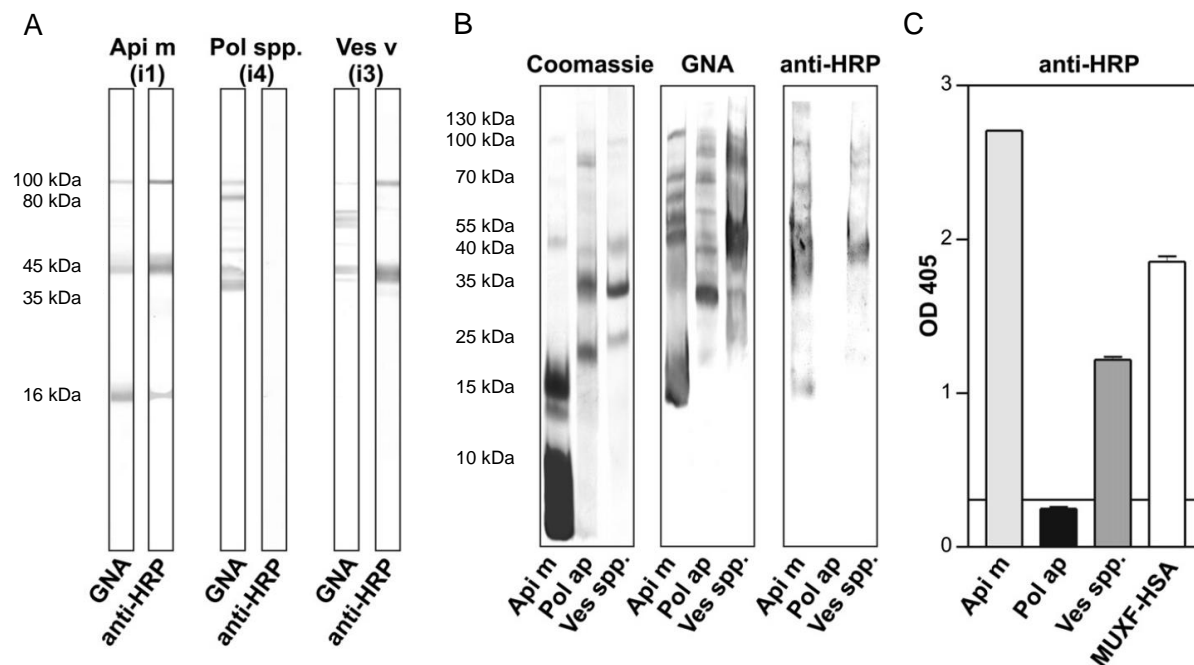


Fig. 3.22 Glycosylation pattern of *Polistes*, *Apis*, and *Vespula* venom preparations

A AlaBlots of *Apis mellifera*, *Polistes* species, and *Vespula vulgaris* venom detected with *Galanthus nivalis* agglutinin indicating the presence of glycosylation or with anti-HRP serum specific for α -1,3-core fucosylation. B SDS-PAGE and immunoblot analysis of *A. mellifera*, *Polistes apachus*, and *Vespula* species venom visualised as above. C ELISA analysis of *A. mellifera*, *P. apachus*, and *Vespula* species venom and MUXF-human serum albumin conjugate by using the anti-HRP serum. GNA, *Galanthus nivalis* agglutinin.

The use of anti-HRP serum in AlaBlots revealed pronounced α -1,3-core fucosylation for honeybee venom (HBV) as well as for yellow jacket venom (YJV). In contrast, *Polistes* species venom, which is a mixture of venoms of different American *Polistes* species, did not show any α -1,3-core fucosylation and hence CCD reactivity (Fig. 3.22A). Comparable results were obtained when we analysed the individual venom of *Polistes apachus* compared with HBV and *Vespula* species venom (Fig. 3.22B). Immunoblot analyses demonstrated pronounced glycosylation of *Polistes apachus* venom allergens but the absence of CCD-based reactivity. ELISA analysis with anti-HRP serum corroborated the absence of any α -1,3 core fucosylation and CCD reactivity of *P. apachus* venom (Fig. 3.22C).

3.5.2 Screening of CCD reactive Hymenoptera venom allergic patients sera

In addition, we analysed sera of 2 patient groups with known IgE reactivity to CCD (as determined by the detection of specific IgE to CCD markers) and a low probability to have

carbohydrate independent specific IgE to *Polistes* venom: (1) patients with confirmed HBV allergy but no history of YJV or PV allergy and (2) patients with grass pollen allergy without clinical history of Hymenoptera venom allergy. Overall, 17 sera of patients with confirmed HBV allergy displayed strong reactivity with sensitizing HBV (Fig. 3.23A) and medium to strong reactivity with MUXF and YJV, indicating the presence of CCD specific IgE antibodies.

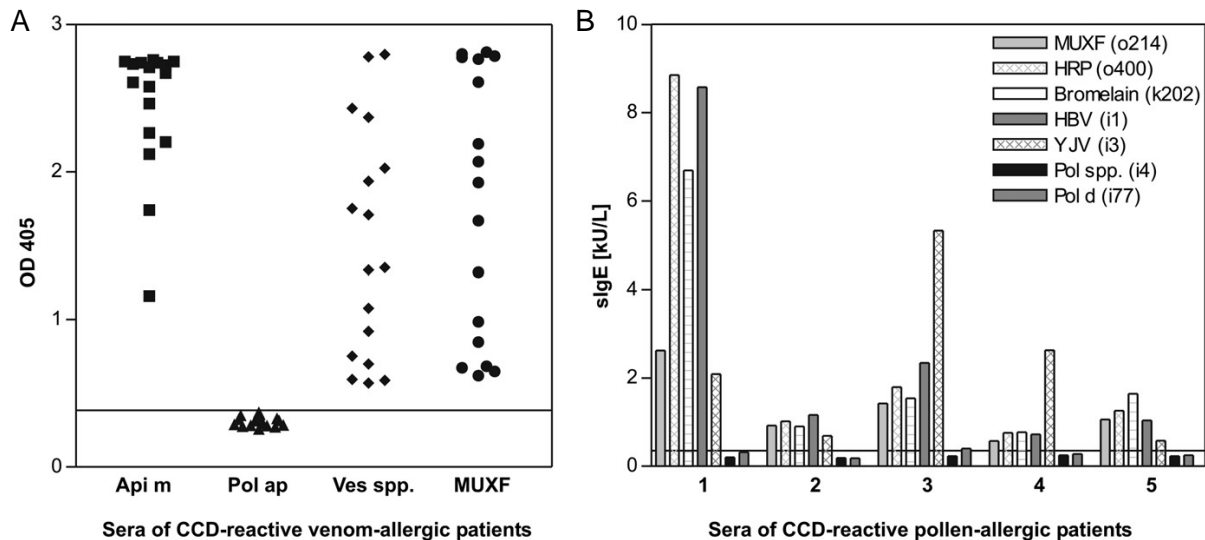


Fig. 3.23 Venom IgE immunoreactivity of individual CCD-reactive patient sera

A IgE reactivity of sera of CCD reactive HBV-allergic patients with *Apis mellifera*, *Polistes apachus*, and *Vespula* species venom and MUXF-HSA conjugate was assessed by using ELISA. The lower end functional cut-off is represented by a solid line. B IgE reactivity of CCD-reactive pollen-allergic patients with MUXF, HRP, bromelain, HBV, and YJV. *Polistes* species venom and *Polistes dominula* venom as determined by ImmunoCAP.

In stark contrast, none of the sera showed any reactivity with *Polistes apachus* venom, suggesting the lack of interference by CCD reactivity. From the grass pollen-allergic patients without clinical history of Hymenoptera venom allergy, 5 sera were selected that exhibited pronounced specific IgE reactivity to the CCD markers MUXF (o214), HRP (o400), and bromelain (k202) as analysed by ImmunoCAP (Thermo Fisher Scientific, Freiburg, Germany) (Fig. 3.23B). As expected, all patients exhibited additional reactivity with HBV (i1) and YJV (i3) extract. In contrast, none of the CCD reactive sera showed reactivity with American (i4) and European (i77) PV. Only 1 serum exhibited a very low reactivity over the cut-off with European PV. Interestingly, this finding appears to be a result of genuine sensitisation to YJV and cross-reactivity because this serum additionally showed minor reactivity with non-glycosylated Ves v 1 and Ves v 5 (not shown).

3.6 Fine specificity of IgE carbohydrate reactivity dissected by establishing xenobiotic epitopes with glyco-engineered cell lines

Glycosylation is probably the most abundant posttranslational modification of proteins and is divided in N-glycosylation of asparagine residues and O-glycosylation of hydroxyl residues of amino acids like serin [89, 91]. Many pathogenic mechanisms, like cancer formation, development disorders and allergic reactions are caused by altered glycosylation [89, 107, 278, 279].

Glycosylation starts in the Endoplasmic reticulum (ER) where a glycan precursor ($\text{Glc}_3\text{Man}_9\text{GlcNAc}_2$) is linked to nascent proteins [89]. Subsequently the glycan precursor is modified in several steps in the ER and the Golgi apparatus (GA) [89].

In general glycosylation is a heterogeneous event due to the synthesis of the glycans by different glycosyltransferases. The structure of the glycan depends on the expression level of the participating glycosyltransferases, which is influenced by tissue-, development- and species-dependent differences. Plants are well known to alter complex N-glycans with β -1,2 xylose and α -1,3-core fucose, the same applies to helminths. Insects, like the honeybee, modify their glycans with α -1,3-core fucose. Compared to that snail glycans are xylosylated to a greater extent and only weakly fucosylated. Key enzymes for these glycosylation motifs, the β -1,2 xylosyltransferase and the α -1,3-core fucosyltransferase, are type II membrane proteins, consisting of a small cytoplasmatic tail, a trans domain, a short linker and the catalytic domain, inside of the GA lumen [24, 123, 139, 144]. In plants the β -1,2 xylosylation of the innermost core mannose is accomplished directly before the fucose residue is linked to the innermost core GlcNAc [144]. β -1,2 xylose and α -1,3-core fucose as well as the α -gal epitope are known as Cross-reactive Carbohydrate Determinants (CCDs); these glycan modifications cannot be found on human glycans and provoke immune reactions [66, 106, 107, 271, 280]. About 20-40% of allergic patients produce specific IgE antibodies against these carbohydrate based epitopes [107, 123]. These antibodies are responsible for pronounced cross-reactivity between e.g. pollen and Hymenoptera allergic patients sera, because these antibodies are able to react with different allergens from a variety of different natural sources (also sources not responsible for true sensitisation), as long as the relevant glycan is present [281]. Prominent CCD bearing allergen sources include plants like tomato, latex and peanut and insects like wasp, honeybee and house dust mite. Red meat is a prominent CCD carrier for the α -gal epitope, which can cause delayed anaphylactic reactions. Furthermore some biologicals could act as CCD carriers, if the therapeutics were produced in expression systems modifying the glycans with CCDs [106, 282]. It's known for a long time that CCDs are often responsible for massive false-positive results in diagnostic approaches [281]. While the diagnostic relevance of the CCDs is

proven, the clinical relevance as well as biological and cellular effects of the CCDs remain elusive and are controversially discussed [123, 283]. Distinguishing specific carbohydrate based reactivity patterns of allergic patient sera is particularly difficult due to non-available tools, which would allow a spatially separated dissection of xylose or fucose specific IgEs. These difficulties are owed to the fact that currently used CCD-markers like bromelain bear fucose as well as xylose.

In this study we dissected immunoglobulin specificity for certain glycotopes by generation of glycoengineered insect cell lines with variable abilities for α -1,3-core fucosylation and β -1,2 xylosylation. For dissection of immunoglobulin reactivity to α -1,3-core fucose or β -1,2 xylose the immunogenic glycotopes were expressed on an immunologically inert scaffold protein as intact glycans. As scaffold glycoprotein for the formation of the CCDs the high abundant human serum protein alpha-2HS-glycoprotein (AHSG) was expressed in the glycoengineered insect cell lines. The resulting molecular tool now allows a dissection of IgE- and IgG-reactivity to certain glycotopes, and will gain insights into the recognition of such epitopes on a molecular level.

3.6.1 Cloning of β -1,2 xylosyltransferase and alpha-2HS-glycoprotein

β -1,2 xylosyltransferase is the key enzyme for the establishment of CCD-reactive allergens in plants. Before a nascent glycan is modified by the α -1,3-core fucosyltransferase the glycan has to be xylosylated otherwise the glycan is not converted by the α -1,3-core fucosyltransferase. To establish insect cell lines capable of xylosylation the culprit enzyme of *G. max* was amplified from leave cDNA. Due to a high GC-content, the 5'-part of the enzyme could not be amplified directly from cDNA in contrast to the 3'-part. Therefore the 5'-part was chemically synthesised using a predicted gene sequence. Finally both parts were joined by PCR based methods and the final sequence was confirmed by sequencing and comparison with the predicted database sequence. The compared sequences showed a homology of the cloned β -1,2 xylosyltransferase of *G. max* and the predicted data file sequences of 100% (Scheme 3).

RESULTS

Scheme 3 Comparison of amplified and predicted sequence of *G.max* β -1,2 xylosyltransferase

Seq 1	MNRRRTLLVRLTLLFLFVLNSFSLFLYFITHKTSSSPSSSLQLKKPRTYLTPLSHQTHFSK	60
Data 1	MNRRRTLLVRLTLLFLFVLNSFSLFLYFITHKTSSSPSSSLQLKKPRTYLTPLSHQTHFSK	60
Seq 61	PWPILPSYLPWSQAPTAPPRSCWAYFGNGFMRRRDLRLSRGGAGWFRCHSDTLRSSVC	120
Data 61	PWPILPSYLPWSQAPTAPPRSCWAYFGNGFMRRRDLRLSRGGAGWFRCHSDTLRSSVC	120
Seq 121	EGGRLRMVPERIAMAKGGEDLSAVMGRREEEELPAFQNGAFEVDGGEVVDREFLVDKKFL	180
Data 121	EGGRLRMVPERIAMAKGGEDLSAVMGRREEEELPAFQNGAFEVDGGEVVDREFLVDKKFL	180
Seq 181	DEYVPRGGIDRHTMRDLIAKIRIVRGKDFQCDEWIEEPALLVTRFEYANLFHTVTDWYSA	240
Data 181	DEYVPRGGIDRHTMRDLIAKIRIVRGKDFQCDEWIEEPALLVTRFEYANLFHTVTDWYSA	240
Seq 241	YVSSRVGTGLPNRPHLIFVDGHCAAPLEETWRALFSSRLRYAKNFGSGVCFRHAILSPLGYE	300
Data 241	YVSSRVGTGLPNRPHLIFVDGHCAAPLEETWRALFSSRLRYAKNFGSGVCFRHAILSPLGYE	300
Seq 301	TALFKGLTEDIDCYGAPAEQELWQNPDDHKTARLSEFGEMVRAAFGLPLNVHRGGKPLFGH	360
Data 301	TALFKGLTEDIDCYGAPAEQELWQNPDDHKTARLSEFGEMVRAAFGLPLNVHRGGKPLFGH	360
Seq 361	NILFVRREDYLAHPRHGGKVESRLSNEQEVFDSLKSASNYKGCKINLVNGLFAHMSMKD	420
Data 361	NILFVRREDYLAHPRHGGKVESRLSNEQEVFDSLKSASNYKGCKINLVNGLFAHMSMKD	420
Seq 421	QVRAIQDASVIIGAAGLTHIVSALPKTVILEIISSYFRRPHFAYISRWKGLEHAINL	480
Data 421	QVRAIQDASVIIGAAGLTHIVSALPKTVILEIISSYFRRPHFAYISRWKGLEHAINL	480
Seq 481	AGSHADTGTVIKELVDIMKSLGC	503
Data 481	AGSHADTGTVIKELVDIMKSLGC	503

Seq indicates the amplified sequence, Data refers to the gene sequence found in the data files.

A comparison of the β -1,2 xylosyltransferase sequences between the genes of *G. max* and *A. thaliana* shows a homology of 62% (Scheme 4).

Scheme 4 Comparison of *G. max* β -1,2 xylosyltransferase and *A. thaliana* β -1,2 xylosyltransferase

G.max	1	MNRRTTLLVRTLLFLFVLNSFSFLYFITHKTS SSPSSSLQLKKPRTYLTPLSHQTHFSK	60
		M++R +++ L++ +LNS L +YF+ H +S SP S + P Y +++Q+ K	
A.thaliana	1	MSKRNP KILKIFLYMLLLNSLFLIIYFVFHSSSF SPEQS---QPPHIYHVSNNQSSI QK	57
G.max	61	PWPILPSYLPWSQAPT TAPPRSCEAYFGNGFMRRRDLLSRGGAG---WFRCRHSDTLR	116
		PWPILPSYLPW+ P SCE YFGNGF +R D L R G G WFR C +S+TL+	
A.thaliana	58	PWPILPSYLPWTPPQRNLPTGSC EGYFGNGFTKRVD FLKPRIGGGGEGSWFR CFYSETLQ	117
G.max	117	SSVCEGGRLRMVPERIAMAKGGEDLSAVMGRREEEELPAFQNGAFEV-----	163
		SS+CEG LRMVP+RI M++GGE L VMGR+EEEEELPAF+ GAFEV	
A.thaliana	118	SSICEGRSLRMVPDRIVMSRGG EKLEEV MGRKEEEELPAFRQGA FEVAEEVSSRLGFKRH	177
G.max	164	-----DGGEVVDREFLVDKKFLDEYVPRGGIDRHTMRDLIAKIRIVRGKDFQCDEWIEE	217
		+GG V R LV+ + L+EY+ GGIDRHTMRDL+A IR V DF C+EW+EE	
A.thaliana	178	RRFGGGEGGSAVSRR-LVNDEMLNEYMQEGGIDRHTMRDLVASIRAVDTNDFVCEEWVEE	236
G.max	218	PALLVTRFEYANLFHTVTDWYSAYVSSRV TGLPNRPHLIFVDGHCAAPLEETWRALFSSL	277
	P	LLVTRFEYANLFHTVTDWYSAYVSSRV TGLPNRPH++FVDGHC LEETW ALFS +	
A.thaliana	237	PTLLVTRFEYANLFHTVTDWYSAYVSSRV TGLPNRPHVVFVDGHCTTQLEETWTALFSGI	296
G.max	278	RYAKNFSGSVCFRHAILSP LGYETALFKGLTEDIDCYGAPAQELWQNPD DHKTARLSEFG	337
		RYAKNF+ VCFRHAILSP LGYETALFKGL+ +IDC G A LWQNPD D +TAR+SEFG	
A.thaliana	297	RYAKNFTKPVCFRHAILSP LGYETALFKGLSGEIDCKGDSAHLN WQNPD DKRTARISEFG	356
G.max	338	EMVRAAFGLPLNVHRG-GKPLFG-----HNILFVRREDYLAHPRHGGKVESR LSNEQEV	390
		EM+RAAFGLP+N HR KPL +N+LFVRREDYLAHPRHGGKV+SRL NE+EV	
A.thaliana	357	EMIRAAFGLPVNRHRSLEKPLSSSSSASVYNVLFVRREDYLAHPRHGGKVQSRLINEEEV	416
G.max	391	FDSLKSW----ASNYKGCKINLVNGLFAHMSMKDQVRAIQDASVIIGA HAGLTHIVSAL	446
		FDSL W ++ C INLVNGL AHMSMKDQVRAIQDASVIIGA HAGLTHIVSA	
A.thaliana	417	FDSLHHWVATGSTGLTKCGINLVNGLLAHMSMKDQVRAIQDASVIIGA HAGLTHIVSAT	476
G.max	447	PKTVILEIISSYFRRPHFAYISRWKGLE YHAINLAGSHADTGTVIKELVDIMKSLGC	503
		P T I EII S F+RPHF I++WKGLE YHA++LA S A+ VI++L +IMKSLGC	
A.thaliana	477	PNTTIFEIISVEFQRP HFELIAKWKGLE YHAMHLANSRAEPTAVIEKLTEIMKSLGC	533

G.max indicates the sequence of the *G. max* xylosyltransferase, A.thaliana refers to the gene sequence of the *A. thaliana* xylosyltransferase.

To evaluate CCD-reactivity of allergic patient sera with certain glycotopes both or only one CCD-structure were expressed on an immunologically inert scaffold protein. As CCD carrier the high abundance serum protein AHSG was chosen as this protein should not show any reactivity on protein level with patient sera. AHSG consists of 2 polypeptide chains and provides two sites for N-glycosylation and one O-glycosylation site. By the expression of AHSG in glyco-engineered insect cells, the N-glycosylation can be modified to create the glycotope of choice. The AHSG cDNA was amplified from human PBMC (peripheral blood mononuclear cells) cDNA.

3.6.2 Establishment of insect cell lines with variant glycosylation

To provide a set of insect cell lines with variant glycosylation for the expression of differently glycosylated AHSG forms, insect cells were transfected with different glycosyltransferases. Insect cells with the capacity of α -1,3-core fucosylation were established by stable

transfection of the *Apis mellifera* α -1,3-core fucosyltransferase (Sf9-FucTA). β -1,2 xylosylating insect cells were established by the transfection with the genetic information of the culprit enzyme from soy bean (Sf9-XylIT). To establish both phenotypes in one cell line, cells derived from *Trichoplusia ni* (High Five) were transfected with the genetic information of β -1,2 xylosyltransferase (High Five-XylIT). In contrast to Sf9 cells, cells derived from *T. ni* are already able to modify glycans with α -1,3-core fucose. As a scaffold protein to provide a non-reactive, non-allergic protein backbone for different glycan structures we employed human fetuin, termed also alpha-2HS-glycoprotein (AHSG), a plasma protein highly abundant in most mammalian species.

To evaluate the capacity of altered glycosylation of the new established insect cell lines, cell lysates from the glyco-engineered cells were analysed using anti-HRP serum from immunised rabbits (Fig. 3.24).

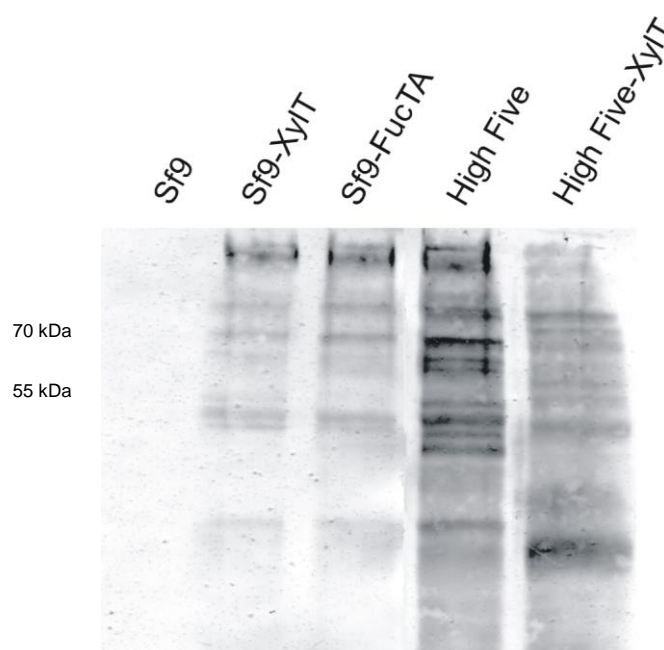


Fig. 3.24 Analysis of CCD-reactivity of glyco-engineered insect cell lines by anti-HRP-serum

Cellular lysates of the different cell lines were analysed by anti-HRP-serum, showing strong reactivity with the glyco-modified cell and High Five cells, but no reactivity with unmodified Sf9 cells.

The CCD-reactivity analysis shows strong reactivity with the glyco-modified insect cell lines and cells derived from *T. ni*, in contrast to unmodified Sf9 cells.

3.6.3 Expression of AHSG in glyco-engineered insect cells lines

The expression of AHSG with different glycotopes for the before mentioned analysis was performed applying the baculovirus expressionsystem [71]. The resulting expression culture supernatans were subjected to Ni-affinity chromatography, and the purified proteins were

analysed by SDS-PAGE and immunoblotting using anti-V5 antibody for detection (Fig. 3.25A and B).

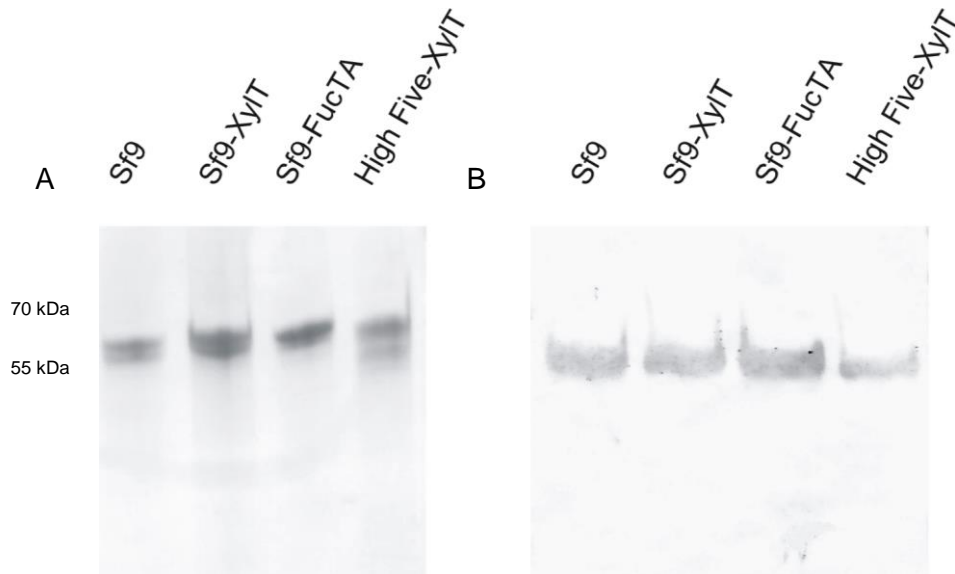


Fig. 3.25 AHSG variants analysis in gel and immunoblots

A The different AHSG glycoforms were analysed in gel by Coomassie staining, B and immunoblot by using anti-V5 antibody.

Protein yields of AHSG after purification were in the range of 2-3 mg in total.

3.6.4 Analyses of CCD-phenotype of AHSG variants

The differently glycosylated AHSG variants were analysed in immunoblot as well as in ELISA using anti-HRP-serum for detection (Fig. 3.26A and B). Anti-HRP serum was derived from rabbits immunised with HRP. Therefore the serum recognises β -1,2 xylose and α -1,3-core fucose. In immunoblot and ELISA the serum showed no reactivity with the AHSG derived from unmodified Sf9 cells, in contrast to the CCD bearing AHSG variants derived from insect cells stably transfected with glycosyltransferases.

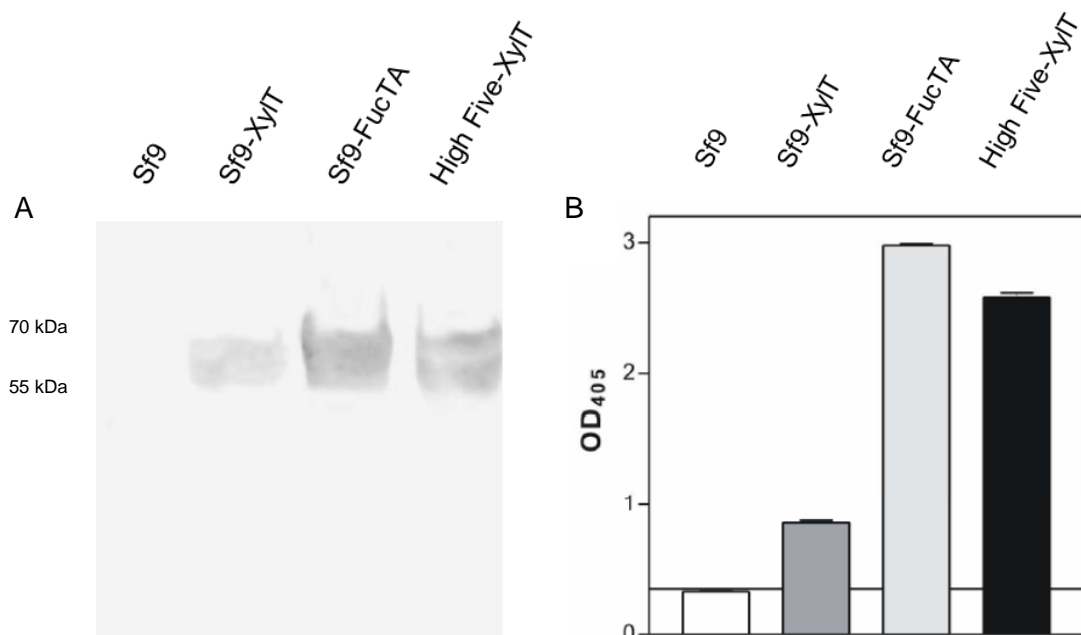


Fig. 3.26 Analysis of CCD-phenotypes of different AHSG variants

The analysed AHSG variants showed pronounced reactivity in immunoblot (A) and ELISA (B), except the AHSG variant expressed in Sf9 cells.

The analysed AHSG variants showed the expected reactivity with the anti-HRP serum. All variants expressed in the glyco-modified insect cells showed a pronounced reactivity, in contrast to the AHSG variant expressed in Sf9 cells, proving Sf9 cells do not establish immunologically detectable CCDs.

3.6.5 Screening of allergic patients sera with diversely glycosylated AHSG variants

After verification of immune reactivity to the CCD bearing AHSG variants with anti-HRP serum from rabbits, the AHSG variants were analysed with allergic patient sera regarding their IgE-reactivity. Therefore 30 sera of Hymenoptera venom allergic patients and 30 sera of pollen allergic patients were analysed in ELISA (Fig. 3.27). Up to 50% of Hymenoptera venom allergic patients showed IgE reactivity to fucosylated AHSG, but only poor reactivity to the exclusively xylosylated variant. Two third of the patients reacted solely with the fucose epitope, while one third reacted with a combined xylose and fucose epitope. 30% of the pollen allergic patients showed medium to high reactivity to the combined epitope, of which one third also recognised the xylose epitope exclusively. On the contrary only two patients showed exclusive reactivity to the fucose epitope (Fig. 3.27).

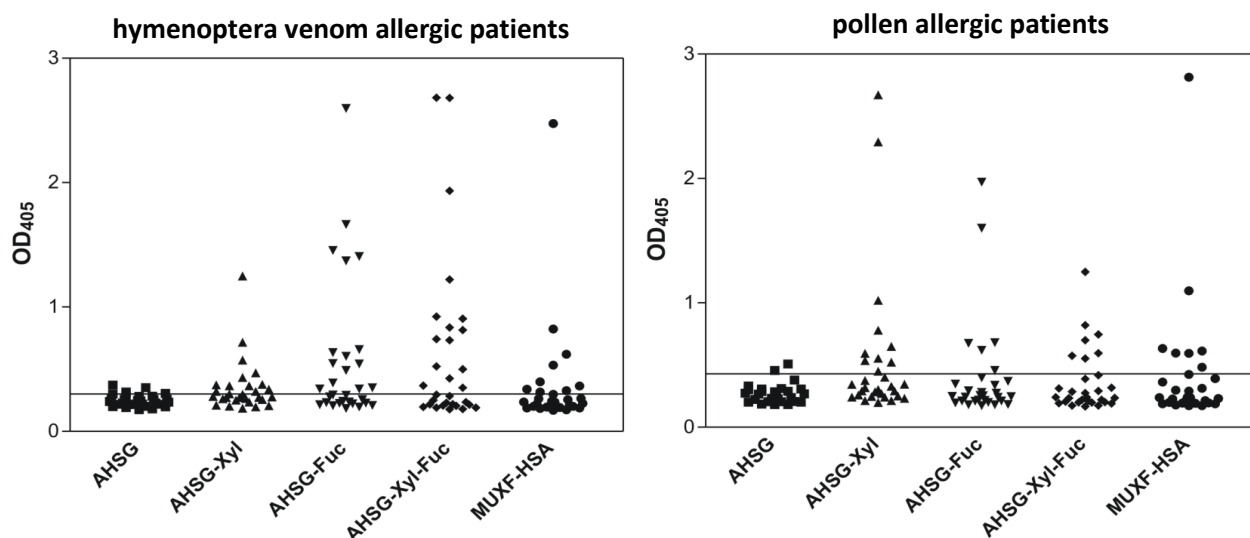


Fig. 3.27 Screening of allergic patients' sera with different glycosylated AHSG variants and MUXF-HSA

Sera of hymenoptera venom and pollen allergic patients were analysed for their reactivity to the certain glycotopes present on the surface of the AHSG variants and MUXF-HSA.

Sera of non-atopic patients served as control and showed no reactivity with the AHSG variants (not shown). Selected individual reactivity profiles demonstrated the particular relevance of the fucose and xylose epitope as well as their variant and separated recognition (Fig. 3.28).

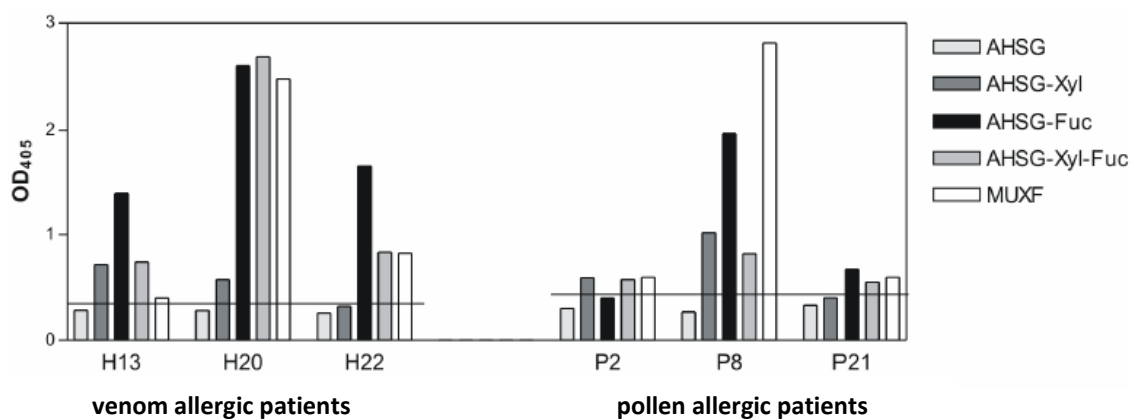


Fig. 3.28 Individual reactivity of selected sera to the glycotopes

Reactivity profiles of selected Hymenoptera venom and pollen allergic patients for the certain glycotopes

In a detailed analysis the Hymenoptera venom allergic patients show either a combined recognition of fucose and xylose (H13 and H20), or an exclusive recognition of the fucose epitope, demonstrated by the absence of reactivity to the xylosylated AHSG by serum H22. None of the Hymenoptera venom allergic patients showed any reactivity to the solely xylosylated AHSG at all.

In contrast the pollen allergic patients show reactivity exclusive to the xylose epitope (P2), and to the fucose epitope (P21) or also a combined recognition of fucose and xylose (P8)

3.7 Structural and functional insights into the high affinity recognition of xenobiotic complex-type N-glycan core structures by mammalian antibodies

Carbohydrate antigens of pathogens and environmental substances can provoke pronounced responses of the adaptive and innate immune system [284]. The interaction of carbohydrate specific immunoglobulins however often is governed by limited affinities. These are compensated by multivalency to enable the physiologically intended effects but pose difficulties in molecular analyses as well as applications targeting oligosaccharide structures. Carbohydrates are considered to be T cell-independent antigens incompetent to raise high affinity responses. Recently even presentation to and recognition by carbohydrate specific T cells could be shown [285]. In contrast to their immunological significance however, little is known about molecular aspects of carbohydrate recognition.

In pathological conditions which are associated with elevated levels of IgE such as type I allergic reactions and parasitic infections pronounced immune responses to xenobiotic carbohydrate structures are found. Although carbohydrate recognition by IgE obeys the same inherent limitations as seen for other antibodies and carbohydrate binding molecules, IgE is an antibody isotype supposed to exhibit extraordinary high affinities which allow potent stimulation of immediate type immune responses even by minute amounts of allergen.

The predominant eukaryotic carbohydrate epitopes recognised by IgE are established by specific glycosyltransferases of non-mammalian species, i.e. helminths, plants and insects. These highly immunogenic glycotopes provoke IgE reactivity and represent the universal principle for cross-reactivity of glycoproteins [119]. The hallmark of these CCDs classically is constituted by α -1,3 linked core fucose residues found on insect glycans, and, additionally, spatially separated β -1,2 linked xylose on plant- and helminth-derived CCDs (Fig. 3.29). The role of the core modifications in allergy and parasitic infection however still is discussed controversially [283]. Although initial studies suggest high antibody affinities for core-modified carbohydrates, the clinical consequences of their interaction however remain open [160]. In contrast, IgE with specificity for the α -gal epitope is the underlying principle of a novel type of severe anaphylaxis and high affinity appears to be a crucial parameter [127]. Apart from phenomenological knowledge, however, molecular knowledge about the interaction of IgE with carbohydrate antigens and the basis for *in vivo* activity remain scarce.

Generally, only few antibody structures in complex with carbohydrate antigens - mostly LPS (lipopolysaccharides) from different species - do exist [286-291]. As examples for mammalian carbohydrate antigens two Lewis structures in complex with murine antibodies

are crystallographically available [158, 292]. Analyses of carbohydrate specific human antibodies are hampered by low affinities, low serum concentrations and a broad unavailability of monoclonal antibodies [151]. Carbohydrate specific IgE antibodies - and thus molecular and structural data - are not available at all, since the evanescent concentrations of IgE producing cells render hybridoma technology and the establishment of IgE derived immune repertoires highly difficult [293, 294].

The missing authenticity of animal derived antibodies used as substitute gets obsolete if such antibodies recognise B cell epitopes identical to those of human antibodies. This requirement is given for small sized epitopes which obey identical immunological mechanisms in animals and men, as true for carbohydrate epitopes that are characterised by a high immunogenicity in mammalian species and a spatially defined architecture.

Although the immunogenicity of xenobiotic core glycan modifications in rodents is given, immunological analyses yielded contradictory findings on specificity and affinity [295]. Hence, a molecular characterisation is imperative for dissection of this immune recognition.

Thus, the aim of our work was to gain access to monoclonal antibodies with specificity for N-glycan core modifications from rabbit immune repertoires for functional and molecular analyses. Recombinant human IgE and IgG isotypes were employed for characterisation of the interaction regarding affinity and molecular assignment of the glycotope by STD NMR, as well as cellular activation assays. This work contributes to the dissection of the antibody carbohydrate interaction and molecular aspects in carbohydrate anaphylaxis.

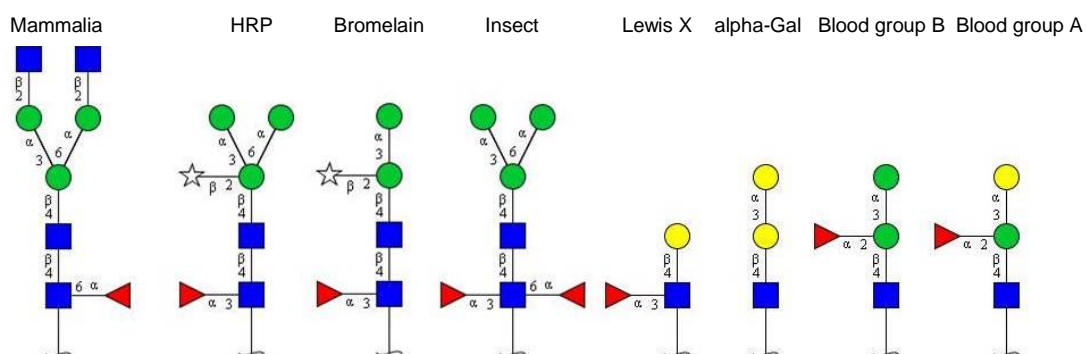


Fig. 3.29 Overview of relevant glycan structures

Exemplary structures of N-glycans found on glycoproteins from plants, insects and parasites as well as blood group antigens are shown.

3.7.1 Establishment of leporid immune repertoire libraries and selection of CCD specific antibodies

Leporid IgG V_H and V_L repertoires were amplified from spleen and bone marrow cDNA after immunisation with HRP and the identity of randomly chosen single V_H and V_L was confirmed by sequence analysis. These repertoires were subsequently combined using a cloning strategy allowing an unbiased assembly of V_H and V_L to scFv. The resulting library of 3×10^7

independent clones in a phagemid vector was subjected to selection by phage display against HRP (H), MUXF-conjugate (M), fucosylated α -1,3-core fucosyltransferase (F) and fucosylated AHSG (A). After iterative panning, ELISA analyses demonstrated significant enrichment of CCD specific clones in the library (Fig. 3.30A and C). Reactive clones were subjected to further ELISA and sequence analysis (Fig. 3.30B and D). Notably, use of different glycoproteins for selection yielded different dominant sequences. The sequences demonstrated enrichment of clones with limited substitutions of particular residues within the V_H or V_L (Fig. 3.31).

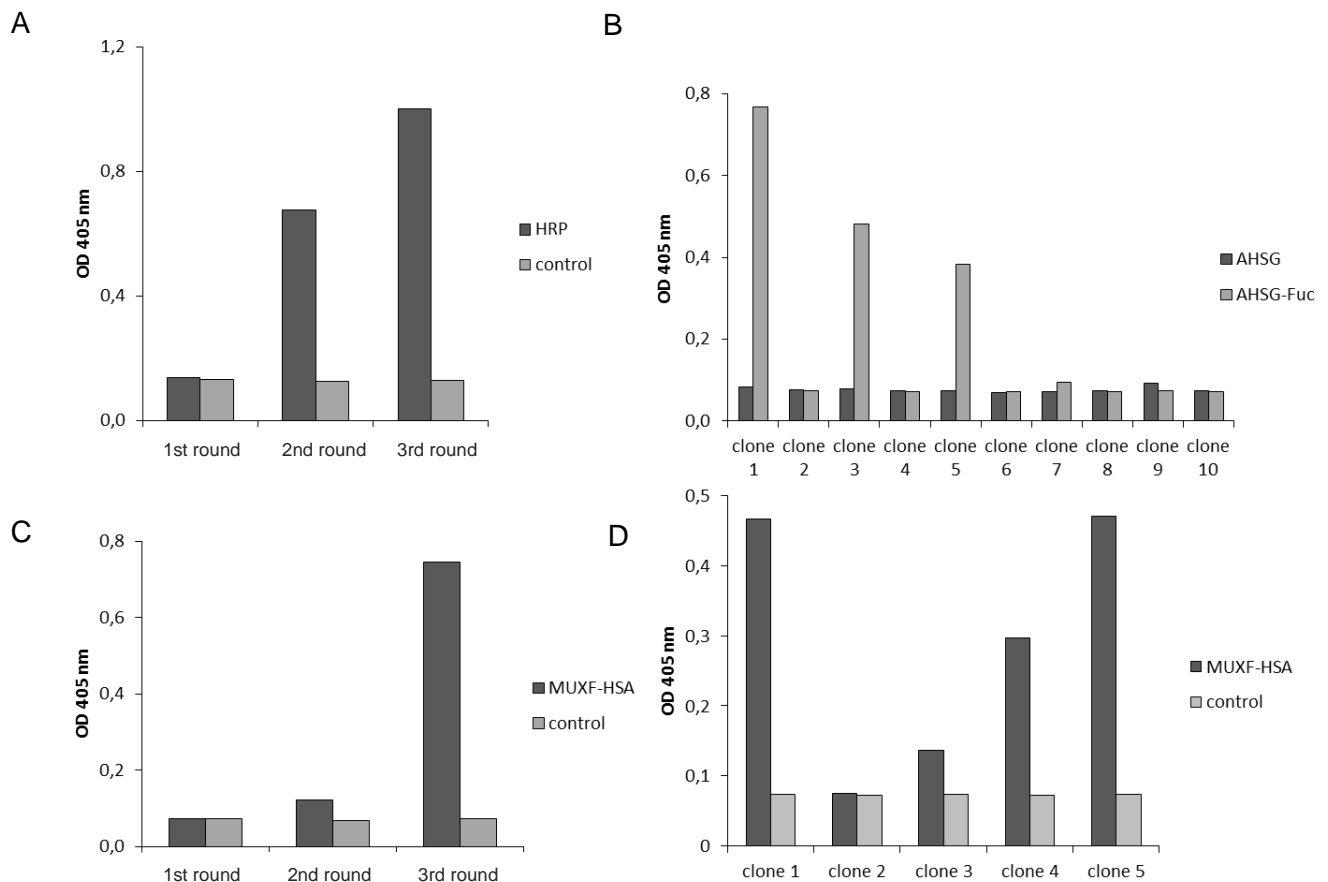


Fig. 3.30 Immunoreactivity of poly- and monoclonal phages

The immunoreactivity of the enriched library (A and C) as well as selected phage clones (B and D) against CCD epitopes was analysed by ELISA.

Subsequently selected clones were converted into IgG and IgE antibodies and antibody constructs.

RESULTS

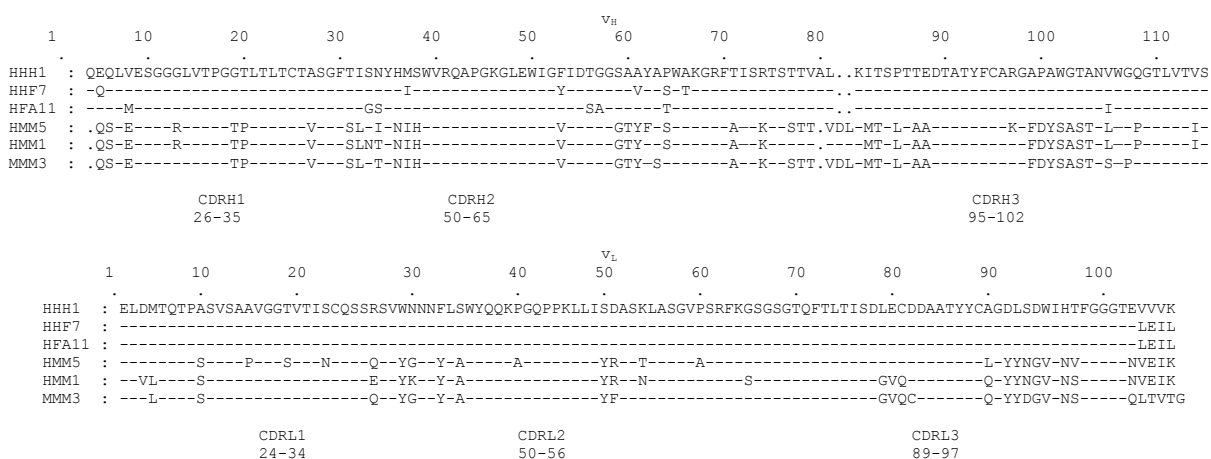


Fig. 3.31 Primary structure alignments of obtained antibody fragments

Numbering and determination of the CDRs was performed according to Kabat [176].

3.7.2 Generation and characterisation of carbohydrate specific IgE and IgG₁ immunoglobulins

The obtained clones were evaluated in ELISA regarding reactivity to a panel of glycoproteins. Thereby, all clones recognised all glycoproteins carrying either the xenobiotic fucose exclusively or additional xylose modifications. Exemplarily the reactivities of the monoclonal phage HHH1 is shown (Fig. 3.32).

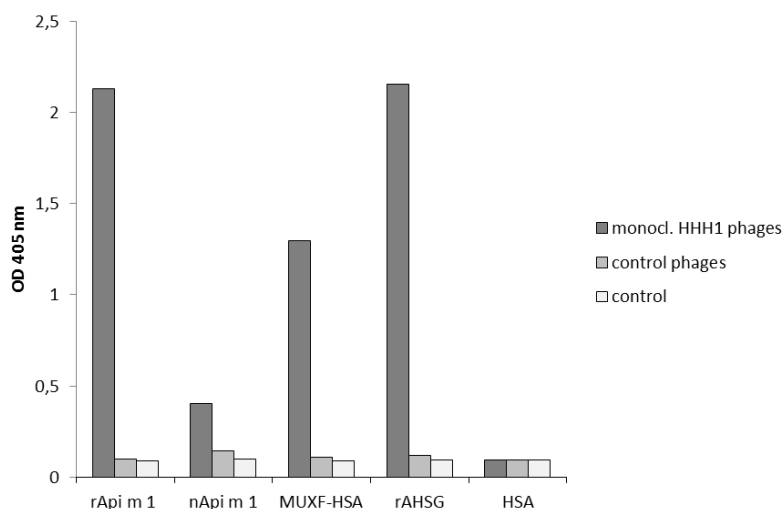


Fig. 3.32 Fine specificity of monoclonal phages using different glycoproteins in ELISA

The immunoreactivity of an exemplary phage clone to a panel of CCD conjugates was analysed by ELISA as described in methods. The recombinant proteins were expressed in High Five cells and therefore carrying α -1,3-core fucose

For subsequent analyses the phages HHH1 and HMM5 were selected for conversion into chimeric IgG₁ and IgE immunoglobulin formats and produced in mammalian cells. Immunoblotting analyses verified the molecular masses suggesting proper folding and glycosylation. Exemplarily the expressed HHH1 IgG_{CH2-4} is shown (Fig. 3.33).

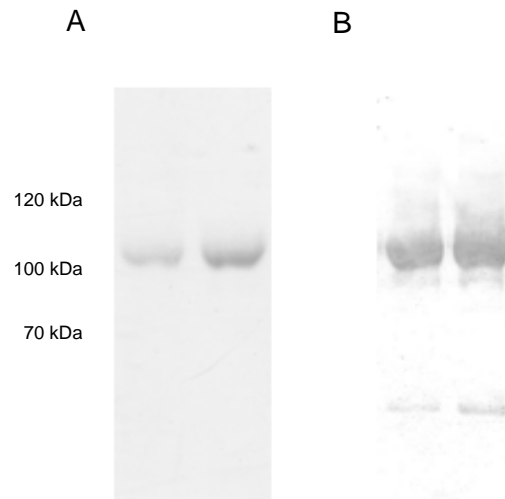


Fig. 3.33 Recombinant expression of carbohydrate specific antibody constructs

Purified proteins were assessed under non-reducing conditions by Coomassie staining (A) and immunoblot (B).

The recombinant antibodies showed the same epitope specificity as their ancestral phages (Fig. 3.34).

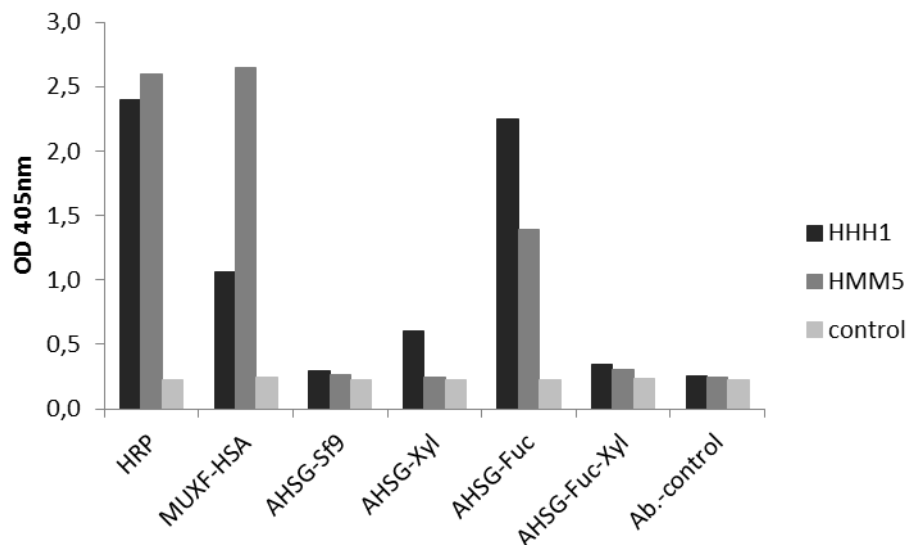


Fig. 3.34 Fine specificity of HHH1 and HMM5 IgG_{CH2-4} using different glycoproteins in ELISA

The immunoreactivity of the clones HHH1 and HMM5 to a panel of CCD conjugates was analysed by ELISA

Interestingly, the antibody HMM5 showed a higher preference in binding to MUXF type glycans compared to HHH1.

Generally it is a tenet that increased avidity has to overcome the mostly limited affinities seen for the interaction of proteins with carbohydrates. Interestingly, CCD specific

immunoglobulins from mammals including men and rabbits are found to have outstanding affinities. The ease in detecting carbohydrate specific monovalent phages in ELISA already suggests a robust immunoreactivity (Fig. 3.30). The concept of high affinity could be validated by SPR analyses yielding K_D s of the HHH1 antibody of $2 \times 10^8 \text{ M}^{-1}$, $4 \times 10^8 \text{ M}^{-1}$ and $3 \times 10^8 \text{ M}^{-1}$ for HRP, AHSF-Fuc and MUXF conjugate (not shown), respectively.

The HMM5 antibody exhibited K_D s of $2 \times 10^8 \text{ M}^{-1}$ and $3 \times 10^9 \text{ M}^{-1}$ for HRP and MUXF conjugate, respectively. In accordance with its monovalency, the HHH1 scFv exhibited K_D s of $3.8 \times 10^7 \text{ M}^{-1}$ and $4.7 \times 10^7 \text{ M}^{-1}$. These data emphasise the outstanding nature of core glycan recognition. Notably, in an inverse setting - mimicking receptor bound antibodies on effector cell surfaces by immobilisation of antibodies and using glycoproteins as analytes - K_D s in a similar range were obtained.

3.7.3 Cellular activation by recombinant CCD specific antibodies

The potential of carbohydrate specific HHH1 and HMM5 IgE for cross-linking of the FcεRI and degranulation of effector cells was assessed by determination of β-hexosaminidase release from rat basophilic leukemia cells (RBL-SX38) (Fig. 3.35). Antigen dependent cellular activation through monoclonal IgE demands the availability of more than one epitope per allergen. Hence, we used CCD carrying glycoproteins with several glycosylation sites (Fig. 3.35A and B).

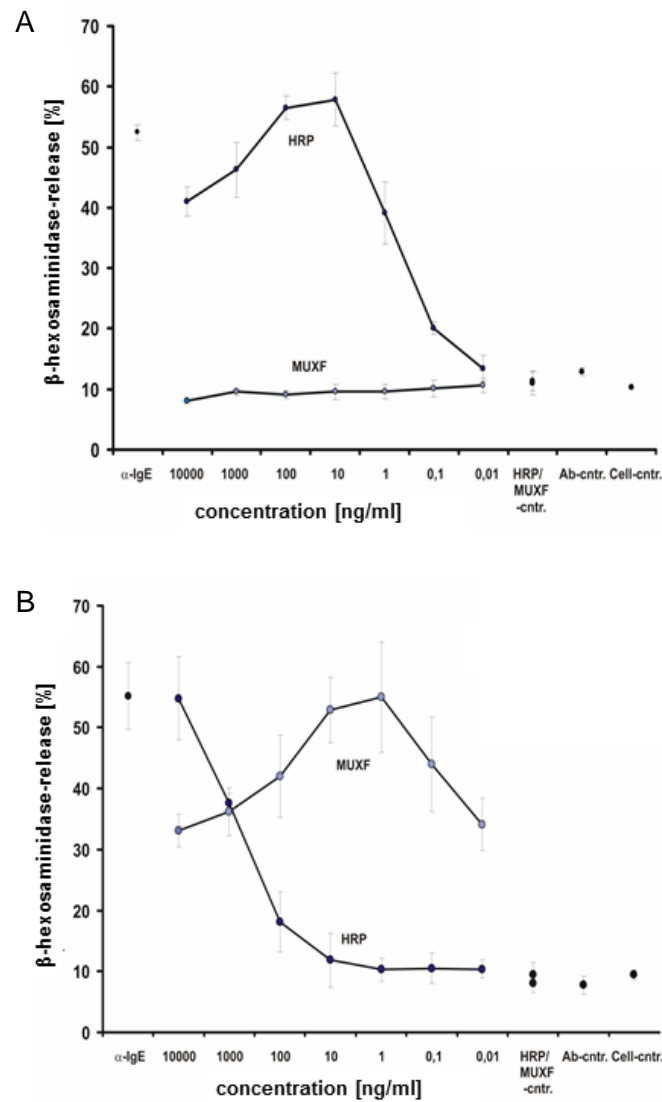


Fig. 3.35 Mediator release of humanised RBL-SX38 by CCD microspheres

RBL-SX38 cells providing the human FcεRI were sensitised with CCD specific IgE HHH1 (A) and HMM5 (B). Degranulation was induced by addition of the glycoproteins HRP and MUXF-HSA conjugate. Degranulation was monitored by β-hexosaminidase activity released into culture supernatants. Data are mean ± SD of triplicate measurements.

Antigen-independent degranulation by anti-IgE verified binding to the FcεRI and its general capability for activation. Using glycoproteins both carbohydrate specific IgE mediated clear antigen-dependent activation (Fig. 3.35A and B). In accordance with the affinities for the HMM5 IgE even lowest concentrations of antigen (10 pg/mL MUXF conjugate) were highly efficient in mediating degranulation. Variations in valency as represented by different glycoproteins such as chemically synthesised MUXF-HSA (6-7 modifications/molecule), and HRP (7-8 glycosylation sites) affected efficacy of mediator release to a limited extent only.

These data clearly suggest that CCD specific IgE exhibits an intrinsic potential to cross-link the FcεRI and activate effector cells in a highly efficient manner. Any limitation observed in a polyclonal setting or *in vivo* does not arise from fundamental molecular incompetence.

3.7.4 Epitope recognition by CCD specific antibodies

Molecular details of the high affinity recognition of carbohydrate antigens by antibodies still remain open. Therefore, we monitored the interaction of affinity purified rabbit polyclonal antibodies as well as two monoclonal IgE by STD NMR, a method enabling molecular analyses of lower molecular weight ligands. As ligands α -1,3- and α -1,6-core fucosylated biantennary N-glycans were generated from the common core glycan enzymatically by honeybee core fucosyltransferase A.

Pronounced STD effects were obtained for the α -1,3,6-core difucosylated carbohydrate ligand (Fig. 3.36).

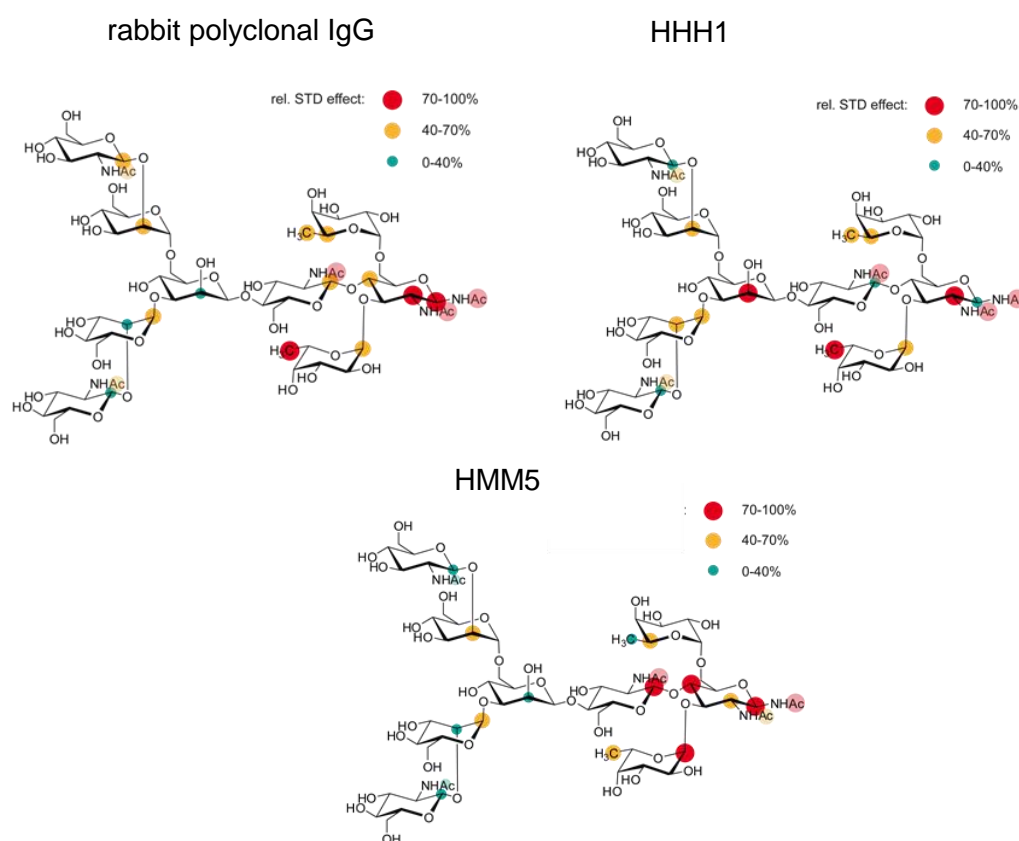


Fig. 3.36 Interaction footprints of monoclonal leporid antibodies and polyclonal immunoglobulins as assessed by STD NMR

Shown are the interaction footprints of α -1,3,6-fucosylated core glycan binding to the monoclonal antibodies and polyclonal antibodies purified from rabbit serum. Circles represent the relative size of the saturation transfer and reflect the vicinity of individual protons to protons in the binding pocket of the immunoglobulin as macromolecular binding partner. The closer the ligand protons are to protons of the binding pocket, the larger is the saturation transfer.

The interaction footprint of the monoclonal antibodies HHH1 and HMM5 revealed dominant interaction with the 1,3-core fucose and the GlcNAc1 (Fig. 3.36). Major contacts of the fucose are defined by the H3 proton having the highest STD signal and to a high extent the H2, and H4 protons. Interestingly, the α -1,6-core fucose located in the opposite hemisphere as well as some residues in the antennae exhibit medium STD effects. Intriguingly, the HHH1 antibody showing exclusive specificity for the HRP glycan, exhibited an additional dominant interaction on the β -mannose suggesting a role in differentiating glycoforms. The interaction footprint of the rabbit polyclonal immunoglobulins revealed an interaction modus comparable to that of the monoclonal antibodies HHH1 and HMM5 (Fig. 3.36).

The glycosidic acetyl group replacing and representing the N-glycosylated asparagine also shows contributions suggesting a potential role of the asparagine linkage.

These findings support the key role of the α -1,3 linkage of core fucose for the recognition of the epitope core glycan epitope by monoclonal IgE as well as polyclonal serum antibodies. Beyond this anchoring different residues spread all over the entire glycan are involved in antibody binding.

4. Discussion

4.1 Identification and characterisation of Hymenoptera venom allergens

The recombinant expression and use of Hymenoptera venom allergens represents a strategy clearly superior to the use of venom extracts. One major advantage of recombinant allergens compared to venom extracts is the reliable availability of substantial amounts of all venom components. In recent studies it could be shown that some allergens in the venom preparations used for diagnostics represent a lower diagnostic sensitivity, although they are present in the preparations. Additionally therapeutic approaches cannot assure complete protection against honeybee venom based on the underrepresentation or even absence of some allergens in the venom preparations used for immunotherapy [72, 266, 296]. Apart from the availability of particular low abundant components it could be shown that the supplementation of one allergen alone could be sufficient to increase the diagnostic sensitivity dramatically. In a study 308 patients with a systemic reaction after a sting of yellow jacket were tested with yellow jacket venom, recombinant Ves v 1 and rVes v 5. 83.4% reacted with the conventional venom extract, 44.2% reacted with rVes v 1 and 89.9% showed reactivity to the rVes v 5 [266]. The lower reactivity to yellow jacket venom extract compared to rVes v 5 suggests an unavailability of this allergen in the diagnostic product [266]. This could be explained by a reduced concentration of Ves v 5 in the processed venom extract, an insufficient coupling of the allergen to the solid phase, or a sterical unaccessibility of Ves v 5 epitopes after coupling [266]. To overcome the limitation of venom extract, recombinant Ves v 5 was added to the venom resulting in an increase of the reactivity from 83.4% to 96.8% [266].

Beside the described advantages in extract based diagnosis of yellow jacket venom allergic patients, recombinant allergens are suitable to improve the diagnosis as individual components of honeybee venom [297]. In our study a large set of recombinant venom allergens was used for diagnostic approaches comprised of Api m 1, Api m 2, Api m 3, Api m 5, Api m 10 and native Api m 4 [297]. By measuring sIgE levels to the individual components, the recombinant allergens were confirmed to be diagnostically relevant emphasizing the importance of the individual components [297]. Thereby the diagnostic relevance of the additional allergens was particularly evident for Api m 10. In the study most of the individual allergens were shown to represent major allergens. Although all the allergens have been described earlier the fact that most of the components constitute major allergens has been underestimated. Beyond the pronounced IgE reactivity of the allergens, Api m 3 and Api m 10 represent species specific marker allergens for honeybee venom allergy.

In the current study involving 144 sera of honeybee allergic patients the diagnostic sensitivity could be increased from 72.2% (using Api m 1 alone) to 94.4% (if the described set was used) [297]. The increased sensitivity nearly closed a diagnostic gap of 22.2%, when using Api m 1 alone. In the present study however 8 patients (5.6%) showed no IgE reactivity to any of the used components [297]. It is open if these patients would become detectable with using an extended set of recombinant allergens. In our study specific sensitisation patterns could be described showing that the sensitisation profiles are more complex than anticipated and include profiles with only one component responsible for sensitisation [297]. Patients showing recognition patterns to Api m 3 and Api m 10 either in combination or to one of the allergens exclusively, have to be particularly considered since these allergens are underrepresented or missing in venom preparations used for immunotherapy [72]. Hence these patients might be more unlikely to profit from therapy and they should be carefully monitored under and after immunotherapy for success of treatment. In addition to improving sensitivity of allergy diagnosis, also the accuracy and specificity of diagnostic approaches could be enhanced by the use of recombinant allergens. A common problem in diagnostic approaches using honeybee or yellow jacket venom is the presence of double-positive sIgE in 50-60% of patients with anaphylactic reactions to Hymenoptera stings, although most of them report an anaphylactic reaction only to one sting [80]. The observed cross-reactions are provoked by homologous allergens in both venoms, like dipetidylpeptidases and/or the new identified vitellogenins, or by CCDs [70, 81, 298]. CCDs are present on most allergens from honeybee venom and also on different allergens of yellow jacket venom [80]. Moreover CCDs are also present on a variety other insect and plant derived allergens, but apparently are missing on allergens from *Polistes spp.* venom [65, 80]. The use of recombinant allergens can help to circumvent this molecular factor provoking double positivity. The absence or strong reduction of CCDs on the glycans of recombinant allergens is a result of the expression system used for the production of the allergens. Sf9 cells derived from *Spodoptera frugiperda* are apparently not able to decorate glycans with CCDs, and these cells were used to express the different allergens.

The quality of the data obtained with the recombinant allergens devoid of CCDs underline the strength of our approach.

Based on our results the potential of individual recombinant honeybee venom allergens for application in immunotherapy has to be evaluated and analysed. The findings suggest that some allergens like Api m 3 or Api m 10 are underrepresented or even missing in therapeutic extracts used for immunotherapy [72]. The reason for this lack of particular venom components most likely relies on the procedures applied for preparing the venom for the therapeutic approach. The lack in the therapeutic extracts however might result in unsafe

immunotherapy for the patient, since a full protection against the venom might not be reached as suggested by the limited induction of IgG₄ against Api m 3 and Api m 10. Hence the lacking venom components could be a factor for the reduced efficacy of VIT using honeybee venom (10-20% not fully protected) compared to yellow jacket venom (2-10% not fully protected) [299, 300]. To circumvent this reduced protection, the addition of recombinant allergens to the extracts might represent an attractive approach [280, 301, 302].

The established recombinant technologies also allow the identification and evaluation of new Hymenoptera venom components. This is reflected in several studies concerning new components and evaluation of their allergenic potential, as shown e.g. for the honeybee allergens Api m 11 and Api m 12 [81, 271]. The future identification of new marker allergens is needed to further improve diagnostic approaches. While marker allergens for honeybee venom and yellow jacket venom, like Api m 1, Api m 10 and Ves v 5, are readily available, marker allergens for other Hymenoptera species, like *Polistes spp.* and *Solenopsis spp.* need to be identified. Especially a marker allergen for *Polistes dominula* venom seems to be important, since the only commercially available allergen Pol d 5 is cross-reactive with Ves v 5 and *Polistes dominula* represents an important species in Southern Europe that is increasingly spreading all over Europe, also increasing the risk of allergies to venom of this particular species [65]. A promising candidate for a marker allergen could be the venom protease Pol d 4, since it is assumed that there is no cross-reactive homologue in yellow jacket venom [303].

4.2 Fine specificity of IgE carbohydrate reactivity

Glycans of glycoproteins derived from allergenic sources are often associated with IgE mediated allergy. Prominent sources include Hymenoptera venoms carrying α -1,3 fucosyl residues and plant glycoproteins additionally carrying β -1,2 xylose residues linked to the glycan core structure. To analyse CCD reactivity the glycoproteins HRP and bromelain are widely used, but due to their plant origin these glycoproteins are decorated with α -1,3-core fucose as well as β -1,2 xylose [82, 304]. Analyses on a molecular level of IgE and IgG reactivities however are hampered by the lack of molecular tools that are capable to distinguish the patterns of reactivity. This is due to the fact that in nature certain xenobiotic modifications often are found simultaneously on the same glycan rendering a dissection on the basis of native glycans difficult.

In this work immunoglobulin specificity was addressed by establishing and employing glyco-engineered cell lines to provide variant capacities of α -1,3-core fucosylation and β -1,2 xylosylation. Different insect cell lines, which differ in the glycosylation patterns they

establish, were used. Sf9 cells derived from *Spodoptera frugiperda* show no immunologically detectable α -1,3-core fucosylation, in contrast to HighFive cells derived from *Trichoplusia ni* with pronounced α -1,3-core fucosylation activity [71]. Two Sf9 derived insect cell lines were engineered, one cell line only modifying its glycans with β -1,2 xylose, another cell line solely capable to decorate their glycans with α -1,3-core fucose. Transfecting cells derived from *Trichoplusia ni* with the β -1,2 xylosyltransferase established a third cell line producing glycans with both glycotopes. Upon expression of the human alpha-2HS-glycoprotein (AHSG) as carrier scaffold in the different insect cell lines, different combinations of xenobiotic glycan modifications were produced.

The resulting glycoconjugates were used to evaluate the IgE and IgG reactivity profile to defined glycotopes of non-allergic, pollen-allergic, and venom-allergic patients.

The Hymenoptera venom allergic patients showed a pronounced IgE reactivity to the fucosylated AHSG variants. The reactivity to the xylosylated variants was scarcely found for these patients. In the group of the pollen allergic patients 30% showed reactivity to the CCD bearing glycoproteins. A more detailed look revealed that 23% reacted to the fucose and xylose epitope in combination and 7% reacted exclusively to the xylose epitope. This screening of individual sera emphasised the particular relevance of the individual carbohydrate epitopes.

The AHSG variants with defined glycosylation allow a dissection of xylose and fucose reactivity with IgE antibodies in epitope resolved diagnostics and will elucidate the role of CCDs in the context of clinical relevance. Moreover the biological activity of the CCDs regarding uptake of allergens by APCs and the ability of CCDs to elicit a T_H2 -based immune response can be analysed more in detail [18, 116].

4.3 Carbohydrate core recognition by glycosyltransferases and affinity purified antibodies

The recognition of core glycans is a highly specific interaction and only scarce molecules are available for analyzing the mechanism. Glycosyltransferases modifying the core glycan constitute an ideal model systems to analyse and understand the recognition of the carbohydrate core structure; moreover their recognition mode could allow for a comparison between these enzymes and core glycan binding antibodies [138, 305].

Different glycosyltransferases were produced as soluble proteins in insect cells in functional form. As shown by STD NMR experiments for the honeybee α -1,3-core fucosyltransferase, the enzyme interacts with large portions of the carbohydrate core [138]. However, core GlcNAc and the 3-mannose branch seem to be closer to the enzyme surface compared to the α -1,6-core fucose and the 6-mannose branch [138]. Beyond the significance of the core

GlcNAcs, also the GlcNAc of the 3-branch is important of the acceptor recognition, because a glycan without these residue is not accepted as substrate by the enzyme at all [138].

A closer look by STD NMR into protein-carbohydrate interaction could also be provided for the human fucosyltransferase 8 and their acceptor substrate [305]. Similar to the honeybee α -1,3-core fucosyltransferase, the fucosyltransferase 8 also recognises a large epitope of the acceptor substrate [305]. However, strongest STD effects could be measured for the innermost GlcNAc and the α -1,3 linked mannose. Other residues of the core are also recognised, but to a weaker extent only [305]. The data obtained by STD NMR and MD simulation suggest that the presence of the donor could contribute significantly to acceptor binding. Strong interactions were observed e.g. between the oxygen atoms of β phosphate and a hydroxyl group of the innermost GlcNAc. Additionally, low affinities of the enzyme to the acceptor (390 μ M) and much higher affinities for the donor (9.3 μ M) underline the relevance of the donor. The obtained data and affinities suggest a prior binding of the donor, changing the affinity of the FUT8/GDP-Fuc and resulting in a 10 to 100fold higher affinity for the acceptor.

These data show that the acceptor core glycan is bound by the enzyme relatively weak. In the case of antibodies binding the core structure without fucose, this binding is weak and immunologically not detectable but the α -1,3-core fucosylated glycan is bound efficiently. Whether this similarity is a simple result of similar molecular events ora defined role of the fucose in high affinity binding is present remains open so far.

To obtain first insights into core glycan binding by antibodies, serum of an HRP-immunised rabbit was affinity purified. The interaction of these antibodies were analysed with a chemo-enzymatically α -1,3-core fucoslyated glycan by STD NMR. As also shown for the fucosyltransferase 8, the interaction involves dominantly the innermost GlcNAc residue. Moreover, the α -1,3-core fucose residue appears to be crucial. As mentioned above the interaction of α -1,3-core fucose with the antibodies probably stabilises the binding and directs antibody recognition and specificity. The obtained STD NMR Data show that the method represents a powerful tool to analyse antibody interactions with carbohydrates even for polyclonal serum [153].

4.4 Generation of α -1,3-core fucose specific antibodies for evaluation of affinity and biological activity

So far no monoclonal antibodies against the α -1,3-core fucose epitope are available hampering molecular, structural and functional analyses of the antibody-CCD interaction. In this study an immune library was generated to select monoclonal antibodies with specificity for the α -1,3-core fucose epitope. These antibodies should have the potential to provide

unique insights into reasons for high affinity for certain glycotopes and potential biological activity.

Rabbit anti-HRP serum is known to recognise the α -1,3-core fucose epitope, therefore the serum is used to analyse allergens for the presence of α -1,3-core fucose [113, 143]. HRP provides multiple copies of glycans on its surface mainly belonging to the MMXF-type, rendering HRP an ideal antigen to obtain antibody fragments and antibodies specific for the α -1,3-core fucose epitope [306]. Hence, to obtain monoclonal antibodies with specificity for CCDs rabbits were immunised with HRP [295]. The rabbit antibody repertoire, which in form of polyclonal antibodies has been used in diagnostic applications for decades, is an attractive source for the generation of monoclonal antibodies. Some epitopes are not immunogenic in mice, a species from which the vast majority of monoclonal antibodies to human antigens has been generated. However, rabbits in some cases show a pronounced immune response to these epitopes, as shown e.g. for the α -1,3-core fucose epitope, which emphasise the great potential of rabbit immune libraries [295]. Due to the fact that the rabbit immunoglobulin gene repertoire is well characterised, the generation of rabbit immune libraries could be a promising approach to obtain specific monoclonal antibodies [307, 308]. Moreover the reduced V gene usage makes the access easier as for human immune libraries [308].

For generation of the immune library total mRNA from HRP-immunised rabbit spleen and bone marrow was used. The final immune library consisted of 3×10^7 single clones, a size comparable to established immune libraries [309] [310]. The number of subsequently obtained sequences of rabbit scFvs further emphasises that the recombinant library mirrors the repertoire and provides the information of CCD specificity.

Monoclonal phages were successfully selected against different glycoproteins including MMXF- or MUXF-type glycans and analysed for their reactivity against different glycotopes. Sequence analysis revealed six different CCD binding clones, which can be classified into two sequence families. For the two families the clones HHH1 and HMM5 are prototypic, the other clones differ in small aberrations of the amino acid composition of the CDRs only. The small number of amino acid changes in the sequences of the obtained CCD specific antibodies could be interpreted as hint for antigen-dependent affinity maturation processes. Clones belonging to the HHH1-family are more reactive to MMXF-type than to MUXF-type glycans, in contrast to clones belonging to the HMM5-family, which exhibit an inverse preference.

The presence of the two antibody families suggests that there are only a few dominant B cell clones specific for the CCDs. The limited clonality of carbohydrate specific B cells was also shown for capsular polysaccharide specific antibodies [311, 312]. The small number of

dominant B cell clones might be explained by the structure of the epitope. Only minor modifications on the core render the whole core glycan from an immunogenically inert antigen to a highly immunogenic antigen. During developmental processes B cells specific for the core glycan need to be eliminated, and only the small number of B cells, recognising additional core fucose and/or xylose can evade these processes. The reduced clonality therefore would be a result of the challenge to focus reactivity to the xenobiotic modification without involving the glycan itself.

Apart from the selection strategies the absence of solely β -1,2 xylose specific antibodies remains unclear. This may indicate the inferior role of the β -1,2 xylose epitope in comparison to the more dominant α -1,3-core fucose epitope. An immunisation of a rabbit with proteins exclusively bearing β -1,2 xylose and the subsequent generation and selection of a derived library could finally result in obtaining antibodies specific for β -1,2 xylose. Additionally the selection of such immune library could be improved by the use of glycoproteins exclusively β -1,2 xylosylated.

The clones HHH1 and HMM5 were converted into human/leporid chimeric IgG and IgE antibody constructs, due to the fact that scFvs are showing different characteristics and functional abilities. The lower affinity of scFvs compared to antibodies is based on the monovalency of scFvs. Additionally some functional assays need receptor-binding, which is mediated by the constant region of the antibody heavy chain.

The antibodies were expressed in a human cell line as different isotypes, which vary in the type number of domains of the heavy chain constant region. After purification from the supernatant the antibodies were analysed regarding their affinity, biological activity and epitope recognition.

The affinity of the antibodies was analysed by SPR (surface plasmon resonance) spectroscopy. Therefor HRP and fucosylated AHSG as CCD bearing molecules were immobilised on a gold surface and the antibodies were directed as a mobile phase over these molecules. A glycoprotein without CCDs served as control. For the clone HHH1 affinities of 7×10^9 M to HRP and 4×10^8 M to fucosylated AHSG were obtained. The slightly lower affinity of the antibody to fucosylated AHSG might be explained by the different numbers of glycosites between the HRP and AHSG. Using scFv of HHH1 to analyse the affinity to HRP and fucosylated AHSG, the obtained affinities were similar ($3,8 \times 10^7$ M and $4,7 \times 10^7$ M respectively). The nearly identical affinities for HRP and the fucosylated AHSG could be explained by the binding mode of the scFv. ScFvs bind in an one to one binding mechanism to the recognised epitope.

Generally, anti-carbohydrate antibodies are supposed to have low to medium affinities as reported for anti-Lewis X antibodies [158]. The selected anti-CCD antibodies exhibit affinities that are roughly in agreement with those reported for polyclonal human and rabbit antibodies with specificity for the CCD-epitopes [160, 295]. These affinities are extraordinarily high for carbohydrate-binding antibodies. There are only a few examples of such high affinity antibodies towards carbohydrate epitopes which mostly have particularities such as a unique structure, like the broadly-neutralizing anti-HIV antibody 2G12, or recognise repetitive glycan elements, as the *Chlamydia* LPS specific antibody S25-2 [156, 313].

The epitopes recognised by the monoclonal antibodies HHH1 and HMM5 were analysed by STD NMR and compared with the epitopes of polyclonal rabbit CCD specific antibodies and the two different fucosyltransferases. All proteins showed a pronounced interaction with the innermost GlcNAc, indicating that this residue is essential for recognising the glycan core structure. In detail the protons of the N-acetyl group and the protons of C2 of the GlcNAc-1 showed strong STD effects. This finding indicates that the innermost GlcNAc is in close contact to the core binding sites. Additionally all antibody preparations showed also interaction with the terminal N-acetyl group used for ring closing, whereby the human fucosyltransferase showed only weak interaction with this residue. This might suggest that the asparagine residue, normally attached to the CCDs is partially involved in antibody binding. Furthermore the antibodies show also a pronounced STD effect for the N-acetyl group of GlcNAc-2. The fucosyltransferase showed only medium STD effects for this group, however additional medium close contacts could be shown for the protons of C6 of GlcNAc-2, protons of the Man-3 and for the antennae, which is in accordance to recognition of the whole core through the enzyme. In contrast the antibodies showed only medium to weak STD effects within the antennae and these interactions were not frequent. The antibody HHH1 however interacted strongly with the protons of C2 of Man-3, indicating that this residue is also crucial for antibody recognition. As expected all CCD specific antibodies showed strong interactions with the α -1,3-core fucose. In immunological analyses glycoproteins without core fucose were not recognised at all by the different antibodies. These data in connection to the pronounced STD effects for α -1,3-core fucose suggest that the fucose residue is crucial to define antibody specificity and intensify the interaction for the antibodies to the fucosylated glycans. In conclusion it still remains unclear, whether the antennae are needed for antibody binding. To analyse the role of the antennae affinity measurements could be performed using a trisaccharide comprising of the two GlcNAc residues and α -1,3 attached fucose. The obtained affinities could be compared to affinities for the whole fucosylated core glycan to analyse the role of the antennae.

To analyse the antibodies HHH1 and HMM5 for a potential correlation of high affinity and cellular activation a β -hexosaminidase release assay was performed. In contrast to previous studies, the generated antibodies showed pronounced cellular activation in response to minute amounts of antigens [122, 314]. The obtained data document reactivities of CCD specific IgE that are equivalent to protein specific IgE, suggesting that CCD specific antibodies do not have inherent functional limitations in cellular activation. These *in vitro* results apparently stand in contrast to the *in vivo* situation where α -1,3-core fucose and β -1,2 xylose specific antibodies are supposed to have no clinical effects. In the human system CCD specific blocking antibodies may counter the potential provoked effects by CCD specific IgE [107]. Additional analyses however are clearly needed to address the discrepancy between the *in vitro* potential and the seemingly missing *in vivo* effects.

4.5 Relevance of glycosylation in immune modulation, vaccination approaches and tumor targeting

The role of glycosylation in different immune aspects have to be considered, especially the role of the CCDs remains in many facets open. Recent studies suggest an important role of allergen glycosylation for the uptake by APCs, especially the role of mannose residues and recognition of these by the MR [18]. A hypermannosylated Der p 1 was taken up by DCs more efficiently than natural or unglycosylated Der p 1 underlining the relevance of glycans in allergen recognition by C-type lectin receptors like MR [18]. Previously it was also demonstrated that Der p 1 binding to the MR plays a key role in downstream allergen induced T_H2 -cell differentiation, probably through the regulation of indoleamine 2,3 dioxygenase activity [315]. It can be speculated if a similar allergen uptake of CCD bearing allergens by a CCD specific receptor of APCs is possible. To date such a receptor was only found in *Drosophila melanogaster*, with a suggested function in the nervous system and specificity for α -1,3-core fucose [316].

In mice infected with *Schistosoma mansoni*, the *S. mansoni*-derived glycans are able to bias the immune response towards a T_H2 phenotype, while antigens pre-treated with metaperiodate could not induce a T_H2 response including IgE production and induction of IL-4 in a mouse model of intranasal sensitisation [116, 317, 318]. Periodate treatment destroys glycan integrity and functionality by disrupting the ring structure of monosaccharides such as mannose, galactose and fucose, abundant constituents of *S. mansoni*-derived glycans [317]. Hence glycans apparently play a relevant role in induction of a T_H2 response in *Schistosoma*-infected mice. In contrast, yellow jacket venom allergen Ves v 1 (only core fucose containing) and hemocyanin from the snail *H. pomatia* (only xylose containing) were

not able to induce the same T cell response, indicating that CCDs require the framework of *S. mansoni*-derived glycoproteins to induce immune modulation [116].

Completely open is the role of CCDs as possible adjuvant during venom immunotherapy. If CCD specific IgG antibodies already exist in a patient undergoing venom immunotherapy, these antibodies would recognise CCD bearing allergens. The complex of IgG antibodies and CCD bearing allergens is recognised by APC, like DC, Langerhans cells of the skin and macrophages, all expressing the Fc γ receptors I and III. The interaction between the Fc portion of the antibodies and Fc γ receptor on APC is considered the most effective mechanism by which APC identify and internalise antigens that should be targeted for an effective immune response. The APCs internalise the allergens and transport them to lymph nodes. Here the APCs present allergen derived peptides on cell surface by MHCII, which result in an activation of CD4⁺ T cells. The activated T cells induces B cells to produce allergen specific IgG antibodies [319]. Moreover allergen specific IgG₁ and IgG₄ levels increase, by the induction of T_{reg} cells [320]. The beneficial role of IgG₄ in immunotherapy is discussed later.

The potential of CCD decorated antigens to improve allergen uptake was shown for the α -gal epitope, however α -gal specific antibodies are suggested to possess low affinities [153, 319]. In contrast to α -gal specific antibodies, α -1,3-core specific antibodies exhibit high affinities [160]. It can be speculated that the higher affinity of these antibodies would result in a much better recognition and uptake of CCD bearing allergens by APCs compared to α -gal carrying antigens.

Moreover, a second mechanism of CCDs to act as adjuvant during venom immunotherapy in patients without pre-existing IgG could be possible. DCs are capable of taking up allergens through Fc ϵ RI-bound IgE molecules, internalising these allergens and presenting the processed allergen peptides to T cells after migrating to the peripheral lymphoid organs [321]. Presumably, allergens applied for the purpose of immunotherapy are also taken up by DCs and presented to T cells [321]. Furthermore, variations in the maturation stage and grade of activation of DCs, the composition of DC subtypes at the different sites of the body, and the dosage of allergens applied, in combination with many other factors, critically modulate the nature of the immune response induced by DCs through immunotherapy [321]. The Fc ϵ RI has an ambivalent role, on the one hand Fc ϵ RI on DCs in the epidermis is involved in the induction of proinflammatory cytokine production and recruitment of more inflammatory cells to the skin of patients with atopic dermatitis [321, 322]. Thus Fc ϵ RI-bearing DCs in the skin perpetuate the allergic inflammation, in contrast there is also a suggested role for the Fc ϵ RI in tolerogenic processes [321]. In this context, ligation of Fc ϵ RI on monocytes and certain subsets of DCs, Fc ϵ RI has been shown to trigger the production of the anti-inflammatory

cytokine IL-10 [321, 323]. During sublingual immunotherapy (SLIT) oral mucosal DCs, so called Langerhans cells (oLCs) take up administered allergens by FcεRI, followed by the secretion of IL-10 and TGF-β (tumor growth factor β) combined with the additional induction and activation of IL-10 -TGF-β-producing regulatory T cells (T_{reg}) [324]. The IL-10 and TGF-β production of T_{reg}-cells induces the production and secretion of allergen specific antibodies like IgG₄ or IgA and the suppression of allergen specific IgE [325]. IgG₄ and IgA are suggested to compete for allergen binding with IgE and to inhibit IgE-mediated crosslinking of FcεRI on mast cells. Moreover IgG₄ inhibit IgE-facilitated allergen uptake by DC, supplementary allergen specific IgA seems to play a protective role at mucosal surface and possibly IgA₂ may also act as blocking antibody at mucosal surfaces [320]. Additional T_{reg}S are also able to directly inhibit mast cell degranulation and induces tolerance by the shift from T_H2- to a T_H1-immuneresponse [326].

Due to the fact that allergen-induced IL-10 production of oLCs is IgE and FcεRI depended, it remains unclear if CCD specific IgEs are also able to induce the production of the anti-inflammatory cytokine during venom immunotherapy. Till now no data exist, in which the influence of CCD specific IgE is discussed and where the levels of anti-CCD IgE before and during immunotherapy are monitored. It might be supposed, if a Hymenoptera venom allergic patient undergoes immunotherapy, that pre-existing anti-CCD IgE facilitates the uptake of CCD bearing venom components by APCs and induces subsequent tolerance, in contrast in patient with no or low levels of CCD specific IgE the activation of APCs could be reduced, resulting in a lower IL-10 secretion and decreased tolerance induction.

Beside the potential role of CCDs during venom immunotherapy, CCDs, like α-gal, might enhance the immunogenicity of viral vaccines by targeting them to APCs. The presence of anti-gal antibodies in human serum provides an opportunity for exploiting this antibody in several clinical settings [327]. One versatile clinical application is to enhance immunogenicity of viral and other microbial vaccines as well as cancer vaccines by targeting vaccines for effective uptake by APCs like DCs and macrophages. The immunogenicity could be enhanced by the decoration of the vaccine with α-gal epitopes [327]. Studies were performed in anti-gal expressing α1,3GT knockout mice (GT-KO mice) with ovalbumin as a vaccine model [327]. If the vaccine expresses α-gal epitopes, anti-gal forms immune complexes with it. These immune complexes are effectively internalized by APCs via interaction between the Fc portion of immune-complexed anti-gal and Fcγ receptors (FcγR) on the APCs [327, 328]. These APCs transport the vaccine to regional lymph nodes where they present the vaccinating peptides on MHC molecules to activate vaccine specific T cells [327]. The efficiency of this method was demonstrated e.g. for influenza virus vaccine [319].

Glycolipids containing α -gal epitopes are an useful tool for cancer immunotherapy, if the glycolipids are injected into the tumor [329]. A successful immune response against tumor antigens (TAs) requires internalisation by APCs which transport the TA to the regional lymph nodes, followed by a subsequent activation of tumor specific cytotoxic and helper T cells [329].

In previous studies the efficiency of this α -gal glycolipid-mediated immunotherapy was demonstrated by the use of GT-KO mice bearing B16 melanoma [329].

To analyse if human tumor cells are able to insert α -gal containing glycolipids, cells from the human mammary carcinoma cell line MCF-7 were incubated with these glycolipids, showing that a dose range from 0.1-1 mg/ml is likely to result in substantial insertion of α -gal lipids into the membrane of cells. In a phase 1 dose-escalation study no α -gal related side effects could be observed, even if 10 mg α -gal glycolipids were injected. The result of this study was an enhanced survival of some patients, indicating that the treatment with α -gal containing glycolipids could help to therapy tumors and micrometastases.

Whether a similar effect is induced if vaccines are decorated with α -1,3-core fucose and/or β -1,2 xylose remains unclear. Some authors speculate on the existence of anti- α 1,3-core fucose and anti- β -1,2 xylose specific IgG antibodies due to daily exposing of plant derived material to the immune system [107, 330]. In a study analyzing blood samples of non-allergic blood donors 50% showed immunoreactivity to the β -1,2 xylose epitope and 25% to α -1,3-core fucose-epitope, in which the antibodies mainly belong to IgG and IgM subclass [330].

The presence of these antibodies allows a potential role of α -1,3-core fucose and/or β -1,2 xylose as adjuvant in vaccines to enhance APC uptake.

The implication of α -1,3-core fucosylated and/or β -1,2 xylosylated lipids represents another possibility to enhance and improve the success of cancer immunotherapy by the α -gal epitope and offers new approaches for cancer treatment.

Many aspects of the influence of the CCDs are still open and subsequent studies have to be performed to elucidate the versatile effects of the CCDs.

5. Summary

The background of this PhD-thesis is based on the Hymenoptera venom allergy and the associated complex of problems of severe anaphylactic reactions. In general around 0.3 to 8.9% of the population suffer from systemic reactions after a Hymenoptera sting. Allergic reactions are frequently provoked by stings of honeybee (*Apis mellifera*) and yellow jacket (*Vespula vulgaris*). In this context 10 to 20 fatal causalities are reported in Germany per annum; in other countries the rate is between 0.1 to 0.5 per million inhabitants and it can be assumed that the estimated number of unreported cases is much higher. As permanent therapy of allergies the so called “specific immunotherapy” (SIT) has been established. In the case of Hymenoptera venom allergy a proper diagnosis and identification of the allergy provoking insect is a prerequisite for such therapy. *In vitro* diagnostic is based i.a on determination of IgE reactivities against the venom; however this is hampered by the complexity of the venoms.

A molecular, component resolved analysis of IgE reactivities offers an opportunity to distinguish relevant IgE reactivities from clinical irrelevant cross-reactivities.

Therefore in the context of this work several different honeybee venom allergens were expressed in insect cells. The choice of the expression system offers the opportunity to avoid the establishment of cross-reactive carbohydrate determinants (CCDs). Beside biochemical and allergogenic characterisation of the allergens, coupling on a diagnostic surface allowed analyses of IgE reactivities to the allergens by the use of a great cohort of patient sera. Thereby for the first time insights into the recognition patterns of allergic patients and the relevance of particular allergens could be obtained. Additional allergens relevant for therapy could be identified and the diagnostic sensitivity could be enhanced and improved from 72 to 94% by this component resolved diagnostic.

Another aspect of this work is represented by the phenomena of IgE reactivities to CCDs. In this case IgE antibodies are binding specific to the α -1,3-core fucose epitope, which is present on glycosylated Hymenoptera venom allergens. The circumvention of the epitope formation offers diagnostic benefits, however the relevance of this reactivity is still unclear. For the detection of such reactivities marker proteins which bear different CCD epitopes are widely used rendering a differentiation and fine analysis difficult. Therefore a set of glyco-engineered insect cell lines was established by the stable transfection of different Lepidoptera species with CCD-relevant glycosyltransferases. These cell lines were used for the expression of a human serum protein with defined glycosylation pattern. The resulting glycoproteins were used to obtain reactivity profiles of Hymenoptera venom and pollen allergic patients and to analyse the prevalence of IgE reactivity for particular carbohydrate

structures. As inert scaffold protein alpha-2HS-glycoprotein was chosen, because as high abundance serum protein it should not show any protein-based cross-reactivity. Additionally it bears two glycosylation-sites, which can be easily modified upon expression in the different glyco-engineered insect cell lines. It could be shown, that IgE reactivities to the fucose epitope dominate compared to the xylose epitope in the case of Hymenoptera venom allergic patients.

Moreover analyses for the establishment and recognition of CCDs by specific antibodies and glycosyltransferases were performed. By the use of recombinant expressed glycosyltransferases and using STD NMR based analyses, first insights into the recognition of the carbohydrate core by human fucosyltransferase 8 and the honeybee α -1,3-core fucosyltransferase could be obtained. Interestingly an appropriate affinity of the enzyme to its acceptor is secured by the previous binding of the donor. To obtain findings of the recognition of CCDs by high affinity antibodies, α -1,3-core fucose specific antibody fragments were selected from a rabbit immune library for the first time. Subsequently this antibody fragments were converted into different human antibodies classes and used for structural as well as for functional analysis. By the recombinant approach the pronounced potential to activate effector cells of these antibodies was demonstrated, which confirms the biological relevance and therefore also the potential clinical significance. In structural analyses the relevance of core fucose as well as the importance of the carbohydrate core for the binding of CCD specific antibodies could be confirmed. The obtained insights contribute significantly to the comprehension of the interaction of the adaptive immune system with the environment and the allergy in particular.

6. Outlook

The use of recombinant allergens for the diagnosis of Hymenoptera venom allergy offers a variety of benefits. A set of CCD free honeybee venom allergens composed of Api m 1, Api m 2, Api m 3, Api m 5 and Api m 10 was expressed in insect cells. This set in combination with native Api m 4 was used to evaluate IgE and IgG₄ reactivities of honeybee venom allergic patients. Thereby the relevance of the individual components was emphasised. Moreover, diagnostic sensitivity could be enhanced by the use of additional allergens compared to the exclusive use of Api m 1. The recombinant approach will help to diagnose honeybee venom allergic patients more reliable. Additionally sensitisation patterns of allergic patients to different allergens were revealed. Patients showing recognition of Api m 3 and Api m 10 either in combination or to one allergen exclusively have to be particularly considered since these allergens are underrepresented or missing in venom preparations presently used for immunotherapy. Hence, these patients might be more unlikely to profit from therapy and they should be carefully monitored prior, under and after immunotherapy for success of treatment. This information may help to assure an effective immunotherapy in the future.

The molecular tools developed by the use of glyco-engineered insect cells emphasised the separated and particular relevance of α -1,3-core fucose and β -1,2 xylose. These tools can be used to dissect IgE reactivities to xylose and fucose in an epitope resolved diagnostic. Moreover the glycoproteins with different CCD configurations could help to elucidate the biological role of CCDs. Therefore animal models will be needed to show whether the CCDs have impact on uptake of CCD-bearing proteins by APCs and simultaneously to support a potential use of α -1,3-core fucose and β -1,2 xylose modified glycans as adjuvants in therapeutic approaches.

The monoclonal CCD specific antibodies generated in this work were analysed regarding epitope recognition, affinities and functionality. The epitope analyses allowed for comparison of the epitope of monoclonal antibodies, polyclonal CCD specific antibodies and core-glycan modifying enzymes. Generally it remains to analyse which residues are essential for specific antibody binding. Core glycan fragments such as a trisaccharide consisting of two GlcNAc residues and a α -1,3-core fucose attached to the reducing GlcNAc might be sufficient for antibody recognition but could show significant decrease of affinity.

The outstanding high affinities for the monoclonal CCD specific antibodies to different CCD structures were revealed. To analyse whether the high affinities and cellular activation of the

antibodies correlate mediator release assays were performed. Thereby the clear biological activity of CCD specific antibodies was confirmed. Hence, it has to be assumed that these antibodies are equivalently potent in cellular activation compared to protein specific antibodies. However, further studies on the characteristics of CCD specific antibodies are needed to address the discrepancy between clear cellular activation *in vitro* and the low clinical effects observed *in vivo*.

Antibodies specific for β -1,2 xylose were not obtained by the selection of the established immune library. To overcome this deficit alternative approaches have to be followed. Establishment of carbohydrate specific antibodies however also has to be performed using patient derived immune repertoire libraries to reliably reflect the *in vivo* situation. Animal models using specific IgE antibodies as well as structural analyses of the CCD specific antibodies in complex with the relevant glycans will reveal further insights into the interaction and recognition of carbohydrates and antibodies. These data will help to enhance our comprehension how carbohydrates are generally recognised by the adaptive immune system and which structural features govern the high affinity interaction of antibodies and carbohydrates.

7. References

1. Pirque, v., *Allergie*. Munch Med Woch, 1906. **53**: p. 1547-48.
2. Galli, S.J., M. Tsai, and A.M. Piliponsky, *The development of allergic inflammation*. Nature, 2008. **454**(7203): p. 445-54.
3. Valenta, R., *The future of antigen-specific immunotherapy of allergy*. Nat Rev Immunol, 2002. **2**(6): p. 446-53.
4. Gell, P. and R. Coombs, *The classification of allergic reactions underlying disease*. Clinical Aspects of immunology (chapter 13). 1963, Oxford: Blackwell Scientific Publications.
5. Rajan, T.V., *The Gell-Coombs classification of hypersensitivity reactions: a re-interpretation*. Trends Immunol, 2003. **24**(7): p. 376-9.
6. Hamilton, R.G., *Diagnosis and treatment of allergy to Hymenoptera venoms*. Curr Opin Allergy Clin Immunol. **10**(4): p. 323-9.
7. Naik, S.R. and S.M. Wala, *Inflammation, allergy and asthma, complex immune origin diseases: mechanisms and therapeutic agents*. Recent Pat Inflamm Allergy Drug Discov. **7**(1): p. 62-95.
8. Rivera, J., et al., *New insights on mast cell activation via the high affinity receptor for IgE*. Adv Immunol, 2008. **98**: p. 85-120.
9. Amin, K., *The role of mast cells in allergic inflammation*. Respir Med. **106**(1): p. 9-14.
10. Descotes, J. and G. Choquet-Kastylevsky, *Gell and Coombs's classification: is it still valid?* Toxicology, 2001. **158**(1-2): p. 43-9.
11. Czarnobilska, E., K. Obtulowicz, and K. Wsolek, *[Type IV of hypersensitivity and its subtypes]*. Przegl Lek, 2007. **64**(7-8): p. 506-8.
12. Kay, A.B., *Overview of 'allergy and allergic diseases: with a view to the future'*. Br Med Bull, 2000. **56**(4): p. 843-64.
13. Johansson, S.G., et al., *A revised nomenclature for allergy. An EAACI position statement from the EAACI nomenclature task force*. Allergy, 2001. **56**(9): p. 813-24.
14. Glimcher, L.H., *Trawling for treasure: tales of T-bet*. Nat Immunol, 2007. **8**(5): p. 448-50.
15. Zhu, J. and W.E. Paul, *CD4 T cells: fates, functions, and faults*. Blood, 2008. **112**(5): p. 1557-69.
16. Chen, Z., et al., *Distinct regulation of interleukin-17 in human T helper lymphocytes*. Arthritis Rheum, 2007. **56**(9): p. 2936-46.
17. Salazar, F., et al., *The role of lectins in allergic sensitization and allergic disease*. J Allergy Clin Immunol. **132**(1): p. 27-36.
18. Al-Ghouleh, A., et al., *The glycosylation pattern of common allergens: the recognition and uptake of Der p 1 by epithelial and dendritic cells is carbohydrate dependent*. PLoS One. **7**(3): p. e33929.
19. Wambre, E., E.A. James, and W.W. Kwok, *Characterization of CD4+ T cell subsets in allergy*. Curr Opin Immunol. **24**(6): p. 700-6.
20. Licona-Limon, P., et al., *TH2, allergy and group 2 innate lymphoid cells*. Nat Immunol. **14**(6): p. 536-42.

21. Saenz, S.A., B.C. Taylor, and D. Artis, *Welcome to the neighborhood: epithelial cell-derived cytokines license innate and adaptive immune responses at mucosal sites*. Immunol Rev, 2008. **226**: p. 172-90.
22. Kitajima, M., et al., *TSLP enhances the function of helper type 2 cells*. Eur J Immunol. **41**(7): p. 1862-71.
23. Hurst, S.D., et al., *New IL-17 family members promote Th1 or Th2 responses in the lung: in vivo function of the novel cytokine IL-25*. J Immunol, 2002. **169**(1): p. 443-53.
24. Angkasekwinai, P., et al., *Interleukin 25 promotes the initiation of proallergic type 2 responses*. J Exp Med, 2007. **204**(7): p. 1509-17.
25. Lefrancais, E. and C. Cayrol, *Mechanisms of IL-33 processing and secretion: differences and similarities between IL-1 family members*. Eur Cytokine Netw. **23**(4): p. 120-7.
26. Nakae, S., et al., *Role of interleukin-33 in innate-type immune cells in allergy*. Allergol Int. **62**(1): p. 13-20.
27. Mjosberg, J. and H. Spits, *Type 2 innate lymphoid cells-new members of the "type 2 franchise" that mediate allergic airway inflammation*. Eur J Immunol. **42**(5): p. 1093-6.
28. Wilhelm, C., et al., *An IL-9 fate reporter demonstrates the induction of an innate IL-9 response in lung inflammation*. Nat Immunol. **12**(11): p. 1071-7.
29. Yamane, H. and W.E. Paul, *Early signaling events that underlie fate decisions of naive CD4(+) T cells toward distinct T-helper cell subsets*. Immunol Rev. **252**(1): p. 12-23.
30. Vercelli, D., *Immunoglobulin E and its regulators*. Curr Opin Allergy Clin Immunol, 2001. **1**(1): p. 61-5.
31. de Vries, J.E., et al., *Regulation of the human IgE response by IL4 and IL13*. Res Immunol, 1993. **144**(8): p. 597-601.
32. Geha, R.S., H.H. Jabara, and S.R. Brodeur, *The regulation of immunoglobulin E class-switch recombination*. Nat Rev Immunol, 2003. **3**(9): p. 721-32.
33. Kraft, S. and N. Novak, *Fc receptors as determinants of allergic reactions*. Trends Immunol, 2006. **27**(2): p. 88-95.
34. Potaczek, D.P. and M. Kabesch, *Current concepts of IgE regulation and impact of genetic determinants*. Clin Exp Allergy. **42**(6): p. 852-71.
35. Zhang, M., R.F. Murphy, and D.K. Agrawal, *Decoding IgE Fc receptors*. Immunol Res, 2007. **37**(1): p. 1-16.
36. Kinet, J.P., *The high-affinity IgE receptor (Fc epsilon RI): from physiology to pathology*. Annu Rev Immunol, 1999. **17**: p. 931-72.
37. Garman, S.C., et al., *Structure of the Fc fragment of human IgE bound to its high-affinity receptor Fc epsilon RI alpha*. Nature, 2000. **406**(6793): p. 259-66.
38. Hulett, M.D., et al., *Fine structure analysis of interaction of Fc epsilon RI with IgE*. J Biol Chem, 1999. **274**(19): p. 13345-52.
39. Voehringer, D., *Regulation of type 2 immunity by basophils*. Adv Exp Med Biol. **785**: p. 37-41.
40. Galli, S.J. and M. Tsai, *Mast cells in allergy and infection: versatile effector and regulatory cells in innate and adaptive immunity*. Eur J Immunol. **40**(7): p. 1843-51.
41. Galli, S.J. and M. Tsai, *IgE and mast cells in allergic disease*. Nat Med. **18**(5): p. 693-704.

42. Stone, K.D., C. Prussin, and D.D. Metcalfe, *IgE, mast cells, basophils, and eosinophils*. J Allergy Clin Immunol. **125**(2 Suppl 2): p. S73-80.
43. Siracusa, M.C., et al., *Basophils and allergic inflammation*. J Allergy Clin Immunol. **132**(4): p. 789-801; quiz 788.
44. Kraft, S. and J.P. Kinet, *New developments in FcepsilonRI regulation, function and inhibition*. Nat Rev Immunol, 2007. **7**(5): p. 365-78.
45. Frandsen, P.M., et al., *The Influence of IgE on Cultured Human Mast Cells*. Allergy Asthma Immunol Res. **5**(6): p. 409-14.
46. Sarin, S., et al., *The role of the nervous system in rhinitis*. J Allergy Clin Immunol, 2006. **118**(5): p. 999-1016.
47. Cevikbas, F., et al., *Neuroimmune interactions in allergic skin diseases*. Curr Opin Allergy Clin Immunol, 2007. **7**(5): p. 365-73.
48. Laloo, U.G., P.J. Barnes, and K.F. Chung, *Pathophysiology and clinical presentations of cough*. J Allergy Clin Immunol, 1996. **98**(5 Pt 2): p. S91-6; discussion S96-7.
49. Sampson, H.A., et al., *Symposium on the definition and management of anaphylaxis: summary report*. J Allergy Clin Immunol, 2005. **115**(3): p. 584-91.
50. He, S.H., et al., *IL-9(+) IL-10(+) T cells link immediate allergic response to late phase reaction*. Clin Exp Immunol. **165**(1): p. 29-37.
51. Pejler, G., et al., *Mast cell proteases*. Adv Immunol, 2007. **95**: p. 167-255.
52. Caughey, G.H., *Mast cell tryptases and chymases in inflammation and host defense*. Immunol Rev, 2007. **217**: p. 141-54.
53. Tamachi, T., et al., *IL-25 enhances allergic airway inflammation by amplifying a TH2 cell-dependent pathway in mice*. J Allergy Clin Immunol, 2006. **118**(3): p. 606-14.
54. Yao, Z., et al., *Human IL-17: a novel cytokine derived from T cells*. J Immunol, 1995. **155**(12): p. 5483-6.
55. Larche, M., D.S. Robinson, and A.B. Kay, *The role of T lymphocytes in the pathogenesis of asthma*. J Allergy Clin Immunol, 2003. **111**(3): p. 450-63; quiz 464.
56. Bonness, S. and T. Bieber, *Molecular basis of atopic dermatitis*. Curr Opin Allergy Clin Immunol, 2007. **7**(5): p. 382-6.
57. Przybilla, B. and F. Rueff, *Hymenoptera venom allergy*. J Dtsch Dermatol Ges. **8**(2): p. 114-27; quiz 128-30.
58. Schäfer, T., *Epidemiologie der Insektengiftallergie*. Allergo J, 2009(18): p. 353-358.
59. Rueff, F., U. Jappe, and B. Przybilla, *[Standards and pitfalls of in-vitro diagnostics of Hymenoptera venom allergy]*. Hautarzt. **61**(11): p. 938-45.
60. Bilo, M.B., *Anaphylaxis caused by Hymenoptera stings: from epidemiology to treatment*. Allergy. **66 Suppl 95**: p. 35-7.
61. Demain, J.G., A.A. Minaei, and J.M. Tracy, *Anaphylaxis and insect allergy*. Curr Opin Allergy Clin Immunol. **10**(4): p. 318-22.
62. Golden, D.B., et al., *Stinging insect hypersensitivity: a practice parameter update 2011*. J Allergy Clin Immunol. **127**(4): p. 852-4 e1-23.
63. Porter, S.D., et al., *Mitigating the allergic effects of fire ant envenomation with biologically based population reduction*. Curr Opin Allergy Clin Immunol. **13**(4): p. 372-8.
64. Bilo, B.M., et al., *Diagnosis of Hymenoptera venom allergy*. Allergy, 2005. **60**(11): p. 1339-49.

65. Blank, S., et al., *Polistes species venom is devoid of carbohydrate-based cross-reactivity and allows interference-free diagnostics*. J Allergy Clin Immunol. **131**(4): p. 1239-42.
66. Blank, S., et al., *Evaluation of different glycoforms of honeybee venom major allergen phospholipase A2 (Api m 1) produced in insect cells*. Protein Pept Lett. **18**(4): p. 415-22.
67. Shipolini, R.A., et al., *The amino-acid sequence and carbohydrate content of phospholipase A2 from bee venom*. Eur J Biochem, 1974. **48**(2): p. 465-76.
68. Markovic-Housley, Z., et al., *Crystal structure of hyaluronidase, a major allergen of bee venom*. Structure, 2000. **8**(10): p. 1025-35.
69. Grunwald, T., et al., *Molecular cloning and expression in insect cells of honeybee venom allergen acid phosphatase (Api m 3)*. J Allergy Clin Immunol, 2006. **117**(4): p. 848-54.
70. Blank, S., et al., *Identification, recombinant expression, and characterization of the 100 kDa high molecular weight Hymenoptera venom allergens Api m 5 and Ves v 3*. J Immunol. **184**(9): p. 5403-13.
71. Seismann, H., et al., *Dissecting cross-reactivity in Hymenoptera venom allergy by circumvention of alpha-1,3-core fucosylation*. Mol Immunol. **47**(4): p. 799-808.
72. Blank, S., et al., *Api m 10, a genuine A. mellifera venom allergen, is clinically relevant but underrepresented in therapeutic extracts*. Allergy. **66**(10): p. 1322-9.
73. Paull, B.R., J.W. Yunginger, and G.J. Gleich, *Melittin: an allergen of honeybee venom*. J Allergy Clin Immunol, 1977. **59**(4): p. 334-8.
74. Mittermann, I., et al., *Recombinant allergen-based IgE testing to distinguish bee and wasp allergy*. J Allergy Clin Immunol. **125**(6): p. 1300-1307 e3.
75. Ebo, D.G., et al., *Component-resolved diagnosis of wasp (yellow jacket) venom allergy*. Clin Exp Allergy. **43**(2): p. 255-61.
76. Hoffman, D.R. and R.S. Jacobson, *Allergens in Hymenoptera venom XII: how much protein is in a sting?* Ann Allergy, 1984. **52**(4): p. 276-8.
77. Schumacher, M.J., M.S. Tveten, and N.B. Egen, *Rate and quantity of delivery of venom from honeybee stings*. J Allergy Clin Immunol, 1994. **93**(5): p. 831-5.
78. Sastre, J., *Molecular diagnosis and immunotherapy*. Curr Opin Allergy Clin Immunol. **13**(6): p. 646-50.
79. Muller, U.R., et al., *Hymenoptera venom allergy: analysis of double positivity to honey bee and Vespula venom by estimation of IgE antibodies to species-specific major allergens Api m1 and Ves v5*. Allergy, 2009. **64**(4): p. 543-8.
80. Muller, U., et al., *IgE to recombinant allergens Api m 1, Ves v 1, and Ves v 5 distinguish double sensitization from crossreaction in venom allergy*. Allergy. **67**(8): p. 1069-73.
81. Blank, S., et al., *Vitellogenins are new high molecular weight components and allergens (Api m 12 and Ves v 6) of Apis mellifera and Vespula vulgaris venom*. PLoS One. **8**(4): p. e62009.
82. Jappe, U., et al., *In vitro Hymenoptera venom allergy diagnosis: improved by screening for cross-reactive carbohydrate determinants and reciprocal inhibition*. Allergy, 2006. **61**(10): p. 1220-9.
83. Kohler, J., et al., *Component resolution reveals additional major allergens in patients with honeybee venom allergy*. J Allergy Clin Immunol.

84. Korosec, P., et al., *Clinical routine utility of basophil activation testing for diagnosis of Hymenoptera-allergic patients with emphasis on individuals with negative venom-specific IgE antibodies*. *Int Arch Allergy Immunol.* **161**(4): p. 363-8.
85. McGowan, E.C. and S. Saini, *Update on the performance and application of basophil activation tests*. *Curr Allergy Asthma Rep.* **13**(1): p. 101-9.
86. Scherer, K., A.J. Bircher, and I.A. Heijnen, *Diagnosis of stinging insect allergy: utility of cellular in-vitro tests*. *Curr Opin Allergy Clin Immunol*, 2009. **9**(4): p. 343-50.
87. Ozdemir, C., et al., *Mechanisms of immunotherapy to wasp and bee venom*. *Clin Exp Allergy.* **41**(9): p. 1226-34.
88. Burks, A.W., et al., *Update on allergy immunotherapy: American Academy of Allergy, Asthma & Immunology/European Academy of Allergy and Clinical Immunology/PRACTALL consensus report*. *J Allergy Clin Immunol.* **131**(5): p. 1288-96 e3.
89. Marino, K., et al., *A systematic approach to protein glycosylation analysis: a path through the maze*. *Nat Chem Biol.* **6**(10): p. 713-23.
90. Spiro, R.G., *Protein glycosylation: nature, distribution, enzymatic formation, and disease implications of glycopeptide bonds*. *Glycobiology*, 2002. **12**(4): p. 43R-56R.
91. Gill, D.J., H. Clausen, and F. Bard, *Location, location, location: new insights into O-GalNAc protein glycosylation*. *Trends Cell Biol.* **21**(3): p. 149-58.
92. Zauner, G., et al., *Protein O-glycosylation analysis*. *Biol Chem.* **393**(8): p. 687-708.
93. Aebi, M., *N-linked protein glycosylation in the ER*. *Biochim Biophys Acta.* **1833**(11): p. 2430-7.
94. Nothhaft, H. and C.M. Szymanski, *Bacterial protein N-glycosylation: new perspectives and applications*. *J Biol Chem.* **288**(10): p. 6912-20.
95. Gomord, V., et al., *Plant-specific glycosylation patterns in the context of therapeutic protein production*. *Plant Biotechnol J.* **8**(5): p. 564-87.
96. Moremen, K.W., M. Tiemeyer, and A.V. Nairn, *Vertebrate protein glycosylation: diversity, synthesis and function*. *Nat Rev Mol Cell Biol.* **13**(7): p. 448-62.
97. Schiller, B., et al., *Complicated N-linked glycans in simple organisms*. *Biol Chem.* **393**(8): p. 661-73.
98. Gray, J.S., B.Y. Yang, and R. Montgomery, *Heterogeneity of glycans at each N-glycosylation site of horseradish peroxidase*. *Carbohydr Res*, 1998. **311**(1-2): p. 61-9.
99. Tian, Y. and H. Zhang, *Characterization of disease-associated N-linked glycoproteins*. *Proteomics.* **13**(3-4): p. 504-11.
100. Jones, J., S.S. Krag, and M.J. Betenbaugh, *Controlling N-linked glycan site occupancy*. *Biochim Biophys Acta*, 2005. **1726**(2): p. 121-37.
101. Gu, J., et al., *Potential roles of N-glycosylation in cell adhesion*. *Glycoconj J.* **29**(8-9): p. 599-607.
102. Roth, J., et al., *Protein N-glycosylation, protein folding, and protein quality control*. *Mol Cells.* **30**(6): p. 497-506.
103. Varki, A., *Biological roles of oligosaccharides: all of the theories are correct*. *Glycobiology*, 1993. **3**(2): p. 97-130.

104. Freeze, H.H., *Human disorders in N-glycosylation and animal models*. Biochim Biophys Acta, 2002. **1573**(3): p. 388-93.
105. Haltiwanger, R.S. and J.B. Lowe, *Role of glycosylation in development*. Annu Rev Biochem, 2004. **73**: p. 491-537.
106. Commins, S.P. and T.A. Platts-Mills, *Delayed anaphylaxis to red meat in patients with IgE specific for galactose alpha-1,3-galactose (alpha-gal)*. Curr Allergy Asthma Rep. **13**(1): p. 72-7.
107. Altmann, F., *The role of protein glycosylation in allergy*. Int Arch Allergy Immunol, 2007. **142**(2): p. 99-115.
108. Gao, P., *Sensitization to cockroach allergen: immune regulation and genetic determinants*. Clin Dev Immunol. **2012**: p. 563760.
109. Taylor, P.R., S. Gordon, and L. Martinez-Pomares, *The mannose receptor: linking homeostasis and immunity through sugar recognition*. Trends Immunol, 2005. **26**(2): p. 104-10.
110. Linehan, S.A., *The mannose receptor is expressed by subsets of APC in non-lymphoid organs*. BMC Immunol, 2005. **6**: p. 4.
111. Salazar, F. and A.M. Ghaemmaghami, *Allergen Recognition by Innate Immune Cells: Critical Role of Dendritic and Epithelial Cells*. Front Immunol. **4**: p. 356.
112. Zuberi, R.I., et al., *Critical role for galectin-3 in airway inflammation and bronchial hyperresponsiveness in a murine model of asthma*. Am J Pathol, 2004. **165**(6): p. 2045-53.
113. Tretter, V., et al., *Fucose alpha 1,3 linked to the core region of glycoprotein N-glycans creates an important epitope for IgE from honeybee venom allergic individuals*. Int Arch Allergy Immunol, 1993. **102**(3): p. 259-66.
114. Poltl, G., et al., *N-glycans of the porcine nematode parasite Ascaris suum are modified with phosphorylcholine and core fucose residues*. Febs J, 2007. **274**(3): p. 714-26.
115. Ishihara, H., et al., *Complete structure of the carbohydrate moiety of stem bromelain. An application of the almond glycopeptidase for structural studies of glycopeptides*. J Biol Chem, 1979. **254**(21): p. 10715-9.
116. Faveeuw, C., et al., *Schistosome N-glycans containing core alpha 3-fucose and core beta 2-xylose epitopes are strong inducers of Th2 responses in mice*. Eur J Immunol, 2003. **33**(5): p. 1271-81.
117. Jang-Lee, J., et al., *Glycomics analysis of Schistosoma mansoni egg and cercarial secretions*. Mol Cell Proteomics, 2007. **6**(9): p. 1485-99.
118. van Kuik, J.A., et al., *Primary structure of the low-molecular-weight carbohydrate chains of Helix pomatia alpha-hemocyanin. Xylose as a constituent of N-linked oligosaccharides in an animal glycoprotein*. J Biol Chem, 1985. **260**(26): p. 13984-8.
119. Aalberse, R.C., V. Koshte, and J.G. Clemens, *Immunoglobulin E antibodies that crossreact with vegetable foods, pollen, and Hymenoptera venom*. J Allergy Clin Immunol, 1981. **68**(5): p. 356-64.
120. Mari, A., *IgE to cross-reactive carbohydrate determinants: analysis of the distribution and appraisal of the in vivo and in vitro reactivity*. Int Arch Allergy Immunol, 2002. **129**(4): p. 286-95.
121. Kochuyt, A.M., E.M. Van Hoeyveld, and E.A. Stevens, *Prevalence and clinical relevance of specific immunoglobulin E to pollen caused by sting- induced*

- specific immunoglobulin E to cross-reacting carbohydrate determinants in Hymenoptera venoms*. Clin Exp Allergy, 2005. **35**(4): p. 441-7.
122. Mertens, M., et al., *Cross-reactive carbohydrate determinants strongly affect the results of the basophil activation test in Hymenoptera-venom allergy*. Clin Exp Allergy. **40**(9): p. 1333-45.
123. Foetisch, K., et al., *Biological activity of IgE specific for cross-reactive carbohydrate determinants*. J Allergy Clin Immunol, 2003. **111**(4): p. 889-96.
124. Jappe, U., *[Update on meat allergy. alpha-Gal: a new epitope, a new entity?]*. Hautarzt. **63**(4): p. 299-306.
125. Galili, U., *The alpha-gal epitope and the anti-Gal antibody in xenotransplantation and in cancer immunotherapy*. Immunology and Cell Biology, 2005. **83**: p. 674-686.
126. Avila, J.L., M. Rojas, and U. Galili, *Immunogenic Gal alpha 1----3Gal carbohydrate epitopes are present on pathogenic American Trypanosoma and Leishmania*. J Immunol, 1989. **142**(8): p. 2828-34.
127. Chung, C.H., et al., *Cetuximab-induced anaphylaxis and IgE specific for galactose-alpha-1,3-galactose*. N Engl J Med, 2008. **358**(11): p. 1109-17.
128. Biedermann, T. and M. Rocken, *[Delayed appearance of symptoms in immediate hypersensitivity: type I sensitization to galactose-alpha-1,3-galactose]*. Hautarzt. **63 Suppl 1**: p. 76-9.
129. Commins, S.P. and T.A. Platts-Mills, *Tick bites and red meat allergy*. Curr Opin Allergy Clin Immunol. **13**(4): p. 354-9.
130. Commins, S.P., et al., *Delayed anaphylaxis, angioedema, or urticaria after consumption of red meat in patients with IgE antibodies specific for galactose-alpha-1,3-galactose*. J Allergy Clin Immunol, 2009. **123**(2): p. 426-33.
131. O'Neil, B.H., et al., *High incidence of cetuximab-related infusion reactions in Tennessee and North Carolina and the association with atopic history*. J Clin Oncol, 2007. **25**(24): p. 3644-8.
132. Saleh, H., et al., *Anaphylactic reactions to oligosaccharides in red meat: a syndrome in evolution*. Clin Mol Allergy. **10**(1): p. 5.
133. Pagny, S., et al., *Structural requirements for Arabidopsis beta1,2-xylosyltransferase activity and targeting to the Golgi*. Plant J, 2003. **33**(1): p. 189-203.
134. Keegstra, K. and N. Raikhel, *Plant glycosyltransferases*. Curr Opin Plant Biol, 2001. **4**(3): p. 219-24.
135. Ma, B., J.L. Simala-Grant, and D.E. Taylor, *Fucosylation in prokaryotes and eukaryotes*. Glycobiology, 2006. **16**(12): p. 158R-184R.
136. Staudacher, E., et al., *GDP-fucose: beta-N-acetylglucosamine (Fuc to (Fuc alpha 1----6GlcNAc)-Asn-peptide)alpha 1----3-fucosyltransferase activity in honeybee (Apis mellifica) venom glands. The difucosylation of asparagine-bound N-acetylglucosamine*. Eur J Biochem, 1991. **199**(3): p. 745-51.
137. Staudacher, E. and L. Marz, *Strict order of (Fuc to Asn linked GlcNAc) fucosyltransferases forming core-difucosylated structures*. Glycoconj J, 1998. **15**(4): p. 355-60.
138. Kotzler, M.P., et al., *Formation of the immunogenic alpha1,3-fucose epitope: elucidation of substrate specificity and of enzyme mechanism of core fucosyltransferase A*. Insect Biochem Mol Biol. **42**(2): p. 116-25.
139. Rendic, D., et al., *Towards abolition of immunogenic structures in insect cells: characterization of a honey-bee (Apis mellifera) multi-gene family reveals both*

- an allergy-related core alpha1,3-fucosyltransferase and the first insect Lewis-histo-blood-group-related antigen-synthesizing enzyme.* Biochem J, 2007. **402**(1): p. 105-15.
140. Fabini, G., et al., *Identification of core alpha 1,3-fucosylated glycans and cloning of the requisite fucosyltransferase cDNA from Drosophila melanogaster. Potential basis of the neural anti-horseadish peroxidase epitope.* J Biol Chem, 2001. **276**(30): p. 28058-67.
141. Wilson, I.B., et al., *Cloning and expression of cDNAs encoding alpha1,3-fucosyltransferase homologues from Arabidopsis thaliana.* Biochim Biophys Acta, 2001. **1527**(1-2): p. 88-96.
142. Kaulfurst-Soboll, H., et al., *Reduced immunogenicity of Arabidopsis hgl1 mutant N-glycans caused by altered accessibility of xylose and core fucose epitopes.* J Biol Chem. **286**(26): p. 22955-64.
143. Jan, L.Y. and Y.N. Jan, *Antibodies to horseradish peroxidase as specific neuronal markers in Drosophila and in grasshopper embryos.* Proc Natl Acad Sci U S A, 1982. **79**(8): p. 2700-4.
144. Kajiura, H., et al., *Arabidopsis beta1,2-xylosyltransferase: substrate specificity and participation in the plant-specific N-glycosylation pathway.* J Biosci Bioeng. **113**(1): p. 48-54.
145. Yuriev, E., et al., *Structural biology of carbohydrate xenoantigens.* Expert Opin Biol Ther, 2009. **9**(8): p. 1017-29.
146. Toledo-Pereyra, L.H. and F. Lopez-Neblina, *Xenotransplantation: a view to the past and an unrealized promise to the future.* Exp Clin Transplant, 2003. **1**(1): p. 1-7.
147. Joziase, D.H., et al., *Characterization of an alpha 1----3-galactosyltransferase homologue on human chromosome 12 that is organized as a processed pseudogene.* J Biol Chem, 1991. **266**(11): p. 6991-8.
148. Macher, B.A. and U. Galili, *The Galalpha1,3Galbeta1,4GlcNAc-R (alpha-Gal) epitope: a carbohydrate of unique evolution and clinical relevance.* Biochim Biophys Acta, 2008. **1780**(2): p. 75-88.
149. Larsen, R.D., et al., *Frameshift and nonsense mutations in a human genomic sequence homologous to a murine UDP-Gal:beta-D-Gal(1,4)-D-GlcNAc alpha(1,3)-galactosyltransferase cDNA.* J Biol Chem, 1990. **265**(12): p. 7055-61.
150. Heimburg-Molinaro, J. and K. Rittenhouse-Olson, *Development and characterization of antibodies to carbohydrate antigens.* Methods Mol Biol, 2009. **534**: p. 341-57.
151. Calarese, D.A., et al., *Antibody domain exchange is an immunological solution to carbohydrate cluster recognition.* Science, 2003. **300**(5628): p. 2065-71.
152. Vollmers, H.P. and S. Brandlein, *Natural antibodies and cancer.* N Biotechnol, 2009. **25**(5): p. 294-8.
153. Plum, M., et al., *Close-up of the immunogenic alpha1,3-galactose epitope as defined by a monoclonal chimeric immunoglobulin E and human serum using saturation transfer difference (STD) NMR.* J Biol Chem. **286**(50): p. 43103-11.
154. Gerstenbruch, S., et al., *Analysis of cross-reactive and specific anti-carbohydrate antibodies against lipopolysaccharide from Chlamydomophila psittaci.* Glycobiology. **20**(4): p. 461-72.
155. Lutz, H., *Naturally Occurring Antibodies (NAbs).* 2009: p. 27 - 43.

156. Muller-Loennies, S., et al., *Characterization of high affinity monoclonal antibodies specific for chlamydial lipopolysaccharide*. Glycobiology, 2000. **10**(2): p. 121-30.
157. Pejchal, R., et al., *A potent and broad neutralizing antibody recognizes and penetrates the HIV glycan shield*. Science. **334**(6059): p. 1097-103.
158. van Roon, A.M., et al., *Structure of an anti-Lewis X Fab fragment in complex with its Lewis X antigen*. Structure, 2004. **12**(7): p. 1227-36.
159. Moore, C.J. and F.I. Auzanneau, *Understanding the Recognition of Lewis X by Anti-Le Monoclonal Antibodies*. J Med Chem.
160. Jin, C., et al., *Affinity of IgE and IgG against cross-reactive carbohydrate determinants on plant and insect glycoproteins*. J Allergy Clin Immunol, 2008. **121**(1): p. 185-190 e2.
161. Tamura, T., M.S. Wadhwa, and K.G. Rice, *Reducing-end modification of N-linked oligosaccharides with tyrosine*. Anal Biochem, 1994. **216**(2): p. 335-44.
162. Manger, I.D., T.W. Rademacher, and R.A. Dwek, *1-N-glycyl beta-oligosaccharide derivatives as stable intermediates for the formation of glycoconjugate probes*. Biochemistry, 1992. **31**(44): p. 10724-32.
163. Cohen-Anisfeld, *A practical, convergent method for glycopeptide synthesis*. J. Am. Chem. Soc., 1993. **115**: p. 10531-10537.
164. Asubel, *Current Protocols in Molecular Biology*. Wiley Interscience, 1996.
165. Kemper, S., et al., *Group epitope mapping considering relaxation of the ligand (GEM-CRL): including longitudinal relaxation rates in the analysis of saturation transfer difference (STD) experiments*. J Magn Reson. **203**(1): p. 1-10.
166. Bowers, C., Huafeng, Dror, Eastwood, Gregersen, Klepeis, Kolossvary, Sacerdoti, Moraes, Salmon, Yibing, Shaw, *Scalable algorithms for molecular dynamics simulations on commodity clusters*. Proceedings of the ACM/IEEE, 2006.
167. Ihara, H., et al., *Crystal structure of mammalian alpha1,6-fucosyltransferase, FUT8*. Glycobiology, 2007. **17**(5): p. 455-66.
168. Jorgensen, *The OPLS [optimized potentials for liquid simulations] potential functions for proteins, energy minimizations for crystals of cyclic peptides and crambin*. J. Am. Chem. Soc., 1988.
169. Berendsen, *Intermolecular Forces*. Dordrecht,, 1981.
170. Darden, *Particle mesh Ewald — an N. Log(N) method for Ewald sums in large systems*. J. Chem. Phys., 1993: p. 10089–10092.
171. Evans, *The Nose–Hoover thermostat*. J. Chem. Phys., 1985: p. 4069–4074.
172. Martyna, *Constant-pressure molecular-dynamics algorithms*. J. Chem. Phys., 1994: p. 4177–4189.
173. Kotzler, M.P., et al., *Donor substrate binding and enzymatic mechanism of human core alpha1,6-fucosyltransferase (FUT8)*. Biochim Biophys Acta. **1820**(12): p. 1915-25.
174. Hofmann, S.C., et al., *Added value of IgE detection to rApi m 1 and rVes v 5 in patients with Hymenoptera venom allergy*. J Allergy Clin Immunol. **127**(1): p. 265-7.
175. Braren, I., et al., *Generation of human monoclonal allergen-specific IgE and IgG antibodies from synthetic antibody libraries*. Clin Chem, 2007. **53**(5): p. 837-44.

176. Hecker, J., et al., *Generation and epitope analysis of human monoclonal antibody isotypes with specificity for the Timothy grass major allergen Phl p 5a*. Mol Immunol. **48**(9-10): p. 1236-44.
177. Rice, K.G. and M.L. Corradi Da Silva, *Preparative purification of tyrosinamide N-linked oligosaccharides*. J Chromatogr A, 1996. **720**(1-2): p. 235-49.
178. Wilson, I.B. and F. Altmann, *Structural analysis of N-glycans from allergenic grass, ragweed and tree pollens: core alpha1,3 linked fucose and xylose present in all pollens examined*. Glycoconj J, 1998. **15**(11): p. 1055-70.
179. Aalberse, R.C., J. Akkerdaas, and R. van Ree, *Cross-reactivity of IgE antibodies to allergens*. Allergy, 2001. **56**(6): p. 478-90.
180. Hemmer, W., et al., *Identification by immunoblot of venom glycoproteins displaying immunoglobulin E-binding N-glycans as cross-reactive allergens in honeybee and yellow jacket venom*. Clin Exp Allergy, 2004. **34**(3): p. 460-9.
181. Kubelka, V., F. Altmann, and L. Marz, *The asparagine linked carbohydrate of honeybee venom hyaluronidase*. Glycoconj J, 1995. **12**(1): p. 77-83.
182. Rendic, D., et al., *Modulation of neural carbohydrate epitope expression in Drosophila melanogaster cells*. J Biol Chem, 2006. **281**(6): p. 3343-53.
183. Nguyen, K., et al., *Molecular cloning and characterization of the Caenorhabditis elegans alpha1,3-fucosyltransferase family*. Glycobiology, 2007. **17**(6): p. 586-99.
184. Leiter, H., et al., *Purification, cDNA cloning, and expression of GDP-L-Fuc:Asn linked GlcNAc alpha1,3-fucosyltransferase from mung beans*. J Biol Chem, 1999. **274**(31): p. 21830-9.
185. Becker, D.J. and J.B. Lowe, *Fucose: biosynthesis and biological function in mammals*. Glycobiology, 2003. **13**(7): p. 41R-53R.
186. Staudacher, E., et al., *Fucose in N-glycans: from plant to man*. Biochim Biophys Acta, 1999. **1473**(1): p. 216-36.
187. Brzezinski, K., et al., *High-resolution structure of NodZ fucosyltransferase involved in the biosynthesis of the nodulation factor*. Acta Biochim Pol, 2007. **54**(3): p. 537-49.
188. Sun, H.Y., et al., *Structure and mechanism of Helicobacter pylori fucosyltransferase. A basis for lipopolysaccharide variation and inhibitor design*. J Biol Chem, 2007. **282**(13): p. 9973-82.
189. Rini, J., J. Esko, and A. Varki, *Glycosyltransferases and Glycan-processing Enzymes*. 2009.
190. Qasba, P.K., B. Ramakrishnan, and E. Boeggeman, *Substrate-induced conformational changes in glycosyltransferases*. Trends Biochem Sci, 2005. **30**(1): p. 53-62.
191. Bencurova, M., et al., *Specificity of IgG and IgE antibodies against plant and insect glycoprotein glycans determined with artificial glycoforms of human transferrin*. Glycobiology, 2004. **14**(5): p. 457-66.
192. Kurosaka, A., et al., *The structure of a neural specific carbohydrate epitope of horseradish peroxidase recognized by anti-horseradish peroxidase antiserum*. J Biol Chem, 1991. **266**(7): p. 4168-72.
193. Kubelka, V., et al., *Primary structures of the N-linked carbohydrate chains from honeybee venom phospholipase A2*. Eur J Biochem, 1993. **213**(3): p. 1193-204.

194. Koizumi, K., *High-performance liquid chromatographic separation of carbohydrates on graphitized carbon columns*. J Chromatogr A, 1996. **720**(1-2): p. 119-26.
195. Pabst, M., et al., *Mass + retention time = structure: a strategy for the analysis of N-glycans by carbon LC-ESI-MS and its application to fibrin N-glycans*. Anal Chem, 2007. **79**(13): p. 5051-7.
196. Mayer, M. and B. Meyer, *Group epitope mapping by saturation transfer difference NMR to identify segments of a ligand in direct contact with a protein receptor*. J Am Chem Soc, 2001. **123**(25): p. 6108-17.
197. Mayer, *Characterization of ligand binding by saturation transfer difference NMR spectroscopy*. Angew. Chem., 1999: p. 1784-1788.
198. Meyer, B. and T. Peters, *NMR spectroscopy techniques for screening and identifying ligand binding to protein receptors*. Angew Chem Int Ed Engl, 2003. **42**(8): p. 864-90.
199. Cheng, Y. and W.H. Prusoff, *Relationship between the inhibition constant (K_1) and the concentration of inhibitor which causes 50 per cent inhibition (I_{50}) of an enzymatic reaction*. Biochem Pharmacol, 1973. **22**(23): p. 3099-108.
200. Blume, A., et al., *Fragment-based screening of the donor substrate specificity of human blood group B galactosyltransferase using saturation transfer difference NMR*. J Biol Chem, 2006. **281**(43): p. 32728-40.
201. Ihara, H., Y. Ikeda, and N. Taniguchi, *Reaction mechanism and substrate specificity for nucleotide sugar of mammalian alpha 1,6-fucosyltransferase--a large-scale preparation and characterization of recombinant human FUT8*. Glycobiology, 2006. **16**(4): p. 333-42.
202. Angulo, J., et al., *Blood group B galactosyltransferase: insights into substrate binding from NMR experiments*. J Am Chem Soc, 2006. **128**(41): p. 13529-38.
203. de Vries, T., et al., *Fucosyltransferases: structure/function studies*. Glycobiology, 2001. **11**(10): p. 119R-128R.
204. Vliegthart, J.F., *The applicability of 500-MHz high-resolution ^1H NMR spectroscopy for the structure determination of carbohydrates derived from glycoproteins*. Pure Appl. Chem, 1981. **53**: p. 45-77.
205. Roitinger, A., et al., *HPLC method for the determination of Fuc to Asn linked GlcNAc fucosyltransferases*. Glycoconj J, 1998. **15**(1): p. 89-91.
206. Uozumi, N., et al., *A fluorescent assay method for GDP-L-Fuc:N-acetyl-beta-D-glucosaminide alpha 1-6fucosyltransferase activity, involving high performance liquid chromatography*. J Biochem, 1996. **120**(2): p. 385-92.
207. Voynow, J.A., T.F. Scanlin, and M.C. Glick, *A quantitative method for GDP-L-Fuc:N-acetyl-beta-D-glucosaminide alpha 1----6fucosyltransferase activity with lectin affinity chromatography*. Anal Biochem, 1988. **168**(2): p. 367-73.
208. Yazawa, S., et al., *A novel method for blood group typing with the aid of monoclonal antibody immobilized dyed microspheres*. Nihon Hoigaku Zasshi, 1992. **46**(6): p. 440-4.
209. Fellenberg, M., A. Coksezen, and B. Meyer, *Characterization of picomole amounts of oligosaccharides from glycoproteins by ^1H NMR spectroscopy*. Angew Chem Int Ed Engl. **49**(14): p. 2630-3.
210. Exnowitz, F., B. Meyer, and T. Hackl, *NMR for direct determination of $K(m)$ and $V(max)$ of enzyme reactions based on the Lambert W function-analysis of progress curves*. Biochim Biophys Acta. **1824**(3): p. 443-9.

211. Duggleby, R.G., *Analysis of enzyme progress curves by nonlinear regression*. Methods Enzymol, 1995. **249**: p. 61-90.
212. Duggleby, R.G. and R.B. Clarke, *Experimental designs for estimating the parameters of the Michaelis-Menten equation from progress curves of enzyme-catalyzed reactions*. Biochim Biophys Acta, 1991. **1080**(3): p. 231-6.
213. Orsi, B.A. and K.F. Tipton, *Kinetic analysis of progress curves*. Methods Enzymol, 1979. **63**: p. 159-83.
214. Goudar, C.T., et al., *Progress curve analysis for enzyme and microbial kinetic reactions using explicit solutions based on the Lambert W function*. J Microbiol Methods, 2004. **59**(3): p. 317-26.
215. Helfgott, M., *Some mathematical and statistical aspects of enzyme kinetics*. J. Online Math. Appl, 2007: p. 1-34.
216. Sinnott, M.L., *Catalytic mechanism of enzymic glycosyl transfer*. Chem. Rev., 1990. **90**: p. 1171-1202.
217. Shoemaker, G.K., et al., *Temperature-dependent cooperativity in donor-acceptor substrate binding to the human blood group glycosyltransferases*. Glycobiology, 2008. **18**(8): p. 587-92.
218. Bisswanger, H., *Multiple Equilibria, Enzyme Kinetics*. 2008: p. 7-58.
219. Wilson, J.R., D. Williams, and H. Schachter, *The control of glycoprotein synthesis: N-acetylglucosamine linkage to a mannose residue as a signal for the attachment of L-fucose to the asparagine linked N-acetylglucosamine residue of glycopeptide from alpha1-acid glycoprotein*. Biochem Biophys Res Commun, 1976. **72**(3): p. 909-16.
220. Miyoshi, E., et al., *The alpha1-6-fucosyltransferase gene and its biological significance*. Biochim Biophys Acta, 1999. **1473**(1): p. 9-20.
221. Takahashi, M., et al., *Core fucose and bisecting GlcNAc, the direct modifiers of the N-glycan core: their functions and target proteins*. Carbohydr Res, 2009. **344**(12): p. 1387-90.
222. Wang, X., et al., *Core fucosylation regulates epidermal growth factor receptor-mediated intracellular signaling*. J Biol Chem, 2006. **281**(5): p. 2572-7.
223. Wang, X., et al., *Dysregulation of TGF-beta1 receptor activation leads to abnormal lung development and emphysema-like phenotype in core fucose-deficient mice*. Proc Natl Acad Sci U S A, 2005. **102**(44): p. 15791-6.
224. Wang, X., et al., *Requirement of Fut8 for the expression of vascular endothelial growth factor receptor-2: a new mechanism for the emphysema-like changes observed in Fut8-deficient mice*. J Biochem, 2009. **145**(5): p. 643-51.
225. Osumi, D., et al., *Core fucosylation of E-cadherin enhances cell-cell adhesion in human colon carcinoma WiDr cells*. Cancer Sci, 2009. **100**(5): p. 888-95.
226. Zhao, Y., et al., *Deletion of core fucosylation on alpha3beta1 integrin down-regulates its functions*. J Biol Chem, 2006. **281**(50): p. 38343-50.
227. Noda, K., et al., *High expression of alpha-1-6 fucosyltransferase during rat hepatocarcinogenesis*. Int J Cancer, 1998. **75**(3): p. 444-50.
228. Noda, K., et al., *Gene expression of alpha1-6 fucosyltransferase in human hepatoma tissues: a possible implication for increased fucosylation of alpha-fetoprotein*. Hepatology, 1998. **28**(4): p. 944-52.
229. Moriwaki, K., et al., *A high expression of GDP-fucose transporter in hepatocellular carcinoma is a key factor for increases in fucosylation*. Glycobiology, 2007. **17**(12): p. 1311-20.

- 230. Shields, R.L., et al., *Lack of fucose on human IgG1 N-linked oligosaccharide improves binding to human Fcγ₃ and antibody-dependent cellular toxicity*. J Biol Chem, 2002. **277**(30): p. 26733-40.
- 231. Shinkawa, T., et al., *The absence of fucose but not the presence of galactose or bisecting N-acetylglucosamine of human IgG1 complex-type oligosaccharides shows the critical role of enhancing antibody-dependent cellular cytotoxicity*. J Biol Chem, 2003. **278**(5): p. 3466-73.
- 232. Nishima, W., et al., *Effect of bisecting GlcNAc and core fucosylation on conformational properties of biantennary complex-type N-glycans in solution*. J Phys Chem B. **116**(29): p. 8504-12.
- 233. Andre, S., et al., *From structural to functional glycomics: core substitutions as molecular switches for shape and lectin affinity of N-glycans*. Biol Chem, 2009. **390**(7): p. 557-65.
- 234. Schaefer, K., et al., *A new concept for glycosyltransferase inhibitors: nonionic mimics of the nucleotide donor of the human blood group B galactosyltransferase*. Chembiochem. **13**(3): p. 443-50.
- 235. Schmidt, R.R., *Glycosyltransferase inhibitors*. Carbohydrate-based Drug Discovery, 2003. **2**: p. 609-659.
- 236. Uozumi, N., et al., *Purification and cDNA cloning of porcine brain GDP-L-Fuc:N-acetyl-beta-D-glucosaminide alpha1-->6fucosyltransferase*. J Biol Chem, 1996. **271**(44): p. 27810-7.
- 237. Yanagidani, S., et al., *Purification and cDNA cloning of GDP-L-Fuc:N-acetyl-beta-D-glucosaminide:alpha1-6 fucosyltransferase (alpha1-6 FucT) from human gastric cancer MKN45 cells*. J Biochem, 1997. **121**(3): p. 626-32.
- 238. Voynow, J.A., et al., *Purification and characterization of GDP-L-fucose-N-acetyl beta-D-glucosaminide alpha 1----6fucosyltransferase from cultured human skin fibroblasts. Requirement of a specific biantennary oligosaccharide as substrate*. J Biol Chem, 1991. **266**(32): p. 21572-7.
- 239. Costache, M., et al., *Evolution of fucosyltransferase genes in vertebrates*. J Biol Chem, 1997. **272**(47): p. 29721-8.
- 240. Yamaguchi, Y., et al., *Genomic structure and promoter analysis of the human alpha1, 6-fucosyltransferase gene (FUT8)*. Glycobiology, 2000. **10**(6): p. 637-43.
- 241. Martinez-Duncker, I., et al., *A new superfamily of protein-O-fucosyltransferases, alpha2-fucosyltransferases, and alpha6-fucosyltransferases: phylogeny and identification of conserved peptide motifs*. Glycobiology, 2003. **13**(12): p. 1C-5C.
- 242. Breton, C., R. Oriol, and A. Imberty, *Conserved structural features in eukaryotic and prokaryotic fucosyltransferases*. Glycobiology, 1998. **8**(1): p. 87-94.
- 243. Oriol, R., et al., *Divergent evolution of fucosyltransferase genes from vertebrates, invertebrates, and bacteria*. Glycobiology, 1999. **9**(4): p. 323-34.
- 244. Takahashi, T., et al., *A sequence motif involved in the donor substrate binding by alpha1,6-fucosyltransferase: the role of the conserved arginine residues*. Glycobiology, 2000. **10**(5): p. 503-10.
- 245. Brzezinski, K., Z. Dauter, and M. Jaskolski, *Structures of NodZ alpha1,6-fucosyltransferase in complex with GDP and GDP-fucose*. Acta Crystallogr D Biol Crystallogr. **68**(Pt 2): p. 160-8.

246. Ihara, H., et al., *Fucosylation of chitooligosaccharides by human alpha1,6-fucosyltransferase requires a nonreducing terminal chitotriose unit as a minimal structure*. *Glycobiology*. **20**(8): p. 1021-33.
247. Longmore, G.D. and H. Schachter, *Product-identification and substrate-specificity studies of the GDP-L-fucose:2-acetamido-2-deoxy-beta-D-glucoside (FUC goes to Asn linked GlcNAc) 6-alpha-L-fucosyltransferase in a Golgi-rich fraction from porcine liver*. *Carbohydr Res*, 1982. **100**: p. 365-92.
248. Shao, M.C., C.W. Sokolik, and F. Wold, *Specificity studies of the GDP-[L]-fucose: 2-acetamido-2-deoxy-beta-[D]-glucoside (Fuc-->Asn linked GlcNAc) 6-alpha-[L]-fucosyltransferase from rat-liver Golgi membranes*. *Carbohydr Res*, 1994. **251**: p. 163-73.
249. Kaminska, J., M.C. Glick, and J. Koscielak, *Purification and characterization of GDP-L-Fuc: N-acetyl beta-D-glucosaminide alpha1-->6fucosyltransferase from human blood platelets*. *Glycoconj J*, 1998. **15**(8): p. 783-8.
250. Paschinger, K., et al., *Fucosyltransferase substrate specificity and the order of fucosylation in invertebrates*. *Glycobiology*, 2005. **15**(5): p. 463-74.
251. Lira-Navarrete, E., et al., *Structural insights into the mechanism of protein O-fucosylation*. *PLoS One*. **6**(9): p. e25365.
252. Goudar, C.T., *Progress curve analysis for enzyme and microbial kinetic reactions using explicit solutions based on the Lambert W function*. *J. Microbiol. Methods*, 2004. **59**: p. 317-326.
253. Chen, C.Y., et al., *Fucosyltransferase 8 as a functional regulator of nonsmall cell lung cancer*. *Proc Natl Acad Sci U S A*. **110**(2): p. 630-5.
254. Schaefer, K., et al., *A nonionic inhibitor with high specificity for the UDP-Gal donor binding site of human blood group B galactosyltransferase: design, synthesis, and characterization*. *J Med Chem*. **56**(5): p. 2150-4.
255. Williams, D.H., et al., *Understanding noncovalent interactions: ligand binding energy and catalytic efficiency from ligand-induced reductions in motion within receptors and enzymes*. *Angew Chem Int Ed Engl*, 2004. **43**(48): p. 6596-616.
256. Paulsen, H., *Conformational analysis, XXIV. Determination of the conformations of tri-and tetrasaccharide sequences of N-glycoproteins. The problem of the 1,6-glycosidic bond*. *Liebigs Ann. Chem*, 1984: p. 951-976.
257. Lairson, L.L., et al., *Glycosyltransferases: structures, functions, and mechanisms*. *Annu Rev Biochem*, 2008. **77**: p. 521-55.
258. Breton, C., et al., *Structures and mechanisms of glycosyltransferases*. *Glycobiology*, 2006. **16**(2): p. 29R-37R.
259. Schimpl, M., et al., *O-GlcNAc transferase invokes nucleotide sugar pyrophosphate participation in catalysis*. *Nat Chem Biol*. **8**(12): p. 969-74.
260. Murray, B.W., et al., *Mechanism of human alpha-1,3-fucosyltransferase V: glycosidic cleavage occurs prior to nucleophilic attack*. *Biochemistry*, 1997. **36**(4): p. 823-31.
261. Eberlein, B., et al., *Double positivity to bee and wasp venom: improved diagnostic procedure by recombinant allergen-based IgE testing and basophil activation test including data about cross-reactive carbohydrate determinants*. *J Allergy Clin Immunol*. **130**(1): p. 155-61.
262. Korosec, P., et al., *Low sensitivity of commercially available rApi m 1 for diagnosis of honeybee venom allergy*. *J Allergy Clin Immunol*. **128**(3): p. 671-3.

263. Korosec, P., et al., *High sensitivity of CAP-FEIA rVes v 5 and rVes v 1 for diagnosis of Vespula venom allergy*. J Allergy Clin Immunol. **129**(5): p. 1406-8.
264. Muller, U.R., *Bee venom allergy in beekeepers and their family members*. Curr Opin Allergy Clin Immunol, 2005. **5**(4): p. 343-7.
265. Sturm, G.J., et al., *Detection of IgE to recombinant Api m 1 and rVes v 5 is valuable but not sufficient to distinguish bee from wasp venom allergy*. J Allergy Clin Immunol. **128**(1): p. 247-8; author reply 248.
266. Vos, B., et al., *Spiking venom with rVes v 5 improves sensitivity of IgE detection in patients with allergy to Vespula venom*. J Allergy Clin Immunol. **131**(4): p. 1225-7, 1227 e1.
267. Jakob, T., et al., *Comparable IgE reactivity to natural and recombinant Api m 1 in cross-reactive carbohydrate determinant-negative patients with bee venom allergy*. J Allergy Clin Immunol. **130**(1): p. 276-8; author reply 278-9.
268. Arbesman, C.E., R.E. Reisman, and J.I. Wypych, *Allergenic potency of bee antigens measured by RAST inhibition*. Clin Allergy, 1976. **6**(6): p. 587-95.
269. Müller, U., *Insektenstichallergie: Klinik, Diagnostik und Therapie*. 1988.
270. Michel, Y., et al., *The putative serine protease inhibitor Api m 6 from Apis mellifera venom: recombinant and structural evaluation*. J Investig Allergol Clin Immunol. **22**(7): p. 476-84.
271. Blank, S., et al., *The major royal jelly proteins 8 and 9 (Api m 11) are glycosylated components of Apis mellifera venom with allergenic potential beyond carbohydrate-based reactivity*. Clin Exp Allergy. **42**(6): p. 976-85.
272. Peiren, N., et al., *Molecular cloning and expression of icarapin, a novel IgE-binding bee venom protein*. FEBS Lett, 2006. **580**(20): p. 4895-9.
273. Bilo, B.M. and F. Bonifazi, *Epidemiology of insect-venom anaphylaxis*. Curr Opin Allergy Clin Immunol, 2008. **8**(4): p. 330-7.
274. Tripodi, S., et al., *Molecular profiles of IgE to Phleum pratense in children with grass pollen allergy: implications for specific immunotherapy*. J Allergy Clin Immunol. **129**(3): p. 834-839 e8.
275. Caruso, B., et al., *Evaluation of the IgE cross-reactions among vespoid venoms. A possible approach for the choice of immunotherapy*. Allergy, 2007. **62**(5): p. 561-4.
276. Monsalve, R.I., et al., *Component-resolved diagnosis of vespoid venom-allergic individuals: phospholipases and antigen 5s are necessary to identify Vespula or Polistes sensitization*. Allergy. **67**(4): p. 528-36.
277. Juarez, C., et al., *Specific IgE antibodies to vespids in the course of immunotherapy with Vespula germanica administered to patients sensitized to Polistes dominulus*. Allergy, 1992. **47**(4 Pt 1): p. 299-302.
278. Freeze, H.H. and M. Aebi, *Altered glycan structures: the molecular basis of congenital disorders of glycosylation*. Curr Opin Struct Biol, 2005. **15**(5): p. 490-8.
279. Moskal, J.R., R.A. Kroes, and G. Dawson, *The glycobiology of brain tumors: disease relevance and therapeutic potential*. Expert Rev Neurother, 2009. **9**(10): p. 1529-45.
280. Chapman, M.D., et al., *Recombinant allergens for diagnosis and therapy of allergic disease*. J Allergy Clin Immunol, 2000. **106**(3): p. 409-18.
281. Hemmer, W., et al., *Antibody binding to venom carbohydrates is a frequent cause for double positivity to honeybee and yellow jacket venom in patients with stinging-insect allergy*. J Allergy Clin Immunol, 2001. **108**(6): p. 1045-52.

- 282. Loos, A. and H. Steinkellner, *IgG-Fc glycoengineering in non-mammalian expression hosts*. Arch Biochem Biophys. **526**(2): p. 167-73.
- 283. Malandain, H., *IgE-reactive carbohydrate epitopes--classification, cross-reactivity, and clinical impact (2nd part)*. Eur Ann Allergy Clin Immunol, 2005. **37**(7): p. 247-56.
- 284. Poltorak, A., et al., *Defective LPS signaling in C3H/HeJ and C57BL/10ScCr mice: mutations in Tlr4 gene*. Science, 1998. **282**(5396): p. 2085-8.
- 285. Avci, F.Y., et al., *A mechanism for glycoconjugate vaccine activation of the adaptive immune system and its implications for vaccine design*. Nat Med. **17**(12): p. 1602-9.
- 286. Gomery, K., et al., *Antibody WN1 222-5 mimics Toll-like receptor 4 binding in the recognition of LPS*. Proc Natl Acad Sci U S A. **109**(51): p. 20877-82.
- 287. Cygler, M., D.R. Rose, and D.R. Bundle, *Recognition of a cell-surface oligosaccharide of pathogenic Salmonella by an antibody Fab fragment*. Science, 1991. **253**(5018): p. 442-5.
- 288. Nguyen, H.P., et al., *Germline antibody recognition of distinct carbohydrate epitopes*. Nat Struct Biol, 2003. **10**(12): p. 1019-25.
- 289. Zdanov, A., et al., *Structure of a single-chain antibody variable domain (Fv) fragment complexed with a carbohydrate antigen at 1.7-A resolution*. Proc Natl Acad Sci U S A, 1994. **91**(14): p. 6423-7.
- 290. Vyas, N.K., et al., *Molecular recognition of oligosaccharide epitopes by a monoclonal Fab specific for Shigella flexneri Y lipopolysaccharide: X-ray structures and thermodynamics*. Biochemistry, 2002. **41**(46): p. 13575-86.
- 291. Villeneuve, S., et al., *Crystal structure of an anti-carbohydrate antibody directed against Vibrio cholerae O1 in complex with antigen: molecular basis for serotype specificity*. Proc Natl Acad Sci U S A, 2000. **97**(15): p. 8433-8.
- 292. Jeffrey, P.D., et al., *The x-ray structure of an anti-tumour antibody in complex with antigen*. Nat Struct Biol, 1995. **2**(6): p. 466-71.
- 293. Steinberger, P., D. Kraft, and R. Valenta, *Construction of a combinatorial IgE library from an allergic patient. Isolation and characterization of human IgE Fabs with specificity for the major timothy grass pollen allergen, Phl p 5*. J Biol Chem, 1996. **271**(18): p. 10967-72.
- 294. Laukkanen, M.L., et al., *Hevein-specific recombinant IgE antibodies from human single-chain antibody phage display libraries*. J Immunol Methods, 2003. **278**(1-2): p. 271-81.
- 295. Jin, C., et al., *Immunoglobulin G specifically binding plant N-glycans with high affinity could be generated in rabbits but not in mice*. Glycobiology, 2006. **16**(4): p. 349-57.
- 296. Cifuentes, L., et al., *Identification of Hymenoptera venom-allergic patients with negative specific IgE to venom extract by using recombinant allergens*. J Allergy Clin Immunol.
- 297. Köhler, S.B., Sabine Müller, Marcel Frick, Frank Bantleon, Johannes Huss-Marp, Jonas Lidholm, Edzard Spillner, Thilo Jakob, *IgE reactivity to a broad panel of CCD free bee venom allergens reveals 1 diverse sensitisation profiles in bee venom allergic patients*. The journal of allergy and clinical immunology, 2013.
- 298. Brehler, R., S. Grundmann, and B. Stocker, *Cross-reacting carbohydrate determinants and Hymenoptera venom allergy*. Curr Opin Allergy Clin Immunol. **13**(4): p. 360-4.

299. Rueff, F. and B. Przybilla, [*Venom immunotherapy. Side effects and efficacy of treatment*]. *Hautarzt*, 2008. **59**(3): p. 200-5.
300. Muller, U., A. Helbling, and E. Berchtold, *Immunotherapy with honeybee venom and yellow jacket venom is different regarding efficacy and safety*. *J Allergy Clin Immunol*, 1992. **89**(2): p. 529-35.
301. Brown, T.C., *Reactions to honeybee stings: an allergic prospective*. *Curr Opin Allergy Clin Immunol*. **13**(4): p. 365-71.
302. Bilo, M.B., L. Antonicelli, and F. Bonifazi, *Honeybee venom immunotherapy: certainties and pitfalls*. *Immunotherapy*. **4**(11): p. 1153-66.
303. Winningham, K.M., et al., *Hymenoptera venom protease allergens*. *J Allergy Clin Immunol*, 2004. **114**(4): p. 928-33.
304. Pike, R.N., D. Bagarozzi, Jr., and J. Travis, *Immunological cross-reactivity of the major allergen from perennial ryegrass (*Lolium perenne*), Lol p I, and the cysteine proteinase, bromelain*. *Int Arch Allergy Immunol*, 1997. **112**(4): p. 412-4.
305. Kotzler, M.P., et al., *Donor assists acceptor binding and catalysis of human alpha1,6-fucosyltransferase*. *ACS Chem Biol*. **8**(8): p. 1830-40.
306. Wuhrer, M., et al., *New features of site-specific horseradish peroxidase (HRP) glycosylation uncovered by nano-LC-MS with repeated ion-isolation/fragmentation cycles*. *Biochim Biophys Acta*, 2005. **1723**(1-3): p. 229-39.
307. Knight, K.L. and M.A. Crane, *Generating the antibody repertoire in rabbit*. *Adv Immunol*, 1994. **56**: p. 179-218.
308. Rader, C., et al., *The rabbit antibody repertoire as a novel source for the generation of therapeutic human antibodies*. *J Biol Chem*, 2000. **275**(18): p. 13668-76.
309. Foti, M., et al., *Rabbit monoclonal Fab derived from a phage display library*. *J Immunol Methods*, 1998. **213**(2): p. 201-12.
310. Popkov, M., et al., *Human/mouse cross-reactive anti-VEGF receptor 2 recombinant antibodies selected from an immune b9 allotype rabbit antibody library*. *J Immunol Methods*, 2004. **288**(1-2): p. 149-64.
311. Lucas, A.H., et al., *Oligoclonality of serum immunoglobulin G antibody responses to *Streptococcus pneumoniae* capsular polysaccharide serotypes 6B, 14, and 23F*. *Infect Immun*, 1997. **65**(12): p. 5103-9.
312. Zhou, J., et al., *Recurrent variable region gene usage and somatic mutation in the human antibody response to the capsular polysaccharide of *Streptococcus pneumoniae* type 23F*. *Infect Immun*, 2002. **70**(8): p. 4083-91.
313. Scanlan, C.N., et al., *The broadly neutralizing anti-human immunodeficiency virus type 1 antibody 2G12 recognizes a cluster of alpha1-->2 mannose residues on the outer face of gp120*. *J Virol*, 2002. **76**(14): p. 7306-21.
314. Westphal, S., et al., *Molecular characterization and allergenic activity of Lyc e 2 (beta-fructofuranosidase), a glycosylated allergen of tomato*. *Eur J Biochem*, 2003. **270**(6): p. 1327-37.
315. Royer, P.J., et al., *The mannose receptor mediates the uptake of diverse native allergens by dendritic cells and determines allergen-induced T cell polarization through modulation of IDO activity*. *J Immunol*. **185**(3): p. 1522-31.
316. Bouyain, S., et al., *An endogenous *Drosophila* receptor for glycans bearing alpha 1,3 linked core fucose residues*. *J Biol Chem*, 2002. **277**(25): p. 22566-72.

- 317. Meevissen, M.H., M. Yazdanbakhsh, and C.H. Hokke, *Schistosoma mansoni* egg glycoproteins and C-type lectins of host immune cells: molecular partners that shape immune responses. *Exp Parasitol*. **132**(1): p. 14-21.
- 318. Okano, M., et al., *Induction of Th2 responses and IgE is largely due to carbohydrates functioning as adjuvants on Schistosoma mansoni egg antigens*. *J Immunol*, 1999. **163**(12): p. 6712-7.
- 319. Abdel-Motal, U.M., et al., *Immunogenicity of influenza virus vaccine is increased by anti-gal-mediated targeting to antigen-presenting cells*. *J Virol*, 2007. **81**(17): p. 9131-41.
- 320. Alvaro, M., et al., *Allergen-specific immunotherapy: update on immunological mechanisms*. *Allergol Immunopathol (Madr)*. **41**(4): p. 265-72.
- 321. Novak, N., *Targeting dendritic cells in allergen immunotherapy*. *Immunol Allergy Clin North Am*, 2006. **26**(2): p. 307-19, viii.
- 322. Bieber, T., *The pro- and anti-inflammatory properties of human antigen-presenting cells expressing the high affinity receptor for IgE (Fc epsilon RI)*. *Immunobiology*, 2007. **212**(6): p. 499-503.
- 323. Novak, N., T. Bieber, and N. Katoh, *Engagement of Fc epsilon RI on human monocytes induces the production of IL-10 and prevents their differentiation in dendritic cells*. *J Immunol*, 2001. **167**(2): p. 797-804.
- 324. Allam, J.P., et al., *Characterization of dendritic cells from human oral mucosa: a new Langerhans' cell type with high constitutive Fc epsilon RI expression*. *J Allergy Clin Immunol*, 2003. **112**(1): p. 141-8.
- 325. Soyer, O.U., et al., *Mechanisms of peripheral tolerance to allergens*. *Allergy*. **68**(2): p. 161-70.
- 326. Fujita, H., et al., *Mechanisms of allergen-specific immunotherapy*. *Clin Transl Allergy*. **2**(1): p. 2.
- 327. Galili, U., *Anti-Gal: an abundant human natural antibody of multiple pathogeneses and clinical benefits*. *Immunology*. **140**(1): p. 1-11.
- 328. Abdel-Motal, U.M., et al., *Increased immunogenicity of HIV-1 p24 and gp120 following immunization with gp120/p24 fusion protein vaccine expressing alpha-gal epitopes*. *Vaccine*. **28**(7): p. 1758-65.
- 329. Whalen, G.F., et al., *Cancer immunotherapy by intratumoral injection of alpha-gal glycolipids*. *Anticancer Res*. **32**(9): p. 3861-8.
- 330. Bardor, M., et al., *Immunoreactivity in mammals of two typical plant glyco-epitopes, core alpha(1,3)-fucose and core xylose*. *Glycobiology*, 2003. **13**(6): p. 427-34.

Appendix

Curriculum vitae

Name: Frank Ingo Bantleon

Date of Birth: 20. September 1984

School:

- Visit of J.G. Fischer Elementary School in Süßen / Germany (1991-1994)
- Visit of Erich-Kästner Gymnasium in Eislingen / Germany (1994-2004)

Studies

- Studies of Biology (2005-2010) at the University of Hamburg / Germany
- Diploma thesis: "Components of the Hymenoptera venoms of *Apis mellifera* and *Vespula vulgaris* and their clinical relevance" (in the group of Prof. Dr. R. Bredehorst, Institute of Chemistry, Department for Biochemistry and Molecular Biology II, University of Hamburg)
- Biology-Diploma (Biochemistry, Microbiology) in Hamburg (30th July 2010)

Doctoral thesis

- Ph.D. thesis (since September 2010): "Molecular evaluation of IgE reactivity in hymenoptera venom allergy" in the group of Prof. Dr. Bredehorst, Institute of Chemistry, Department for Biochemistry and Molecular Biology II, University of Hamburg

Stipend

- Stipendiary of the "Studienstiftung des deutschen Volkes" (since 2008).

Main research

- Insect venom allergy
- Recombinant allergens
- Recombinant IgE antibodies
- Epitope characterization
- Cross-reactive carbohydrate determinants

Publications

Close-up of the immunogenic α 1,3-galactose epitope as defined by a monoclonal chimeric immunoglobulin E and human serum using saturation transfer difference (STD) NMR.

Plum M, Michel Y, Wallach K, Raiber T, Blank S, **Bantleon FI**, Diethers A, Greunke K, Braren I, Hackl T, Meyer B, Spillner E.

J Biol Chem. 2011 Dec 16;286(50):43103-11. doi: 10.1074/jbc.M111.291823. Epub 2011 Oct 11

Originalarbeit, Anteil 6%

Formation of the immunogenic α 1,3 fucose epitope: elucidation of substrate specificity and of enzyme mechanism of core fucosyltransferase A.

Kötzler MP, Blank S, Behnken HN, Alpers D, **Bantleon FI**, Spillner E, Meyer B.

Insect Biochem Mol Biol. 2012 Feb;42(2):116-25. doi: 10.1016/j.ibmb.2011.11.004. Epub 2011 Dec 13.

Originalarbeit, Anteil 13%

The major royal jelly proteins 8 and 9 (Api m 11) are glycosylated components of Apis mellifera venom with allergenic potential beyond carbohydrate-based reactivity.

Blank S, **Bantleon FI**, McIntyre M, Ollert M, Spillner E.

Clin Exp Allergy. 2012 Jun;42(6):976-85. doi: 10.1111/j.1365-2222.2012.03966.x.

Originalarbeit, Anteil 13%

Donor substrate binding and enzymatic mechanism of human core α 1,6-fucosyltransferase (FUT8).

Kötzler MP, Blank S, **Bantleon FI**, Spillner E, Meyer B.

Biochim Biophys Acta. 2012 Dec;1820(12):1915-25. doi: 10.1016/j.bbagen.2012.08.018.

Epub 2012 Sep 7.

Originalarbeit, Anteil 15%

Polistes species venom is devoid of carbohydrate-based cross-reactivity and allows interference-free diagnostics.

Blank S, Neu C, Hasche D, **Bantleon FI**, Jakob T, Spillner E.

J Allergy Clin Immunol. 2013 Apr;131(4):1239-42. doi: 10.1016/j.jaci.2012.10.047. Epub 2012 Dec 8. No abstract available.

Originalarbeit, Anteil 13%

Vitellogenins are new high molecular weight components and allergens (Api m 12 and Ves v 6) of Apis mellifera and Vespula vulgaris venom.

Blank S, Seismann H, McIntyre M, Ollert M, Wolf S, **Bantleon FI**, Spillner E.

PLoS One. 2013 Apr 23;8(4):e62009. doi: 10.1371/journal.pone.0062009. Print 2013.

Originalarbeit, Anteil 8%

Donor Assists Acceptor Binding and Catalysis of Human α 1,6-Fucosyltransferase.

Kötzler MP, Blank S, **Bantleon FI**, Wienke M, Spillner E, Meyer B.

ACS Chem Biol. 2013 Aug 16;8(8):1830-40. doi: 10.1021/cb400140u. Epub 2013 Jun 19.

Originalarbeit, Anteil 10%

Component resolution reveals additional major allergens in bee venom allergic patients

Julian Köhler; Simon Blank; Sabine Müller; **Frank Bantleon**; Marcel Frick; Johannes Huss-Marp; Jonas Lidholm; Edzard Spillner; Thilo Jakob, MD

JACI-D-13-00620R1, 2013 Status: akzeptiert

Originalarbeit, Anteil 15%

Conference Contributions

EAACI

EAACI 2011 in Istanbul TRAVEL-GRANT

Poster: Dissecting IgE reactivities in Hymenoptera venom allergy by assessing insect alpha-1,3-core fucosyltransferase activities

EAACI 2012 in Genf

Oral Presentaion: Fine specificity of IgE and IgG carbohydrate reactivity dissected by establishing xenobiotic epitopes with glycoengineered cell lines (EAACI award)

EAACI 2013 in Mailand

Poster-Discussion: Insights into high affinity recognition of cross-reactive carbohydrate determinants by mammalian antibodies prove their functional relevance

Mainzer Allergieworkshop (Oral Presentations)

2011: Dissecting IgE reactivities in Hymenoptera venom allergy by assessing insect alpha-1,3-core fucosyltransferase activities

2013: Fine specificity of IgE and IgG carbohydrate reactivity dissected by establishing xenobiotic epitopes with glycoengineered cells

GlycoT 2012 Hannover

Poster: Establishing xenobiotic epitopes with glycoengineered cell lines for fine specificity dissection of carbohydrate based immunoreactivity

Deutscher Allergiekongress

2012 in München:
















Oral Presentation and Poster: *Polistes spp.* Venom glycoproteins are devoid of CCD reactivity (Posterpresentation was awarded with the price in the Junior Members Postersession)














2013 in Bochum














Poster: Insights into high affinity recognition of cross-reactive carbohydrate determinants by mammalian antibodies prove their functional relevance (Posterpresentation was awarded with the price in the Junior Members Postersession)

Sicherheit und Entsorgung

Folgende Reagenzien und Lösungsmittel waren mit Gefahrenhinweisen und Sicherheitsratschlägen gemäß §6 der Gefahrstoffverordnung versehen:

Substanz	Gefahrensymbol	H-Sätze	P-Sätze
2-Propanol	 	<u>H225-H319-H336</u>	<u>P210-P261-P305</u> + <u>P351 + P338</u>
5-Brom-4-chlor-3-indoxylphosphat	Kein gefährliches Produkt im Sinne der Richtlinie 67/548/EWG		
ABTS		<u>H315-H319-H335</u>	<u>P261-P305 + P351 +</u> <u>P338</u>
Acrylamid	 	301-312-315-317- 319- 332-340-350- 361f.-372	201-280-301+352- 305+351+338
Agar	Kein gefährliches Produkt im Sinne der Richtlinie 67/548/EWG		
Ammoniumpersulfat	  	<u>H272-H302-H315-</u> <u>H317-H319-H334-</u> <u>H335</u>	<u>P220-P261-P280-</u> <u>P305 + P351 + P338-</u> <u>P342 + P311</u>
Ampicillin	 	315-317-319-334- 335	261-280- 305+351+338- 342+311
Anhydrotetrazyklin Hydrochlorid	Kein gefährliches Produkt im Sinne der Richtlinie 67/548/EWG		
Bovines Serumalbumin	Kein gefährliches Produkt im Sinne der Richtlinie 67/548/EWG		
Bromphenolblau	Kein gefährliches Produkt im Sinne der Richtlinie 67/548/EWG		
Calciumchlorid Dihydrat		<u>H319</u>	<u>P305 + P351 + P338</u>
Chloroform	 	302-315-351-373	302+352-314
Diethylpyrocarbonat		<u>H302-H315-H319-</u> <u>H335</u>	<u>P261-P305 + P351 +</u> <u>P338</u>
Dimethylsulfoxid	Kein gefährliches Produkt im Sinne der Richtlinie 67/548/EWG		
Dithiothreitol		302-315-319	302+350- 305+351+338

Substanz	Gefahrensymbol	H-Sätze	P-Sätze
EDTA-Dinatriumsalz-Dihydrat		319	305+351+338
Essigsäure (100%)		226-314	280-301+330+331- 305+351+338
Ethanol		225	210
Ethidiumbromid		332-341	281-308+313
Glukose	Kein gefährliches Produkt im Sinne der Richtlinie 67/548/EWG		
Glutardialdehyd, 25%		<u>H302-H314-H317-</u> <u>H332-H334-H370-</u> <u>H400</u>	<u>P260-P273-P280-</u> <u>P305 + P351 + P338-</u> <u>P310</u>
Glycerin	Kein gefährliches Produkt im Sinne der Richtlinie 67/548/EWG		
Imidazol		302-314-361d	280-301+330+331- 305+351+338
Kanamycin Sulfat		<u>H360</u>	<u>P201-P308 + P313</u>
Methanol		225-301+311+331- 370	210-280-302+352- 403+235
NaOH		<u>H314</u>	<u>P280-P305 + P351 +</u> <u>P338-P310</u>
Natriumchlorid	Kein gefährliches Produkt im Sinne der Richtlinie 67/548/EWG		
NBT		<u>H302-H370</u>	<u>P260-P307 + P311</u>
Ni-NTA-Agarose	Kein gefährliches Produkt im Sinne der Richtlinie 67/548/EWG		
Nickel(II)-sulfat		<u>H302-H315-H317-</u> <u>H332-H334-H341-</u> <u>H350i-H360D-H372-</u> <u>H410</u>	<u>P201-P261-P273-</u> <u>P280-P308 + P313-</u> <u>P501</u>
Phenol (Tris-gesättigt)		<u>H301-H312-H314-</u> <u>H330-H341-H351-</u> <u>H373</u>	<u>P260-P280-P284-</u> <u>P301 + P310-P305 +</u> <u>P351 + P338-P310</u>
Salzsäure, konz.		<u>H314-H335</u>	<u>P261-P280-P305 +</u> <u>P351 + P338-P310</u>

Substanz	Gefahrensymbol	H-Sätze	P-Sätze
SDS	 	<u>H228-H302-H311-</u> <u>H315-H319-H335</u>	<u>P210-P261-P280-</u> <u>P305 + P351 + P338-</u> <u>P312</u>
TEMED	  	<u>H225-H302-H314-</u> <u>H332</u>	<u>P210-P280-P305</u> + <u>P351 + P338-P310</u>
Triethylamin	  	<u>H225-H302-H312-</u> <u>H314-H332</u>	<u>P210-P280-P305</u> + <u>P351 + P338-P310</u>
Tris		<u>H315-H319-H335</u>	<u>P261-P305 + P351 +</u> <u>P338</u>
Wasserstoffperoxid 30%	 	<u>H302-H318</u>	<u>P280-P305 + P351 +</u> <u>P338</u>
Xylen Cyanol FF		<u>H315-H319-H335</u>	<u>P261-P305 + P351 +</u> <u>P338</u>
Zitronensäure		<u>H319</u>	<u>P305 + P351 + P338</u>

Alle in dieser Arbeit verwendeten Chemikalien wurden entsprechend ihrer H- und P-Sätzen gehandhabt und nach der Gefahrgutverordnung entsorgt. Organische halogenfreie und halogenhaltige Lösungsmittel wurden getrennt in gekennzeichnete Behälter überführt. Kontaminierte Betriebsmittel wurden in dafür vorgesehenen Behältern gesammelt. Ethidiumbromid-Abfälle wurden in gesondert gekennzeichnete Behälter entsorgt. Der Umgang mit humanen Zellen wurde ausschließlich auf Laboratorien der Sicherheitsstufe S1 nach §7 GenTG be-schränkt. S1-kontaminierter Abfall wurde vor der Entsorgung in einem Autoklav durch unter Druck (5 bar) stehenden Wasserdampf 20 Minuten bei 120 °C hitzesterilisiert.

Liste der verwendeten KMR-Stoffe

Nachname: Bantleon

Matrikelnummer: 5758290

Vorname: Frank Ingo

Studiengang: Promotion Biologie

Arbeitsbereich: Arbeitskreis Bredehorst, Institut für Biochemie und Molekularbiologie,
Universität Hamburg

Zeitraum: 15.10.2010 - 15.04.2014

Auflistung der verwendeten KMR-Substanzen, Kategorie 1A und 1B

CAS-Nummer	Stoffname	Verfahren und eingesetzte Menge	Kategorie (I oder II)
67-66-3	Trichlormethan (Chloroform)	DNA-Extraktion aus Lösungen ca. 100 µL pro Ansatz	1B
79-06-1	Acrylamid	PAGE ca. 10 mL pro Ansatz	1B
68-12-2	N,N-Dimethylformamid	Detektion Immunprint 125 µL pro Ansatz	1B
1239-45-8	Ethidiumbromid	Agarosegel, DNA Interkalation	2
7786-81-4	Nickelsulfat	IMAC	1A
108-95-2	Phenol	DNA-Extraktion aus Lösungen ca. 100 µL pro Ansatz	2
288-32-4	Imidazol	IMAC Elution 300 mM Lösung, ca. 50 mL pro Reinigung	1B

Datum:

Unterschrift Doktorand

Stellungnahme zu den Beiträgen der unterschiedlichen Kooperationen

- Formation of the immunogenic α 1,3 fucose epitope: elucidation of substrate specificity and enzyme mechanism of core fucosyltransferase A
Transfektion von Insektenzellen mit Sequenz-überprüften Vektoren die das Gen zur Expression der α -1,3 core Fucosyltransferase der Honigbiene enthielten, Generierung von Baculovirus-haltigen Kulturüberständen zur Expression der α -1,3 core Fucosyltransferase in Sf9 Insektenzellen, Expression der α -1,3 core Fucosyltransferase und affinitäts-chromatographische Reinigung aus Kulturüberstand, Analyse der Expressionsausbeute und Aktivitätstest des gereinigten Enzyms mittels div. immunologischer Verfahren (ELISA und Immunoblot)
- Donor substrate binding and enzymatic mechanism of human core α -1,6-fucosyltransferase (FUT8)
und
- Donor Assists Acceptor Binding and Catalysis of Human α -1,6-Fucosyltransferase
Extraktion von mRNA aus humanen embryonalen Nierenzellen (HEK293), Umschreiben der mRNA in cDNA, Amplifikation der genetischen Information der α -1,6 Fucosyltransferase, Klonierung der genetischen Information in Expressionsvektoren zur Expression in Insektenzellen, Transfektion von Insektenzellen mit Sequenz-überprüften Vektoren, Generierung von Baculovirus-haltigen Kulturüberständen zur Expression der α -1,6 Fucosyltransferase in Sf9 Insektenzellen, Expression der α -1,6 Fucosyltransferase und affinitäts-chromatographische Reinigung aus Kulturüberstand, Analyse der Expressionsausbeute der α -1,6 core Fucosyltransferase mittels ELISA und Immunoblot
- Component resolution reveals additional major allergens in patients with bee venom allergy
Generierung expressionsfähiger Baculovirus-Stocks der Bienengift-Allergene Api m 1, Api m 2, Api m 3, Api m 5 und Api m 10, Expression der unterschiedlichen Allergene in Sf9 Insektenzellen, Reinigung der Allergene aus Kulturüberständen mittels affinitäts-chromatographischer Verfahren, Analyse zur Expressionsausbeute der Allergene (ELISA, Immunoblot und photometrische Konzentrationsbestimmung), initiale Evaluierung der IgE-Reaktivität ausgewählter Spender-Seren mittels

immunologischer Verfahren (ELISA), Interpretation der kooperativ erhaltenen IgE-Reaktivitätsanalysen

- Polistes species venom is devoid of carbohydrate-based cross-reactivity and allows interference-free diagnostics

Initiale Analyse zur CCD-Reaktivität unterschiedlicher Hymenopterengifte, Bereitstellung benötigter Antiseren, Interpretation der kooperativ erhaltenen CCD-Reaktivitätsanalysen

- Fine specificity of IgE carbohydrate reactivity dissected by establishing xenobiotic epitopes with glycoengineered cell lines

Extraktion von mRNA aus Giftdrüsen der Honigbiene und Blättern der Sojabohne, Umschreiben der mRNA in cDNA, Amplifikation der genetischen Information der α -1,3 core Fucosyltransferase und β -1,2 Xylosyltransferase, Klonierung der genetischen Information in Expressionsvektoren zur Expression der Enzyme in Sf9 und HighFive Insektenzellen, Generierung unterschiedlicher glykomodifizierter Insektenzellen, Generierung expressionsfähigen Baculovirus-Stocks des humanen α -(2HS)-Glykoproteins (AHSG), Expression des Trägerproteins in glykomodifizierten Insektenzellen, Reinigung des Proteins aus Kulturüberständen mittels affinitätschromatographischer Verfahren, Immunologische Analyse der Zelllinien und der unterschiedlich glykosylierten AHSG-Varianten (ELISA und Immunoblot), Analyse der IgE-Reaktivität von Spenderseren zu unterschiedlichen CCD-Strukturen unter Nutzung der verschiedenen AHSG-Varianten (ELISA), Interpretation der erhaltenen Daten, Textbeiträge Einleitung, Methoden und Ergebnisse, Erstellung der entsprechenden Ergebnisabbildungen

- Structural and functional insights into the high affinity recognition of xenobiotic complex-type N-glycan core structures by mammalian antibodies

Extraktion von mRNA aus Milz und Knochenmark immunisierter Kaninchen, Umschreiben der mRNA in cDNA, Amplifikation der genetischen Information des Immunrepertoires, Einbringen der genetischen Information in Phagmid-Vektoren, Selektion von Antikörperfragment-tragender Phagen gegen unterschiedlichen CCD-tragenden Glykoproteinen, Reaktivitätsanalyse von poly- und monoklonalen Phagen, Überführen der genetischen Information ausgewählter monoklonaler Klone in Vektoren zur Expression humaner IgG- und IgE-Formate, Expression CCD-spezifischer Antikörper in humanen Zelllinien, Reinigung humaner Antikörper aus

Kulturüberständen mittels affinitäts-chromatographischer Verfahren, Reaktivitätsanalyse gereinigter Antikörper, zelluläre und biophysikalische Analysen der CCD-spezifischen Antikörper, vorbereitende Präparation der verschiedenen Antikörper für STD NMR Messungen, Textbeiträge Methoden und Ergebnisse, Erstellung der entsprechenden Ergebnisabbildungen

Danksagung

Herrn Prof. Dr. Reinhard Bredehorst möchte ich an dieser Stelle für die Möglichkeit danken diese Arbeit in seinem Arbeitskreis erstellen zu dürfen. Herrn Prof. Dr. Bernd Meyer danke ich für die Übernahme des Koreferats, sowie Prof. Dr. Markus Fischer und Dr. Thomas Hackl für die Begutachtung der Disputation.

Bei Herrn Prof. Dr. Edzard Spillner möchte ich mich aufrichtig für die Betreuung dieser Arbeit, seine Geduld und Hilfe bedanken. Ohne Ihn wäre diese Arbeit schlicht nicht möglich gewesen.

Frau Dr. Melanie Plum und Frau Dipl.-Chemikerin Sara Wolf danke ich für die hilfreichen Anmerkungen, Korrekturen und Diskussionen im Laufe meiner Doktorarbeit. Besonders möchte ich mich bei Frau Dipl.-Chemikerin Sara Wolf für ihre Geduld und ihre unschlagbare Hilfe in allen Bereichen der EDV bedanken.

Bei den Herren Dr. Simon Blank und Thorsten Mix möchte ich mich für die jahrelange Hilfe und Unterstützung bedanken.

Für die kooperative Zusammenarbeit bedanke ich mich bei Frau Dr. Miriam Kötzler, Herrn Dipl.-Chemiker Felix Niemeyer und Frau Dipl.-Chemikerin Alena Wiegandt.

Bei allen Kooperationspartnern in Deutschland und der Welt bedanke ich mich für die gute Zusammenarbeit.

Bei Frau Dipl.-Biologin Julia Eckenberger bedanke ich mich für die grandiose Zusammenarbeit während ihrer Diplomarbeit und für das Seepferdchen mit Mütze.

Zudem möchte ich mich bei allen aktuellen und ehemaligen Kollegen für die schöne Zeit in und außerhalb des Labors bedanken.

Allen Diplom-, Master-, Bachelor-Studenten und BTA-Schüler danke ich für ihre fleißigen und hilfreichen Beiträge.

Herrn M.Sc Frederick Jabs danke ich für seine konstruktiven Beiträge im Rahmen seiner Projektstudien, Bachelor- und Master-Arbeit.

Meinen Eltern, Herrn Prof. Dr. Werner Bantleon und Frau Brigitte Bantleon, und meiner Familie danke ich für die jahrelange Unterstützung, Hilfe und Zuspruch.

Bei Sara bedanke ich mich von ganzem Herzen für die wunderschöne Zeit, die wir zusammen verbracht haben und freue mich auf unser gemeinsames Abenteuer in Dänemark.

Abschließend möchte ich meinen guten Freund Dr. Robert Nickl darauf hinweisen, dass diese Arbeit noch vor meinen 30. Geburtstag eingereicht wurde.

Eidesstattliche Versicherung

Hiermit versichere ich an Eides statt, die vorliegende Arbeit selbstständig und ohne fremde Hilfe sowie nur mit den angegebenen Hilfsmitteln und Quellen erstellt zu haben. Ergebnisse aus Bachelor- oder Schwerpunktarbeiten, die in diesem Arbeitskreis angefertigt wurden und die teilweise in diese Arbeit eingeflossen sind, wurden von mir initiiert und unter meiner Anleitung angefertigt.

Ebenfalls versichere ich, keinen weiteren Promotionsversuch an einer anderen Einrichtung unternommen zu haben.

Hamburg, den 14.02.2014

Frank Ingo Bantleon

